Charring Rates for Different Cross Sections

of

Laminated Veneer Lumber (LVL)

By

Wei-heng (Kevin) Tsai

Supervised by

Professor Andrew H. Buchanan

Associate Professor Peter J Moss

Dr. David Carradine

A thesis submitted in partial fulfilment of the requirements for the degree of Master of Engineering in Fire Engineering

Department of Civil and Natural Resources Engineering
University of Canterbury
Private Bag 4800
Christchurch, New Zealand

July 2010

Abstract

Current research at the University of Canterbury is investigating the performance of a new type of timber floor system made of a timber-concrete composite. This newly proposed timber floor system uses double LVL members connected together with screwed connections to form one larger LVL member. Recent large scale fire tests showed that the joint between these two screwed LVL members opened up during fire exposure. This opening phenomenon causes concerns as the overall charring rate of the joint LVL members is subsequently increased.

The main focus of this research, therefore, was to examine the charring rate for different cross sections of single and double LVL members, with different connection types for the double members. The single LVL member examined was 63mm width whereas the double LVL members examined were 90mm and 126mm width. Three connection types were investigated which were nails, screws and glue. Their corresponding charring rates and burning characteristics were examined both in the small furnace provided by the University of Canterbury and in the pilot furnace at the Building Research Association of New Zealand (BRANZ) in Wellington.

The overall finding from the small furnace testing shows that the overall average side charring rate for a 30 minute fire exposure was 0.76mm/min; whereas the overall average side charring rate for a 60 minute fire exposure was 0.66mm/min. Moreover for a 30 minute fire exposure, the average bottom charring rates for nail, screw and glue connected double LVL members were 1.00mm/min, 0.83mm/min and 0.83mm/min, respectively. For a 60 minute fire exposure, the average bottom charring rates for screw and glue connected double LVL members were 0.97mm/min and 0.57mm/min, respectively. The nail connected double LVL members experienced the highest bottom charring rate as it suffered the largest bottom separation which allowed the heat to travel into the mid-span resulting in a higher bottom charring rate. Out of these three connection types, the glued connection was the best connection type.

Experimental findings were compared with the simulated results generated by the SAFIR finite element program. Experimental findings were also used to modify the spreadsheet design tool which predicts the fire resistance rating of a timber-concrete composite floor under user defined load conditions and floor geometries.

Acknowledgements

First of all I would like to thank my supervisors, Professor Andy Buchanan, Associate Professor Peter Moss and Dr. David Carradine for their continuous support and guidance in this research. A special thanks to Dr. Carradine for his company and aid for that three days pilot furnace test at BRANZ in Wellington.

I would also like to say thank you to the Structural Timber Innovation Company (STIC) for their funding in this research. Meanwhile a special thanks for the scholarship offered by the New Zealand Fire Service Commission for this research.

A special thanks to the University of Canterbury technicians for their help in my small furnace test, especially Bob Wilsea-Smith.

I would also like to acknowledge Mark Gannon and technical staff at BRANZ for their help while I was up there performing my pilot furnace testing.

A special thanks to Lumberworx Ltd Christchurch for their generosity in providing some free Nelson Pine LVL timber.

A special thanks to the Firepro Christchurch for their generosity in providing free intumescent sealants.

I would also like to give a special thanks to Jeong-ki Min, a current PhD student at the University of Canterbury, who kindly offered support in the SAFIR thermal analysis out of his busy schedule.

A special thanks to all my lecturers and classmates for their feedbacks during the research meeting.

Last but not the least I would like to express my deepest thanks to my parents and my wife for their continuous support and help throughout my study.

Table of Contents

List of Figures

List of Tables

1. INTRODUCTION

Timber is known to be one of the oldest materials used in construction. The tradition of using timber houses varies between different parts of the world. Northern Europe and parts of Asia are areas known for their old timber buildings, but also New Zealand has a history of timber houses (Thelandersson and Larsen, 2002). In New Zealand, timber is widely used in the construction of residential housing notably thanks to the fast growing radiata pine. The tree is processed to make laminated veneer lumber (LVL), similar to glue laminated timber (glulam), which offers superior mechanical properties compared to sawn timber and comparable to reinforced concrete.

1.1. Structural Timber Innovation Company (STIC)

Although New Zealand has vast reserves of renewable forests, very little of these timbers are used in the commercial sector for large buildings. In 2008, the Structural Timber Innovation Company (STIC) was established as a research consortium developing and commercialising new structural timber technologies enabling timber to compete more effectively in the commercial sector of the construction industry. STIC's mission (STIC, 2010) is:

1. *To contract and manage the required research and development to enable the vision to be achieved.*
2. *To manage the intellectual property developed and to ensure its availability to relevant segments of the building and construction industry value chain.*
3. *To facilitate and promote the implementation and transfer of the newly developed intellectual property into the Trans-Tasman building and construction industries.*
4. *To provide new timber building solutions to the industry and add value to building owners/developers, constructors, architects, engineers and fabrications.*

The current research and development programme carried out by STIC runs in 3 parallel objectives (STIC, 2010):

Objective 1: *'Single storey timber roofs and portal frames', is being conducted at University of Auckland.*

Objective 2: *'Timber floors for multi-storey timber buildings', is being conducted at University of Technology, Sydney.*

Objective 3: *'Timber frames for multi-storey timber building', is being conducted at University of Canterbury.*

1.2. Background Leading to this Research

Current research at the University of Canterbury is investigating the performance of a new type of timber floor system made of a timber-concrete composite. Figure 1-1 shows an underside view of this timber-concrete composite floor system taken at the University of Canterbury.

This newly proposed timber floor system uses two identical 63mm width LVL members connected together with screwed connections to form one single 126mm width LVL member. In theory, the charring rate of this joined 126mm cross section LVL member should have the same charring rate as one single 126mm cross section LVL member.

Figure 1-1: Timber-concrete composite floor at the University of Canterbury

Recent fire tests carried out by O'Neill (2009) in an ISO standard fire test at BRANZ Fire Research facility showed that the joint between these two screwed LVL members separated during fire exposure as shown in Figure 1-2. This opening phenomenon causes concerns as it allows heat to travel into the mid section of the screwed joined LVL member which consequently increases the overall charring rate of the LVL members. This is especially critical at the corners of the LVL section where it experiences double-sided fire exposure. As As a result, the timber floor system may fail prematurely and endanger the overall structural stability of the building.

Figure 1-2: Opening of the double LVL member (O'Neill, 2009)

1.3. Objectives

The objectives of this research are:

- To investigate the charring rate for different cross sections of LVL members, with different connection types for double members.
- To modify the existing spreadsheet model which predicts the fire resistance rating of the timber-concrete composite floor system.
- To investigate the rate of charring after the fire is out for the glue connected 90mm width LVL member.

1.4. Scope of Research

The majority of this research is experimental in nature, involving the construction and experimental testing of different cross sections of LVL members utilising different connection types. Essentially there are two main phases for this research:

1. Small Furnace Tests at the University of Canterbury

    - The first phase of this research was to carry out experimental testing in the small furnace at the University of Canterbury. Different cross sections of LVL members ranging from 63mm to 126mm width were constructed and tested in a small furnace. For double LVL members, three different connection types which were nails, screws and glue were investigated. Experimental charring rates for each specimen were recorded and compared.

2. Pilot Furnace Tests at the BRANZ Fire Research facility

   - The second phase of this research was to expose LVL members to the Standard ISO 834 (ISO 834, 1975) design fire curve in the pilot furnace at the Building Research Association of New Zealand (BRANZ) Fire Research facility in Wellington. Three tests were conducted at BRANZ. The first test was to investigate the charring rate for 63mm, 90mm and 126mm width glued LVL members where thermocouples were installed at various depths for each specimen. Meanwhile, the second and third tests were to examine the effect of different screwed connection layouts on the separation and charring of LVL members for both 90mm and 126mm width double LVL members.

1.5. Outline of Report

Chapter 1 of this thesis describes a brief background and the objectives of this research. Prior literature relevant to this research project was reviewed and is outlined in Chapter 2. Chapter 3 and 4 focus on the small furnace testing conducted in the small furnace provided by the University of Canterbury. Chapter 5, 6 and 7 discuss the pilot furnace testing conducted in the pilot furnace provided by BRANZ in Wellington. SAFIR thermal analysis was carried out and is described in more detail in Chapter 8. Chapter 9 describes the modifications made to the exiting spreadsheet design tool based on the experimental findings from this research. Lastly chapter 10 discusses the conclusions of this research and recommendations for further research.

2. LITERATURE REVIEW

This chapter gives a summary of literature relevant to this research project.

2.1. Laminated Veneer Lumber (LVL)

Laminated veneer lumber (LVL) is a structural engineering wood product which is manufactured from thin peeled veneers of wood glued with a durable adhesive with the grain running parallel to the main axis of the member (NZ Wood, 2010). The uniformity of LVL is the key to its high strength and stiffness properties as well as its reputation for reliable and predictable performance.

2.1.1. Characteristics of LVL

Due to the number of layers of veneer used in LVL, the material properties of LVL are much more closely spread about their average value compared to sawn timber and glue laminated timber (glulam). Sawn timber is known to have the greatest variability in material characteristics as its weakest point; generally the largest knot within a sawn timber may penetrate through the entire depth of the timber. As for the glulam timber its characteristics characteristics are less varied due to the fact that multiple members are glued together. Hence the weak point of glulam can be limited within the thickness of one lamination and the odds of having multiple weak points aligned is negligible. In a similar way to glulam, LVL LVL further reduces the depth of weak point penetration by decreasing the thickness of each lamination. Due to a large number of veneer layers, the weak points can be considered as randomly distributed within the LVL so that the LVL can be assumed to have negligible defects. This is supported by fracture mechanic studies which show that in thin veneers of 3mm or less, the effects of defects can be ignored and the properties are the same as defect free wood. Thus the material properties of LVL can be determined much more confidently and closer to the mean value than the sawn timber as illustrated in Figure 2-1. This Hyspan shown on Figure 2-1 is a type of LVL product manufacture by Carter Holt Harvey (CHH) Limited (2008).

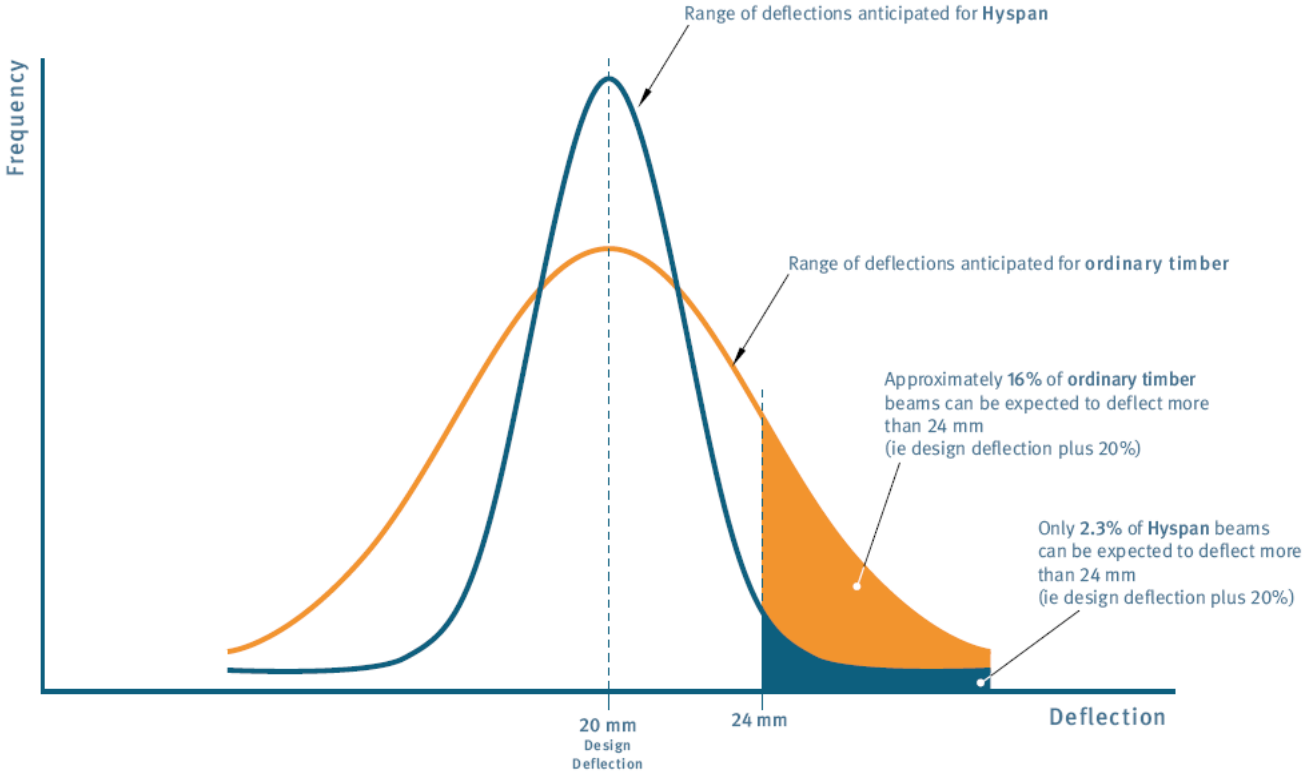

Figure 2-1: Property variances between LVL and sawn timber (CHH, 2008)

2.2. Moisture-related Movement in Timber

All wood contains water. The water can exist as free water within cell lumens and cavities or as bound water within cell walls (Forest Products Society, 1999). When the wet wood is heated, the free water is lost first which causes little change in wood properties other than reducing weight. However if heating is continued to the point where all free water is lost, further loss can only come from bound water. As a result, shrinkage and changes to properties such as strength and modulus of elasticity will occur due to the loss of bound water (Buchanan, 2007).

2.2.1. Moisture Content

Moisture content (m.c.) of wood, usually expressed as a percentage, is defined as the weight of water in wood over the weight of oven dry wood. In trees, moisture content can range from 30% to more than 200% of the weight of wood substance (Forest Products Society, 1999).

Moisture content of wood can be measured in two ways. It can either be measured directly by oven drying of weighed samples, which is the most accurate method, or indirectly with hand-held moisture meters.

2.2.2. Shrinkage and Swelling

Wood is dimensionally stable as long as the wood is not heated to the point when the cell walls start to lose bound water. This threshold is commonly known as the fibre saturation point and is usually 30% moisture content as listed in Table 2-1 (Buchanan, 2007). Shrinkage of timber is usually expressed as the change in dimension from green (fibre saturation point) to 12% moisture content, divided by the green dimension, expressed as a percentage.

Table 2-1: Shrinkage properties of some New Zealand timbers (Buchanan, 2007)

Species	% shrinkage, when drying from green to 12% m.c.		Fibre Saturation Point (% m.c.)
	Tangential	Radial	
Radiata	3.9	2.1	29
Douglas fir	4.9	2.87	27
Macrocarpa	3.2	1.8	25
Redwood	2.2	1.3	25
Eucalyptus sp.	6.0	3.5	30
Kauri	4.1	2.3	26
Matai	3.5	1.9	24
Rimu	4.2	3.0	27
Beech, red	7.1	3.3	24
Tawa	6.7	3.4	30

As shown in Figure 2-2, wood will shrink as it loses moisture and swell as it gains moisture for moisture changes below the fibre saturation point. The amount of movement is proportional to the change in moisture content and varies with species, density and the direction of the grain (Buchanan, 2007). Dense woods generally shrink and swell more than lighter woods.

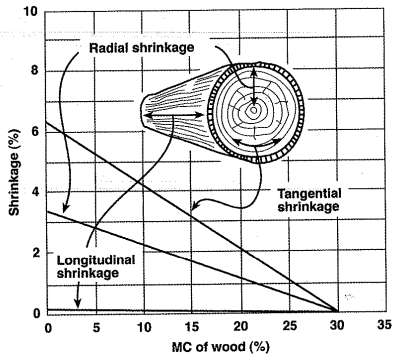

Figure 2-2: Shrinkage at various directions to the grain (Buchanan, 2007)

2.3. Timber Connections

2.3.1. Nailed Connections

Nails are probably one of the most common forms of mechanical fastening because they penetrate the wood much better than surface adhesives. Moreover, they do not weaken the wood with drilled holes and they can distribute forces over a larger part of the surface than bolts (Buchanan, 2002). Large nailed connections often have many nails passing through perforated steel plates providing excellent structural behaviours but poorer fire behaviour because of the large surface area of steel exposed to the fire.

2.3.2. Screwed Connections

Screws possess many of the advantages of nails and they also have much better withdrawal capacity than nails because of the threaded shaft. A disadvantage is the poorer ductility of screws compared with nails because of the steel used. The fire performance of screwed connections in wood has not been studied extensively (Buchanan, 2002).

2.3.3. Glued Connections

Adhesives are often used to connect many timber structures and timber members in construction. When exposed to fire, glued wood members generally behave in the same way as solid wood provided that thermosetting adhesives such as resorcinol or melamine adhesives, are used (Buchanan, 2002). Lane (2005), a former University of Canterbury Fire Engineering graduate, used heat resistant resorcinol adhesive to join his LVL members together. His finding showed that the resorcinol adhesive performed well as the glued LVL members did not show any sign of separation when exposed to fire. However some adhesives such as elastomerics and epoxies are sensitive to elevated temperature and should not be relied on in fire conditions (Buchanan, 2002).

2.4. Thermal Decomposition of Wood

When exposed to high temperature, wood undergoes thermal degradation (pyrolysis) causing physical, structural and chemical changes. The most important parameters to be considered are the exposure time and the impact temperature. Under certain conditions, changes can occur at temperatures as low as 100^{o}C, and chemical changes can appear under 100^{o}C. The phases of thermal decomposition of wood summarised by Bobacz (2006) are as follows

100 °C	- Drying of wood, loss of free and bonded water
150 °C – 200 °C	- Degradation of lignin and hemicelluloses - Composition of gases (70% $C0_2$, 30% CO) - Start of pyrolysis - Slow development of the reactions - Oxidation process becomes exothermic - Spontaneous ignition is possible in case of a long-time temperature exposure
≤ 275 °C	- Slow pyrolysis - Calorific value about 5.02MJ/kg
> 275 °C	- Decomposition of cellulose - Fast development of the reactions - Development of combustible hydrocarbons - Calorific value about 8.3MJ/kg - Beginning of development of a charring zone - Possible ignition by a pilot flame
290 °C	- Massive weight loss of wood (up to 39 % of mass)
400 °C	- Open flame combustion - Maximum production of combustible hydrocarbons - Calorific value about 18.84MJ/kg
500 °C	- Reduction of the gas production - Rise of the production of charcoal
700 °C	- Burn down of the charring residua
1100 °C	- Total destruction of the material - Remaining of non-combustible mineral residua of wood in the form of ash

2.5. Charring of Wood

2.5.1. Overview

Charring can be described as a process of a char layer forming on the burning surface of a timber member when exposed to high temperature. The charring process initiates when the the timber member heats up to a temperature of approximately 300^{o}C. Figure 2-3 illustrates the distinguished char, pyrolysis and residual timber layers when exposed to fire (White, 2008).

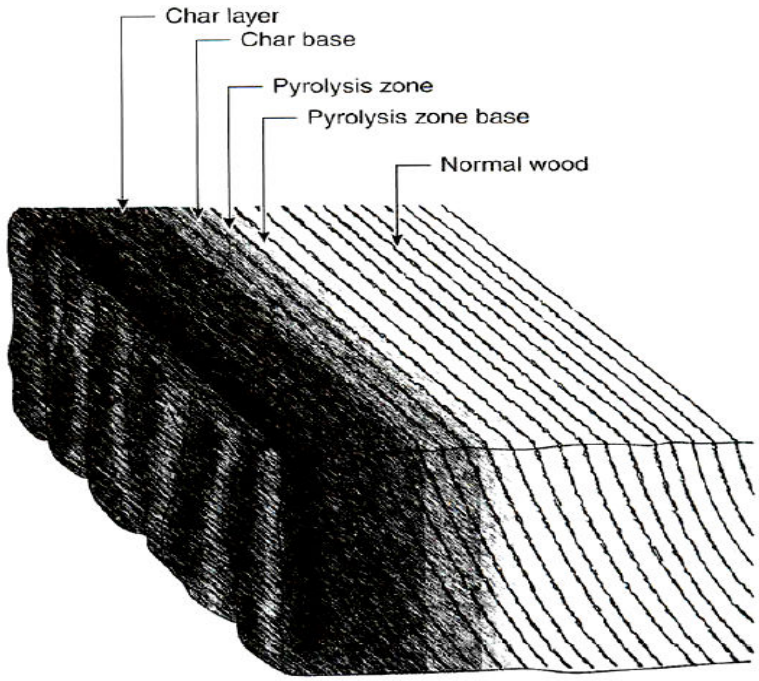

Figure 2-3: Degradation zones in a wood section (White, 2008)

Charring of timber members is divided into:

- One-dimensional charring as a physical property for a specific species, or timber of specific density or strength class.
- Two-dimensional charring, including the effects of cross-sectional dimensions and other effects.

2.5.2. One Dimensional Charring

One dimensional charring rate is the charring rate observed for one-dimensional heat transfer under standard fire exposure of an unprotected semi-infinite timber slab (European guideline, 2010). It is commonly known as the linear rate which tends to be relatively

constant after a higher initial char rate. As illustrated in Figure 2-4, the charring depth, d_c, is the absolute reduction of the wood cross-section at a point in time due to a fire. Since the charring depth is measured as a function of time, the charring rate, β, then can be calculated based on Equation 2-1 below.

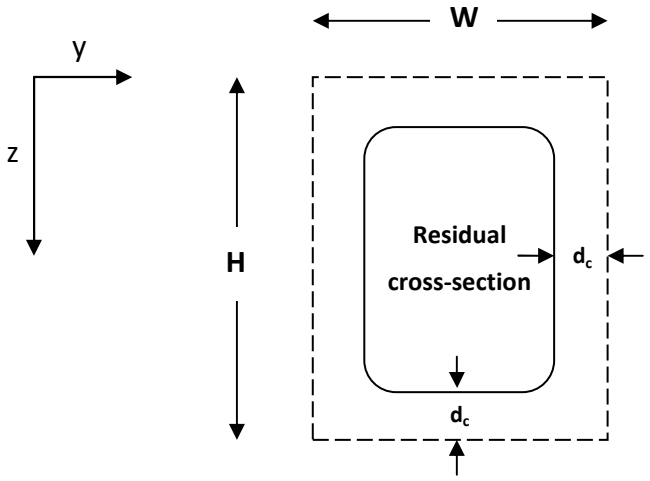

Figure 2-4: Charred cross-section of wood

$$\beta(t) = \frac{\Delta d_c}{\Delta t} \qquad \text{Equation 2-1}$$

Where: $\beta(t)$ = charring rate (mm/min)
d_c = charring depth (mm)
t = duration of fire (min)

2.5.3. Two-dimensional Charring

When a rectangular timber section is exposed to fire, corners of the timber section are subjected to heat transfer from two surfaces creating some rounding of the corners (Buchanan, 2002). At first, the arris rounding is about equal to the one-dimensional charring charring depth. However due to the eventual superposition of rounding of the two opposite opposite arrises, the charring depth on the narrow side of a rectangular cross section increases more than it does on the wide side. Figure 2-5 illustrates the effect of arris rounding.

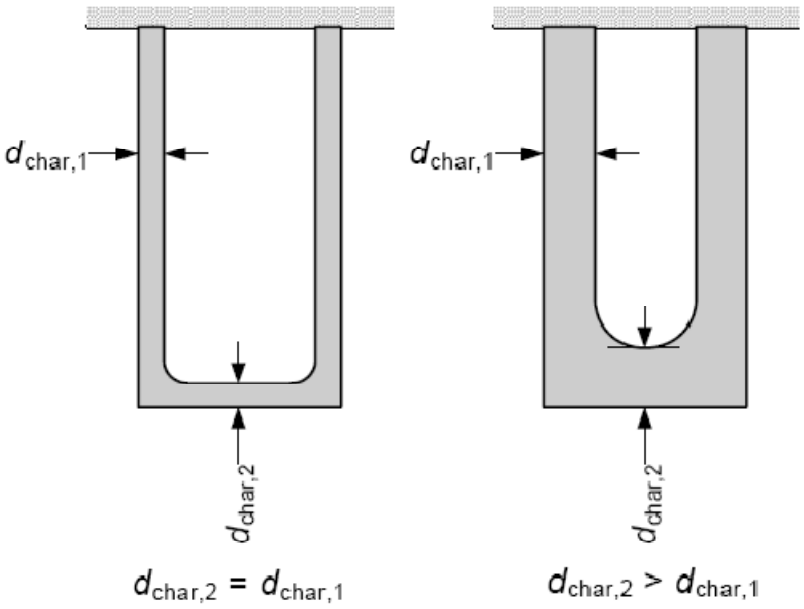

Figure 2-5: Effect of arris rounding on charring on the wide and narrow sides of cross-section (European guideline, 2010)

In the design process, the rounding may be ignored for large timber sections subject to a low fire rating as the effect of any additional loss on the section is small and its effect on the calculated section properties may be ignored (Purkiss, 1996). For small timber sections, however, allowance for charring around the corners must be considered.

For most design codes, the radius of the rounding is considered equal to the depth of the charred layer and the cross sectional area lost due to rounding has magnitude of $0.215r^2$. Refer to Figure 2-6 for details.

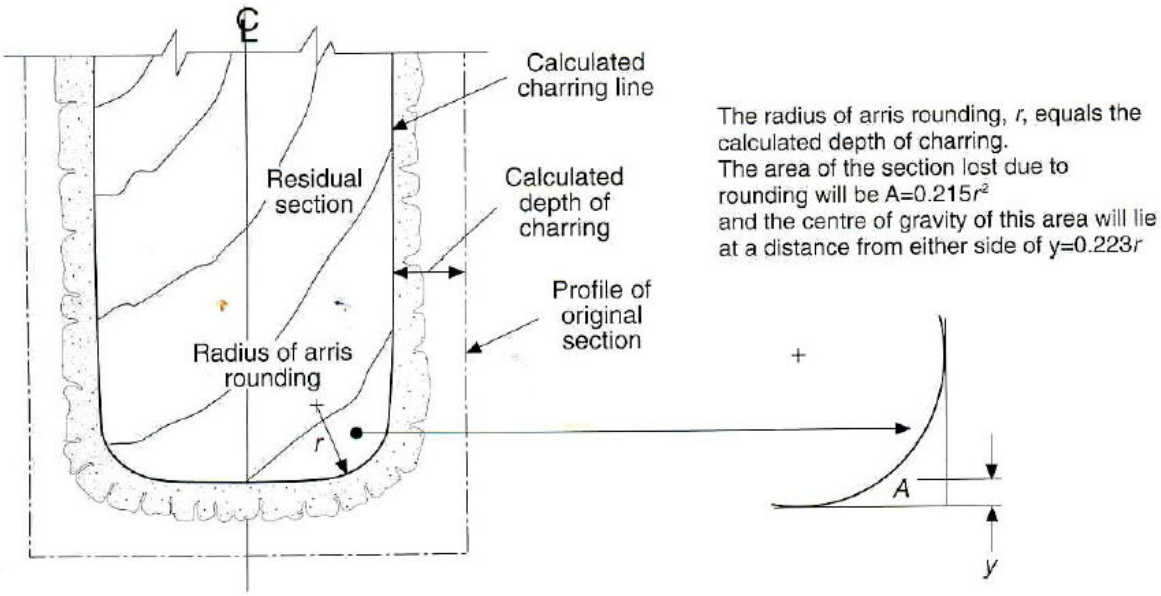

Figure 2-6: Residual cross section of timber beam exposed to fire (Buchanan, 2002)

2.5.4. Charring Depth Measurement Methods

As depicted in Figure 2-7, there are many different existing techniques to measure the charring depth of wood in a fire test. The main distinction is the time dependency of the measurements. The measurement of the charring depth is achieved either after the fire test test or during the fire test, which is normally done in a continuous way.

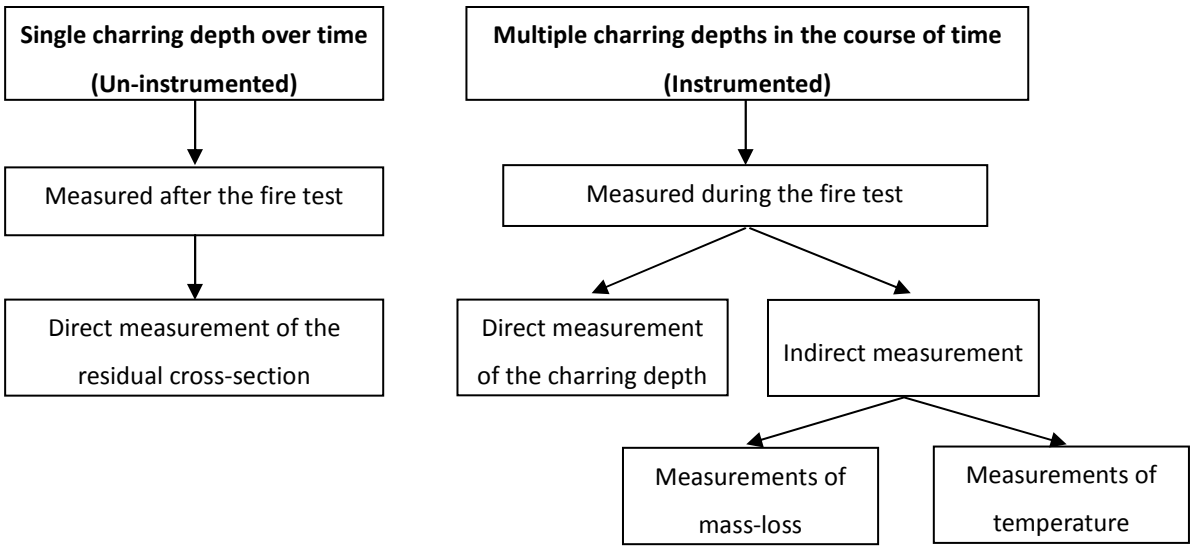

Figure 2-7: Measurement methods of the charring depth

2.5.5. Single Charring Depth Measurement

After a fire test, the charred layer of the specimen is physically removed. From the direct measurement of the residual cross-section, an average charring depth over the whole fire duration is then determined. Although this method provides the most accurate result it does not reveal any information on the course of charring during the fire.

2.5.6. Multiple Charring Depths Measurement

Multiple charring depth measurement involves continuously recording the charring depth of the specimen throughout the entire fire duration. This can be achieved by either a direct measurement of the location of the surface of healthy wood (location of the pyrolysis zone) or an indirect measurement. Auxiliary values are used for indirect measurements which can be accurately measured to derive the corresponding charring depth.

2.5.6.1. Continuous Direct Measurement of Charring Depth

The continuous direct measurement is based on the disparity of physical properties such as

the material strength, stiffness and density around the pyrolysis zone. This disparity is detected by using a mechanical probe which follows the course of the pyrolysis zone during the fire exposure. Knublauch and Rudolphi (1971), described by Bobacz (2006), used a drilling probe to measure the charring depth as shown in Figure 2-8. The drilling probe is rigidly connected to the wagon and is twisted slowly by the electric drilling engine. The movement of the wagon corresponds to the charring depth of the wood specimen.

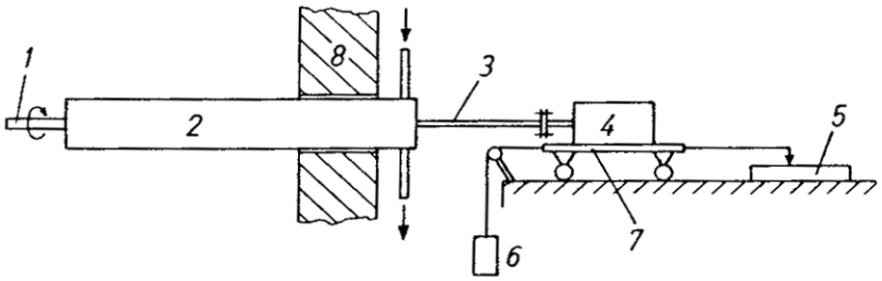

1	ceramic drill bit	5	displacement sensor
2	water-cooled probe guidance	6	pulling weight
3	probe	7	wagon
4	drilling engine	8	furnace wall

Figure 2-8: Drilling probe for continuous charring depth measurement (Knublauch and Rudolphi, 1971)

Bobacz (2006) used ceramic probes with tungsten spearheads as shown in Figure 2-9. These probes are inserted into the charred wood until they reach the pyrolysis zone where the disparity of density prevents a further penetration of the spearheads. The charring depth during the fire exposure can be measured by following the fire exposed surface of healthy wood.

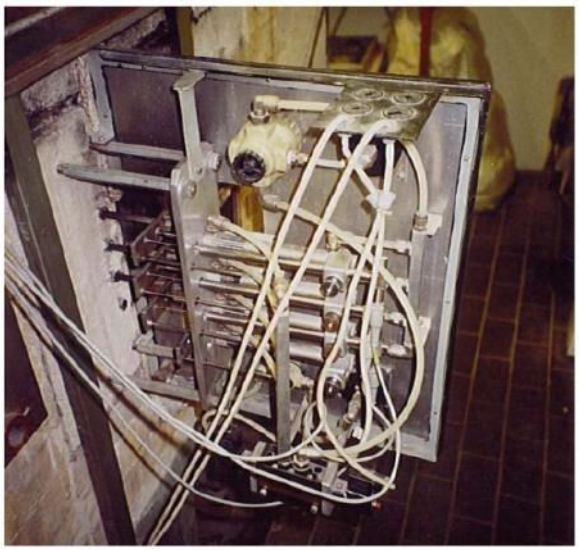

Figure 2-9: Configuration of pneumatic driven probes for continuous charring measurement (Bobacz, 2006)

2.5.6.2. Indirect Measurement based on Mass-Loss

The mass-loss of a wood specimen during a fire test can be measured directly by a weighting machine or derived by the oxygen consumption method. If the density of wood is known, the charring rate can then be calculated based on Equation 2-2 (Bobacz, 2006).

$$\beta = 6\frac{\dot{m}}{\rho \cdot A} \qquad \text{Equation 2-2}$$

Where: β = charring rate (mm/min)
$\dot{m}$ = mass loss rate (mg/s)
ρ = density (kg/m^3)
A = reference area (mm^2)

2.5.6.3. Indirect Measurement based on Temperatures

Based on the fact the temperature of the pyrolysis zone can be considered as constant, the corresponding temperature-isotherm can then describe the border of charring and its location of the charring depth. Thermocouples are buried at various depths of the cross-section which measure and record the temperature continuously during a fire test. Temperature distribution derived out of the gathered data can then indicate the border of charring based on the location of the pyrolysis temperature.

There are many previous papers which give different pyrolysis temperatures, i.e. temperature of the border of charring. They range generally between 250°C and 350°C which is shown in Table 2-2, summarised by Bobacz (2006).

Table 2-2: Summary of Pyrolysis temperature (Bobacz, 2006)

Wood Species	Pyrolysis Temp. (°C)	Source
Spruce	225	Dorn, Egner (1976)
Spruce	300	Klingsch (1993)
Spruce	300	König, Walleij (1999)
Spruce	300	Kordina and Meyer-ottens (1983)
Spruce	260	Lache (1992)
Spruce	350-360	Mikkola (1999)
Spruce	300	prEN 1995-1-2:2003 (2003)
Douglas fir, southern pine, white oak	288	Schaffer (1967)

2.5.7. Experimental Charring Rates

Table 2-3, presented by Bobacz (2006), lists the experimental charring rates of different wood species determined by various researchers. The charring rate of wood is primarily affected by its density and moisture content (Collier, 1992). A wood with high density as well as low moisture content will usually have a lower charring rate. Based on Table 2-3, charring rate of wood can range from 0.50mm/min to 1.02mm/min.

Table 2-3: Selected charring rate of wood under STC exposure (Bobacz, 2006)

Wood Species	Density (kg/m^3)	Moisture Content (%)	Charring Rate (mm/min)	Source
Spruce	430~530	12	0.66	Dorn, Egner (1976)
Spruce	462	12	0.55	Fornather (2000)
Spruce	456	12	0.66	Fornather (2001)
Spruce	470~480	12	0.6~0.7	König, Walleij (1999)
Spruce	433	8	0.71	Lache (1992)
Spruce	458	20	0.63	Lache (1992)
Spruce	490	10	0..56~1.02	Mikkola (1999)
Spruce	490	20	0.60	Mikkola (1999)
Beech	700	8	0.80	Lache (1992)
Beech	689	20	0.72	Lache (1992)
Softwood & beech	≥ 290	12	0.65	prEN 1995-1-2:2003 (2003)
Douglas fir	300~500	12	0.63~0.92	Schaffer (1967)
Hardwood	≥ 290	12	0.65	prEN 1995-1-2:2003 (2003)
Hardwood	≥ 450	12	0.50	prEN 1995-1-2:2003 (2003)
Oak	656	8	0.60	Lache (1992)
Oak	664	20	0.55	Lache (1992)
White oak	350~650	12	0.58~0.83	Schaffer (1967)
Oak	491	10~15	0.59	Topf, Röll (1971)
Pine	560	10	0.80	Mikkola (1999)
Pine (sapwood)	497	8	0.81	Lache (1992)
Pine (heartwood)	491	8	0.69	Lache (1992)
Southern pine	300~600	12	0.76~0.85	Schaffer (1967)

Collier (1992) carried out tests to verify the accepted charring rates of timber, both solid and glulam, at Building Research Association of New Zealand (BRANZ). He used White's Model (1988) for char prediction as the basis for his experimental programme. After several models models were evaluated this model was selected because it was relatively easy to apply and

was able to quantify a range of internal wood properties which influence charring rates. Overall results from his study showed that the current practice of assuming a charring rate of 0.6mm/min was found to be valid only for higher density timbers (density $\geq$ 600kg/m^3 with 12% moisture content). Selection of a charring rate based on the timber density would be more reliable especially for timber with lower densities. Therefore results of his study indicated that a revision of methods used to design timber structures for fire resistance was warranted.

Based on Collier's finding (1992) the New Zealand code NZS 3603 (1993) Clause 9.4.2 specifies:

> *The charring rate of radiate pine and other timber species of approximately the same density shall be taken as 0.65mm/min. The charring rate of species with significantly greater density may be established by test or by calculation in accordance with BRANZ Study Report No. 42, 1992.*

Lane (2005) investigated the charring rate for LVL members using a cone calorimeter and a pilot furnace. His overall findings showed that for New Zealand manufactured radiata pine LVL, the cumulative char rate of 0.72mm/min should be used, and was representative for fire exposure in both edge grain and face grain orientations. As for the end grain orientation, his results showed an end grain charring rate of 0.44mm/min. During the pilot furnace test, Lane (2005) also discovered that the charring rate occurring at the corner of the LVL section averaged 0.93mm/min due to double-sided fire exposure.

O'Neill (2009) tested two full scaled timber-concrete composite floors at BRANZ fire research facility. The first floor specimen was the smaller 300mm beam floor, which was tested to destruction (approximately 75 minutes); whereas the second specimen was the 400mm beam floor, where the test was terminated shortly after 60 minutes of fire exposure. Both timber beams were made of double LVL members with a cross-section of 126mm by joining two single 63mm LVL members with screwed connections. Figure 2-10 shows the specifications from the timber-concrete composite floor system.

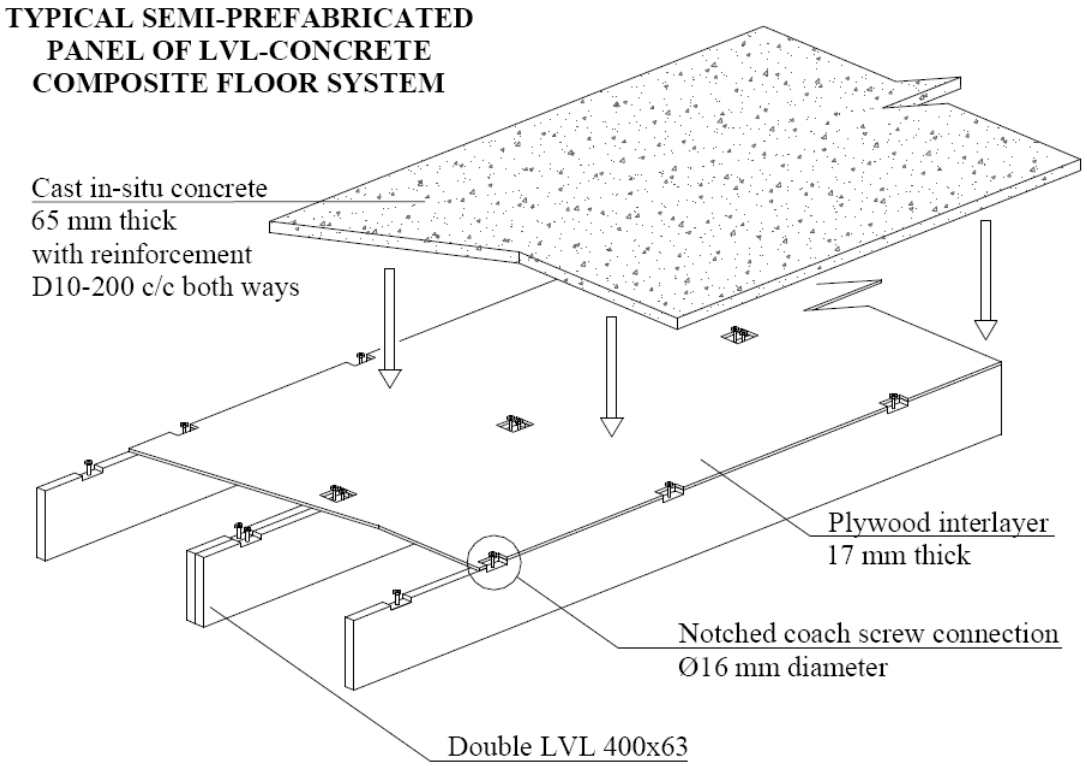

Figure 2-10: The composite floor under study (Yeoh, 2009)

After the fire tests, O'Neill (2009) calculated the average charring rates for each floor shown in Table 2-4.

Table 2-4: Calculated average charring rates for the tested floors (O'Neill, 2009)

Test Specimen	Side Charring Rate (mm/min)	Bottom Charring Rate (mm/min)	Overall Charring Rate (mm/min)
300 mm	0.55	2.27	1.12
400 mm	0.62	2.42	1.22
Both Floors Combined	0.58	2.35	1.17

A sketch of the both beams with initial and final cross-section sizes is shown in Figure 2-11.

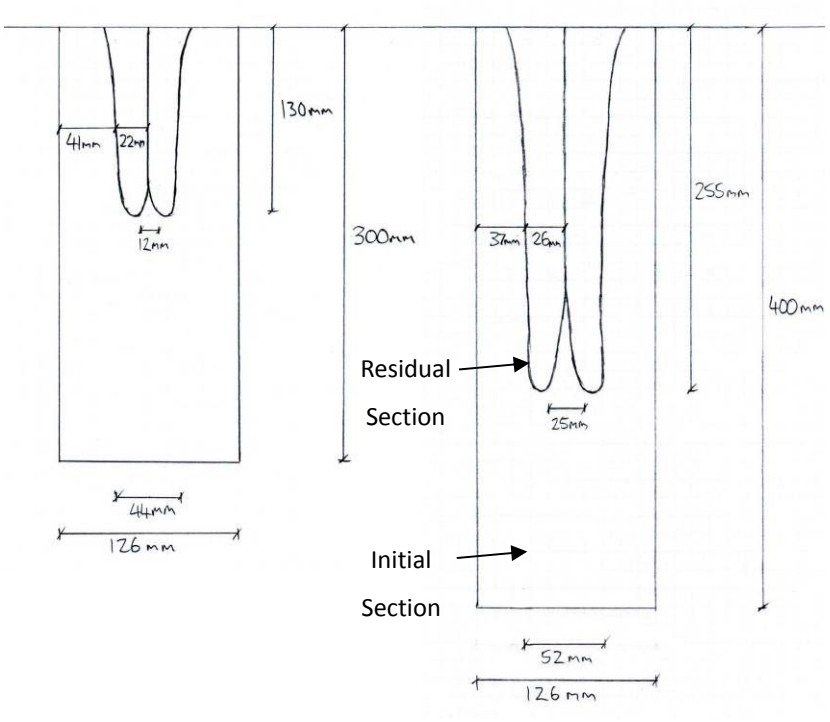

Figure 2-11: Sketches of the initial and residual remains of both beam cross sections after furnace testing (O'Neill, 2009)

O'Neill (2009) discovered in his full scale test that an average charring rate on the sides of the LVL beams was 0.58mm/min (Table 2-4). This was lower than reported values of 0.72mm/min described by Lane (2005) on similar New Zealand produced LVL at the BRANZ facilities. Such a difference was most likely due to the double-tee configuration of the floor beams such that convection of flames and hot gases throughout the space was slightly impeded, and the nearest beam was spaced away far enough that re-radiation off this surface was negligible.

Moreover, based on the results presented in Table 2-4, the charring rate on the underside of the beams was observed to be on average four times higher than the charring rate from either side of the beams. O'Neill (2009) suggested such phenomenon may be partly due to the uneven heating inside the furnace and the configuration of the beams in floor units. However the difference in side and bottom charring rates is much too significant to be attributed to these factors alone.

One of the major factors causing such a high charring rate on the underside of the beam may be due to the separation of the double beams after significant burning shown in Figure 1-2. This opening phenomenon was mainly caused by the uneven drying of the timber beams during the fire and the loss of integrity of the fixing around the fasteners holding the beams together. This opening behaviour could have induced extra charring on the insides of the beam sections and exposed the connections to further fire damage.

2.5.8. Analytical Modelling on Timber Charring

Fragiacomo et al (2009) performed analytical modelling on timber charring by using a finite element program known as Abaqus (2006). He compared his numerical results with the experimental results which were performed at both the University of Canterbury and BRANZ Fire Research facility in Wellington on 146x60, 300x105 and 360x133mm LVL members. His overall finding showed the simulated results from Abaqus predicted the temperature distribution of small cross-sections with acceptable approximation whereas the heating process of the larger cross-sections was predicted with a delayed temperature rise, particularly in the interior fibres.

2.5.9. Summary

In this literature review, it was determined that many experiments had been carried out in the past in determining the charring rate of wood. However the charring rates for the double LVL members joined by different connection types, such as nailed and screwed, have never been conducted. Traditionally a double LVL member is usually achieved by gluing two single LVL members together by using thermosetting adhesives such as resorcinol. Previous research showed that the adhesive performed well in fire and no separation of the double LVL members was observed. In this research, alternative connection methods, such as nails or screws, to join two single LVL members together were investigated. Their corresponding behaviour and charring rates were compared with the glue connected double LVL members.

It was also observed that little analytical analysis on the charring of the LVL member was conducted by using the SAFIR finite element program. Therefore in this research, experimental results were compared with the simulated results obtained from the SAFIR program. This will give us a better insight on how the SAFIR simulations compare with the test results.

3. SMALL FURNACE TESTS

This chapter describes experimental tests which were conducted by using the small furnace at the University of Canterbury.

3.1. Charring Depth Measurement for Small Furnace Tests

For small furnace tests, charring depths, which subsequently allow us to determine charring rates, were determined and compared by both un-instrumented and instrumented analysis. Charring depths determined by the un-instrumented analysis were derived from the un-charred LVL residual thickness measured after the char layer was physically removed at the end of the fire test. Meanwhile charring depths determined by the instrumented analysis were based on where the thermocouples located the 300^{o}C isotherm, which was taken as representing the char front within the samples, throughout the fire test.

3.2. Furnace System

The furnace system used at the University of Canterbury is shown in Figure 3-1.

Figure 3-1: Furnace system at the University of Canterbury

The furnace system is a 500mm long cylinder which has a square opening of 180mm by 180mm at each end. It was constructed from an outer stainless steel skin, with 100mm of Kaowool mineral insulation and a stainless steel inner skin. The furnace is powered by

electricity which heats up three spiral heating coils inside the furnace. The temperature of each heating coil was measured by using a thermocouple which was connected to the temperature control system. The temperature control system was monitored electronically by using a feedback loop method from the average temperature measured from the three coils. Due to limitations of the furnace, the maximum temperature the furnace could be used was 750^{o}C.

3.3. Specimen Details

3.3.1. Overview

Table 3-1 gives a brief summary of tests carried out in the small furnace.

Table 3-1: Test specification for the furnace system at the University of Canterbury

Exposure Time (min)	Single LVL (mm)	Double LVL (mm)							
		No Connection		Nailed Connection		Screwed Connection		Glued Connection	
	63	90	126	90	126	90	126	90	126
30	√	√	-	√	-	√	-	√	-
60	-	-	√	-	-	-	√	-	√

Due to the limitation of the LVL specimen size allowed in the small furnace, all specimens underwent either 30 minutes or 60 minutes fire exposure. Single LVL specimens with a cross-sectional width of 63mm went through a 30 minute fire exposure. As for the double LVL specimens, these with a cross-sectional width of 90mm underwent a 30 minute fire exposure whereas specimens with a cross-sectional width of 126mm underwent a 60 minute fire exposure.

Double LVL specimens with a cross-sectional width of 90mm and 126mm were constructed by joining two single LVL specimens together with a cross-sectional width of 45mm and 63mm, respectively. Due to the limitation of the opening size of the small furnace, all test specimens were 450mm long by 125mm deep. Figure 3-2 shows schematic views of the side and front elevations of the specimens in the small furnace.

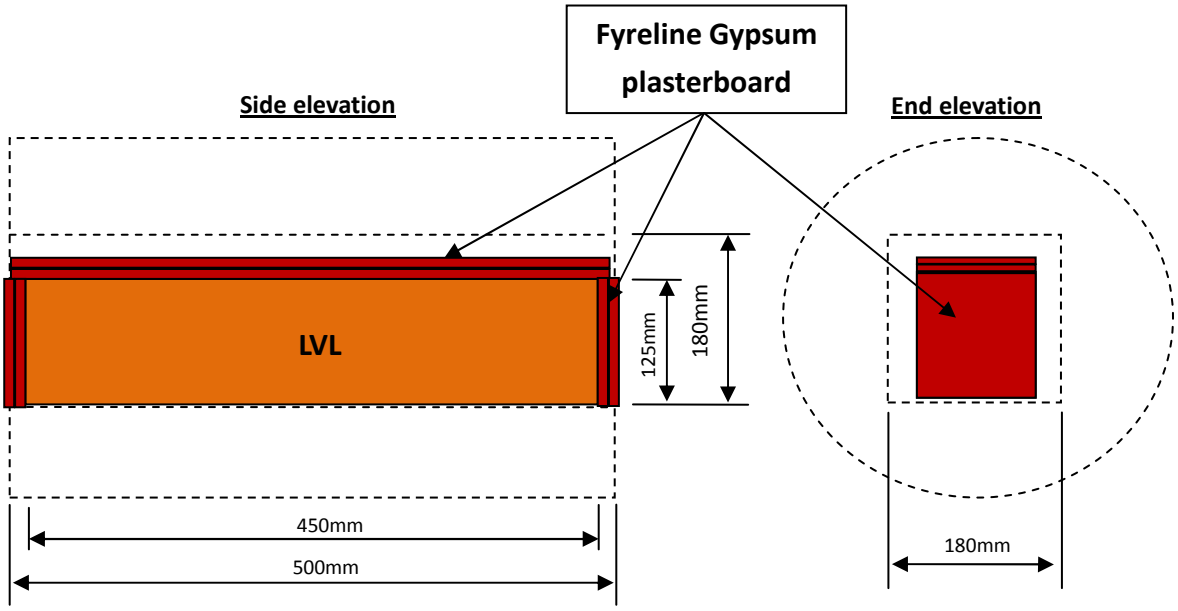

Figure 3-2: Schematic side and front views of the specimens in the small furnace (NOT TO SCALE)

Top and end surfaces of the LVL specimen were insulated by the Fyreline gypsum plasterboard. This was to simulate the three-faced (two sides and bottom) fire exposure of the timber-concrete composite floor as shown in Figure 1-1.

Figure 3-3 show pictures of a typical constructed LVL specimen where the specimen was insulated by the Fyreline gypsum plasterboard on both the top and end surfaces.

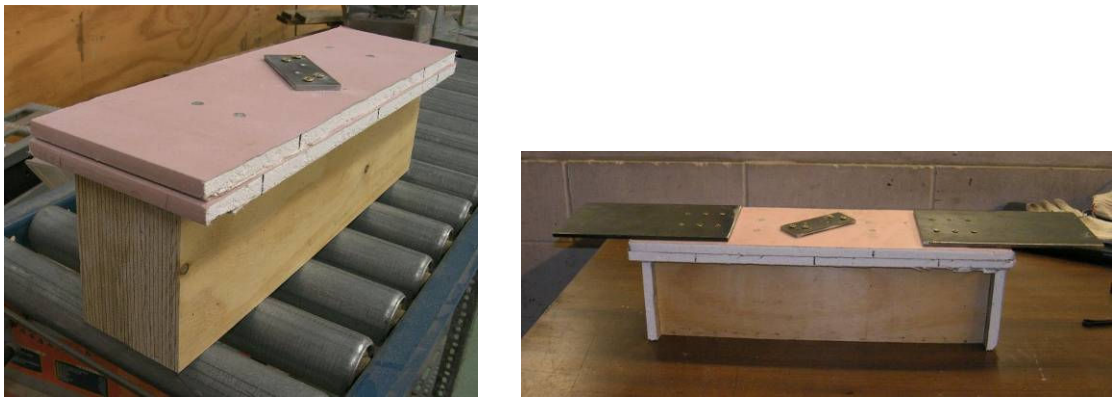

Figure 3-3: Constructed 90mm width double LVL specimen

As shown in Figure 3-3, one small 5mm thick metal bracing was screwed centrally on top of the LVL specimen. This small bracing was for double LVL specimen only which served to prevent any undesired separation of the double LVL sample before fire testing. Meanwhile two metal plates were screwed on top of the plasterboard so that they could extend out of the furnace and be supported by a steel leg at each end of the furnace. This allowed the specimen to be suspended inside the furnace. Figure 3-4 shows a picture of the extended metal plate and the supporting steel leg on one side of the furnace.

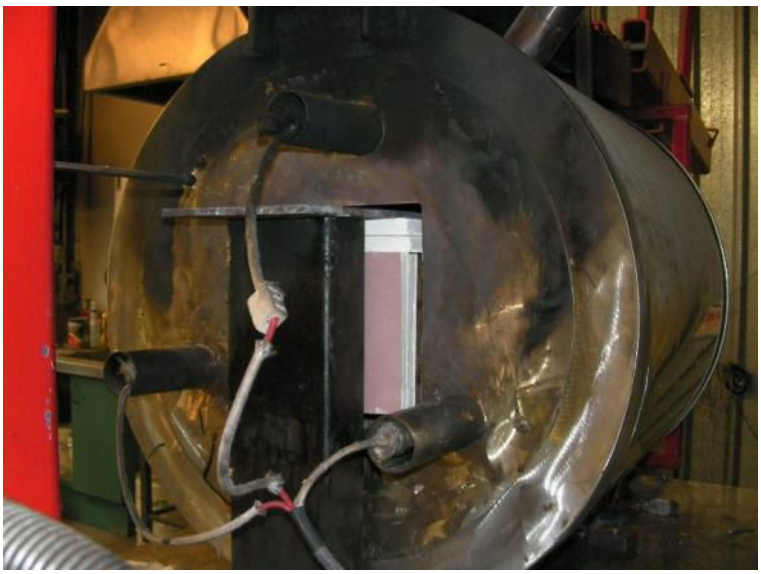

Figure 3-4: Suspending the testing specimen inside the furnace

The baseline model for the double LVL specimen was without any connection holding the two single LVL members together. This was to examine if the double LVL specimen would induce more separation in the joint when there was no fastener holding the two single LVL members together. Meanwhile three different connection systems, nail, screw and glue, were examined for the double LVL specimens, which are discussed in more detail in Section 3.3.2 to Section 3.3.4 below.

3.3.2. Double LVL Specimen with Nailed Connection

An example of nails used for the small furnace test is shown in Figure 3-5. It was the Paslode nail used for the automatic nail gun, which had a length of 90mm and a shank diameter of 3mm. This nail was tested because it was commonly used in construction.

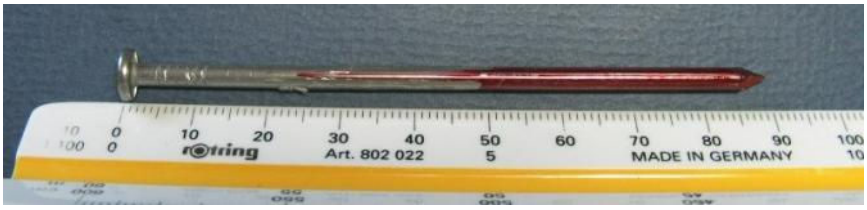

Figure 3-5: Paslode nail used for the small furnace test

This nail was only tested for the 90mm width double LVL specimen for the initial test. This was to see if the nailed connection would perform well in fire due to the fact that nail generally had poor fire performance.

Figure 3-6 shows the location of the nail in the specimen. The nail was installed at the centre of the testing specimen.

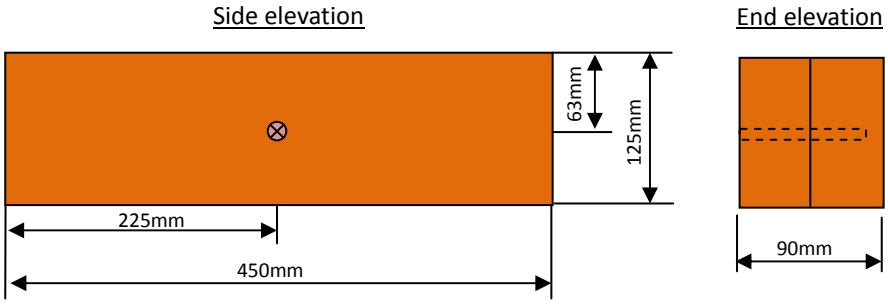

Figure 3-6: Nail layout for the small furnace test (NOT TO SCALE)

3.3.3. Double LVL Specimen with Screwed Connection

Screws used to connect the double 90mm or 126mm LVL specimens were the typical number 8 screw or number 10 screw shown in Figure 3-7. The number 8 screw was 75mm long with a shank diameter of 5mm whereas the number 10 screw was 100mm long with a shank diameter of 5mm as well.

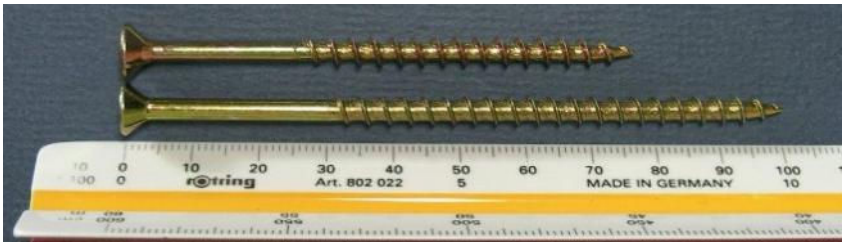

Figure 3-7: Number 8 and number 10 screws used for the small furnace test

Two different screw layouts were examined for the 90mm cross section LVL only. This was to to examine if an increase in the numbers of connections would affect the overall charring rate. Figure 3-8 shows schematic drawings for these different connection layouts.

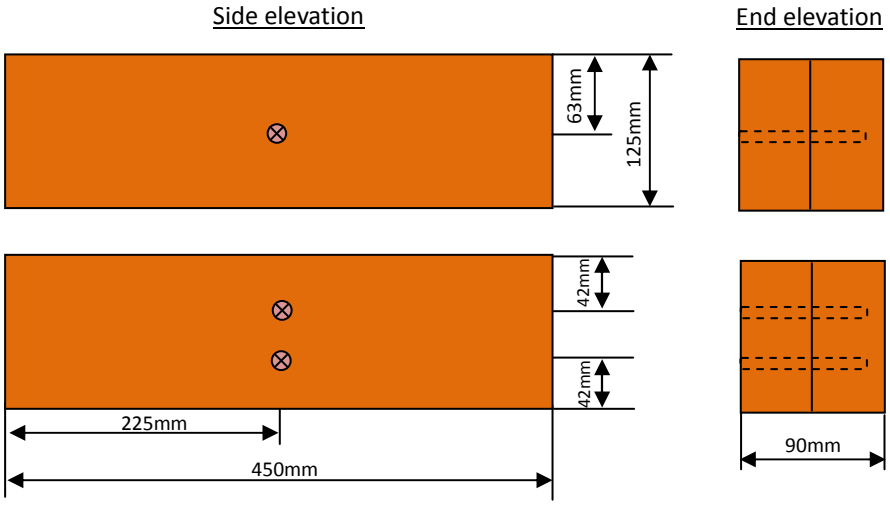

Figure 3-8: Screw layout for the small furnace test (NOT TO SCALE)

3.3.4. Double LVL Specimen with Glued Connection

The glue used to join two single LVL members together was the resorcinol adhesive of the same type used by Lane (2005). His experimental results showed that resorcinol performed well in fire and provided excellent fire resistance.

Glued LVL specimens were left to cure for at least 24 hours before being tested. Figure 3-9 shows a picture of a glued LVL specimen.

Figure 3-9: Glued double LVL specimen

3.3.5. Thermocouple Layouts

The charring rates determined from the un-instrumented tests were compared to the instrumented tests performed on the sample sized LVL specimens. Thermocouples were installed at the various depths of the LVL specimen located at the mid-span. The numbers of thermocouples installed were based on the residual charred width and depth determined from the un-instrumented tests.

The thermocouple layouts for the 63mm width single LVL specimen is shown in Figure 3-10.

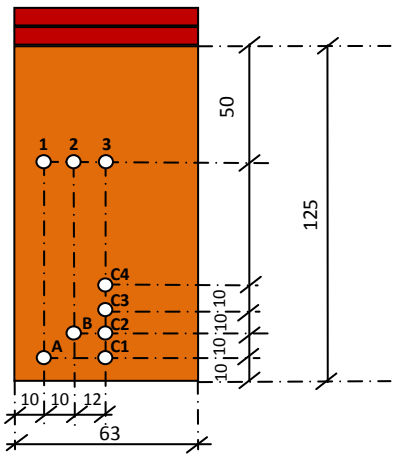

Figure 3-10: Thermocouple layouts for the 63mm width single LVL specimens (NOT TO SCALE)

The thermocouple layouts for the 90mm and 126mm width double LVL specimen are shown

in Figure 3-11 and Figure 3-12. Two thermocouple layouts were applied. One layout was for the glued connection whereas the other layout was for the other connections, which included no fastener, nailed and screwed. The main difference between these two thermocouple layouts was the additional central thermocouple located near the centre of the cross-section. This thermocouple was intended to measure the wood temperature around the nailed or screwed connection located at the mid-span.

The thermocouples at the corners were exposed to the fire on two faces, whereas all other thermocouples had single face exposure.

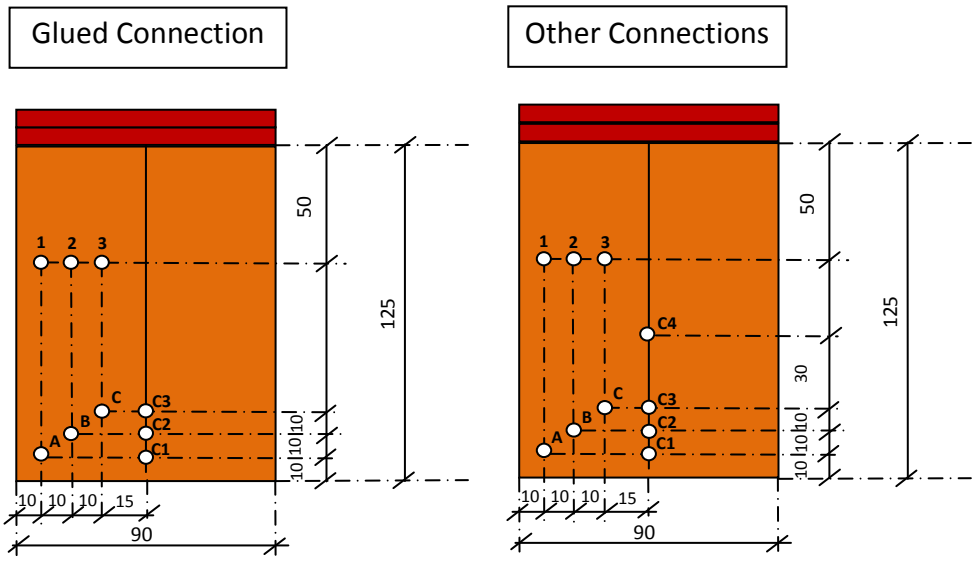

Figure 3-11: Thermocouple layouts for the 90mm width double LVL specimens (NOT TO SCALE)

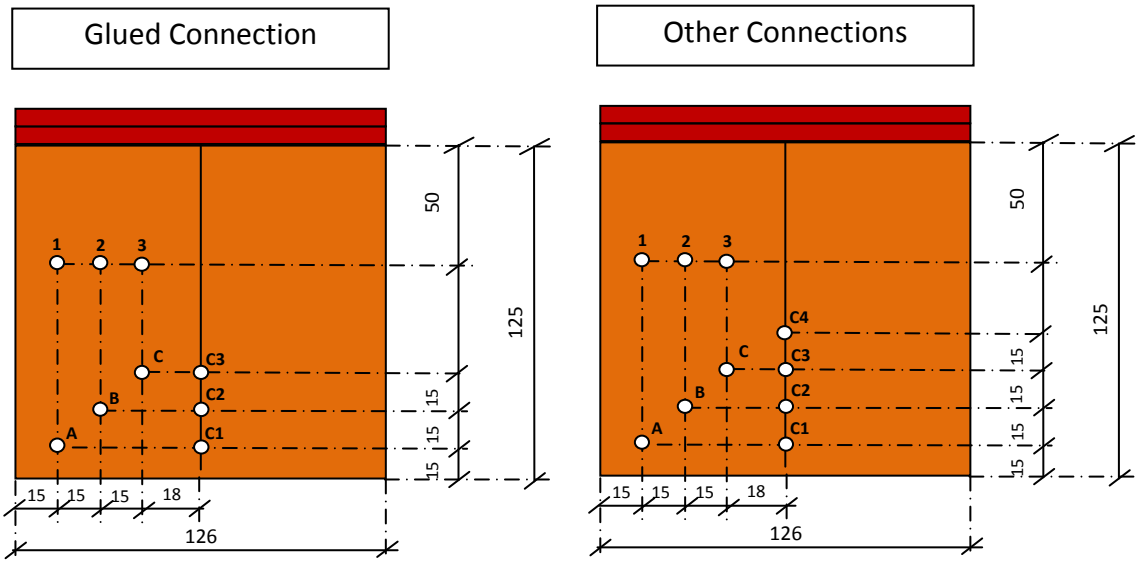

Figure 3-12: Thermocouple layouts for the 126mm width double LVL specimens (NOT TO SCALE)

Once the sections were instrumented, the two sections of LVL were then glued back together using resorcinol adhesive and cured for at least 24 hours. The thermocouple wires were then then led out of the furnace and connected to the electronic data recorder (Figure 3-13).

Figure 3-13: Connecting thermocouples to the electronic data recorder

3.4. Small Furnace Tests Results and Discussions

3.4.1. Un-instrumented Tests Results and Discussions

For un-instrumented tests, the char layer was physically removed and the un-charred LVL residual thickness was measured at the end of each fire test. Refer to Appendix A to Appendix C for comparative pictures between the initial and the residual cross-section of the LVL specimen.

3.4.1.1. 63mm Width Single LVL Specimens

The un-instrumented test results for the 63mm width single LVL specimen are shown in Table 3-2. Two identical specimens were tested and compared.

Table 3-2: Un-instrumented test result for 63mm width single LVL specimen

Single LVL Specimen: 63mm Wide x 125mm Deep x 450mm Long **Fire Duration:** 30 minutes				
Sample No.	**Residual Width (mm)**	**Residual Depth (mm)**	**Avg. Side Charring Rate (mm/min)**	**Avg. Bottom Charring Rate (mm/min)**
1	17	93	0.77	1.07
2	18	94	0.75	1.03
Average			**0.76**	**1.05**

Test results in Table 3-2 showed that both 63mm width specimens produced almost identical results. It was also observed that the average bottom charring rate was approximately 0.3mm/min higher than the average side charring rate. Theoretically, if both side and bottom faces experienced one dimensional charring throughout the entire fire exposure, both charring rates should be identical. However the test results showed that the bottom charring rate accelerated at some stage, which was when the rounding of two opposite arrises superimposed on each other, causing a change from one-dimensional charring to two-dimensional charring. As a result, the bottom charring rate was slightly higher than the side charring rate. Since the test only lasted for 30 minutes, the acceleration of the bottom charring rate was not distinctive. However if the test went longer than 30 minutes, the average bottom charring rate may increase even more.

3.4.1.2. 90mm Width Double LVL Specimens

The un-instrumented test results for the 90mm width double LVL specimen are shown in

Table 3-3. Likewise, each connection type was duplicated and tested to compare results.

Table 3-3: Un-instrumented test results for 90mm width double LVL specimens

Double LVL Specimen:		**90mm Wide x 125mm Deep x 450mm Long**				
Fire Duration:		**30 minutes**				
Sample No.	**Connection Type**	**Residual Width**	**Residual Depth**	**Avg. Side Charring Rate**	**Avg. Bottom Charring Rate**	**Separation Distance (tip to tip)**
		(mm)	**(mm)**	**(mm/min)**	**(mm/min)**	**(mm)**
1	Nil	48	95	0.70	1.00	45
2	Nil	48	95	0.70	1.00	45
Average				**0.70**	**1.00**	**45**
3	Nailed	45	95	0.75	1.00	35
4	Nailed	48	95	0.70	1.00	35
Average				**0.73**	**1.00**	**35**
5	Screwed	48	100	0.70	0.83	30
6	Screwed	48	100	0.70	0.83	25
Average				**0.70**	**0.83**	**28**
7	Glued	47	105	0.72	0.67	0
8	Glued	47	105	0.72	0.67	0
Average				**0.72**	**0.67**	**0**
9	2 screws	47	100	0.72	0.83	25

It was also observed that test results in Table 3-3 showed each set of connection type produced almost identical results. Meanwhile the average side charring rate for all connection types was approximately the same, ranging from 0.70mm/min to 0.75mm/min. However it was noticed that the bottom charring rate for the no connection type was the highest whereas the glued connection type was the lowest. This phenomenon may be due to the opening phenomenon of the double LVL specimen during the fire test (refer to Appendix B for pictures). This opening phenomenon occurred due to the moisture gradient across the width of the LVL specimen during fire exposure. As a result, the face which was exposed to fire started to shrink causing the LVL to distort outwardly. Consequently, this opening behaviour induced extra charring on the insides of the LVL sections causing a rise in the bottom charring rate. The separation distance shown in Table 3-3 indicated that the no connection type had the highest separation distance followed by nailed and screwed connection types, which corresponded well to the average bottom charring rate.

Meanwhile it was also observed that the bottom charring rates between no connection and

nailed connection were almost identical. This shows the poor fire behaviour of the nailed connection. Due to the slippage effect, the nail could not provide sufficient withdrawal resistance to hold the double LVL together once they began to open up. Unlike the screwed connection, however, due to the threaded effect of the screw bridging across the double LVL specimen, the screw was able to hold the double LVL much more securely when they were trying to separate.

The comparative results between the one screw and two screws connection type also showed similar results. This may due to the fact that the depth our LVL specimen was only 125mm deep and hence it was too excessive or conservative to introduce an additional screw. Therefore it was decided to only test one screwed connection type for the 126mm width double LVL specimens.

Lastly, it was also seen that the side and bottom charring rates for the glued double joined LVL were almost identical. This shows that the bottom face was experiencing one dimensional charring in the entire 30 minutes fire exposure.

3.4.1.3. 126mm Width Double LVL Specimens

The un-instrumented test results for the 126mm width single LVL specimen are shown in Table 3-4. Similarly, each connection type was duplicated and tested to compare results.

Table 3-4: Un-instrumented test results for 126mm width double LVL specimens

Double LVL Specimen: 126mm Wide x 125mm Deep x 450mm Long **Fire Duration:** 60 minutes						
Sample No.	**Connection Type**	**Residual Width**	**Residual Depth**	**Avg. Side Charring Rate**	**Avg. Bottom Charring Rate**	**Separation Distance (tip to tip)**
		(mm)	**(mm)**	**(mm/min)**	**(mm/min)**	**(mm)**
1	Nil	46	67	0.67	0.97	30
2	Nil	51	67	0.63	0.97	30
Average				**0.65**	**0.97**	**30**
3	Screwed	49	80	0.64	0.75	10
4	Screwed	47	78	0.66	0.78	5
Average				**0.65**	**0.77**	**8**
5	Glued	47	90	0.66	0.58	0
6	Glued	50	92	0.63	0.55	0
Average				**0.62**	**0.57**	**0**

Similarly, test results in Table 3-4 also show that each set of connection type produced approximately identical results. Meanwhile the average side charring rate for all connection connection types was very similar, ranging from 0.63mm/min to 0.67mm/min. This averaging side charring rate was observed to be slower than the averaging side charring rate for the 90mm width double LVL specimen, which ranged from 0.70mm/min to 0.75mm/min. This difference could be explained by the fact that the 126mm width LVL specimen experienced a 60 minute fire exposure whereas the 90mm width LVL specimen experienced only a 30 minute fire exposure. It is known that the initial burning of wood is generally higher due to the fact that the wood is not initially insulated by the char layer. As the char layer slowly forms, the initial charring rate decreases to a slower steady rate which continues throughout the fire exposure (Buchanan, 2002).

Meanwhile the average bottom charring rate for the 126mm LVL specimens were observed to be similar to the 90mm width LVL specimen, where the no connection type had the highest bottom charring rate whereas the glued connection type had the lowest. However it was noticed the separation distance for the 126mm width LVL specimens was smaller than the 90mm width LVL specimens. This may be due to the fact that the 90mm width LVL specimens were much more slender in comparison with the 126mm width LVL specimens. As a result the 90mm width LVL specimens distorted much more significantly than the 126mm width LVL specimens during the fire test.

Test results from Table 3-4 also show the side and bottom charring rate for the glued double LVL were similar. Again this shows that the bottom face was only experiencing one dimensional charring even though the wood underwent 60 minutes fire exposure. This shows that an increase in the width of the specimen, which causes a decrease in the slenderness ratio, would further delay the time for the two opposite arrises to superimpose on each other.

3.4.2. Instrumented Tests Results and Discussions

3.4.2.1. 63mm Width Single LVL Specimen

Table 3-5 below summarises the instrumented charring rates for the 63mm width single LVL specimen. The time for each thermocouple to reach 300°C was extracted from the thermocouple readings recorded in the Excel spreadsheet. Refer to Appendix D for the thermocouple readings of the 63mm width single LVL specimen.

Table 3-5: Instrumented charring rates for the 63mm width single LVL specimen

	Side			Corner		Bottom			
Thermocouples	**1**	**2**	**3**	**A**	**B**	**C1**	**C2**	**C3**	**C4**
Depth (mm)	10	20	32	14	28	10	20	30	40
Time to 300°C (min)	13	25	-	9	19	11	22	30	-
Charring Rate, β, (mm/min)	0.80	0.80	-	1.57	1.52	0.92	0.93	1.00	-
Average β (mm/min)	**0.80**			**1.54**		**0.97**			

Test results in Table 3-5 shows that charring rates for thermocouple 1 and 2 corresponded well with thermocouple C1 and C2. Meanwhile it is also observed that the charring rate for thermocouple C3 was higher. These results show that during the 30 minutes fire exposure thermocouple C1 and C2 were experiencing one dimensional charring. However thermocouple C3 was beginning to experience two dimensional charring, which was supported by an exponential increase in the temperature reading towards the end of the fire test as shown in Figure D-1 in Appendix D. Moreover test results in Table 3-5 also show that both thermocouple A and B had a charring rate of 1.57 and 1.52 mm/min respectively, which were higher than the other thermocouples. This was expected due to the fact that they were located at the corner where two dimensional charring were occurring.

Table 3-6 below shows the comparative average side and bottom charring rates between the un-instrumented and the instrumented test results for the 63mm width single LVL specimen.

Table 3-6: Comparative un-instrumented and instrumented test results for 63mm width single LVL specimen

	Average Side β (mm/min)	**Average Bottom β (mm/min)**
Un-instrumented Test	0.76	1.05
Instrumented Test	0.80	0.97
Difference	5%	7%

Comparative test results shown in Table 3-6 suggest both the un-instrumented and instrumented test corresponded quite well. The difference between the un-instrumented test and the instrumented test were only 5% and 7% respectively. A difference in measurement may due to uncertainties such as thermocouple installation or the assumption that the 300^{o}C isotherm was taken as representing the char front within the samples.

3.4.2.2. 90mm Width Double LVL Specimens

Table 3-7 summarises the instrumented charring rates for the 90mm width double LVL specimens. Similarly, the time for each thermocouple to reach 300^{o}C was extracted from the the thermocouple readings recorded in the Excel spreadsheet. Refer to Appendix E and Appendix F for the thermocouple readings of the 90mm width double LVL specimen.

Test results in Table 3-7 show the comparative average side and corner charring rates between all connection types were relatively close, ranging from 0.71 to 0.84mm/min and 1.28 to 1.45mm/min, respectively.

It was also observed that the double LVL specimen with no connection had the highest average bottom charring rate whereas the glued connected double LVL specimen had the lowest. This result was expected due to the fact that the no connection double LVL specimen specimen had the highest separation distance based on the un-instrumented test results previously. Due to this separation phenomenon, the heat was able to travel into the mid-mid-span of the double LVL specimen causing a sudden increase in the bottom charring rate. This was supported by comparative temperature graphs shown in Figure F-7 to Figure F-9 in Appendix F, where an exponential temperature increase in thermocouples C1 to C3 for no connection, nail connected and screw connected doubled LVL specimens were observed.

However as for the glued connected doubled LVL specimen, it was observed both the side and bottom average charring rates were similar. This suggests the bottom surface was still experiencing one dimensional charring during the 30 minutes fire exposure. Temperature graphs shown in Figure F-7 to Figure F-9 in Appendix F also indicate a steady temperature increase in thermocouples C1 to C3 for the glued connected LVL specimen.

Table 3-7: Instrumented charring rates for the 90mm width double LVL specimens

	No Connection									
	Side			Corner			Bottom			
Thermocouples	**1**	**2**	**3**	**A**	**B**	**C**	**C1**	**C2**	**C3**	**C4**
Depth (mm)	10	20	30	14	28	42	10	20	30	60
Time to 300°C (min)	11	28	-	11	22	-	12	18	27	-
Charring Rate, β, (mm/min)	0.9	0.72	-	1.25	1.32	-	0.86	1.1	1.1	-
Average β (mm/min)	**0.81**			**1.28**			**1.02**			

	Nailed Connection									
	Side			Corner			Bottom			
Thermocouples	**1**	**2**	**3**	**A**	**B**	**C**	**C1**	**C2**	**C3**	**C4**
Depth (mm)	10	20	30	14	28	42	10	20	30	60
Time to 300°C (min)	14	22	-	10	23	-	12	19	29	-
Charring Rate, β, (mm/min)	0.71	0.92	-	1.38	1.21	-	0.87	1.03	1.03	-
Average β (mm/min)	**0.81**			**1.29**			**0.98**			

	Screwed Connection									
	Side			Corner			Bottom			
Thermocouples	**1**	**2**	**3**	**A**	**B**	**C**	**C1**	**C2**	**C3**	**C4**
Depth (mm)	10	20	30	14	28	42	10	20	30	60
Time to 300°C (min)	12	24	-	10	20	-	12	21	29	-
Charring Rate, β, (mm/min)	0.84	0.84	-	1.42	1.42	-	0.82	0.95	1.03	-
Average β (mm/min)	**0.84**			**1.42**			**0.93**			

	Glued Connection								
	Side			Corner			Bottom		
Thermocouples	**1**	**2**	**3**	**A**	**B**	**C**	**C1**	**C2**	**C3**
Depth (mm)	10	20	30	14	28	42	10	20	30
Time to 300°C (min)	14	29	-	10	19	-	14	-	-
Charring Rate, β, (mm/min)	0.74	0.69	-	1.41	1.49	-	0.7	-	-
Average β (mm/min)	**0.71**			**1.45**			**0.70**		

Table 3-8 below shows the comparative average side and bottom charring rates between the un-instrumented and the instrumented test results for 90mm width double LVL specimens.

Table 3-8: Comparative un-instrumented and instrumented test results for 90mm width double LVL specimens

Connection Type	Average Side Charring Rate (mm/min)			Average Bottom Charring Rate (mm/min)		
	Un-instrumented	Instrumented	Diff.	Un-instrumented	Instrumented	Diff.
Nil	0.70	0.81	14%	1.00	1.02	2%
Nailed	0.73	0.81	10%	1.00	0.98	2%
Screwed	0.70	0.84	17%	0.83	0.93	11%
Glued	0.72	0.71	2%	0.67	0.70	4%

Comparative test results shown in Table 3-8 suggest both the un-instrumented and instrumented test corresponded relatively well. The highest difference between the un-un-instrumented test and the instrumented test was 17%. Again, a difference in measurement is expected due to experimental uncertainties or the assumption of the 300^{o}C isotherm.

3.4.2.3. 126mm Width Double LVL Specimens

The summary of the instrumented test results for 126mm double LVL specimens is shown in Table 3-9. In the same way, the time for each thermocouple to reach 300^{o}C was extracted from the thermocouple readings recorded in the Excel spreadsheet. Refer to Appendix G and and Appendix H for the thermocouple readings of the 126mm width double LVL specimen.

Table 3-9 shows that the comparative average side and corner charring rates between all connection types were approximately the same, ranging from 0.64 to 0.69mm/min and 1.36 to 1.39mm/min, respectively. These ranges were observed to be smaller in comparison with with the 90mm width double LVL specimen test results. As discussed previously, this was due to the fact the 126mm width LVL specimens experienced a 60 minute fire exposure whereas the 90mm width LVL specimens experienced only a 30 minute fire exposure. The initial burning of wood is generally higher due to the fact that the wood is not initially insulated by the char layer. As the char layer slowly forms, the initial charring rate decreases decreases to a slower steady rate which continues throughout the fire exposure.

It was also observed that the double LVL specimen with no connection had the highest average bottom charring rate whereas the glued connected double LVL specimen had the lowest. Again this was due to the separation phenomenon causing the heat to travel into the the mid-span of the double LVL specimen causing a sudden increase in the bottom charring rate. This was supported by comparative temperature graphs shown in Figure H-7 to Figure

H-9 in Appendix H, where an exponential temperature increase in thermocouples C1 to C3 for no connection and screw connected doubled LVL specimens were also observed.

Meanwhile it was also noticed both the side and bottom average charring rates were approximately the same for the glued connected doubled LVL specimen. This suggests the bottom surface was still experiencing one dimensional charring during the 60 minute fire exposure. Temperature graphs shown in Figure H-7 to Figure H-9 in Appendix H also indicate a steady temperature increase in thermocouples C1 to C3 for the glued connected LVL specimen.

Table 3-9: Instrumented charring rates for the 126mm width double LVL specimens

	No Connection									
	Side			Corner			Bottom			
Thermocouples	**1**	**2**	**3**	**A**	**B**	**C**	**C1**	**C2**	**C3**	**C4**
Depth (mm)	15	30	45	21	42	64	15	30	45	60
Time to 300°C (min)	21	45	-	12	34	54	15	29	44	58
Charring Rate, β, (mm/min)	0.72	0.67	-	1.76	1.23	1.19	1.03	1.04	1.03	1.04
Average β (mm/min)	**0.69**			**1.39**			**1.03**			

	Screwed Connection									
	Side			Corner			Bottom			
Thermocouples	**1**	**2**	**3**	**A**	**B**	**C**	**C1**	**C2**	**C3**	**C4**
Depth (mm)	15	30	45	21	42	64	15	30	45	60
Time to 300°C (min)	20	48	-	13	34	52	13	34	54	-
Charring Rate, β, (mm/min)	0.76	0.63	-	1.64	1.24	1.21	1.14	0.88	0.84	-
Average β (mm/min)	**0.69**			**1.36**			**0.95**			

	Glued Connection								
	Side			Corner			Bottom		
Thermocouples	**1**	**2**	**3**	**A**	**B**	**C**	**C1**	**C2**	**C3**
Depth (mm)	15	30	45	21	42	64	15	30	45
Time to 300°C (min)	21	53	-	13	38	-	22	56	-
Charring Rate, β, (mm/min)	0.71	0.57	-	1.69	1.10	-	0.69	0.53	-
Average β (mm/min)	**0.64**			**1.40**			**0.61**		

The comparative average side and bottom charring rates between the un-instrumented and the instrumented test results for 126mm width double LVL specimens are shown in Table 3-10 below.

Table 3-10: Comparative un-instrumented and instrumented test results for 126mm width double LVL specimens

Connection Type	Average Side Charring Rate (mm/min)			Average Bottom Charring Rate (mm/min)		
	Un-instrumented	Instrumented	Diff.	Un-instrumented	Instrumented	Diff.
Nil	0.65	0.69	6%	0.97	1.03	6%
Screwed	0.65	0.69	6%	0.77	0.95	19%
Glued	0.62	0.64	3%	0.57	0.61	7%

Table 3-10 shows both the un-instrumented and instrumented test results corresponded relatively well. The highest different between the un-instrumented test and the instrumented test was 19%. Again, a difference in measurement is expected due to experimental uncertainties or the assumption of the 300^{o}C isotherm.

3.5. Summary

Table 3-11 and Table 3-12 summarise the un-instrumented and instrumented charring rates results from small furnace tests.

Table 3-11: Summary of the un-instrumented tests results from the small furnace testing

UN-INSTRUMENTED TESTS Specimen Dimension: 125mm Deep x 450mm Long				
Width (mm)	**Fire Duration (min)**	**Connection Type**	**Avg. Side β (mm/min)**	**Avg. Bottom β (mm/min)**
63	30	NA	0.76	1.05
90		Nil	0.70	1.00
		Nailed	0.73	1.00
		1 Screw	0.70	0.83
		2 Screws	0.72	0.83
		Glued	0.72	0.83
Average β (mm/min)			**0.72**	
126	60	Nil	0.65	0.97
		1 Screw	0.65	0.77
		Glued	0.62	0.57
Average β (mm/min)			**0.64**	

Table 3-12: Summary of the instrumented tests results from the small furnace testing

INSTRUMENTED TESTS Specimen Dimension: 125mm Deep x 450mm Long					
Width (mm)	**Fire Duration (min)**	**Connection Type**	**Avg. Side β (mm/min)**	**Avg. Corner β (mm/min)**	**Avg. Bottom β (mm/min)**
63	30	NA	0.80	1.54	0.97
90		Nil	0.81	1.28	1.02
		Nailed	0.81	1.29	0.98
		Screwed	0.84	1.42	0.93
		Glued	0.71	1.45	0.70
Average β (mm/min)			**0.79**	**1.40**	
126	60	Nil	0.69	1.39	1.03
		Screwed	0.69	1.36	0.95
		Glued	0.64	1.40	0.61
Average β (mm/min)			**0.67**	**1.38**	

- In Table 3-11 and Table 3-12 test results show that for 30 minute fire exposure, the average side charring rate was between 0.72 to 0.79mm/min. For 60 minute fire exposure, the average side charring rate was between 0.64 to 0.67mm/min. A higher charring rate for the 30 minute fire exposure was expected as the initial burning of wood is generally higher due to the fact that the wood is not initially insulated by a char layer.

- In Table 3-12, test results also show that the overall corner charring rates for the 30 and 60 minute fire exposures were 1.38mm/min and 1.40mm/min, respectively. These rates were approximately twice higher than their average side charring rate due to the fact that the corner of the LVL member was experiencing two dimensional charring.

- Based on the average bottom charring rates as shown in Table 3-11 and Table 3-12, the nailed connection performed the worst whereas the glued connection performed the best in holding the double LVL members together in fire. It was also observed that for the glue connected double LVL specimens, their respective average side and bottom charring rates were relatively approximate due to one-dimensional charring.

4. ADDITIONAL SMALL FURNACE TESTS

This chapter describes additional small furnace tests conducted at the University of Canterbury.

4.1. Oven-Dried LVL Specimen

4.1.1. Overview

The aim of this experiment was to investigate if the moisture in the LVL played a major influence in the separation of the double LVL in fire. To achieve this, two 90mm width double LVL specimens were dried in the oven with a constant temperature of 102^{o}C for at least 48 hours, where the weight of the LVL specimens were measured and found constant. As a result, the moisture inside the samples was driven to the minimum. After they were conditioned, they were immediately tested in the small furnace for 30 minutes without any fastener to hold them together.

4.1.2. Experimental Results and Discussions

The moisture contents, determined by a moisture metre, for both LVL specimens before and after drying were:

Before drying: ≈ 11%
After drying: ≈ 8%

Figure 4-1 shows the comparative pictures between the initial and the residual cross-section for those two LVL specimens.

Figure 4-1: Comparative mid-span cross-sectional pictures between the initial and the residual specimens (Left: sample 1; Right: sample 2)

It was observed in Figure 4-1 that although both double LVL specimens were oven-dried for more than 48 hours, they still experienced separation after 30 minutes of fire exposure. This This opening phenomenon may due to the permanent deformation of the LVL specimen. It is is shown in Figure 2-2 under Section two of this report that when the wood is dried below 30% moisture content, the wood would undergo a linear shrinkage behaviour. Therefore when the wood is burnt into char, i.e. zero % moisture content, the wood would experience this permanent deformation.

Table 4-1 summarises the un-instrumented test results for the oven-dried 90mm width double LVL specimens.

Table 4-1: Un-instrumented test results for the oven-dried 90mm width double LVL specimens

Single LVL Specimen: **63mm Wide x 125mm Deep x 450mm Long** **Fire Duration:** **30 minutes**						
Sample	**Connection Type**	**Residual Width**	**Residual Depth**	**Avg. Side Charring Rate**	**Avg. Bottom Charring Rate**	**Separation Distance (tip to tip)**
		(mm)	**(mm)**	**(mm/min)**	**(mm/min)**	**(mm)**
1	Nil	35	73	0.92	1.75	25
2	Nil	32	85	0.97	1.33	23
Average				**0.95**	**1.53**	**24**

Table 4-1 shows the average side and bottom charring rates for the oven-dried double LVL specimens were 0.95mm/min and 1.53mm/min, respectively. These charring rates were actually higher than the average side and bottom charring rates for the non-oven-dried double LVL specimens, which were 0.7mm/min and 1.00mm/min respectively summarised in Table 3-3. This was due to the drying effect on the LVL specimens inside the oven which evaporated the moisture out of the wood. As a result, these oven-dried LVL specimens contained less moisture in the wood which resulted in a higher charring rate in comparison with the non-oven-dried LVL specimens.

4.2. Rate of Charring after the Fire is Out

4.2.1. Overview

The aim of this experiment was to examine the charring rate of the LVL member after the fire was extinguished. Two scenarios were examined for the glued 90mm width double LVL specimens. The first scenario was to expose the LVL specimen with 30 minutes fire duration duration inside the small furnace and was then left inside the furnace for another two hours while the furnace was switched off. Thermocouples were instrumented at various depths in the mid-span of the LVL specimen as shown in Figure 4-2. Temperature of the furnace was also measured and recorded.

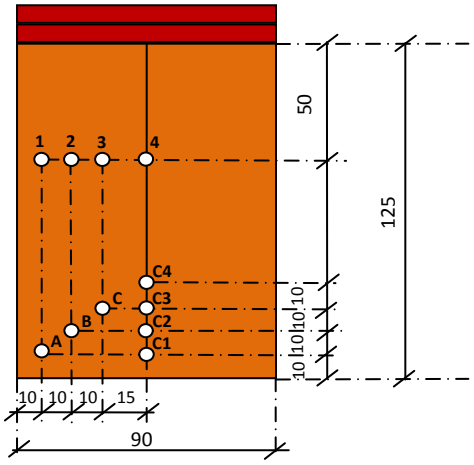

Figure 4-2: Thermocouple layouts for the LVL specimen tested after the fire is out (NOT TO SCALE)

Meanwhile the second scenario was to expose the LVL specimen with 30 minutes fire exposure inside the small furnace and then removed from the furnace for another two hours un-extinguished burning. The LVL specimen for the second scenario was not instrumented due to the limitation that the configuration of the small furnace does not allow the specimen to be removed out the furnace while the thermocouples are connected to the electronic data logger.

4.2.2. Experimental Results and Discussions

4.2.2.1. Scenario One: LVL Specimen Left Inside the Furnace

Thermocouple readings for the LVL specimen are shown in Figure 4-3 below.

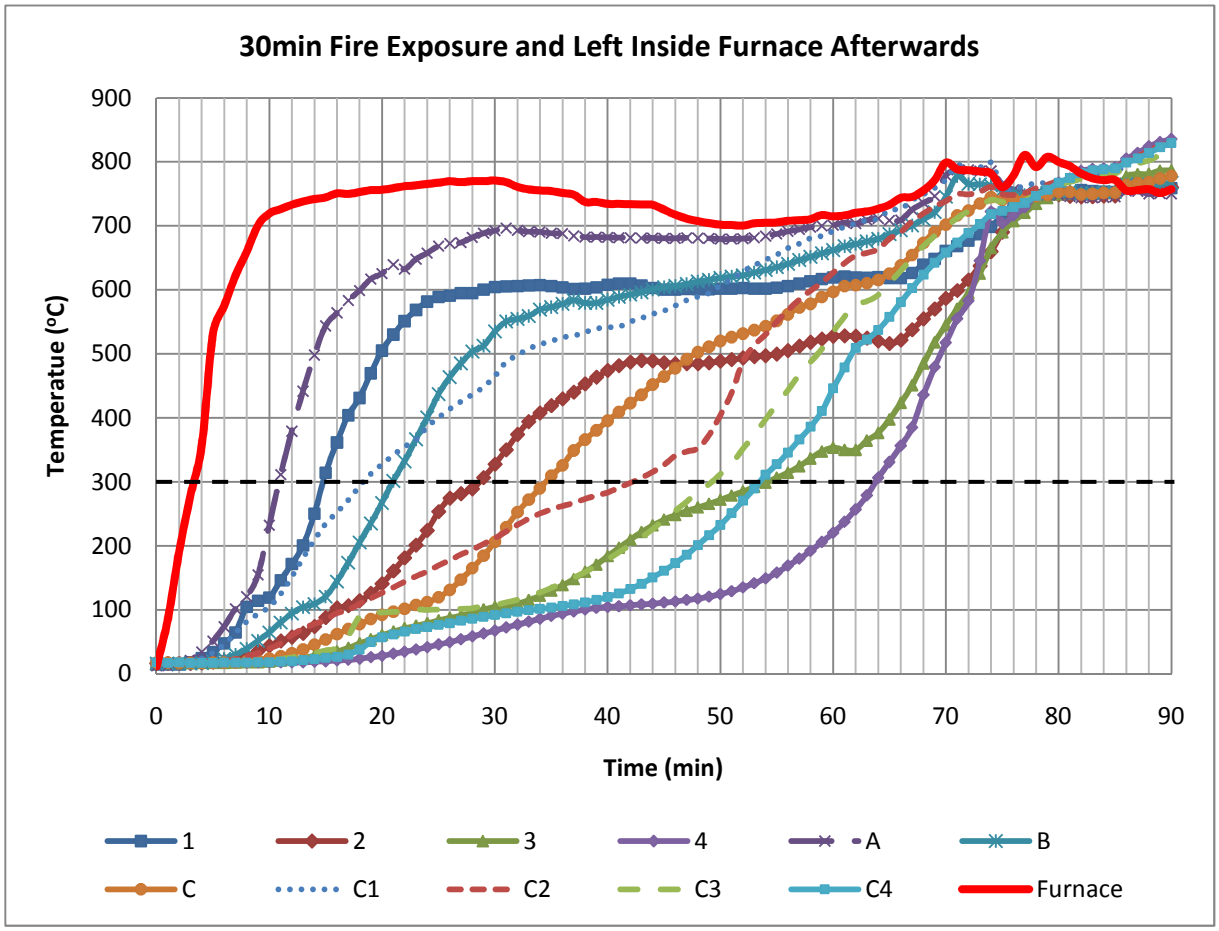

Figure 4-3: Thermocouple readings for scenario one

It was observed in Figure 4-3 that although the furnace was switched off after 30 minutes, the temperature inside the furnace was still reaching over 700°C for more than another hour. Thermocouple 4, which was located at the centre of the specimen reached 300°C at around 65 minutes. This indicates that the entire LVL specimen was completely charred at around this time.

Table 4-2 summarises the instrumented charring rate for scenario one.

Table 4-2: Instrumented charring rates for scenario one

	Side				Corner			Bottom			
Thermocouple	**1**	**2**	**3**	**4**	**A**	**B**	**C**	**C1**	**C2**	**C3**	**C4**
Depth (mm)	10	20	30	45	14	28	42	10	20	30	40
Time to 300°C (min)	15	29	54	64	11	21	34	18	42	49	53
Charring Rate, β, (mm/min)	0.68	0.70	0.55	0.71	1.30	1.35	1.23	0.55	0.47	0.61	0.75
Average β (mm/min)	**0.66**				**1.29**			**0.59**			

Test results in Table 4-2 show that side charring rates measured by thermocouples 1 to 4, which were one-dimensional charring, were reasonably consistent. Meanwhile corner charring rates measured by thermocouples A to C, which were two dimensional charring, were also reasonably uniform. However by comparing the bottom charring rates between thermocouples C1 to C4, it was noticed the charring rate measured by thermocouples C3 and C4 started to increase. This may indicate a change from one-dimensional charring to two-two-dimensional charring due to the superimposition of the two opposite arrises.

4.2.2.2. Scenario Two: LVL Specimen Left Outside the Furnace

Two LVL specimens were tested for scenario two. Figure 4-4 shows the comparative pictures between the initial and residual side elevation for these two LVL specimens.

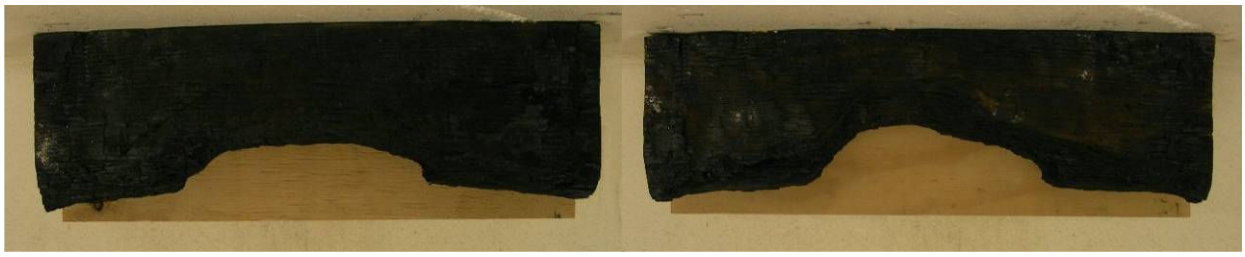

Figure 4-4: Comparative side elevation pictures between the initial and the residual LVL specimens (Left: specimen 1; Right: specimen 2)

Figure 4-5 shows the comparative mid-span cross-sectional pictures between the initial and the residual specimens.

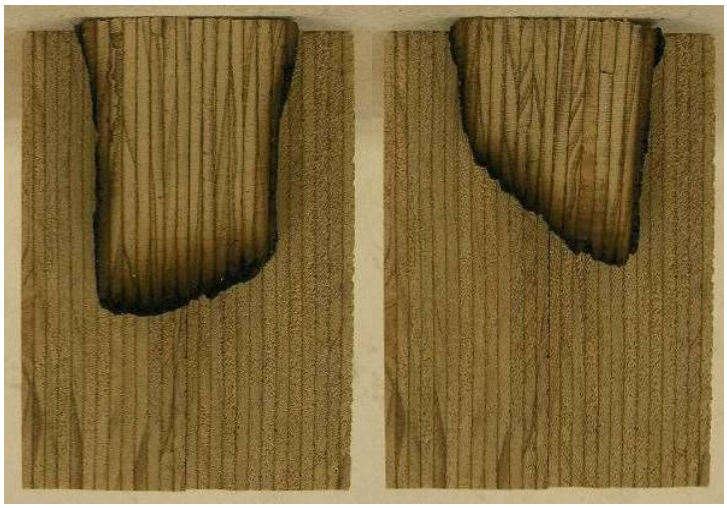

Figure 4-5: Comparative mid-span cross-sectional pictures between the initial and residual LVL specimens (Left: specimen 1; Right: specimen 2)

Comparative pictures in Figure 4-4 and Figure 4-5 show that only the centre part of the tested LVL specimens continued to char after they were left outside for two hours. This phenomenon was due to the insulation effect of the charred layer which sustained the burning in the mid section of the LVL specimens. If these two tested LVL specimens were left left for more than 2 hours, they may be burnt all the way through.

Table 4-3 summarises the charring rates before and after the fire is out for specimens 1 and 2. The average side and bottom charring rate before the fire is out were assumed to be the same as the previously tested glue connected double LVL specimens summarised in Table 3-3.

Table 4-3: Charring rates before and after the fire is out for specimen 1 and 2 for scenario 2

			Inside the Furnace (0~30 minutes)		Outside the Furnace (30~120 minutes)	
Specimen	Residual Width (mm)	Residual Depth (mm)	Avg. Side Charring Rate (mm/min)	Avg. Bottom Charring Rate (mm/min)	Avg. Side Charring Rate (mm/min)	Avg. Bottom Charring Rate (mm/min)
1	45	67	0.72	0.67	0.02	0.32
2	45	45	0.72	0.67	0.02	0.50

4.3. Superwool 607 Blanket

4.3.1. Overview

The aim of this experiment was to investigate the effectiveness of an insulation product, known as the Superwool 607 Blanket (Foreman, 2010), on the bottom charring rate of the screw connected double LVL. Superwool 607 Blanket is made from spun, low bio-persistent glass fibres and has a classification temperature of 1100^{o}C. It is 3mm in thickness and exhibits outstanding insulation properties at elevated temperatures.

In the experiment, Superwool 607 Blanket was sandwiched in between the screwed 90mm width double LVL specimen as shown in Figure 4-6. This experiment was to examine if an introduction of this insulation will allow the screw connected 90mm width double LVL specimen to produce similar or identical bottom charring rate results comparable with the glued 90mm width double LVL specimen. This experiment was an attempt to find an alternative product which will minimise the bottom charring of the screwed double LVL comparable to the glued double LVL. A 30 minute fire exposure was applied to this LVL specimen.

Figure 4-6: (a) Left: Superwool 607 Blanket placed in between the double LVL specimen; (b) Right: Superwool 607 Blanket sandwiched in between the screwed 90mm width double LVL specimen

4.3.2. Experimental Results and Discussions

Comparative pictures between the initial and the residual cross-section for the screw connected, screw connected with the Superwool 607 Blanket and glue connected 90mm width double LVL specimens are shown in Figure 4-7.

Figure 4-7: Comparative mid-span cross-sectional pictures between the initial and residual LVL specimens (From left to right: screw connected, screw connected with Superwool and glue connected)

It was observed in Figure 4-7 that the Superwool 607 Blanket still could not prevent the separation of the screw connected double LVL specimen. However visually it was observed that an introduction of this Superwool 607 Blanket reduced the interior surface charring. This may be due to the fact that the blanket acted as a shield to protect the interior furnaces from being attacked by the fire coming in the opposite direction.

The comparative charring rates between screw connected, screw connected with Superwool 607 Blanket and glue connected double LVL specimens are shown in Table 4-4.

Table 4-4: Comparative charring rates between screwed, screwed with Superwool and glued double LVL specimens

Single LVL Specimen: **63mm Wide x 125mm Deep x 450mm Long** **Fire Duration:** **30 minutes**				
Connection Type	**Residual Width (mm)**	**Residual Depth (mm)**	**Avg. Side Charring Rate (mm/min)**	**Avg. Bottom Charring Rate (mm/min)**
Screwed	48	100	0.70	0.83
Screwed (Superwool)	50	100	0.67	0.83
Glued	47	105	0.72	0.67

Comparative results in Table 4-4 show both screw connected and screw connected with Superwool 607 Blanket double LVL specimens produced approximately identical side and bottom charring rates. Although it was visually observed that the Superwool 607 Blanket reduced the interior surface charring, it still could not prevent the separation of the double LVL specimen. As a result heat was still able to travel into the mid-span which increased the overall bottom charring. Hence the bottom charring rate was still higher in comparison with with the bottom charring rate achieved by the glue connected double LVL specimen.

4.4. Intumescent Sealant

4.4.1. Overview

The aim of this investigation was to examine the effectiveness of intumescent sealant, which swells up into a thick chary mass when it is exposed to fire, on the bottom charring rate of the screw connected double LVL. Likewise, this experiment was to examine if the application of the intumescent sealant will allow the screw connected 90mm width double LVL specimen to produce similar or identical bottom charring rate results comparable with the glued 90mm width double LVL specimen. A 30 minute fire exposure was applied.

In this investigation, a channel was cut in between the double LVL specimen which was then filled with the intumescent sealant. Two different channelling layouts were examined and are shown in Figure 4-8.

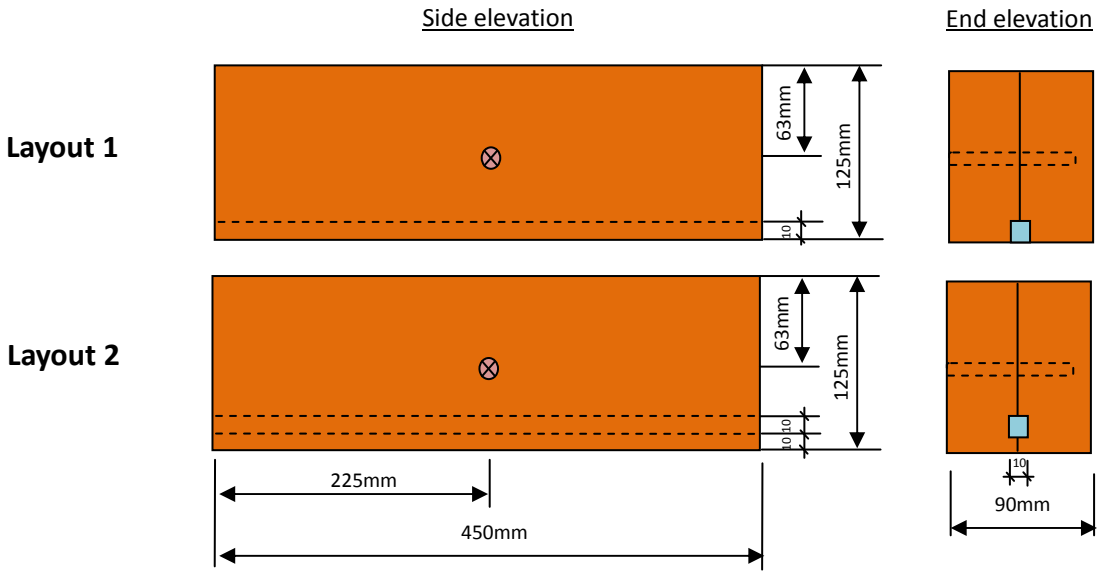

Figure 4-8: Two different intumescent sealant application layouts (NOT TO SCALE)

As shown in Figure 4-8, both channels were 10mm wide by 10mm deep which ran the entire length of the LVL specimen. For Layout 1, the channel was located at the bottom of the double LVL specimen where the intumescent sealant was exposed to the outside. Meanwhile for Layout 2, the channel was located 10mm from the bottom of the double LVL specimen where the intumescent sealant was concealed within the LVL.

Figure 4-9 shows a picture of the constructed LVL specimens for these two intumescent sealant channels.

Figure 4-9: A picture showing the constructed LVL specimens for the two intumescent sealant channels (Top: Layout 2; Bottom: Layout 1)

4.4.2. Experimental Results and Discussions

Comparative pictures between the initial and the residual cross-section for the screw connected, screw connected with Layout 1, screw connected with Layout 2 and glue connected 90mm width double LVL specimens are shown in Figure 4-10.

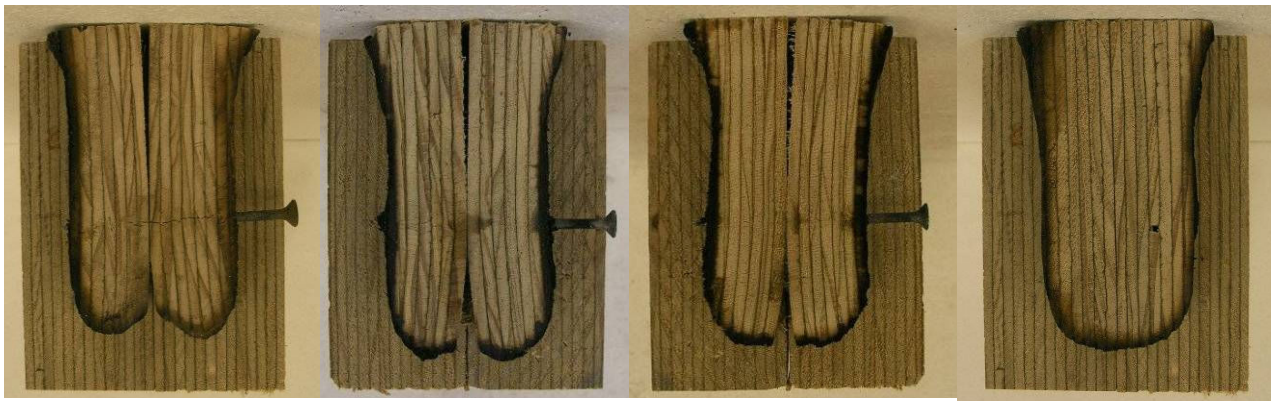

Figure 4-10: Comparative mid-span cross-sectional pictures between initial and residual LVL specimens (From left to right: screw connected, screw connected with Layout 1, screw connected with Layout 2 and glue connected)

It was observed in Figure 4-10 that both intumescent Layouts 1 and 2 were still not able to prevent the separation of the screw connected double LVL specimen. However visually it was noticed that the application of the intumescent sealant lessened the interior surface charring. This may due to the swelled intumescent sealant which protected the interior surface from being charred by fire when the LVL was separating apart. However once the

bottom surface charred to the depth where it passed the depth of the intumescent sealant, this protection would be gone. As a result the interior surface would once again be exposed exposed to heat.

The comparative charring rates between screw connected, screw connected with Layout 1, screw connected with Layout 2 and glue connected 90mm width double LVL specimens are summarised in Table 4-5.

Table 4-5: Comparative charring rates between screwed, screwed with Layouts 1 & 2 and glued double LVL specimens

Single LVL Specimen: 63mm Wide x 125mm Deep x 450mm Long **Fire Duration:** 30 minutes				
Connection Type	**Residual Width (mm)**	**Residual Depth (mm)**	**Avg. Side Charring Rate (mm/min)**	**Avg. Bottom Charring Rate (mm/min)**
Screwed	48	100	0.70	0.83
Screwed (Layout 1)	46	104	0.73	0.70
Screwed (Layout 2)	47	104	0.72	0.70
Glued	47	105	0.72	0.67

Comparative results in Table 4-5 show that both screw connected Layouts 1 and 2 double LVL specimens produced a lower average bottom charring rate than the screw connected double LVL specimen. Moreover it was also observed that they both produced approximately identical side and bottom charring rates in comparison with the glue connected double LVL specimen. This shows that although the intumescent sealant was not able to prevent the separation of the double LVL in fire, it was effective enough to swell up into a chary mass to prevent the heat from attacking the interior surface of the double LVL. As a result, the bottom charring rate for screw connected Layouts 1 and 2 double LVL specimens was comparable with the bottom charring rate achieved by the glue connected double LVL specimen.

5. PILOT FURNACE TESTS

5.1. Overview

Four pilot furnace tests were conducted in the Building Research Association of New Zealand (BRANZ) Fire Research facility in Wellington. In each fire test, LVL members were exposed to the standard ISO 834 (ISO 834, 1975) design fire curve.

The first fire test was to investigate the charring rate for 63mm, 90mm and 126mm width LVL members with thermocouples instrumented at various depths. The second and third tests were to examine different screwed connection layouts for both 90mm and 126mm width double LVL members. Two different screwed connection layouts were proposed for the second fire test. However the screwed connection layouts for the third fire test would only be decided based on the result obtained after the second fire test. The fourth test was to re-test two instrumented 90mm width LVL members as the experimental results obtained from the first pilot furnace test were inconsistent. These four fire tests are described in more detail in Section 5.3.2., Section 5.3.3., Section 5.5. and Section 5.6. of this report.

5.2. Pilot Furnace System

The pilot furnace provided by BRANZ fire research facility is shown in Figure 5-1. The furnace can be rotated into either horizontal or upright positions allowing the fire test to be conducted either horizontally or vertically. The furnace can accommodate complete assemblies such as doors or windows etc.

Figure 5-1: Pilot furnace system at BRANZ

The pilot furnace is a 1 metre by 2.2 metre by 0.5 metre deep fire box fuelled by 8 diesel injection burners. Four thermocouples are fitted in the furnace, which monitor the furnace temperature during the test. The pilot furnace control panel, shown in Figure 5-2, was monitored by the BRANZ operator to ensure the furnace temperature achieve the desirable time temperature curve. The temperature curve in the pilot furnace is based on the Standard ISO 834 design fire (ISO 834, 1975) shown in Figure 5-3. It is used as it is one of the most commonly used and recognised standard design fires around the world.

Figure 5-2: Pilot furnace control panel

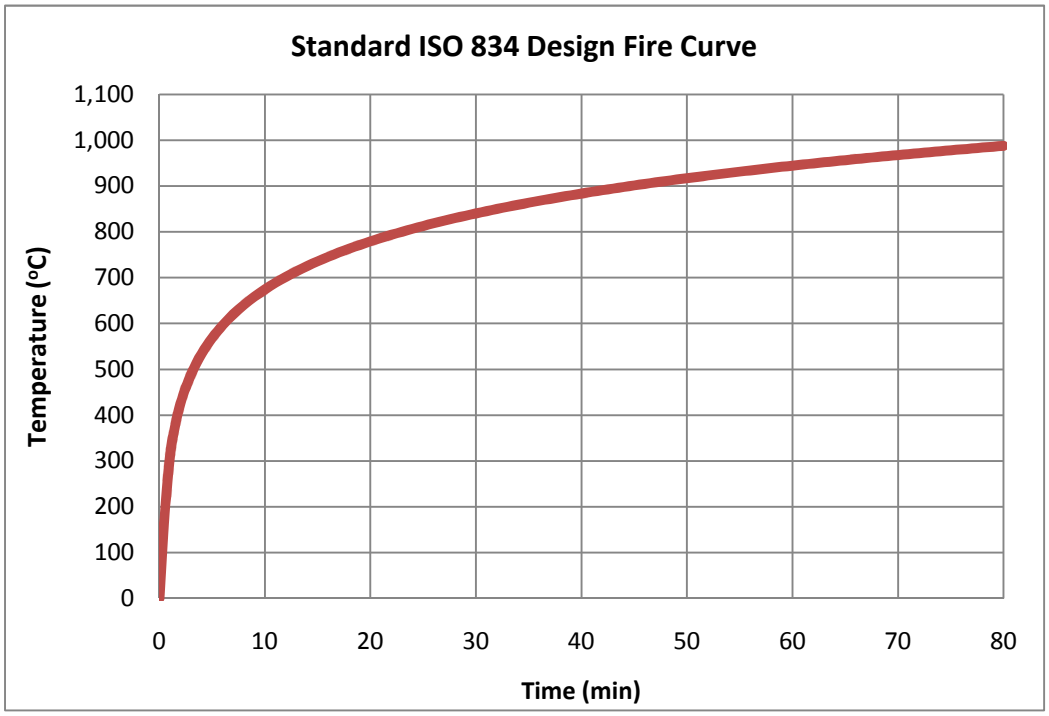

Figure 5-3: Standard ISO 834 design fire curve

5.3. Specimen Details

5.3.1. Overview

In first three pilot furnace tests, three LVL specimens were tested simultaneously. They were spaced 600mm centre to centre which was based on the design of these systems in practice.

In order to simulate three-faced (two sides and bottom) fire exposure of the LVL specimen, all LVL specimens were cut to 1,000mm long, which corresponded to the width of the pilot furnace specimen holder, and 300mm deep. When they were placed across the holder, the ends of the LVL specimens were flush to the concrete wall allowing them to be protected from fire exposure (see Figure 5-4). Meanwhile the top surface of all LVL specimens was insulated with two layers of 15mm Fyreline gypsum plasterboard.

Figure 5-4: LVL specimen installed inside the concrete specimen holder

In order to suspend the LVL specimens securely inside the furnace, a custom-made timber frame was made. As shown in Figure 5-5, those two layers of plasterboards were initially screwed onto the timber frame. Once they were screwed on, the whole assembly was then lifted and placed above the concrete specimen holder. Finally each LVL specimen was fastened to the timber frame by screwing four 100mm long type 17 self-drilling screws through the timber frame into the LVL specimen (see Figure 5-6).

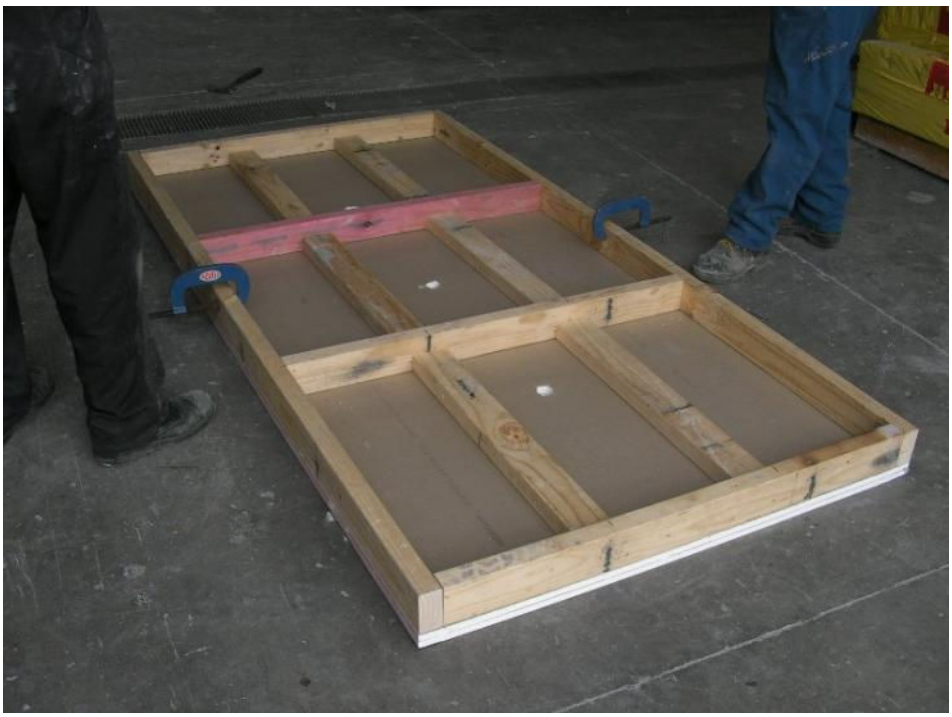

Figure 5-5: Two layers of plasterboard screwed unto the custom-made timber frame

Figure 5-6: Screwing type 17 self-drilling screws through the timber frame into the LVL specimen

Once the LVL specimens were suspended inside the concrete specimen holder, all the edges of the LVL specimens were sealed with intumescent sealant (see Figure 5-7).

Figure 5-7: Suspended LVL specimen with intumescent sealant sealing all edges

After the sealant was applied, the complete assembly was then craned and positioned above the pilot furnace ready for testing (see Figure 5-8).

Figure 5-8: The complete assembly placed above the pilot furnace ready for testing

5.3.2. First Pilot Furnace Test

The aim of the first pilot furnace test, which lasted for 75 minutes, was to investigate the charring rate for the 63mm, 90mm and 126mm LVL members. In order to achieve this, each each LVL member was instrumented with thermocouples at various depths in the mid-span. Charring depths were based on where the thermocouples located the 300^{o}C isotherm, which was taken as representing the char front within the samples. An example of LVL specimen instrumented with thermocouples is shown in Figure 5-9. Once instrumented, the sections of LVL were glued back together using resorcinol adhesive and cured for at least 24 hours (Figure 5-10). The thermocouple layout and dimensions are shown in Figure 5-11.

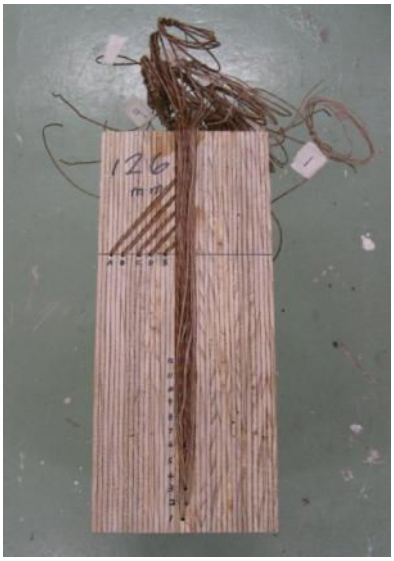

Figure 5-9: Thermocouple layout

Figure 5-10: Resorcinol adhesive joint after thermocouple instrumentation

Side Elevation

(NOT TO SCALE)

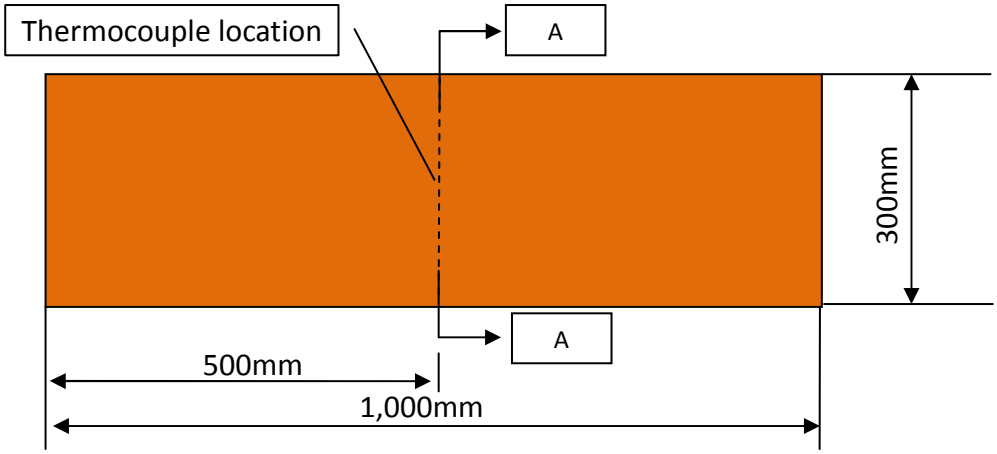

Section AA

(NOT TO SCALE)

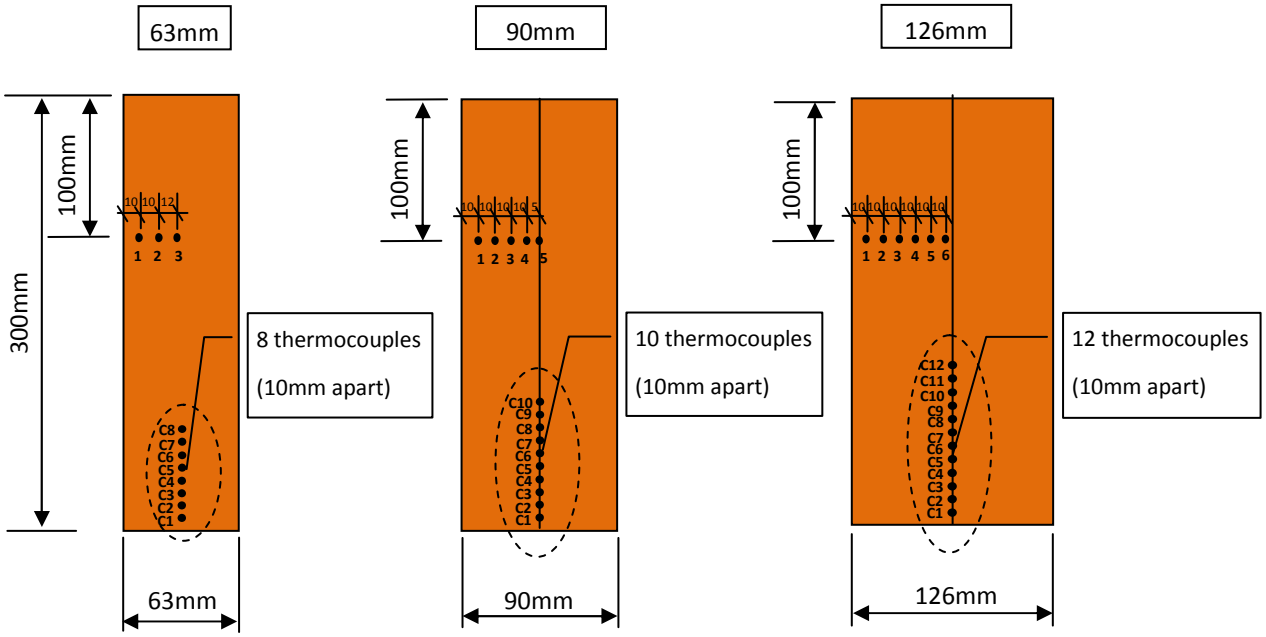

Figure 5-11: Thermocouple layout and dimensions for first pilot furnace test

When the complete testing assembly was positioned above the pilot furnace, thermocouples from LVL specimens were then connected to the electronic data recorder (see Figure 5-12). Each thermocouple was checked for position and recorded during the fire test.

Figure 5-12: Connecting thermocouples to the electronic data recorder

5.3.3. Second Pilot Furnace Test

The aim of the second pilot furnace test, which lasted for 60 minutes, was to determine the optimum screwed connection layouts for the double LVL members. One 90mm width double double LVL specimen and two 126mm width double LVL specimens were tested. Screws used for the double 90mm and 126mm LVL specimens were number 8 and 10 screws, respectively shown in Figure 3-7.

The connection specification for the second pilot furnace test is shown in Figure 5-13. Two different screwed connection layouts were examined. The first screw layout was implemented on Samples 1 and 2 where one row of three screws was fitted. The spacing between these three screws was 300mm centre-to-centre apart and they were installed 50mm from the bottom. Meanwhile the second screw layout was in a staggered fashion where it was implemented on Sample 3. The first row of two screws was fitted 25mm from the base whereas the second row of three screws was fitted 75mm from the base. The spacing between them was 150mm centre-to-centre apart.

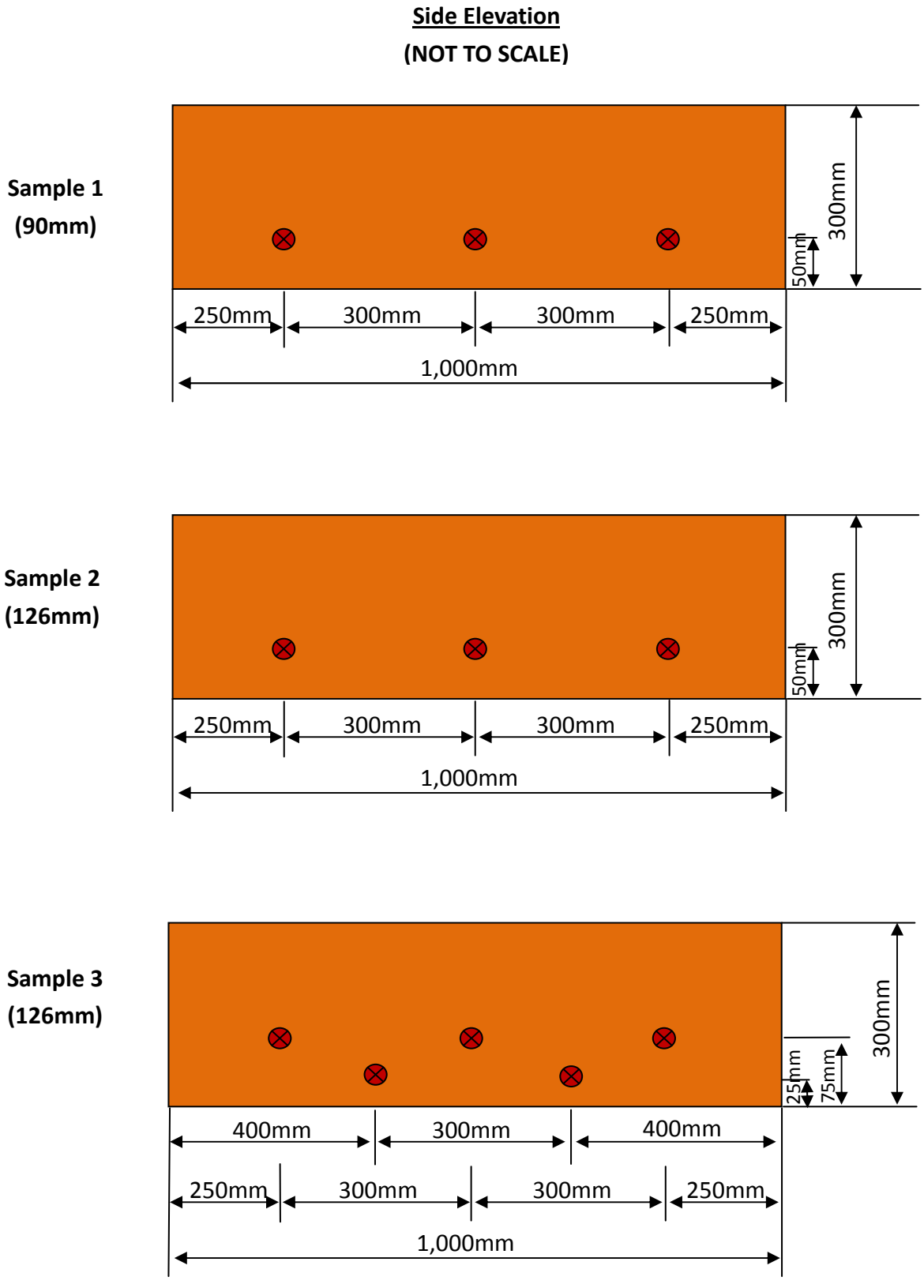

Figure 5-13: Connection specification for the second pilot furnace test

5.4. Pilot Furnace Tests Results and Discussions

5.4.1. First Pilot Furnace Test Results and Discussions

After 75 minutes of fire exposure, the specimen holder was lifted away from the furnace. It was observed that both the 63mm width and the 90mm width double LVL specimens were completed charred away whereas the 126mm width double LVL specimen was still burning. A picture showing the underside of the specimen holder after 75 minutes fire exposure is shown in Figure 5-14.

Figure 5-14: Underside of the specimen holder after the first pilot furnace test

Table 5-1 below summarises the instrumented side and bottom charring rates for each LVL specimen at various depths. The time for each thermocouple to reach 300^{o}C was extracted from the thermocouple readings recorded in the Excel spreadsheet. Refer to Appendix I for thermocouple readings of each specimen.

Figure 5-15 to Figure 5-17 show the comparative side and bottom thermocouple readings for each LVL specimen. Meanwhile Figure 5-18 and Figure 5-19 show the side and bottom charred depth as a function of time for each LVL specimen.

Table 5-1: Summary of charring rate at various depths for the first pilot furnace test

	63mm Width										
	Side			Bottom							
Thermocouples	**1**	**2**	**3**	**C1**	**C2**	**C3**	**C4**	**C5**	**C6**	**C7**	**C8**
Depth (mm)	10	20	32	10	20	30	40	50	60	70	80
Time to 300°C (min)	22	34	41	11	18	32	37	37	38	40	40
Charring Rate, β, (mm/min)	0.45	0.58	0.78	0.89	1.10	0.93	1.10	1.37	1.60	1.77	2.01
Average β (mm/min)	**0.60**			**1.35**							

	90mm Width														
	Side					Bottom									
Thermocouples	**1**	**2**	**3**	**4**	**5**	**C1**	**C2**	**C3**	**C4**	**C5**	**C6**	**C7**	**C8**	**C9**	**C10**
Depth (mm)	10	20	30	40	45	10	20	30	40	50	60	70	80	90	100
Time to 300°C (min)	13	58	52	56	56	17	27	34	45	49	53	55	56	54	52
Charring Rate, β, (mm/min)	0.80	0.34	0.57	0.72	0.81	0.59	0.74	0.88	0.89	1.03	1.13	1.28	1.44	1.68	1.92
Average β (mm/min)	**0.65**					**1.16**									

	126mm Width																	
	Side						Bottom											
Thermocouples	**1**	**2**	**3**	**4**	**5**	**6**	**C1**	**C2**	**C3**	**C4**	**C5**	**C6**	**C7**	**C8**	**C9**	**C10**	**C11**	**C12**
Depth (mm)	10	20	30	40	50	60	10	20	30	40	50	60	70	80	90	100	110	120
Time to 300°C (min)	15	24	40	51	65	-	15	23	42	49	63	73	-	-	-	-	-	-
Charring Rate, β, (mm/min)	0.66	0.82	0.76	0.79	0.77	-	0.68	0.87	0.71	0.82	0.80	0.82	-	-	-	-	-	-
Average β (mm/min)	**0.76**						**0.78**											

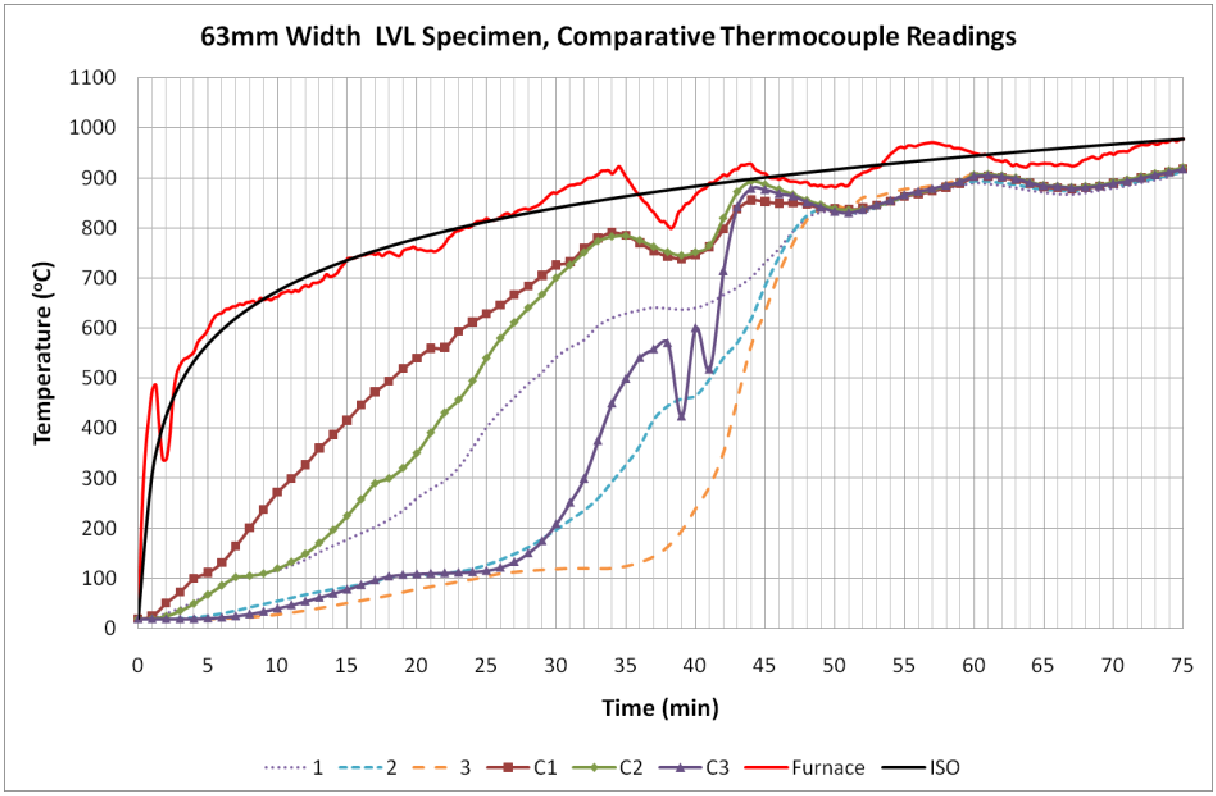

Figure 5-15: Comparative thermocouple readings for 63mm width LVL specimen

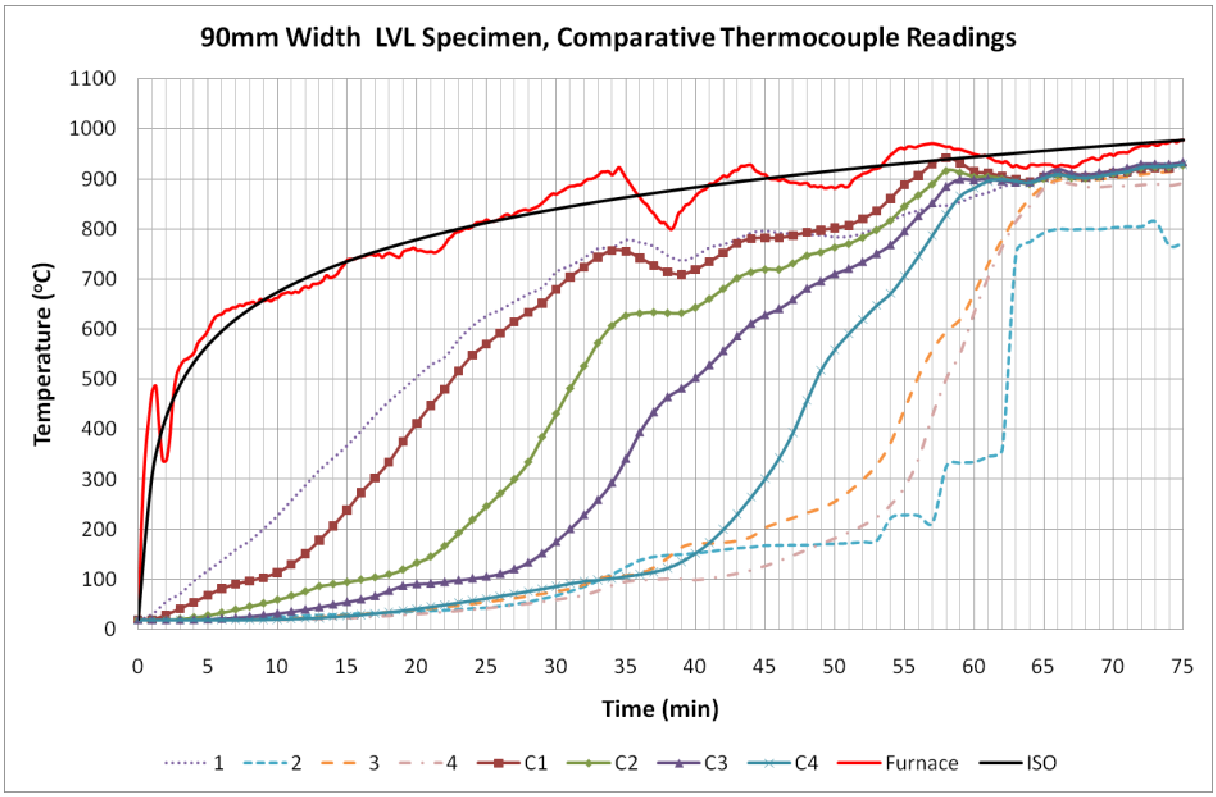

Figure 5-16: Comparative thermocouple readings for 90mm width LVL specimen

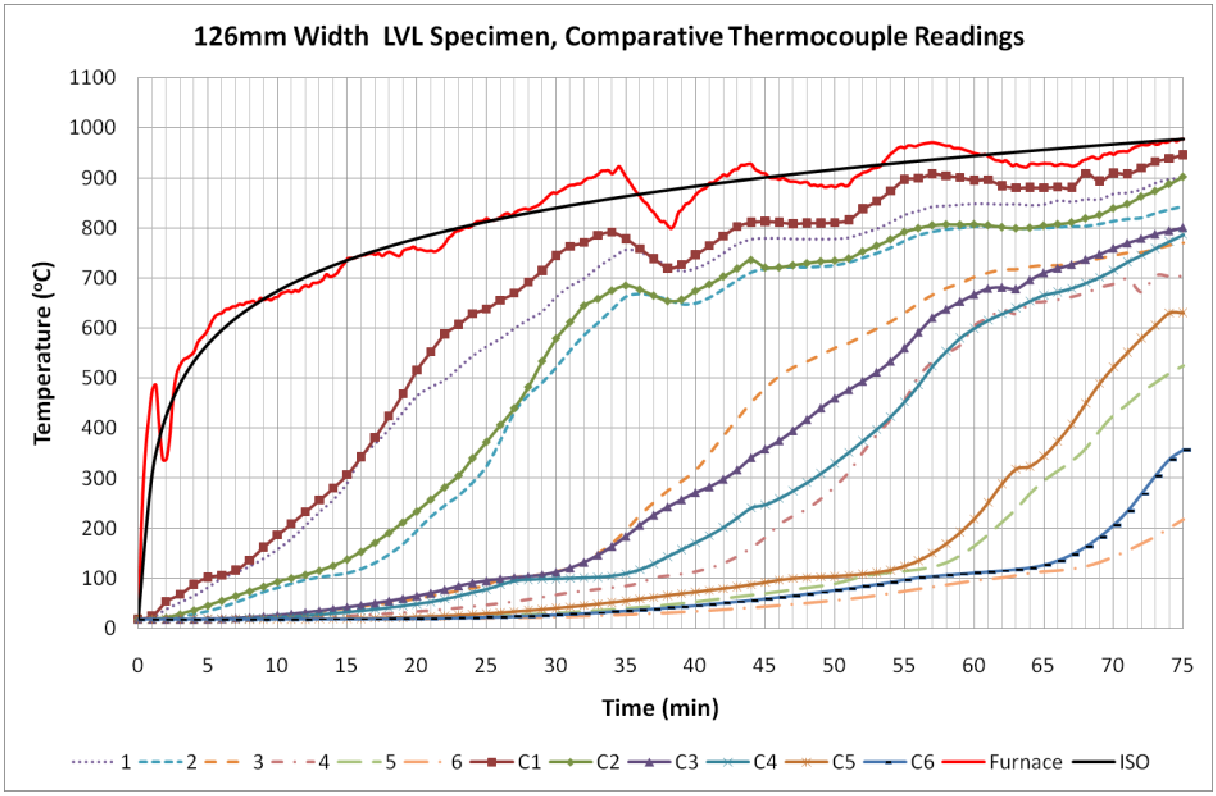

Figure 5-17: Comparative thermocouple readings for 126mm width LVL specimen

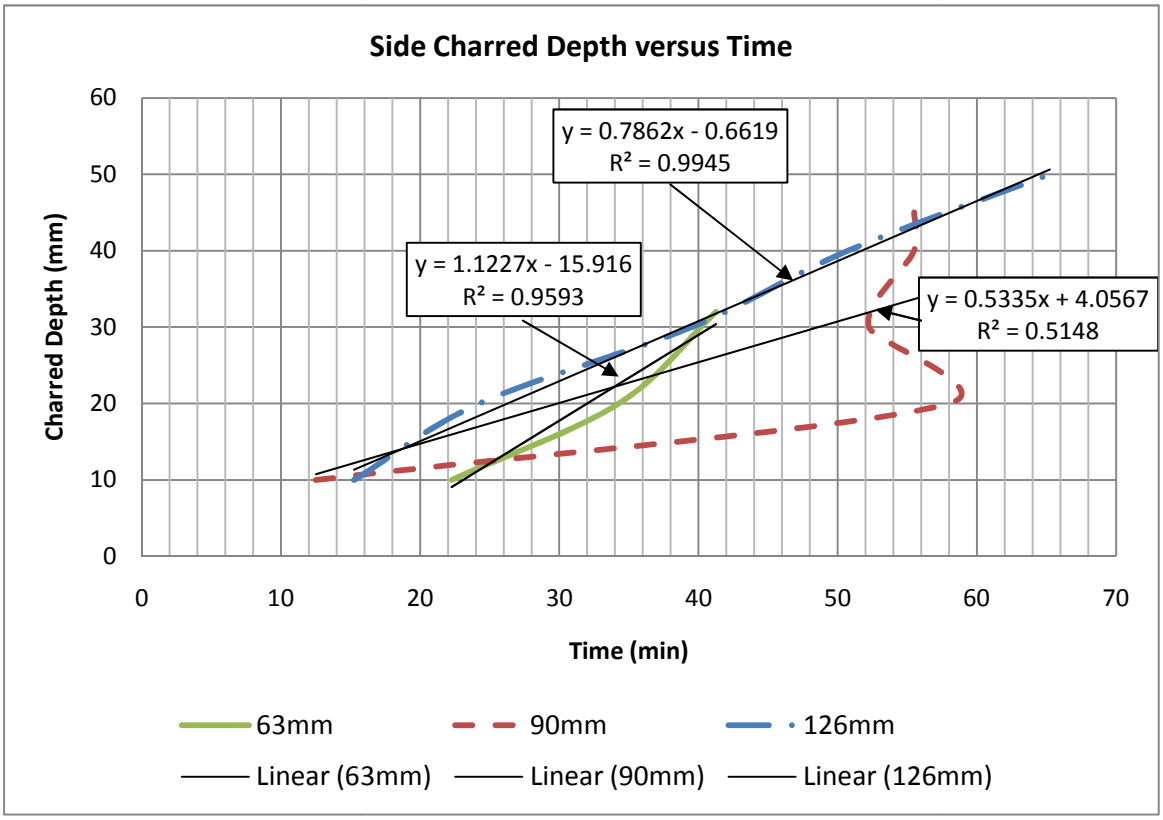

Figure 5-18: Side charred depth as a function of time for each LVL specimen

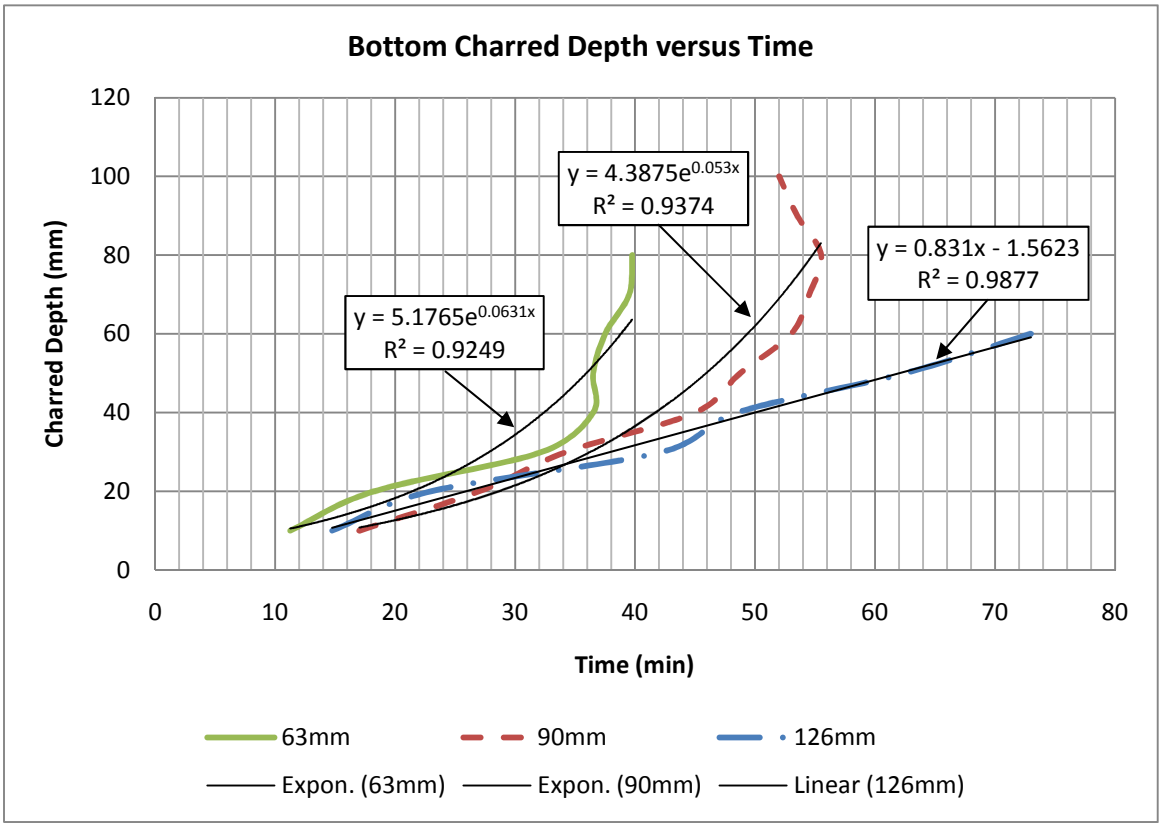

Figure 5-19: Bottom charred depth as a function of time for each LVL specimen

Test results in Table 5-1 show that average side charring rates for 63mm, 90mm and 126mm width LVL specimens were 0.60mm/min, 0.65mm/min and 0.76mm/min, respectively. They were relatively close since the side only experienced one dimensional charring. However it was observed that the side charring rates of thermocouples 1 and 2 for 63mm width LVL specimen and the side charring rates of thermocouple 2 and 3 for 90mm width LVL specimen were uncharacteristically lower than the other thermocouples. These poor results were also also evidenced in the comparative thermocouple readings for the 63mm and 90mm width LVL specimens shown in Figure 5-15 and Figure 5-16. For the 63mm width LVL specimen, thermocouple C1 to C4 would experience one dimensional charring during the initial stage of burning which means their temperature readings should correspond relatively close with the temperature readings measured by thermocouples 1 to 4. Similarly for the 90mm width LVL LVL specimen, thermocouple C1 to C5 should correspond relatively similar with thermocouples 1 to 5. However it was observed that except for the comparative thermocouples 1 and C1 readings for the 90mm width LVL specimens, all other comparative thermocouple readings were vastly inconsistent with each other. These inconsistent thermocouple readings may due to the thermocouple wiring issues. Therefore it was decided that a re-test for the 90mm width LVL specimens was required. This re-test was described in more detail in Section 5.6. of this report. Meanwhile the 63mm width LVL

specimen was not re-tested due to the reason that it was not a common width used for structural purposes.

On the other hand, it was observed that for the 126mm width LVL specimen both the side and bottom charring rates were comparatively close to each other. These similarities were also shown in the comparative thermocouple temperature readings as shown in Figure 5-17.

In terms of the bottom charring rate as shown in Table 5-1, it was noticed the average bottom charring rate for 63mm, 90mm and 126mm width LVL specimens were 1.35mm/min, 1.16mm/min and 0.78mm/min respectively. The average bottom charring rates for the 63mm and the 90mm width LVL specimens were significantly higher than the 126mm width LVL specimen, which suggested that both the 63mm and the 90mm width LVL specimens experienced a change from one-dimensional to two-dimensional bottom charring. For the 63mm width LVL specimen, a large increase in the bottom charring rate was observed at the depth of 50mm which corresponded to the residual width of approximately 10mm. This indicates that the beginning of the two-dimensional bottom charring may occur in between the depth of 40 and 50mm. Meanwhile for the 90mm width LVL specimen, , a large increase increase in the bottom charring rate was observed at the depth of 60mm which corresponded to the residual width of approximately 10mm. This suggests the beginning of the two-dimensional charring may occur between the depth of 50 and 60mm. These results results corresponded well with what it was observed in Figure 5-19 where both 63mm and 90mm width LVL specimen started to experience an exponential bottom charring rate at the depth of approximately 45mm and 55mm, respectively.

As for the 126mm width LVL specimen, however, the average bottom charring rate was observed to be similar to the average side charring rate. This shows that the bottom charring rate of the 126mm width LVL specimen did not go into a two-dimensional charring for a 75 minutes fire exposure.

In Figure 5-18, a bad correction for the 90mm width LVL specimen was noticed. Meanwhile the average side charring rate for the 63mm and 126mm width LVL specimens generated by the Excel spreadsheet were 1.12mm/min and 0.79mm/min. In comparison with the average average side and bottom charring rates summarized in Table 5-1, the 63mm width LVL specimen did not correlate well whereas the 126mm width LVL specimen did correlate well. in Figure 5-19, it was observed that both the 63mm and the 90mm width LVL specimens showed an exponential increase in the bottom charred depth after around 36^{th} and 50^{th} minutes respectively. These increases may be due to the two-dimensional charring occurring occurring at the bottom. Meanwhile a linear 0.83mm/min bottom charring rate was generated by the Excel spreadsheet for the 126mm width LVL specimen, which correlated reasonably well with the average bottom charring rate summarized in Table 5-1 .

5.4.2. Second Pilot Furnace Test Results and Discussions

Figure 5-20 shows the underside of the specimen holder after the 60 minute fire exposure.

Figure 5-20: Underside of the specimen holder after the second pilot furnace test

It was observed that after 60 minutes of fire exposure, Sample 1 had completely disappeared whereas Samples 2 and 3 were still burning. The disappearance of Sample 1 was not due to the complete charring away of the LVL specimen but it was instead due to the separation of Sample 1 away from the concrete specimen holder which fell into the pilot furnace during the test (refer to Figure 5-21). This falling, which hit one of the thermocouples inside the furnace, caused a sudden change in the pilot furnace temperature reading at around 46th minute noticed by the BRANZ operator.

Figure 5-21: Remains of Sample 1 inside the pilot furnace

Meanwhile Figure 5-22 shows a picture of Samples 2 and 3 after they were removed away from the specimen holder. It was observed that Sample 2 underwent a large separation at the bottom of the double LVL specimen whereas Sample 3 experienced a large separation at the top of the double LVL specimen.

Figure 5-22: Separation of Samples 2 (left) and 3 (right) after the second pilot furnace test

The falling of Sample 1 and the separation of Sample 3 at the top of the LVL specimens were all due to an unsecured fastening between the timber framing and the specimens. In full scale construction, timber notches and a concrete slab on top of the timber joists would hold the joists securely in place. Therefore this disconnection between the specimens and the timber framing was undesired. Hence in the third pilot furnace test, additional screws were introduced on top to ensure a secure fastening between all testing specimens and the timber framing. The third pilot furnace is described in more detail in Section 5.5. of this report.

Figure 5-23 shows the comparative mid-span cross–sectional pictures between the initial and the residual LVL specimens for Samples 2 and 3. Meanwhile Table 5-2 summarises the average side and the bottom charring rates for Samples 2 and 3 of the second pilot furnace test.

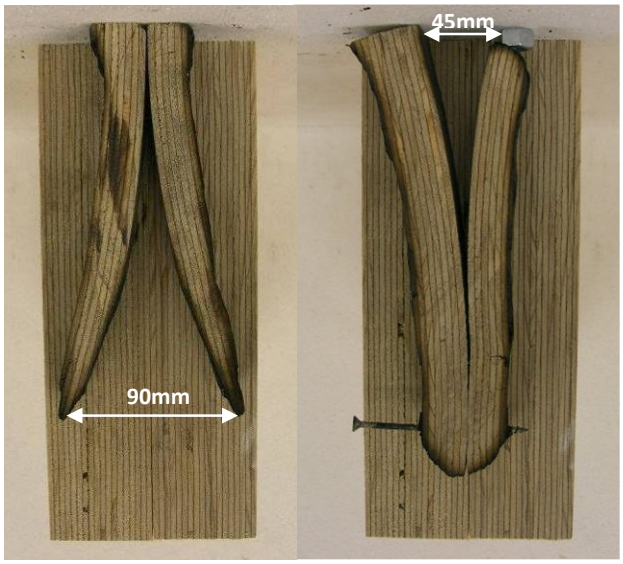

Figure 5-23: Comparative mid-span cross-sectional pictures between the initial and residual LVL specimens (Left: Sample 2; Right: Sample 3)

Table 5-2: Average side and bottom charring rates for Samples 2 and 3 of the second pilot furnace test

Sample	Fire Duration	Initial Width	Initial Depth	Residual Width	Residual Depth	Avg. Side Charring Rate	Avg. Bottom Charring Rate
	(min)	(mm)	(mm)	(mm)	(mm)	(mm/min)	(mm/min)
2	60	126	300	46	210	0.66	1.50
3	60	126	300	52	245	0.62	0.92

In Figure 5-23, the bottom separation for Sample 2 was approximately 90mm whereas the top separation for Sample 3 was approximately 45mm. Due to this large bottom separation for Sample 2, it caused an intensive bottom charring of 1.5mm/min in comparison with a 0.92mm/min bottom charring rate for Sample 3 as shown in Table 5-2. Meanwhile the average side charring rates between the Samples 2 and 3 were approximately the same.

It was also observed in Figure 5-23 that due to this bottom separation of Sample 2, the double LVL specimens experienced 6 faced fire exposure. As a result, the double LVL specimens became two single LVL specimens which significantly reduce the time for the opposite arrises to superimpose on each other. In other words, the bottom charring for Sample 2 changed from one-dimensional charring to two-dimensional charring in a much earlier stage of burning. Hence it was observed that the Sample 2 was much too slender in comparison with the Sample 3 as shown in Figure 5-23.

Therefore it could be concluded that for a 60 minute fire exposure the proposed screw layout for Sample 2 was inadequate to hold the double LVL member together whereas the screw layout for Sample 3 was somehow effective although Sample 3 separated at the top due to the insecure fastening between the LVL specimen and the timber framing.

5.5. Third pilot furnace test

5.5.1. Overview

The objective of the third pilot furnace test, which lasted 45 minutes, was to re-adjust the screwed connection layouts for the 90mm and 126mm width double LVL members based on the results obtained from the second pilot furnace test.

5.5.2. Test Specification

Figure 5-24 shows the testing specification for the third pilot furnace test specimens.

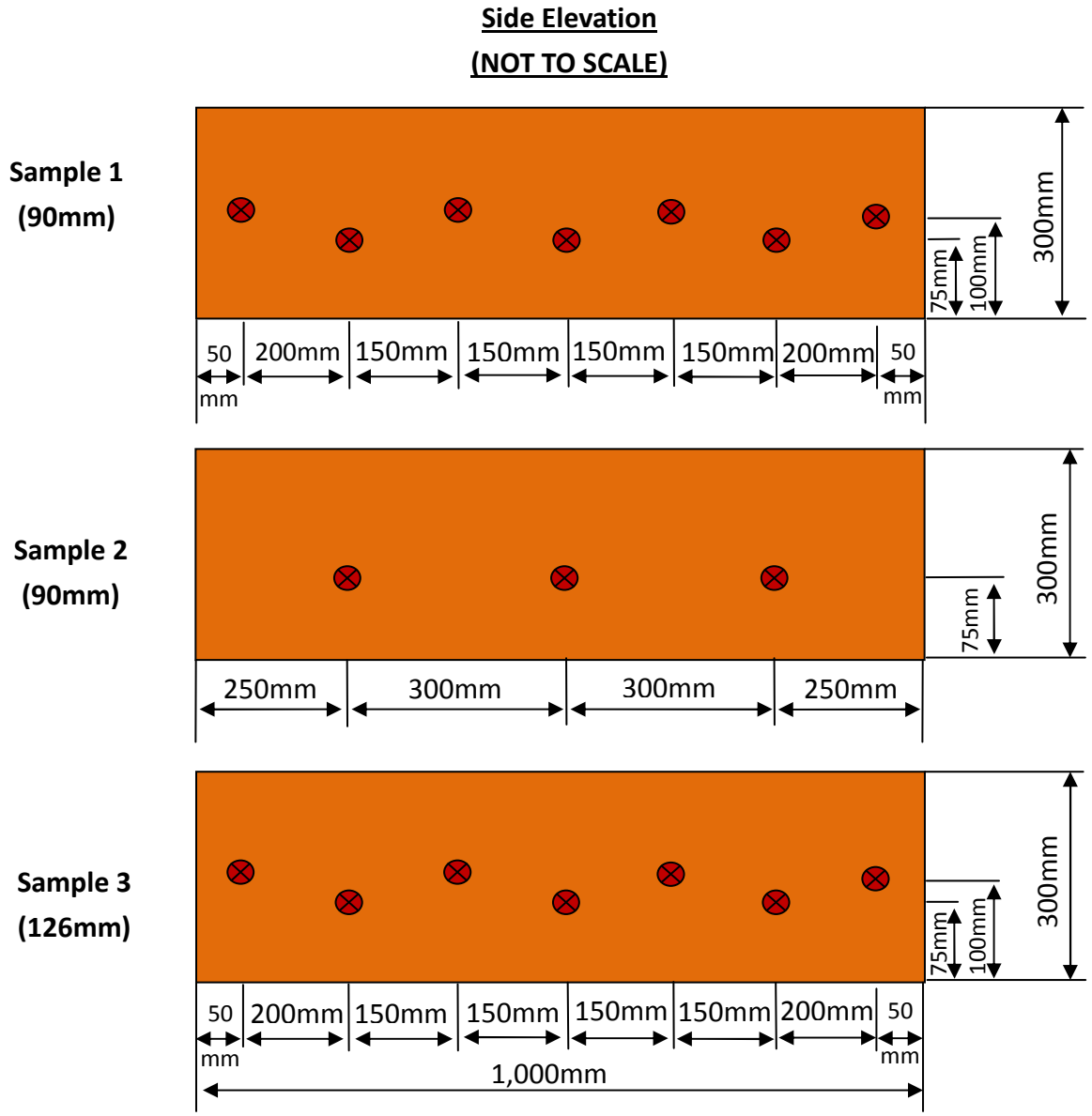

Figure 5-24: Connection specification for the third pilot furnace test specimens (NOT TO SCALE)

As shown in Figure 5-24, two 90mm and one 126mm width double LVL specimens were tested. Screws used for the double 90mm and 126mm LVL specimens were typical number 8 8 and number 10 screws respectively shown in Figure 3-7.

Based on the test results from the second pilot furnace test, two different screwed connection layouts were examined. The first screw layout was implemented on Sample 2 which was treated as the baseline layout. This layout was to re-adjust the screw layout implemented on Sample 3 of the second pilot furnace test. The difference was that the top row of four screws was removed. This was to see if three screws were adequate enough to hold the 90mm width double LVL specimen together. These three screws were installed 75mm from the bottom and were spaced 300mm centre-to-centre apart.

Meanwhile the second screw layout for the third pilot furnace test was a staggered screw layout, which was implemented on Samples 1 and 3. In this layout an additional row of four screws was fitted 100mm from the bottom. Out of these four screws, two of them were installed 50mm from the end. This was to examine if these two screws would prevent the separation of the double LVL specimen at the end. The rest of the screws were spaced 150mm centre-to-centre.

In order to prevent disconnection between the LVL specimens and the timber framing like the second pilot furnace test, eight 150mm long type 17 self-drilling screws were screwed through the timber framing into each LVL specimen. Four screws were screwed on either side of the double LVL specimen as shown in Figure 5-25.

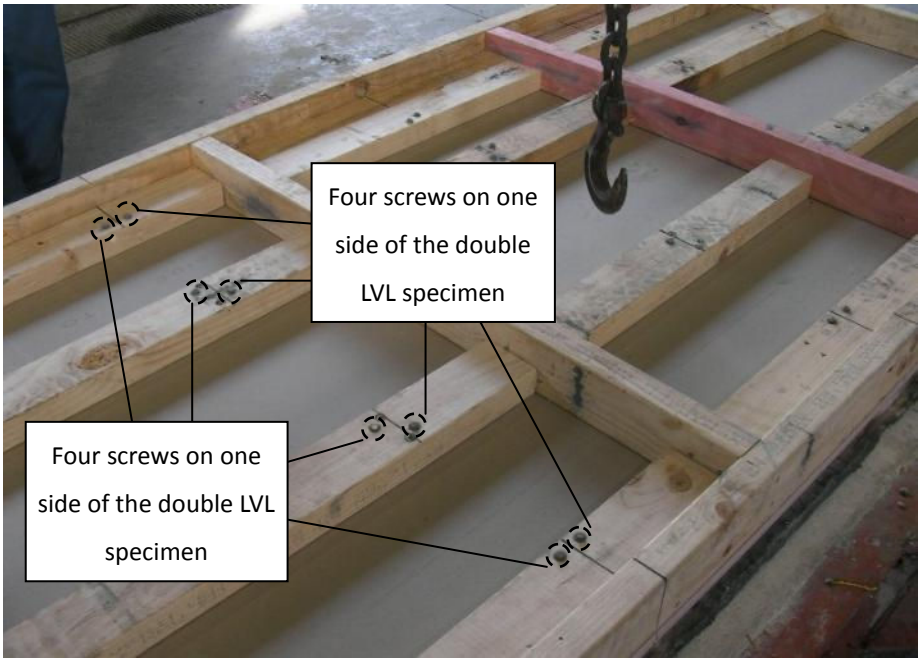

Figure 5-25: Eight sell-drilling screws introduced for each double LVL specimen in the third pilot furnace test

5.5.3. Third Pilot Furnace Test Results and Discussions

Figure 5-26 shows the underside of the specimen holder after a 45 minute fire exposure.

Figure 5-26: Underside of the specimen holder after the third pilot furnace test

Figure 5-27 shows the end view of these three tested LVL specimens after a 45 minute of fire exposure.

Figure 5-27: End view of these three tested LVL specimens after a 45 minute of fire exposure
(Left to right: Samples 1, 2 and 3)

It was observed in Figure 5-27 that all three LVL specimens did not suffer any top separation or disconnection from the timber framing after a 45 minute fire exposure. This shows the proposed eight 150mm long type 17 screws were effective in securing the LVL specimen. Meanwhile, the end view in Figure 5-27 also shows that comparatively Sample 2 suffered the greatest end and bottom separation in comparison with Samples 1 and 3. This indicates the effectiveness of the additional row of four screws introduced 100mm from the bottom. Moreover the screw located 50mm from the end also proved to be effective enough to prevent the end separation of Samples 1 and 3.

Figure 5-28 shows the comparative mid-span cross-sectional view between the initial and the residual LVL specimens for Samples 1, 2 and 3. Meanwhile Table 5-3 summarises the side and the bottom charring rates for Samples 1, 2 and 3 of the third pilot furnace test.

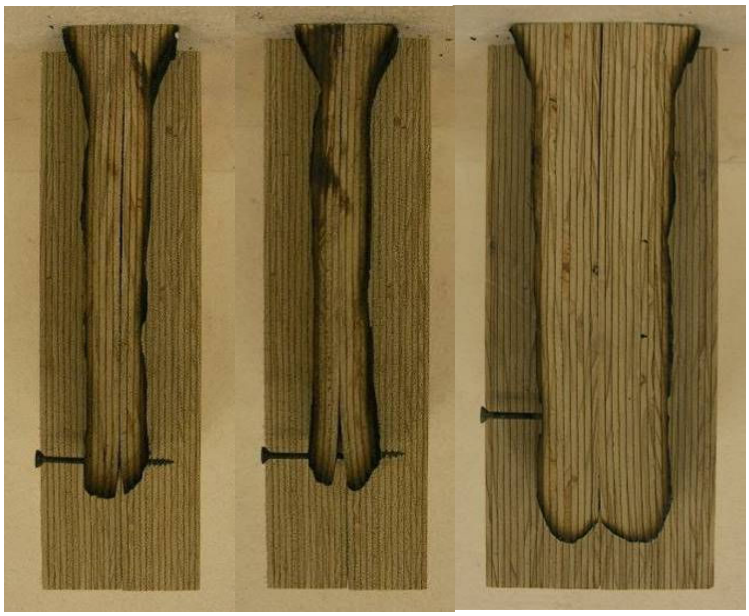

Figure 5-28: Comparative mid-span cross-sectional view between the initial and the residual LVL specimens (From left to right: Samples 1, 2 and 3)

Table 5-3: Average side and bottom charring rates for Samples 1, 2 and 3 of the third pilot furnace test

Sample	Fire Duration	initial Width	Initial Depth	Residual Width	Residual Depth	Avg. Side Charring Rate	Avg. Bottom Charring Rate
	(min)	(mm)	(mm)	(mm)	(mm)	(mm/min)	(mm/min)
1	45	90	300	34	238	0.62	1.38
2	45	90	300	29	234	0.68	1.47
3	45	126	300	67	264	0.65	0.80

Test results in Table 5-3 show that the average side charring rates between Samples 1 to 3 were approximately the same ranging from 0.62 to 0.68mm/min. However it was noted that the average bottom charring rate for Sample 2 was higher than Sample 1. This may be due to a bigger bottom separation for Sample 2 in comparison with Sample 1 observed in Figure 5-28, which caused a higher bottom charring rate. Meanwhile the average bottom charring rate for Sample 3 was only 0.80mm/min.

Therefore it could be concluded that for a 45 minute fire exposure, the screw layout for Samples 1 and 3 were much more effective than the screw layout for Sample 2 in preventing a large separation of the double LVL members.

5.6. Fourth Pilot Furnace Test

5.6.1. Overview

The aim of this fourth pilot furnace test was to re-test the instrumented 90mm width glued LVL specimen in BRANZ. Two identical 90mm width glued LVL specimens, which were spaced spaced 700mm apart, were tested simultaneously for 60 minute fire duration. The thermocouple layout and dimensions for this re-test are shown in Figure 5-29. Figure 5-30 and Figure 5-31 show the experimental setup prior to testing.

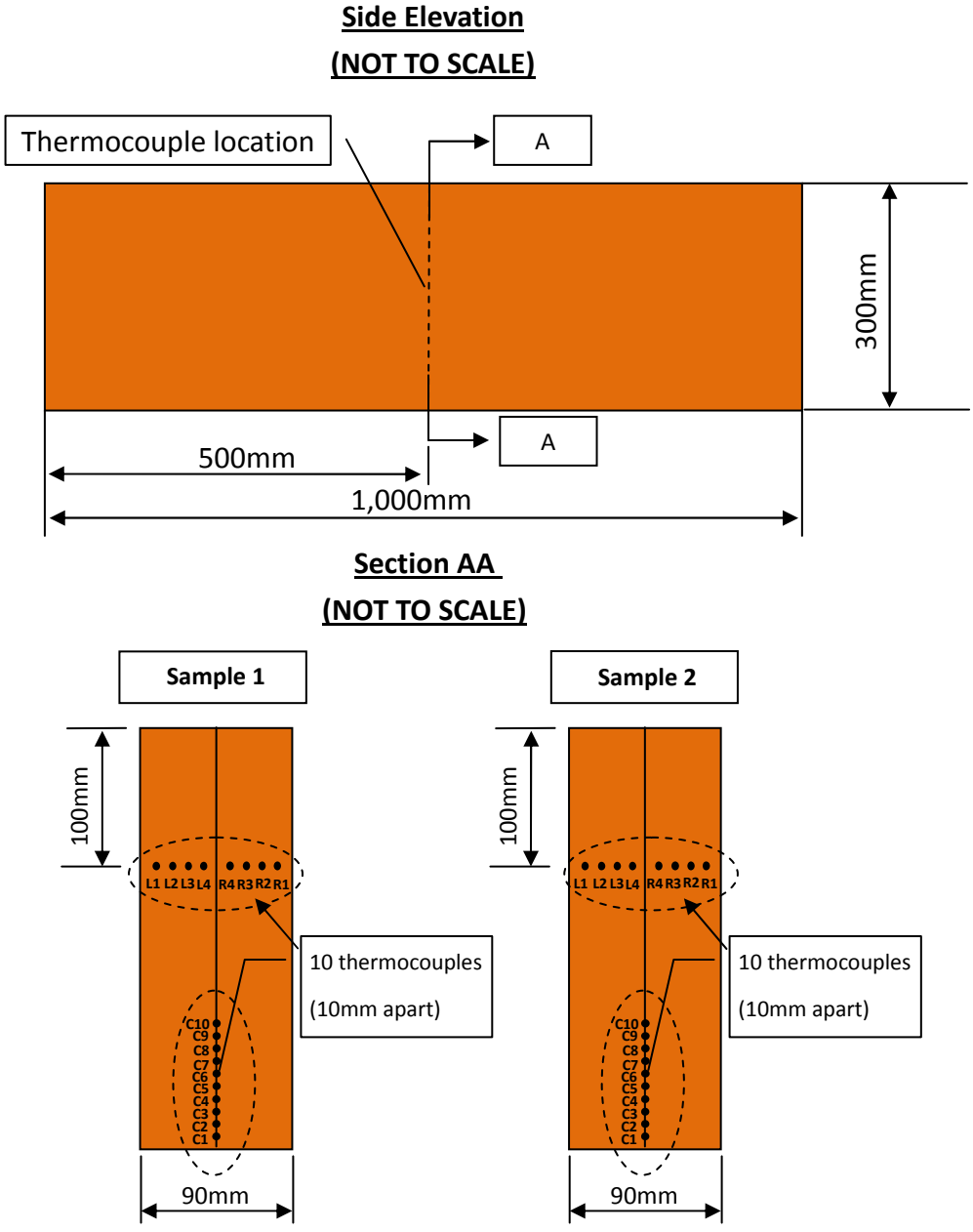

Figure 5-29: Thermocouple layout and dimensions for the fourth pilot furnace test

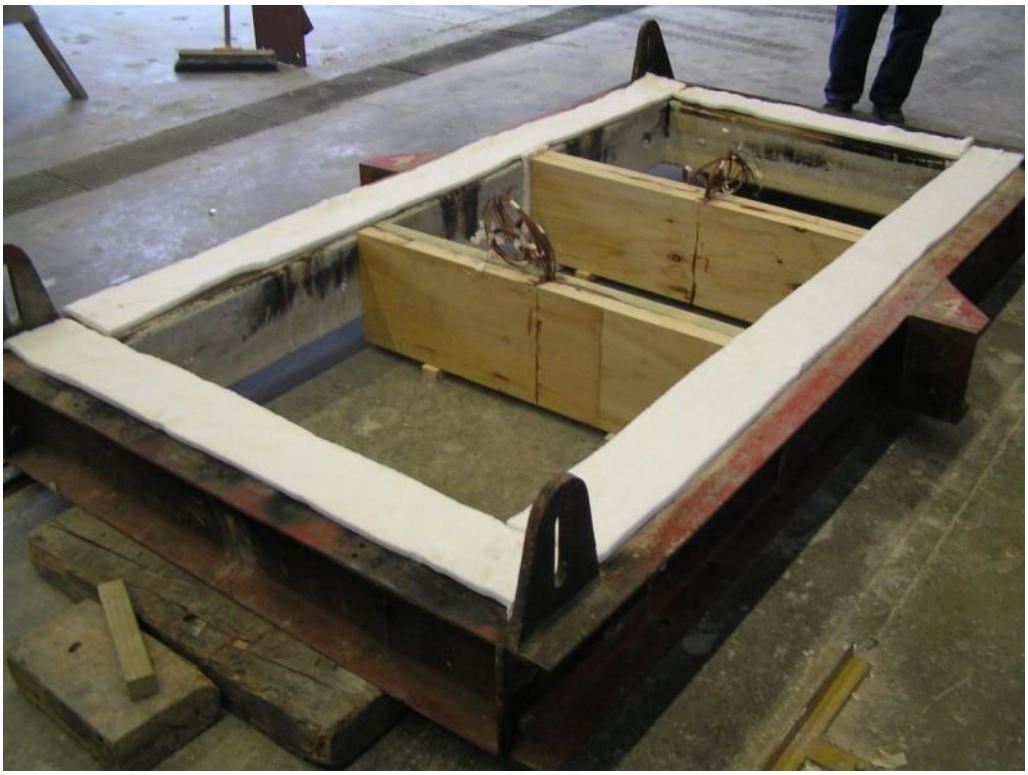

Figure 5-30: LVL specimens installed inside the concrete specimen holder

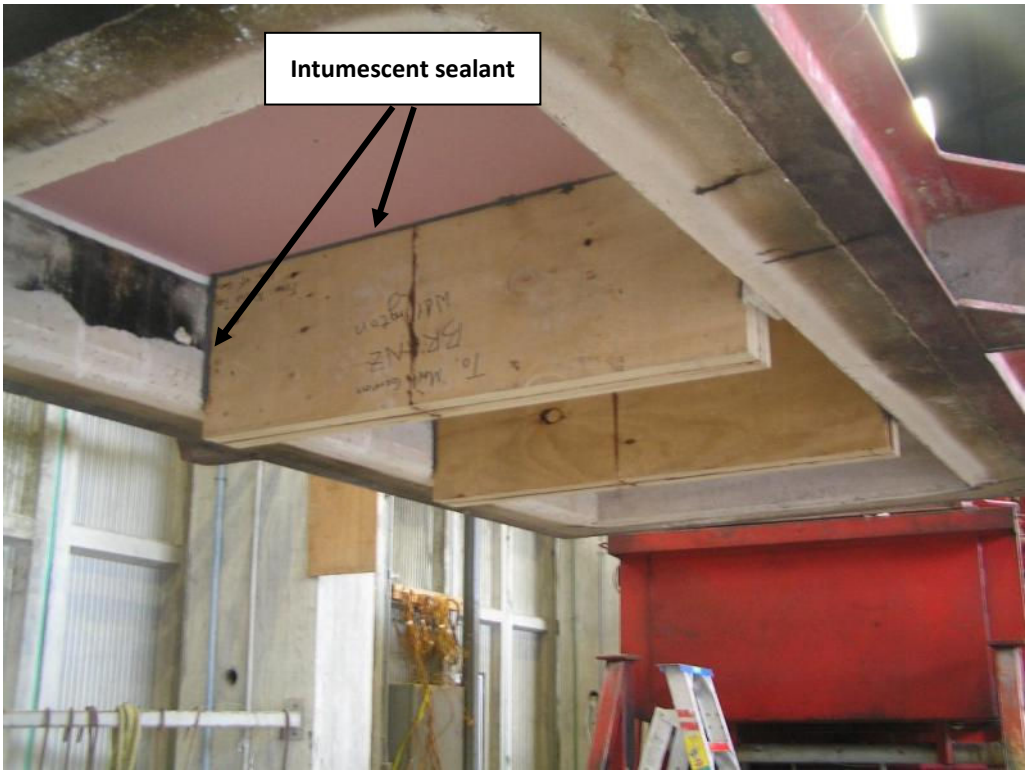

Figure 5-31: Suspended LVL specimens with intumescent sealant sealing all edges

5.6.2. Experimental Results and Discussions

After 60 minutes of fire exposure the specimen holder was lifted away from the pilot furnace. It was observed that both 90mm width double LVL specimens were completely charred away. The underside of the specimen holder after a 60 minute fire exposure is shown in Figure 5-32.

Figure 5-32: Underside of the specimen holder after the fourth pilot furnace test

Table 5-4 below summarises the instrumented side and bottom charring rates for each LVL specimen at various depths. The time for each thermocouple to reach 300^{o}C was extracted from the thermocouple readings recorded in the Excel spreadsheet. Refer to Appendix J for thermocouple readings of each specimen.

Figure 5-33 to Figure 5-38 show the comparative side and bottom thermocouple readings for each LVL specimen, Figure 5-39 and Figure 5-40 show the side and bottom charred depth as a function of time for each LVL specimen.

Table 5-4: Summary of charring rate at various depths for the fourth pilot furnace test

	Sample 1																	
	Left Side				Right Side				Bottom									
Thermocouple	**L1**	**L2**	**L3**	**L4**	**R1**	**R2**	**R3**	**R4**	**C1**	**C2**	**C3**	**C4**	**C5**	**C6**	**C7**	**C8**	**C9**	**C10**
Depth (mm)	10	20	30	40	10	20	30	40	10	20	30	40	50	60	70	80	90	100
Time to 300°C (min)	17	25	43	57	28	38	42	58	17	33	45	52	56	58	59	58	58	58
Charring Rate, β, (mm/min)	0.61	0.81	0.71	0.70	0.36	0.53	0.71	0.69	0.60	0.61	0.67	0.77	0.89	1.03	1.20	1.37	1.55	1.72
Average β (mm/min)	**0.70**				**0.58**				**1.04**									

	Sample 2																	
	Left Side				Right Side				Bottom									
Thermocouple	**L1**	**L2**	**L3**	**L4**	**R1**	**R2**	**R3**	**R4**	**C1**	**C2**	**C3**	**C4**	**C5**	**C6**	**C7**	**C8**	**C9**	**C10**
Depth (mm)	10	20	30	40	10	20	30	40	10	20	30	40	50	60	70	80	90	100
Time to 300°C (min)	16	33	41	56	15	33	-	-	15	28	42	52	54	57	57	57	57	57
Charring Rate, β, (mm/min)	0.65	0.62	0.74	0.72	0.68	0.61	-	-	0.66	0.72	0.72	0.78	0.93	1.05	1.22	1.40	1.59	1.77
Average β (mm/min)	**0.68**				**0.64**				**1.08**									

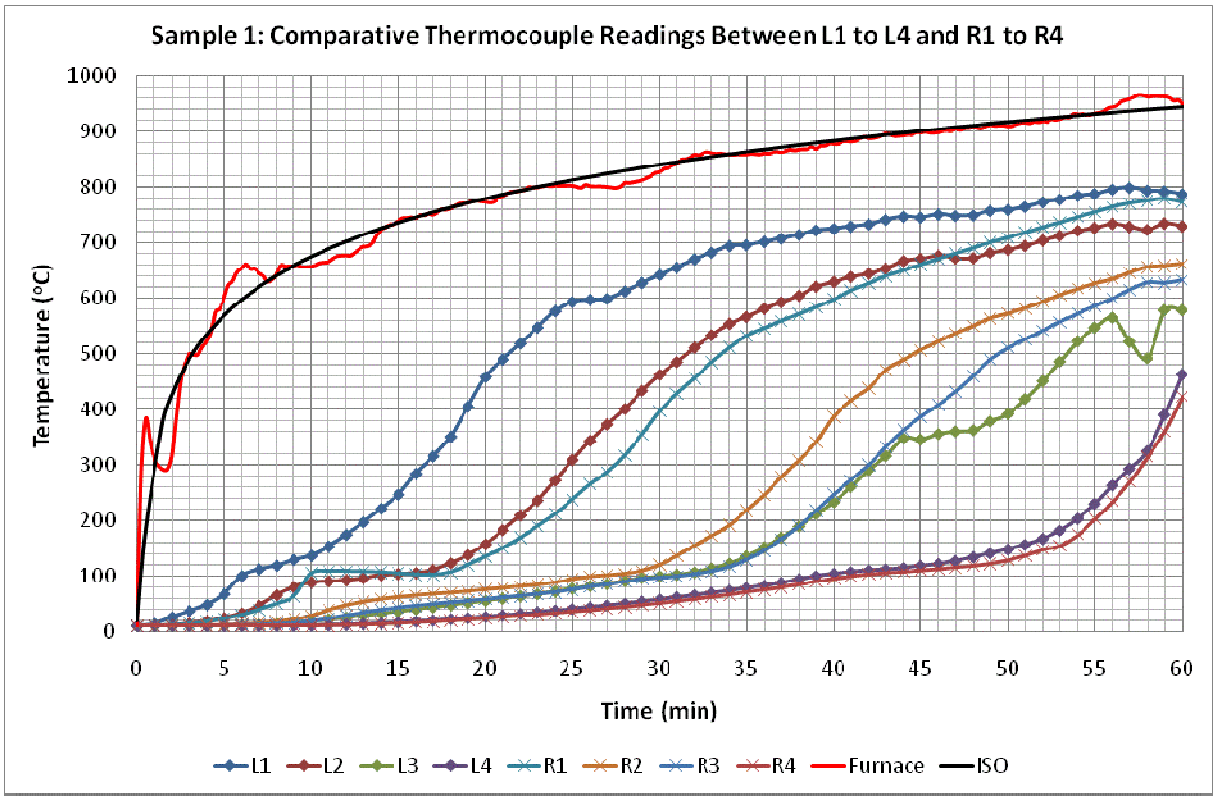

Figure 5-33: Comparative thermocouple readings between L1 to L4 and R1 to R4 for Sample 1

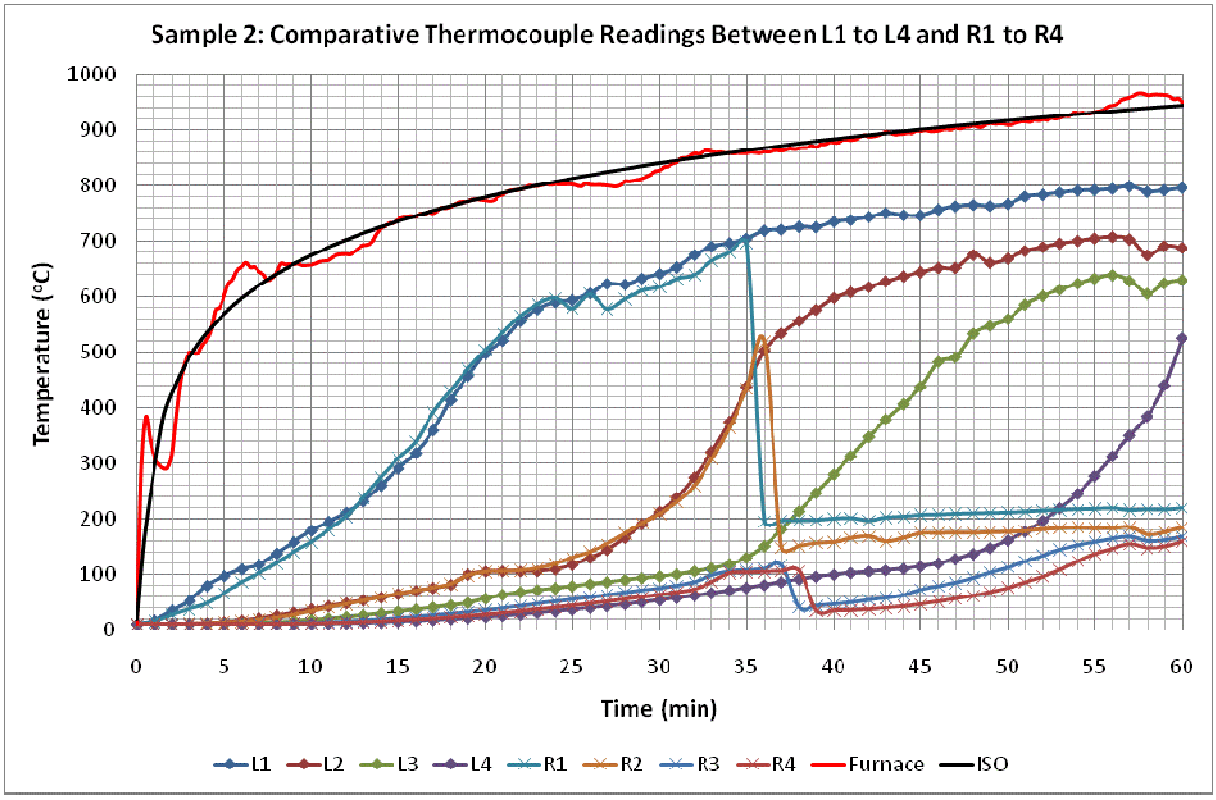

Figure 5-34: Comparative thermocouple readings between L1 to L4 and R1 to R4 for Sample 2

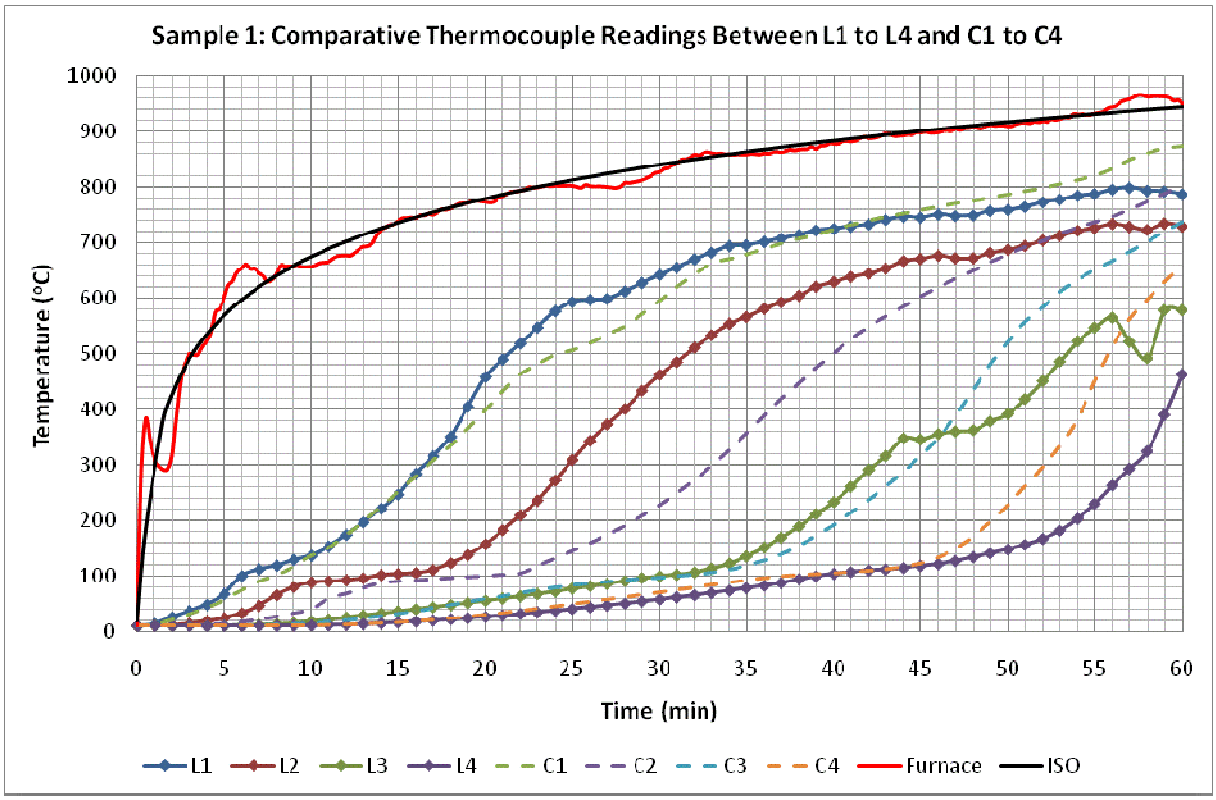

Figure 5-35: Comparative thermocouple readings between L1 to L4 and C1 to C4 for Sample 1

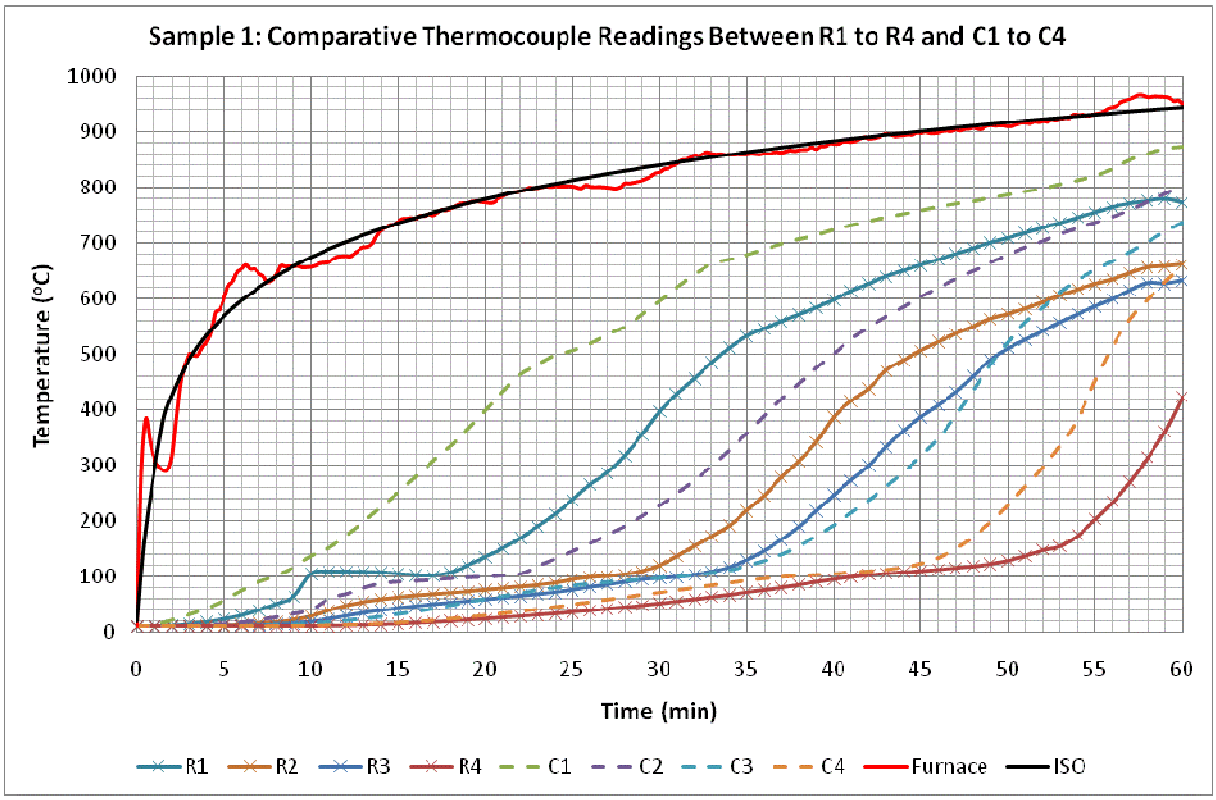

Figure 5-36: Comparative thermocouple readings between R1 to R4 and C1 to C4 for Sample 1

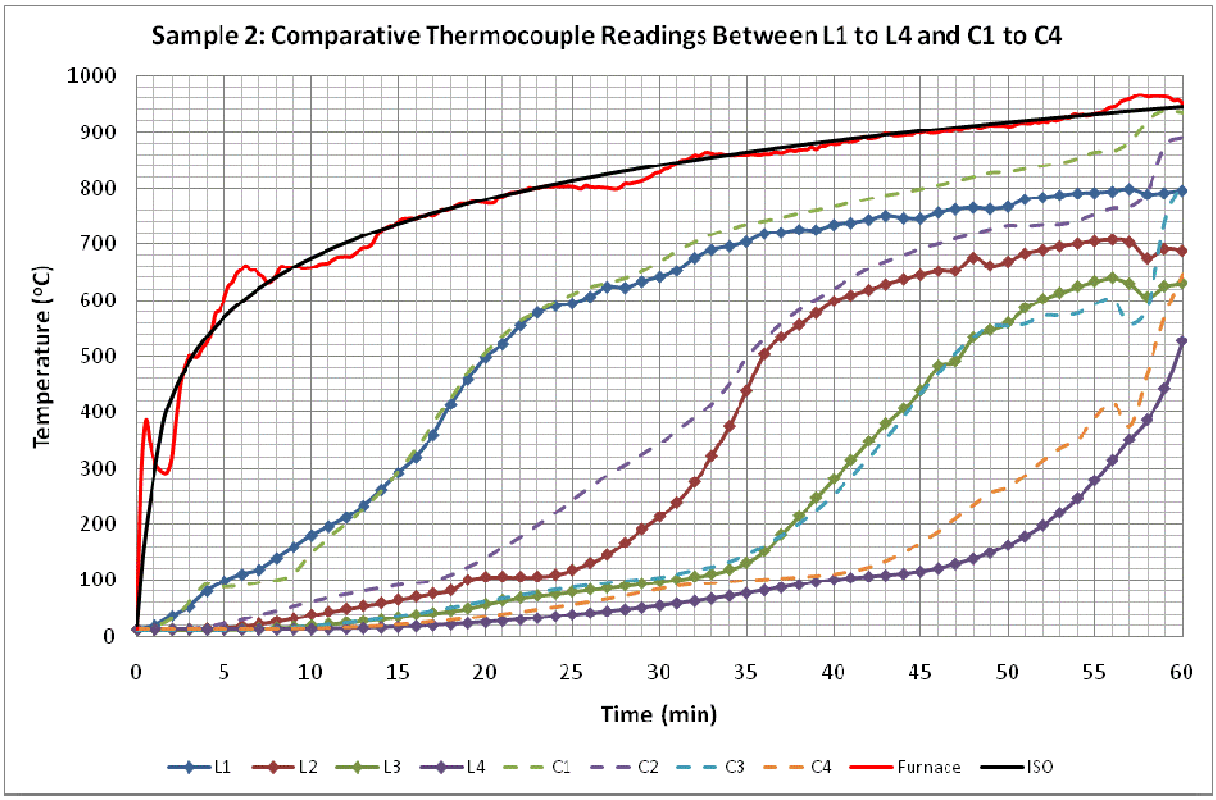

Figure 5-37: Comparative thermocouple readings between L1 to L4 and C1 to C4 for Sample 2

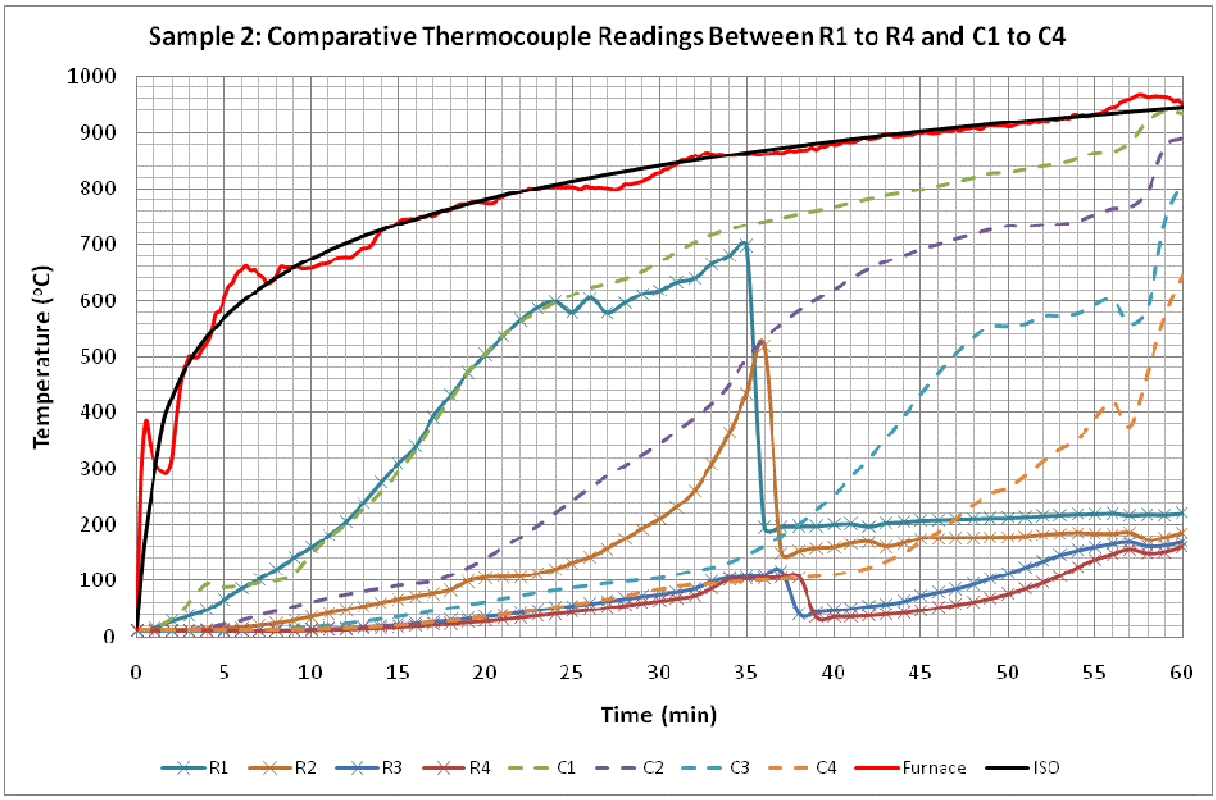

Figure 5-38: Comparative thermocouple readings between R1 to R4 and C1 to C4 for Sample 2

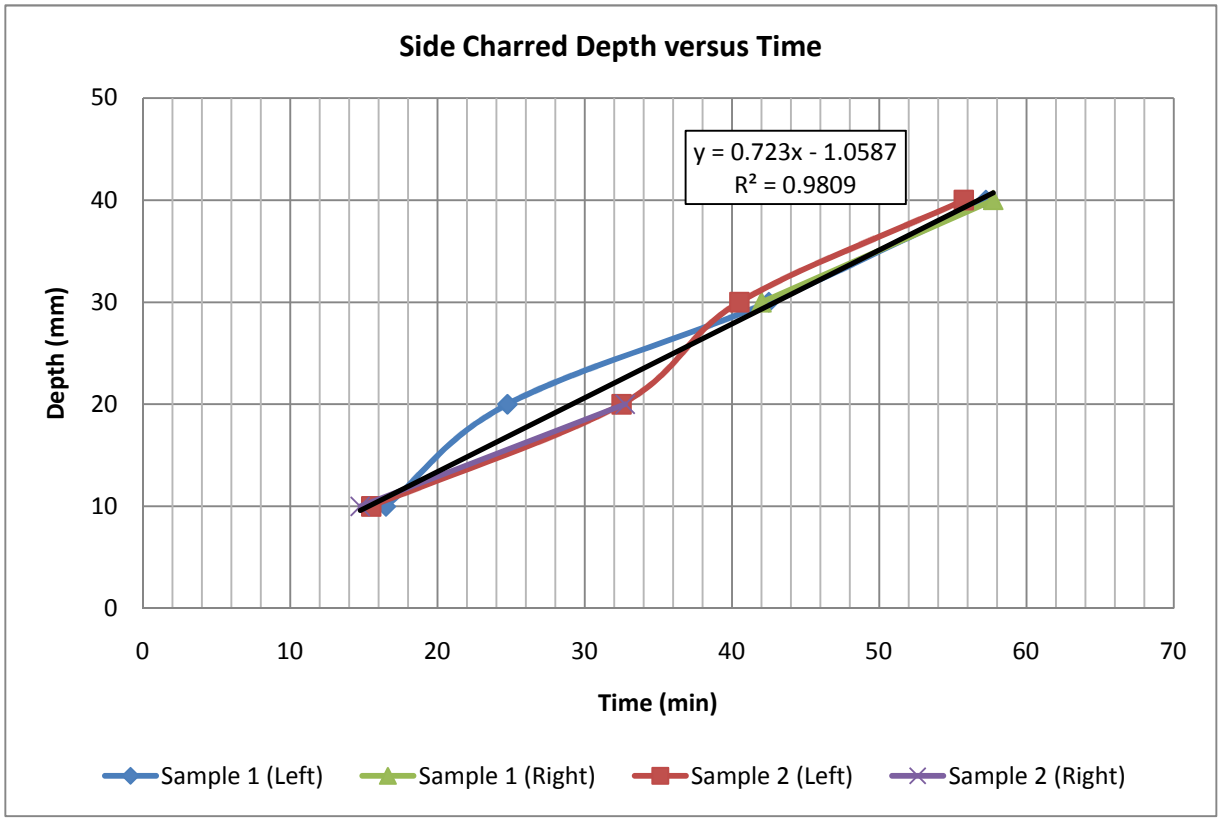

Figure 5-39: Side charred depth versus time for both Samples 1 and 2

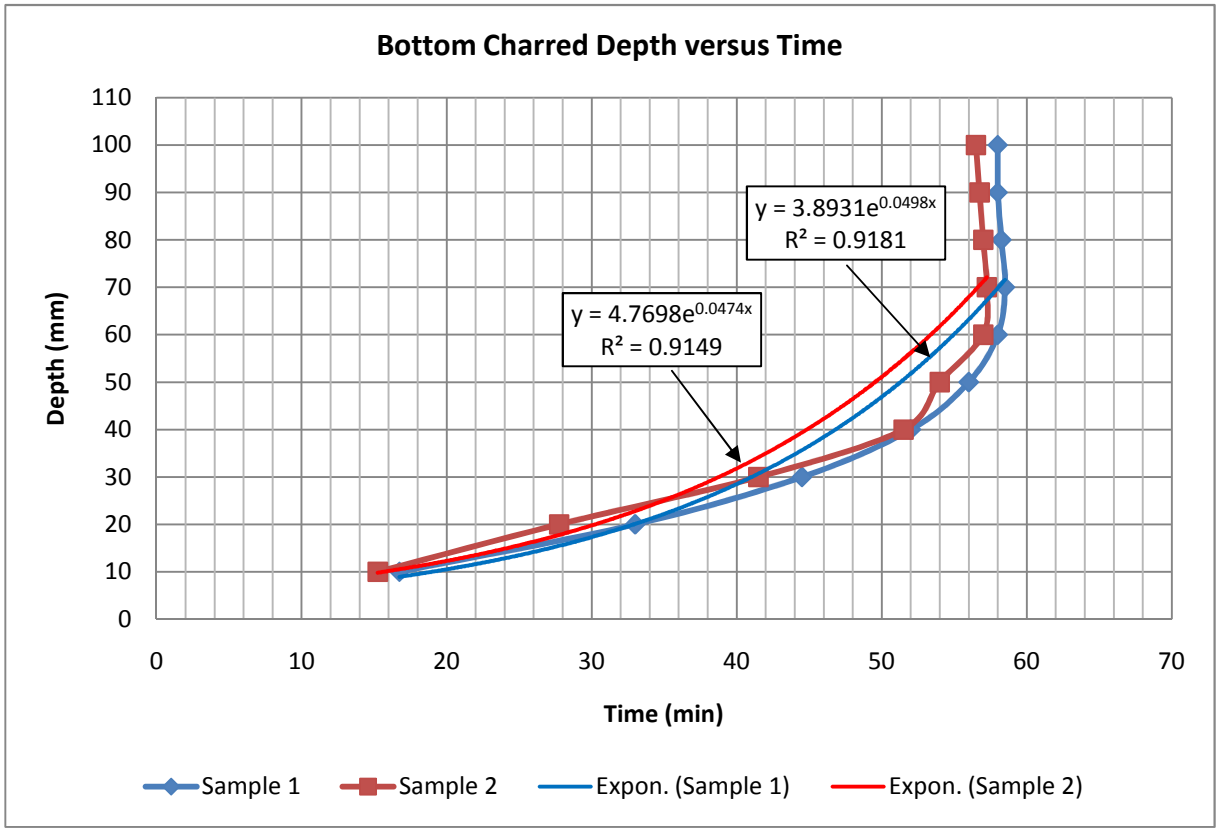

Figure 5-40: Bottom charred depth versus time for both Samples 1 and 2

In Table 5-4, test results show that for Sample 1, the average left side charring rate was 0.70mm/min which was higher than the average right side charring rate of 0.58mm/min. In theory both charring rates should be identical or close to each other since they were both one-dimensional charring. This inconsistency was due to the low charring rates measured by thermocouples R1 and R2, which were 0.36mm/min and 0.53mm/min respectively. This was supported by the comparative thermocouple readings between L1 to L4 and R1 to R4 as shown in Figure 5-33 where both thermocouples R1 and R2 produced much lower temperature readings in comparison with the thermocouples L1 and L2. Such low temperature readings may be caused by experimental uncertainties such as the installation or the failure of the thermocouples.

As for Sample 2, conversely, it was observed that the average right and left side charring rates were approximately identically, which were 0.68mm/min and 0.64mm/min, respectively. However it was noted that both thermocouples R3 and R4 did not reach 300^{o}C isotherm which was unlikely. It was observed in Figure 5-38 that at around the 35th minute of the fire testing, thermocouples R1 to R4 experienced some forms of failure which resulted in a drastic fall in the temperature reading. As a result, both thermocouples R3 and R4 did not reach the 300^{o}C isotherm. Having said that, comparative temperature readings between thermocouples L1 to L4 and R1 to R4 shown in Figure 5-34 were relatively close before the failure occurred.

In terms of the bottom charring rate, it was observed in Table 5-4 that both Samples 1 and 2 produced near identical average bottom charring rates, which were 1.04mm/min and 1.08mm/min respectively. They were much higher than their average side charring rate which was due to the fact that a change from the one-dimensional charring to the two-dimensional charring had occurred at the bottom face. For both Samples 1 and 2, a large increase in the bottom charring rate was observed approximately at the depth of 50mm which corresponded to the residual width of approximately 10mm. This indicates that the beginning of the two-dimensional charring may occur approximately at the depth in between 40 and 50mm. This corresponded well with the observation in Figure 5-40 that both Samples 1 and 2 started to experience an exponential bottom charred depth at a depth of approximately 45mm from the bottom. Meanwhile both test results in Table 5-4 and Figure 5-40 show that when the two-dimensional charring began, the remaining residual wood started to char relatively instantaneously at around the 57th or 58th minute of the fire testing.

Thermocouples C1 to C4 would experience one-dimensional charring during the initial stage of burning which means that their temperature readings should correspond relatively close with the temperature readings measured by thermocouples L1 to L4 or R1 to R4. The comparative thermocouple readings from Figure 5-35 to Figure 5-38 show that they all

showed a relatively close match in temperature trends except for the comparison between thermocouples R1 to R2 and C1 to C2 for Sample 1 and thermocouples R1 to R4 and C1 to C4 for Sample 2 as shown in Figure 5-36 and Figure 5-38, respectively.

In Figure 5-39, the side charred depths as a function of time for both Samples 1 and 2 were plotted. However experimental results for thermocouple R1 and R2 of Sample 1 were not plotted in this graph as they were considered erroneous. The linear trend line for all results suggests an averaging 0.72mm/min side charring rate with a R^2 value of 0.98. This result was similar to the value Lane (2004) determined in his research. His overall findings showed that for New Zealand manufactured radiata pine LVL, the cumulative char rate of 0.72mm/min should be used, and is representative for fire exposure in both edge grain and face grain orientations.

In Figure 5-40, it was observed that for both Samples 1 and 2 the initial bottom charring rate was relatively constant until at a depth of approximately 45mm which corresponds to the 52^{nd} minute. After the 52^{nd} minute, an exponential bottom charring rate was observed. This signifies that the two-dimensional charring occurred at a depth of approximately 45mm.

5.7. Summary

- Based on the first pilot furnace test, inconsistent side charring rates were observed for the 63mm width and the 90mm width LVL specimens. However the side charring rates for the 126mm width LVL specimen were consistent. For the 63mm width LVL specimen, a large increase in the bottom charring rate was observed at the depth of 50mm which corresponded to the residual width of approximately 10mm. This indicates that the beginning of the two-dimensional bottom charring may occur in between the depth of 40 and 50mm. Meanwhile for the 90mm width LVL specimen, , a large increase in the bottom charring rate was observed at the depth of 60mm which corresponded to the residual width of approximately 10mm. This suggests the beginning of the two-dimensional charring may occur between the depth of 50 and 60mm. For the 126mm width LVL specimen, the average bottom charring rate was observed to be similar to the average side charring rate. This shows that the bottom charring rate of the 126mm width LVL specimen did not go into a two-dimensional charring for a 75 minute fire exposure.

- Based on the second and the third pilot furnace tests, a staggered screw layout with a centre-to-centre spacing of 150mm is recommended if screws are used to join the double LVL members. The bottom row of screws is installed at 75mm from the bottom whereas the top row of screws is installed at 100mm from the bottom. One screw located 50mm from either ends of the LVL member is also recommended to prevent the

separation of the double LVL member at the ends.

- Based on the fourth pilot furnace test, the average side charring rate for the 90mm width LVL specimens were 0.72mm/min. Meanwhile a large increase in the bottom charring rate was observed approximately at the depth of 50mm which corresponded to the residual width of approximately 10mm. This indicates that the beginning of the two-dimensional charring may occur approximately at the depth in between 40 and 50mm.

6. SAFIR THERMAL ANALYSIS

6.1. Overview

SAFIR (Franssen, 2007) is a finite element program which uses the Finite Element Method (FEM) for the analysis of one, two or three-dimensional structures under ambient and elevated temperature conditions. The aim in using the SAFIR program in this research was to simulate the thermal behaviour of 63mm, 90mm and 126mm width LVL members under fire conditions. These simulated results were subsequently compared with the experimental results obtained from pilot furnace tests. In SAFIR, LVL members were also exposed to the standard ISO 834 (ISO 834, 1975) design fire curve.

6.2. Required LVL Thermal Properties in SAFIR

The required thermal properties In SAFIR for the LVL members are:

1. Specific mass of the material, including moisture (kg/m^3)
   - All experimentally tested LVL timbers were manufactured by Nelson Pine Industries Limited (Nelson, 2010). The Nelson Pine product specification states the specific mass of Nelson Pine LVL is 550kg/m^3.
2. Percentage of water content (%) relative to the dry mass (moisture content)
   - The average moisture content of Nelson Pine LVL is 8 to 15% according to the Nelson Pine product specification. Sensitivity analysis was carried in SAFIR using different moisture content (refer to Section 8.3.2. of this report).
3. Convection coefficients on hot and cold surfaces
   - From Drysdale (Drysdale, 1999), the natural convection in air is between 5 to 50 W/m^{2}K. Sensitivity analysis was carried out in SAFIR using different convection coefficients on hot and cold surfaces (refer to Section 8.3.3. of this report).
4. Relative emissivity
   - From Incorpera et al (Incorpera et al, 2007), the relative emissivity of wood is between 0.82 and 0.92. Sensitivity analysis was carried out in SAFIR using different relative emissivity (refer to Section 8.3.4. of this report).
5. Ratio between conductivity in the direction of the grain and in the transverse direction (orthotropy), usually greater than 1.0.
   - From the Forest Products Society (Forest Products Society, 1999), it states that the average ratio between the conductivity along the grain and across the grain is about 1.8.

6.3. Sensitivity Analysis

In this section sensitivity analyses such as the grid size and thermal properties of wood are described. They were conducted so that realistic thermal input values for the LVL wood could be determined and used in the SAFIR thermal analysis later on in this research.

63mm width by 300mm depth LVL member was analysed in the sensitivity analysis.

6.3.1. Mesh Size

Three different mesh sizes summarised in Table 6-1 were examined in this sensitivity analysis.

Table 6-1: Summary of the three different mesh sizes examined in SAFIR

Mesh Size	Width (mm)	Height (mm)	Number of Solids
1	15.75	15	80
2	6.3	6	500
3	3	3	2,100

Thermal properties input in the mesh size sensitivity analysis are summarised in Table 6-2. Thermal properties for the water content, conductivity and the relative emissivity were taken as the mean values.

Table 6-2: Thermal properties inputted in SAFIR for the mesh size sensitivity analysis

Specific Mass (kg/m^3)	Moisture Content (%)	Convection Coefficient (W/m^2K)		Relative Emissivity	Conduction Ratio
		Hot Faces	Cold Faces		
550	12	25	25	0.87	1.8

Figure 6-1 shows the comparative temperature distributions of the cross-section generated by SAFIR for these three different mesh sizes. These distributions were captured in different different time steps.

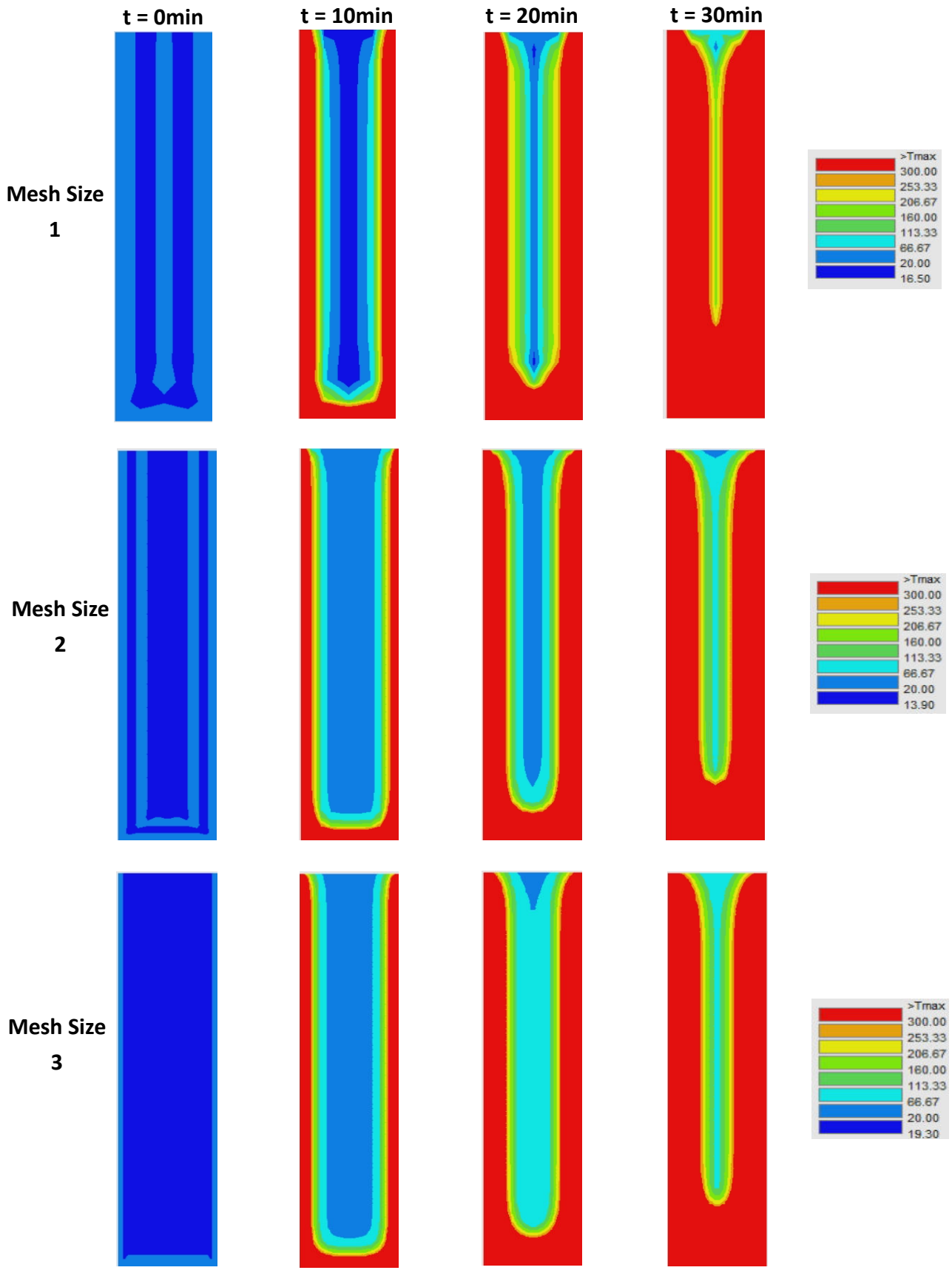

Figure 6-1: Comparative temperature distributions generated by SAFIR for these three different mesh sizes

In Figure 6-1 it was observed mesh size 1 appeared too coarse judging by their temperature distributions. Such coarse mesh size created a negative wood temperature in the early stage stage of the simulation. Meanwhile comparative temperature distributions between mesh size 2 and 3 showed that both mesh size 2 and 3 produced relatively similar results. This was was further supported by their comparative temperature curves generated by SAFIR as shown in Figure 6-2. These nodes taken for comparison were located at the mid-height of the LVL member. Their distances from the edge of the LVL member were summarized in Table 6-3. Due to a slight offset in the nodal distance, those comparative temperature readings were therefore slightly offset. Overall they were relatively the same.

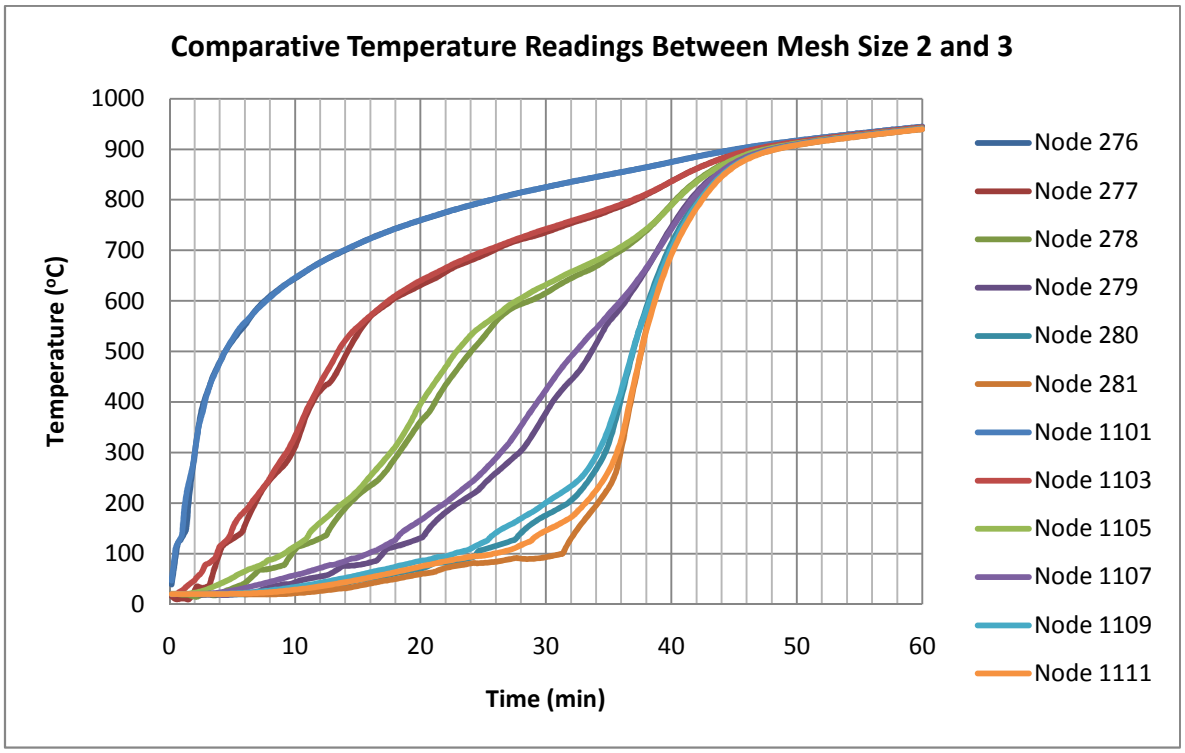

Figure 6-2: Comparative temperature readings between mesh size 2 and 3

Table 6-3: Comparative nodal numbers between mesh size 2 and 3

Mesh Size 2						
Nodal Number	276	277	278	279	280	291
Distance from Edge (mm)	0	6.3	12.6	18.9	25.2	31.5
Mesh Size 3						
Nodal Number	1101	1103	1105	1107	1109	1111
Distance from Edge (mm)	0	6	12	18	24	30

Therefore mesh size 2 is recommended after this sensitivity analysis and will be used in the SAFIR thermal analysis.

6.3.2. Moisture Content (%)

According to the Nelson Pine product specification, the average moisture content of Nelson Pine LVL is 8% to 15%. Hence in this sensitivity analysis, 8%, 12% and 15% moisture contents contents were examined in SAFIR. Other thermal properties inputted in SAFIR for the moisture content sensitivity analysis were summarised in Table 6-4.

Table 6-4: Other thermal properties inputted in SAFIR for the moisture content sensitivity analysis

Specific Mass (kg/m^3)	Convection Coefficient (W/m^2K)		Relative Emissivity	Conduction Ratio
	Hot Faces	Cold Faces		
550	25	25	0.87	1.8

Figure 6-3 below shows the comparative temperature readings generated by SAFIR between 8%, 12% and 15% moisture content at node 276 to 280.

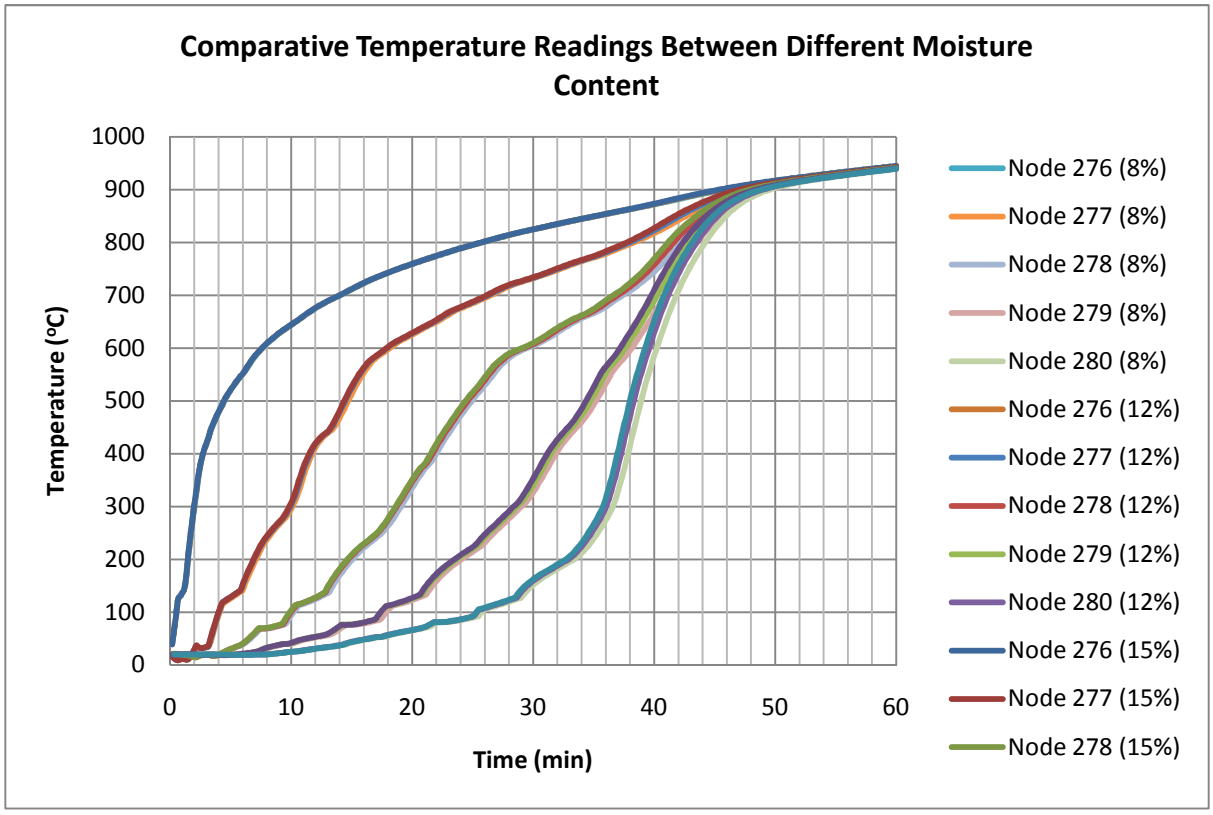

Figure 6-3: Comparative temperature readings between different moisture content

Simulation results in Figure 6-3 show that the effect of change in the moisture content was negligible in the SAFIR thermal analysis. Hence an average 12% moisture content will be used in the SAFIR thermal analysis.

6.3.3. Convection Coefficients on Hot and Cold Surfaces

It was stated by Drysdale (Drysdale, 1999) that the natural convection in air is between 5 W/m^2K to 50 W/m^2K. Hence four different sets of convection coefficients on hot and cold surfaces, summarised in Table 6-5, were examined. Other thermal properties inputted in SAFIR for the convection coefficient sensitivity analysis were summarised in Table 6-6.

Table 6-5: Summary of the four sets of convection coefficients examined in SAFIR

		Set 1	Set 2	Set 3	Set 4
Convection Coefficient (W/m^2K)	Hot Surface	13	25	25	50
	Cold Surface	5	10	25	20

Table 6-6: Other thermal properties inputted in SAFIR for the convection coefficient sensitivity analysis

Specific Mass (kg/m^3)	Moisture Content (%)	Relative Emissivity	Conduction Ratio
550	12	0.87	1.8

Figure 6-4 shows the comparative temperature readings generated by SAFIR between these four sets of convection coefficients at node 276 to 280.

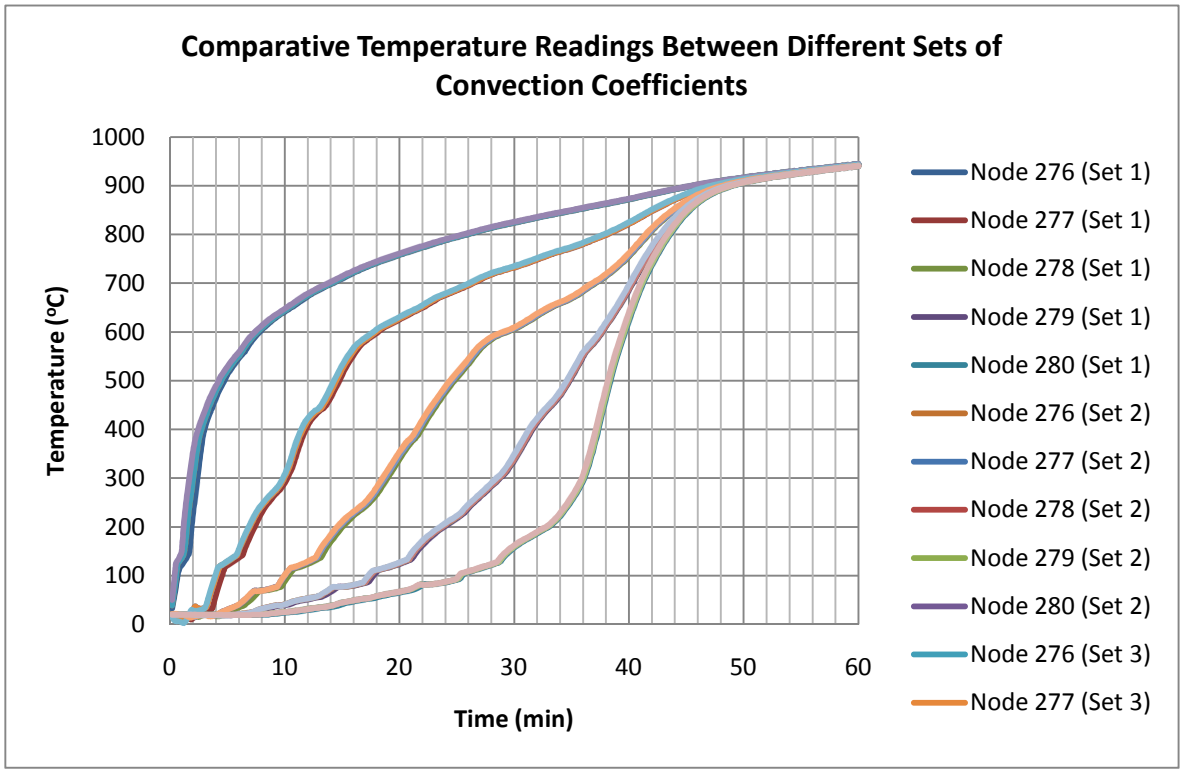

Figure 6-4: Comparative temperature readings between different sets of convection coefficients

It was observed in Figure 6-4 that the effect of change in the convection coefficient on the temperature readings generated by SAFIR was minor. Therefore an average 25W/m^{2}K convection coefficients on both hot and cold surfaces, i.e. Set 3, will be used in the SAFIR thermal analysis.

6.3.4. Relative Emissivity

From Incorpera et al (Incorpera et al, 2007), the relative emissivity of wood is between 0.82 and 0.92. Therefore three different relative emissivity, which were 0.82, 0.87 and 0.92, were were examined. Other thermal properties inputted in SAFIR for the relative emissivity sensitivity analysis were summarised in Table 6-7.

Table 6-7: Other thermal properties inputted in SAFIR for the relative emissivity sensitivity analysis

Specific Mass (kg/m^3)	Moisture Content (%)	Convection Coefficient (W/m^{2}K)		Conduction Ratio
		Hot Faces	Cold Faces	
550	12	25	25	1.8

Figure 6-5 shows the comparative temperature readings generated by SAFIR between these three different relative emissivity at node 276 to 280.

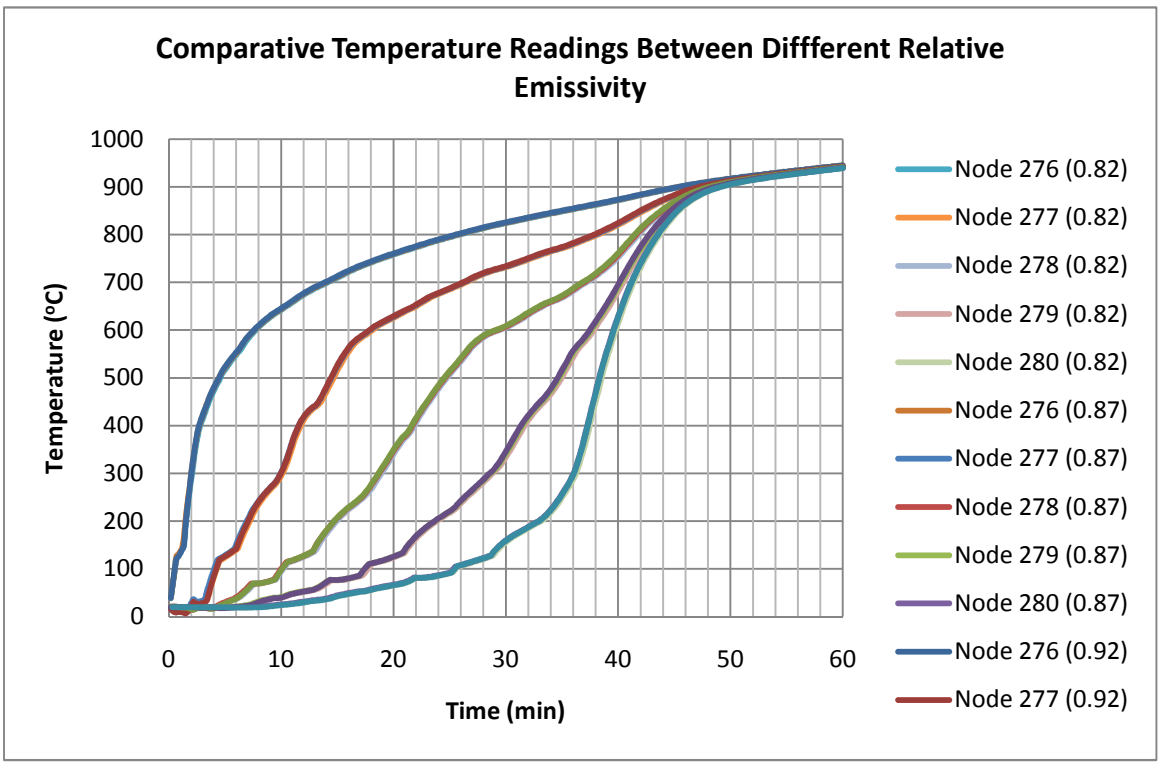

Figure 6-5: Comparative temperature readings between different relative emissivity

It was observed in Figure 6-5 that the effect of change in the relative emissivity on the temperature readings generated by SAFIR was negligible. Therefore an average 0.87 relative emissivity will be used in the SAFIR thermal analysis.

6.3.5. Summary

In conclusion, the mesh size and thermal properties used for the 63mm, 90mm and 126mm width LVL members in the SAFIR thermal analysis are summarised in Table 6-8.

Table 6-8: Summary of the mesh size and thermal properties used for the LVL member inputted in SAFIR

LVL Width (mm)	Mesh Size (mm)		Specific Mass (kg/m^3)	Moisture Content (%)	Convection Coefficient (W/m^2K)		Relative Emissivity	Conduction Ratio
	Width	Height			Hot Faces	Cold Faces		
63	6.3	6	550	12	25	25	0.87	1.8
90	6	6						
126	6	6						

6.4. SAFIR Thermal Analysis on 63mm, 90mm and 126mm Width LVL Members

In this section, descriptions of LVL members with 63mm, 90mm and 126mm width which were analysed in the SAFIR program are provided. Figure 6-6 to Figure 6-8 show some temperature distributions of the cross-section of the 63mm, 90mm and 126mm width by 300mm depth LVL members generated by SAFIR. These temperature distributions were based on the mesh size and thermal properties summarised in Table 6-8. Refer to Appendix K to Appendix M for more temperature distributions at various time steps.

Meanwhile Table 6-9 summarises the side and bottom charring rates at various nodal points generated by the SAFIR thermal analysis. Those nodal points were located at the mid-height mid-height and depth of the LVL members. Their depths also corresponded to the experimental depths of the thermocouples. Their temperature profiles are shown in Figure 6-9 to Figure 6-14.

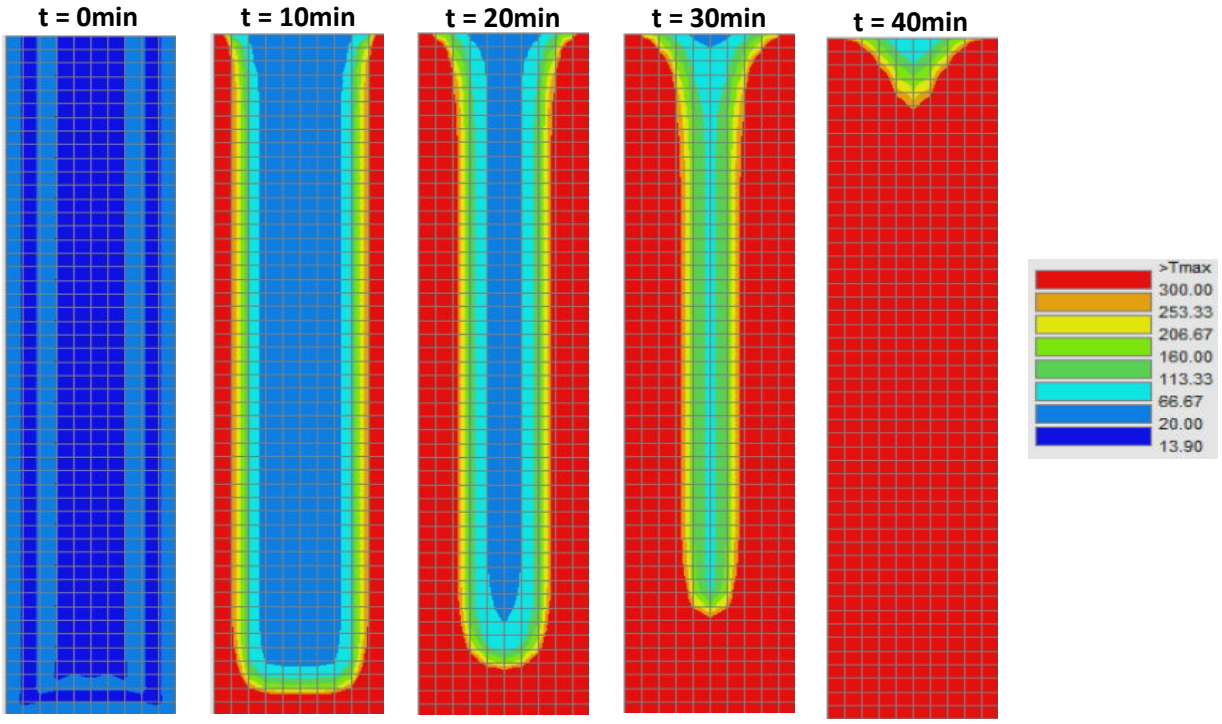

Figure 6-6: Temperature distributions of the 63mm width LVL member generated by SAFIR

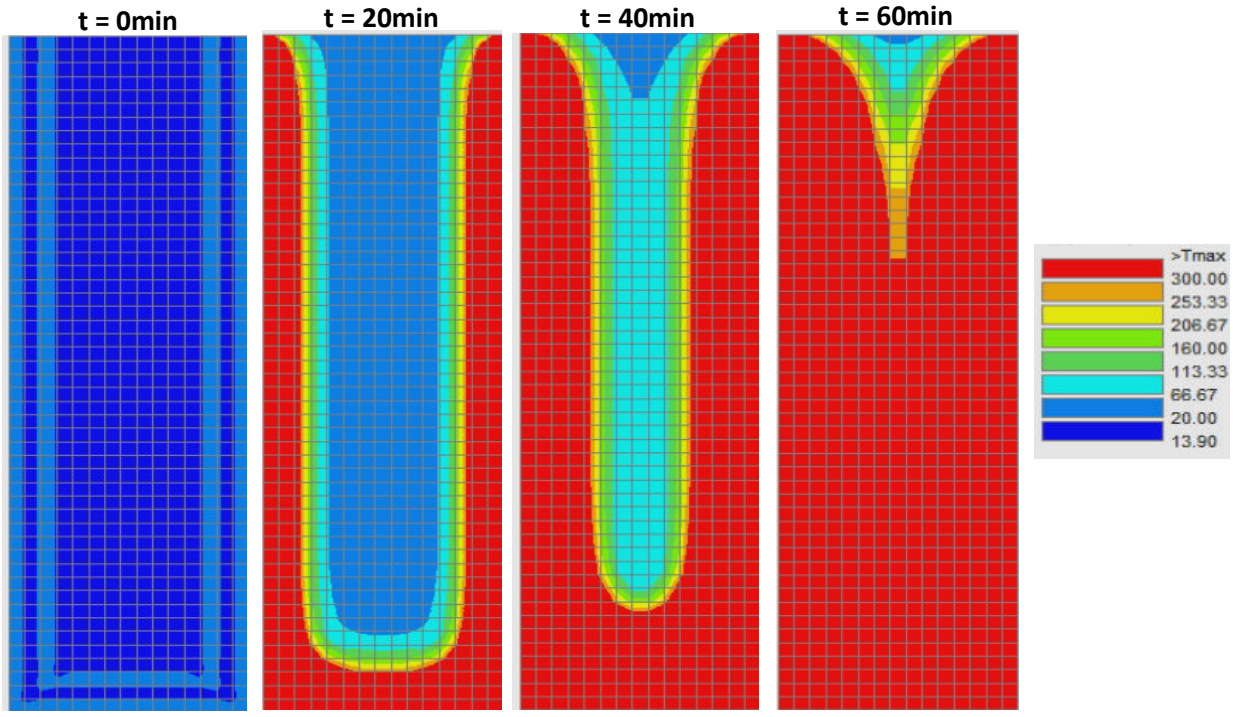

Figure 6-7: Temperature distributions of the 90mm width LVL member generated by SAFIR

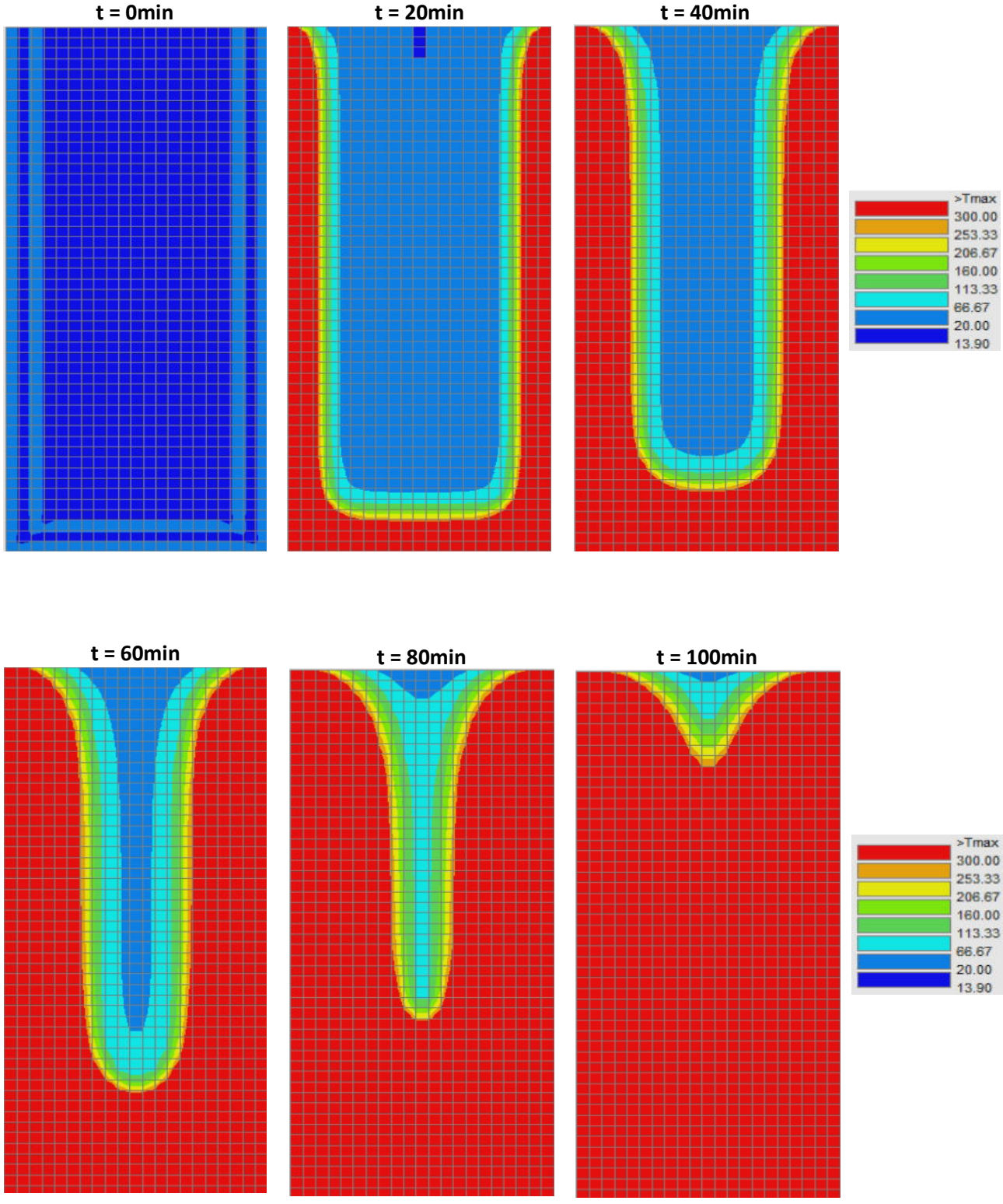

Figure 6-8: Temperature distributions of the 1260mm width LVL member generated by SAFIR

Table 6-9: Summary of the side and bottom charring rates at various nodal points generated by SAFIR

	63mm Width										
	Side			Bottom							
Node	**107**	**108**	**109**	**11**	**18**	**25**	**32**	**39**	**46**	**53**	**60**
Depth (mm)	10	20	33	10	20	30	40	50	60	70	80
Time to 300°C (min)	14	30	36	12	20	25	28	31	33	34	35
Charring Rate, β (mm/min)	0.71	0.67	0.93	0.81	1.01	1.22	1.42	1.63	1.85	2.07	2.31
Average β (mm/min)	**0.77**			**1.54**							

	90mm Width													
	Side					Bottom								
Node	**167**	**168**	**169**	**170**	**171**	**17**	**28**	**39**	**50**	**61**	**72**	**83**	**94**	**105**	**116**
Depth (mm)	10	20	30	40	45	10	20	30	40	50	60	70	80	90	100
Time to 300°C (min)	14	30	47	58	59	12	23	32	38	43	47	50	53	55	56
Charring Rate, β (mm/min)	0.71	0.67	0.64	0.69	0.76	0.85	0.88	0.95	1.05	1.16	1.27	1.39	1.51	1.64	1.78
Average β (mm/min)	**0.69**					**1.25**									

	126mm Width																
	Side						Bottom										
Node	**197**	**198**	**199**	**200**	**201**	**202**	**20**	**33**	**46**	**59**	**72**	**85**	**98**	**111**	**124**	**137**	**150**	**163**
Depth (mm)	10	20	30	40	50	63	10	20	30	40	50	60	70	80	90	100	110	120
Time to 300°C (min)	14	30	48	66	84	89	12	23	35	46	54	61	67	71	75	79	81	84
Charring Rate, β (mm/min)	0.71	0.67	0.63	0.61	0.60	0.71	0.85	0.87	0.86	0.88	0.92	0.98	1.05	1.12	1.19	1.27	1.35	1.43
Average β (mm/min)	**0.65**						**1.07**											

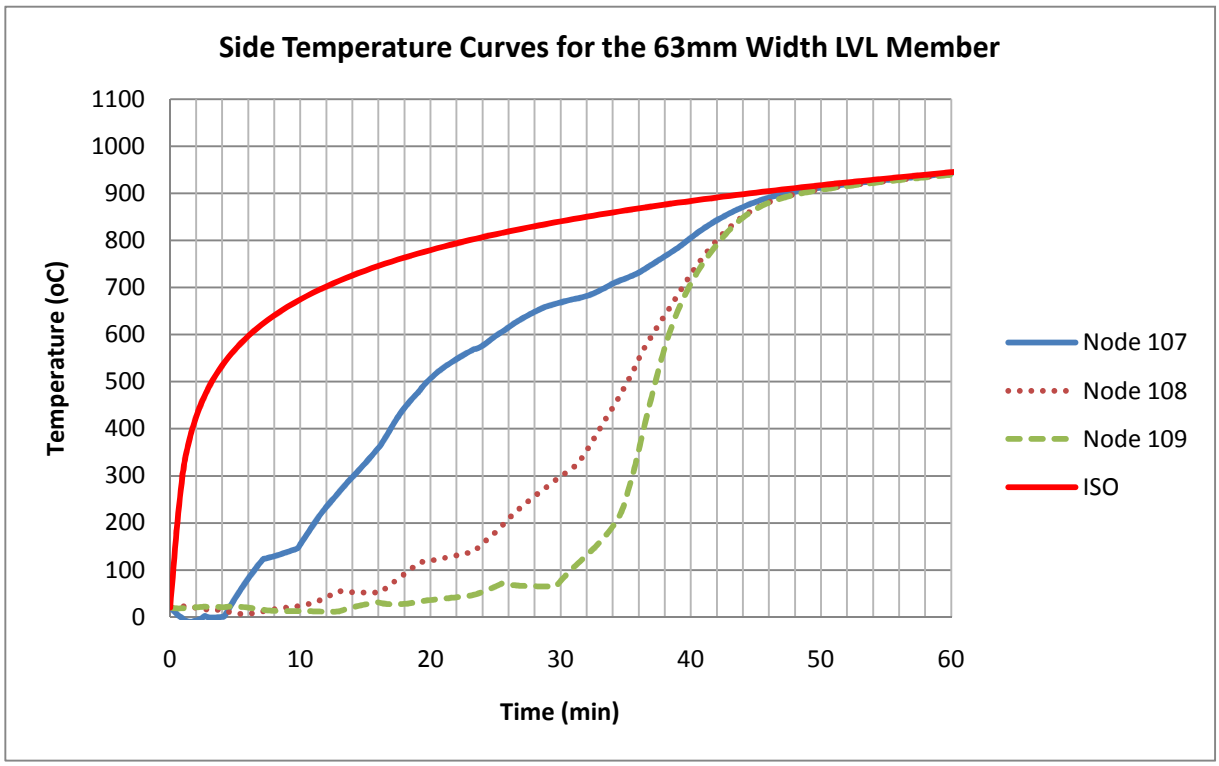

Figure 6-9: Side temperature curves for the 63mm width LVL member

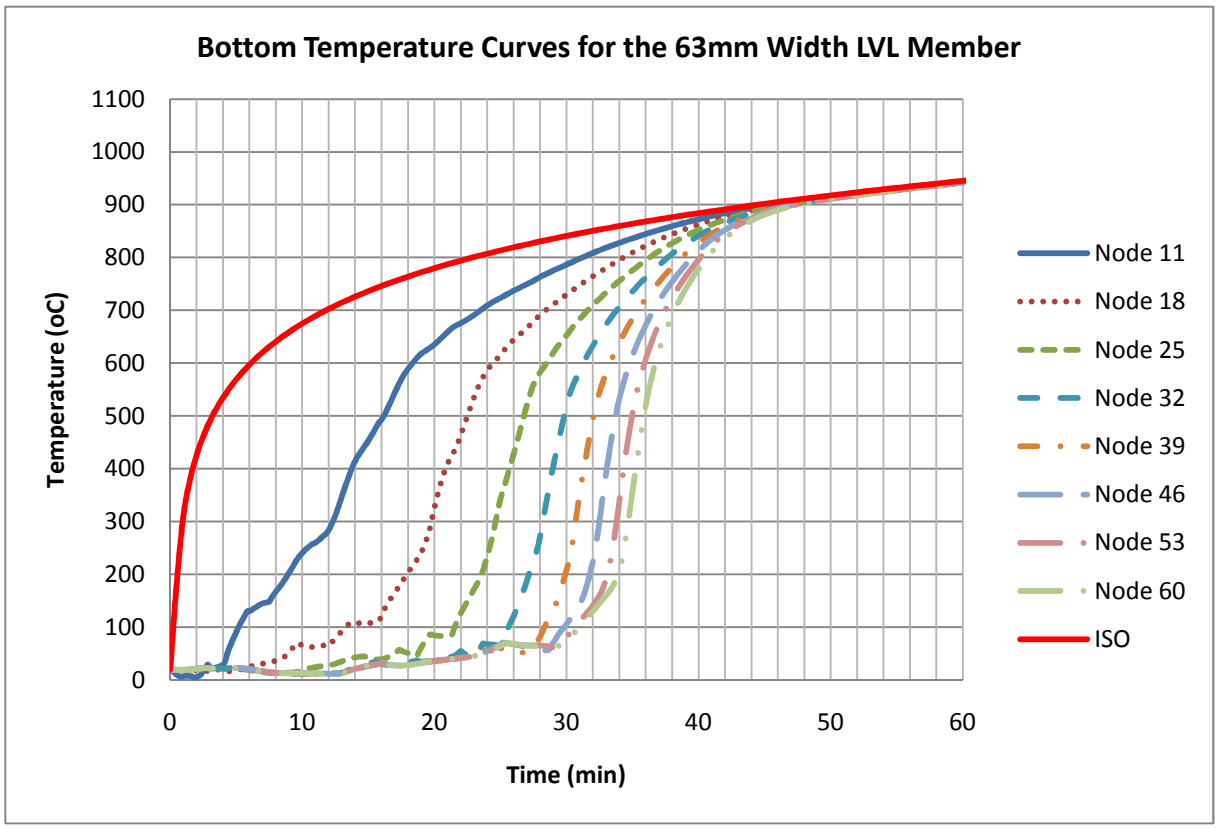

Figure 6-10: Bottom temperature curves for the 63mm width LVL member

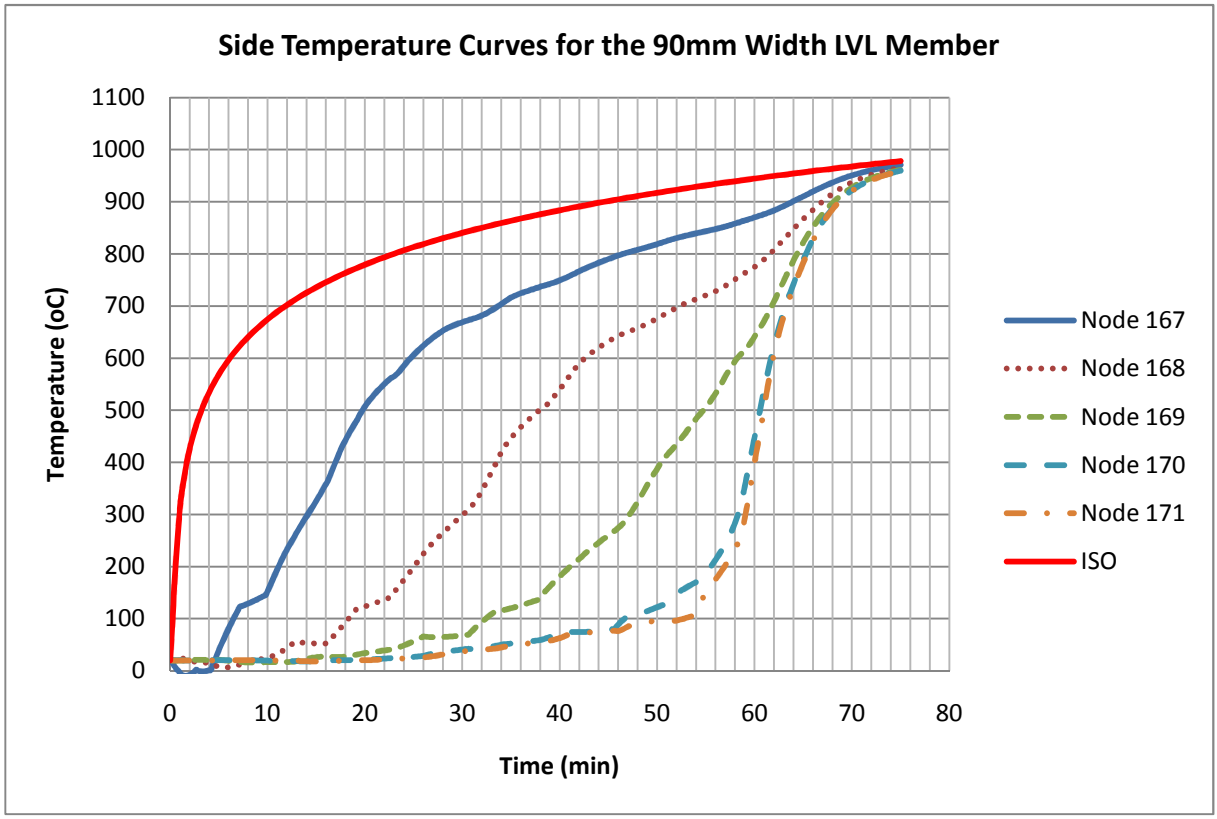

Figure 6-11: Side temperature curves for the 90mm width LVL member

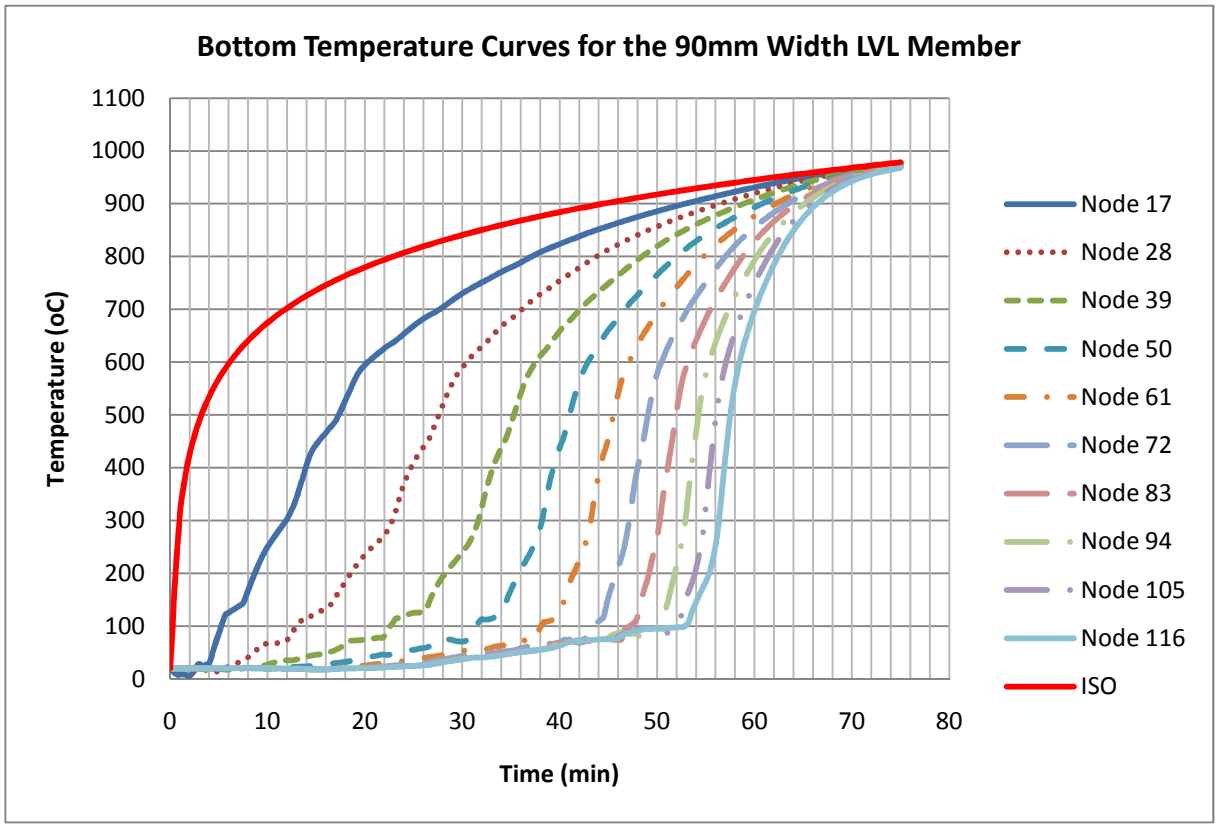

Figure 6-12: Bottom temperature curves for the 90mm width LVL member

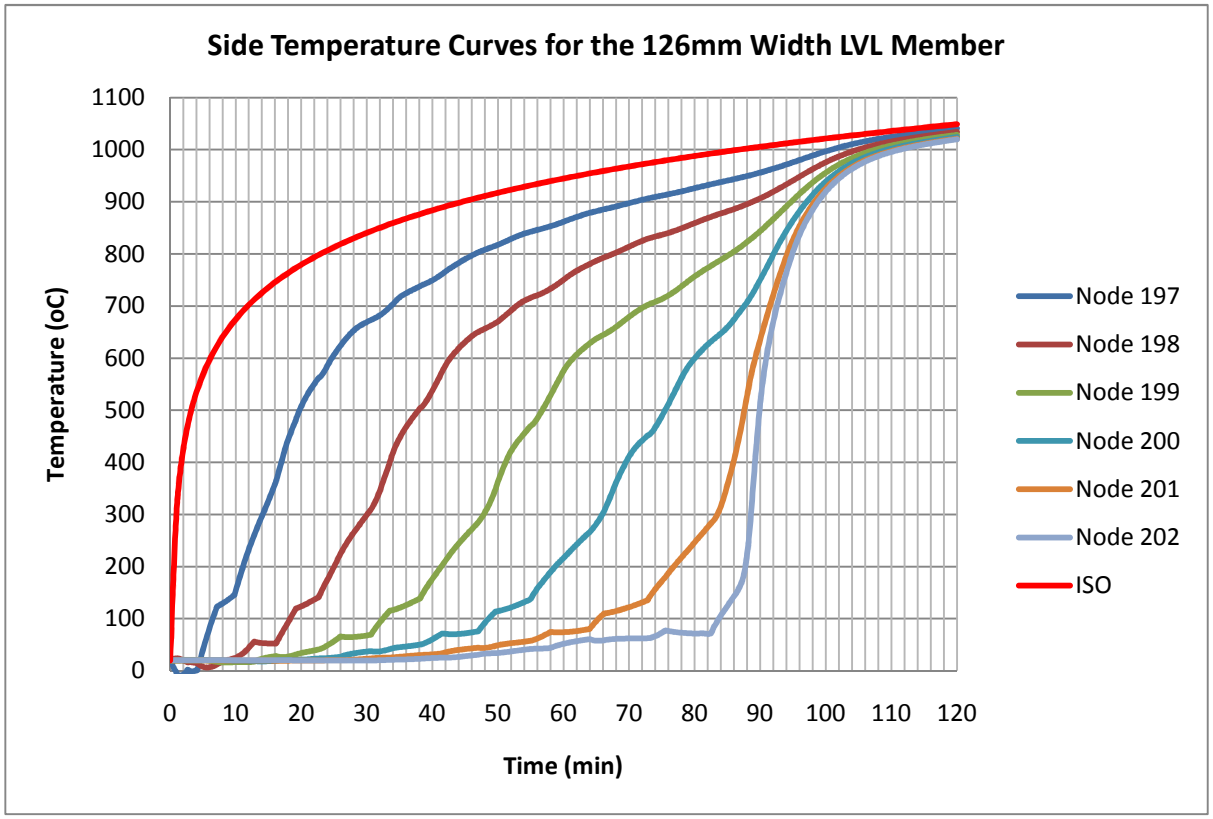

Figure 6-13: Side temperature curves for the 126mm width LVL member

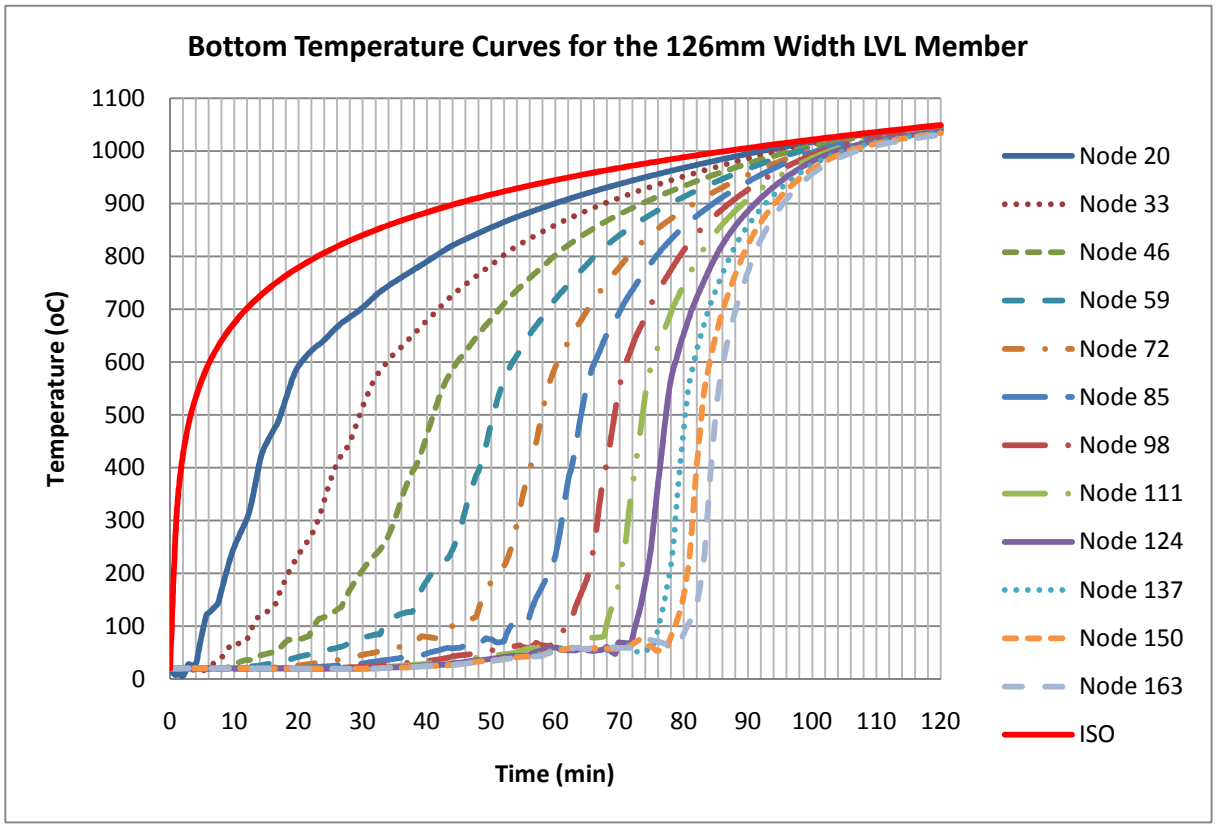

Figure 6-14: Bottom temperature curves for the 126mm width LVL member

In Table 6-9, it is observed that the average side charring rate between the 63mm, 90mm and 126mm width LVL members generated by SAFIR were approximately the same. This is expected as they were experiencing one-dimensional charring throughout the entire fire exposure. However nodes 109, 171 and 202 of the 63mm, 90mm and 126mm width LVL members respectively, which were located at the centre of the member, were observed to have an increase in the charring rate. This was due to the last stage of the burning when the residual cross section of the LVL was so thin and thus resulted in an instantaneous burning of the entire cross-section of the wood.

It was also observed that all bottom charring rates for all three LVL members were higher than their respective side charring rate. In theory, the bottom face should be experiencing one-dimensional charring rate at the initial stage of burning. Hence the initial bottom charring rate should correspond similarly with the side charring rate which is supported by the BRANZ experimental results shown in Table 5-1 and Table 5-4. However it was observed that the initial bottom charring rate was already higher than the side charring rate. This suggests that the bottom charring rate generated by SAFIR was more conservative than in practice.

Temperature curves generated by SAFIR in Figure 6-9 to Figure 6-14 show they all followed a similar trend and were in a consistent manner.

6.5. Comparison between BRANZ Experimental Results and SAFIR Simulation

The comparative temperature readings between the BRANZ experimental results and the SAFIR simulation for the 63mm, 90mm and 126mm width LVL members are shown in Figure 6-15 to Figure 6-21.

In Figure 6-15 to Figure 6-21, it was observed that overall the comparative temperature readings between the BRANZ test results and the SAFIR simulation did not correspond very well. Although both the BRANZ test results and the SAFIR simulation showed reasonable approximation close to the surface, the mismatch became more and more pronounced for interior fibres. One possible reason behind such discrepancy may be due to the difference in the heating condition of the LVL member in the pilot furnace and in the SAFIR modelling. In the pilot furnace, the heating condition around the LVL specimens may be non-uniform whereas in SAFIR, a uniform heating condition is applied around the LVL member.

In a study carried out by Fragiacomo et al (2009), test results obtained from the small furnace and the pilot furnace were compared with those from an Abaqus computer model (2006). The overall findings also showed that both the experimental results and the Abaqus simulation were acceptably close near the surface but the accuracy reduced for deeper fibres.

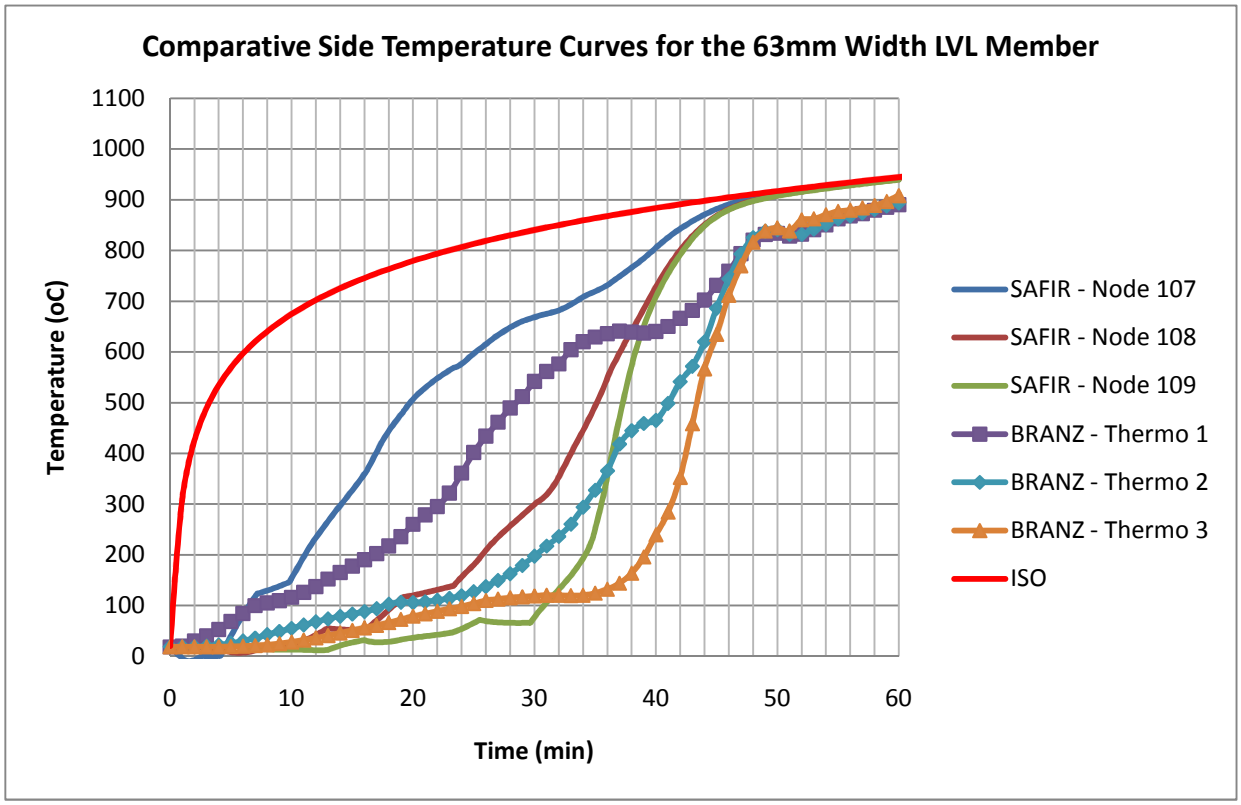

Figure 6-15: Comparative side temperature curves for the 63mm width LVL member

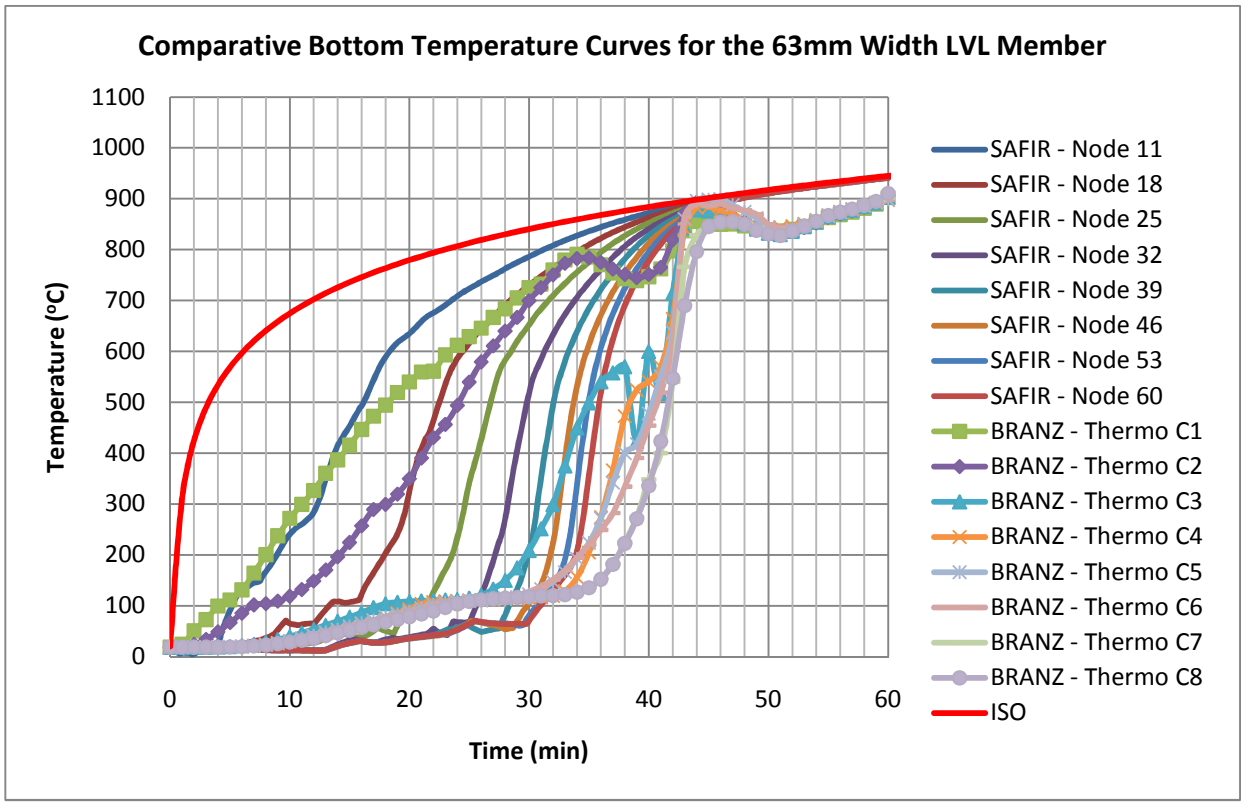

Figure 6-16: Comparative bottom temperature curves for the 63mm width LVL member

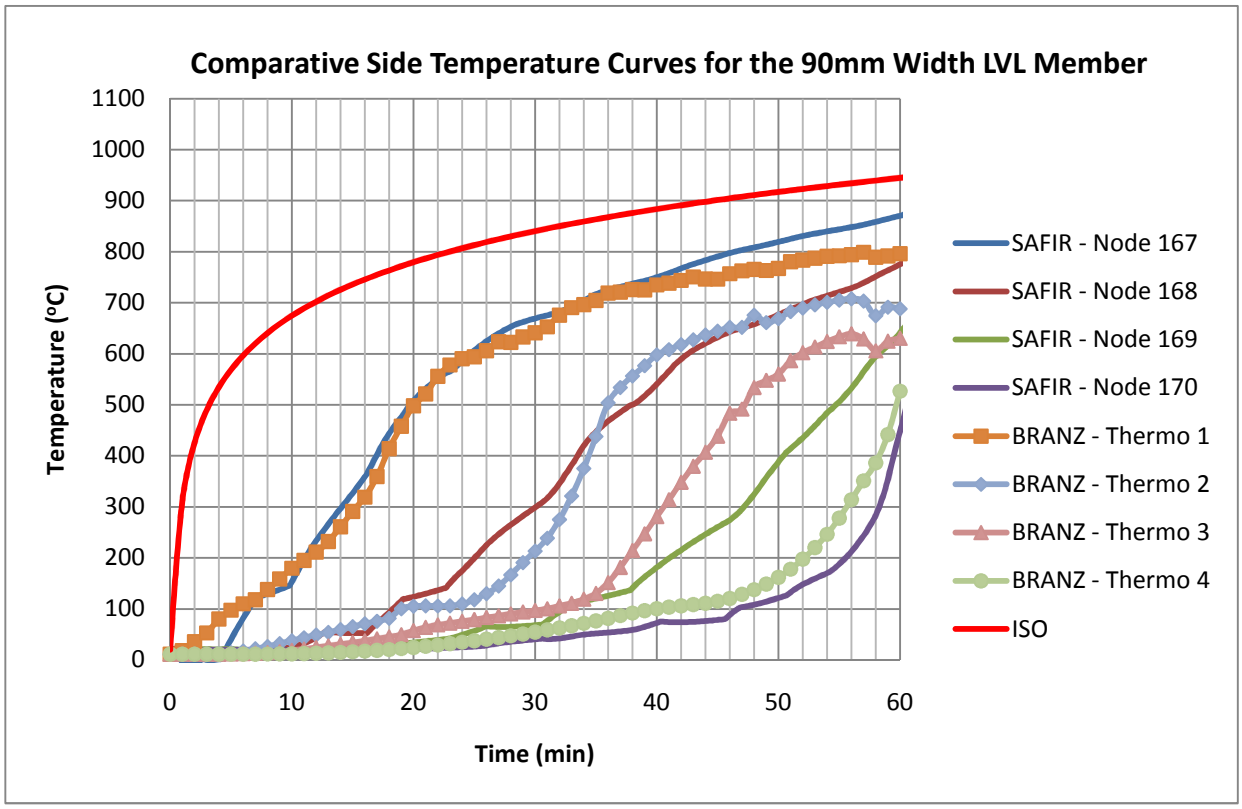

Figure 6-17: Comparative side temperature curves for the 90mm width LVL member

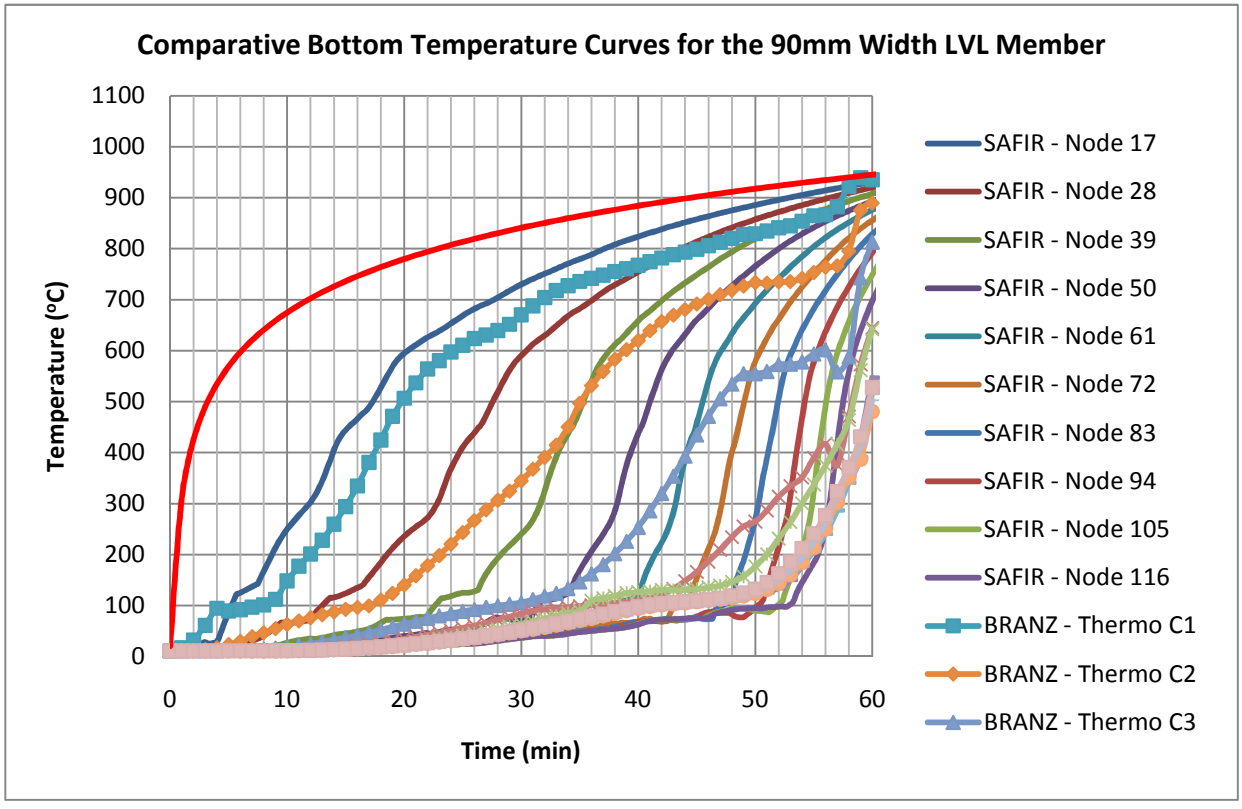

Figure 6-18: Comparative bottom temperature curves for the 90mm width LVL member

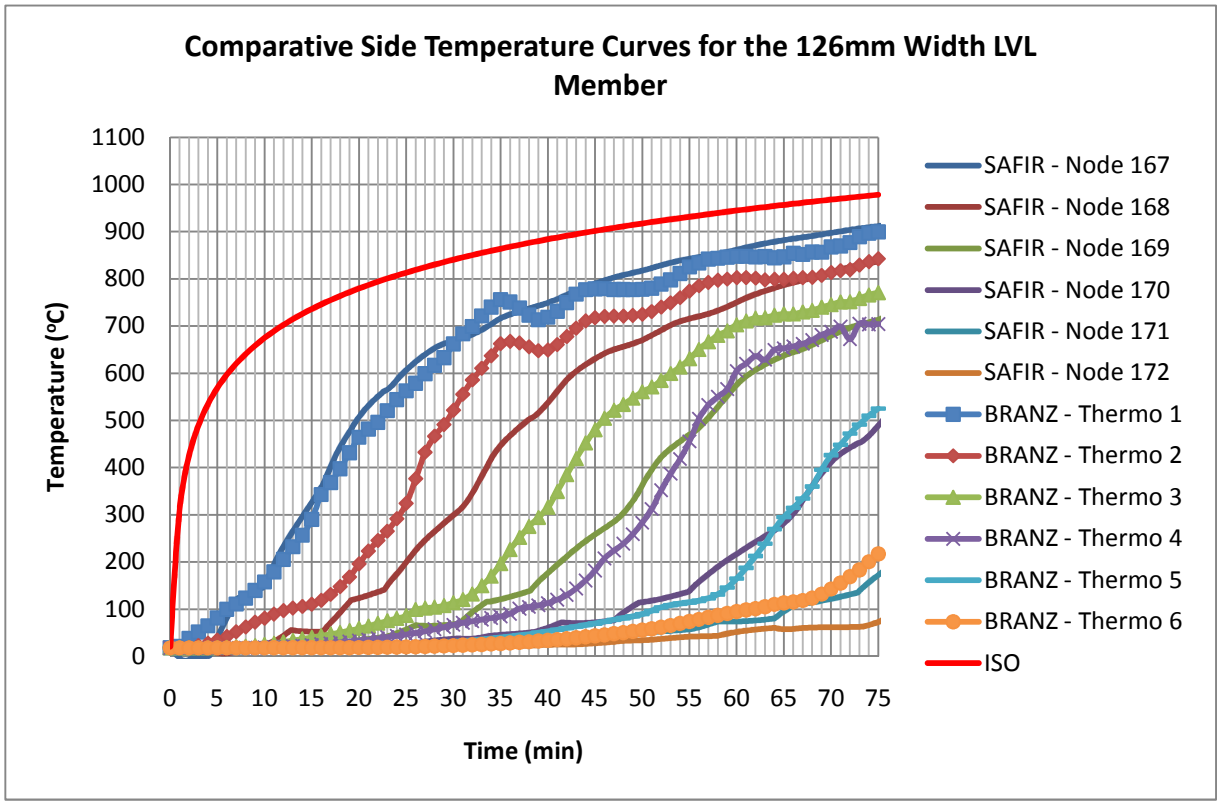

Figure 6-19: Comparative side temperature curves for the 126mm width LVL member

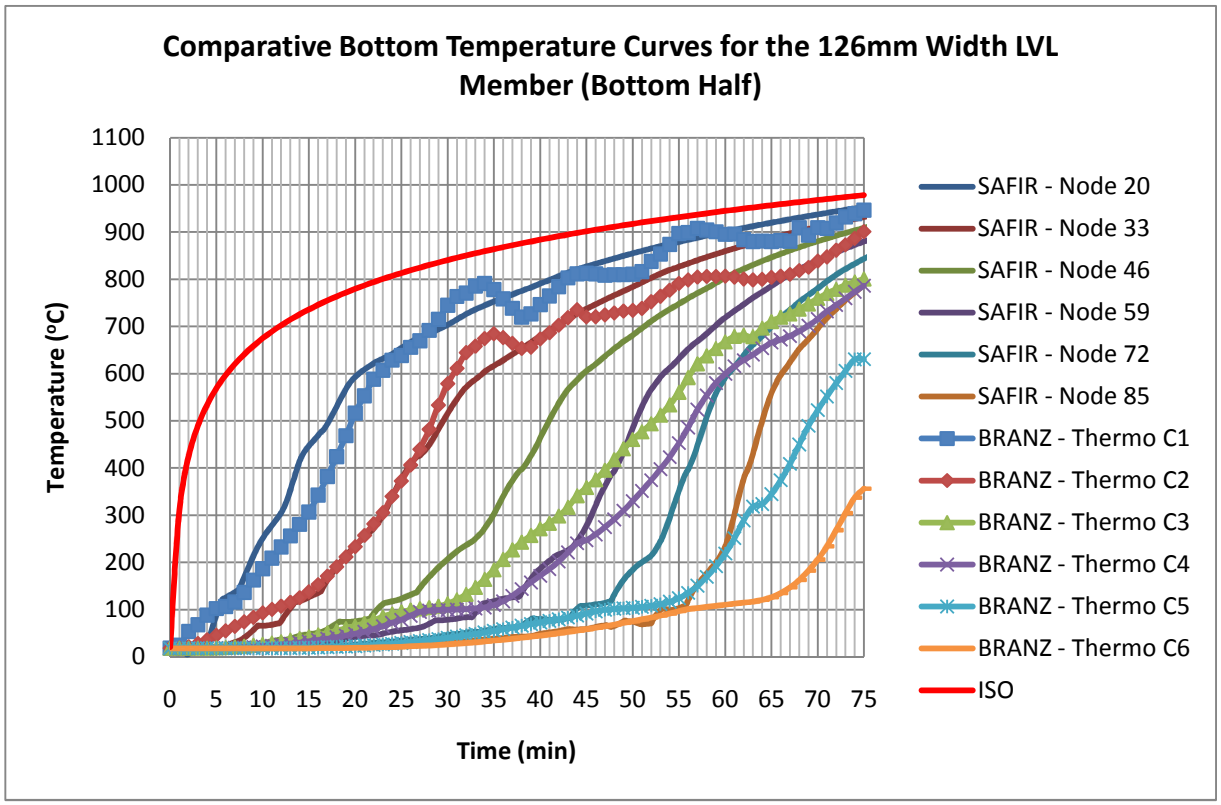

Figure 6-20: Comparative bottom temperature curves for the 126mm width LVL member (Bottom Half)

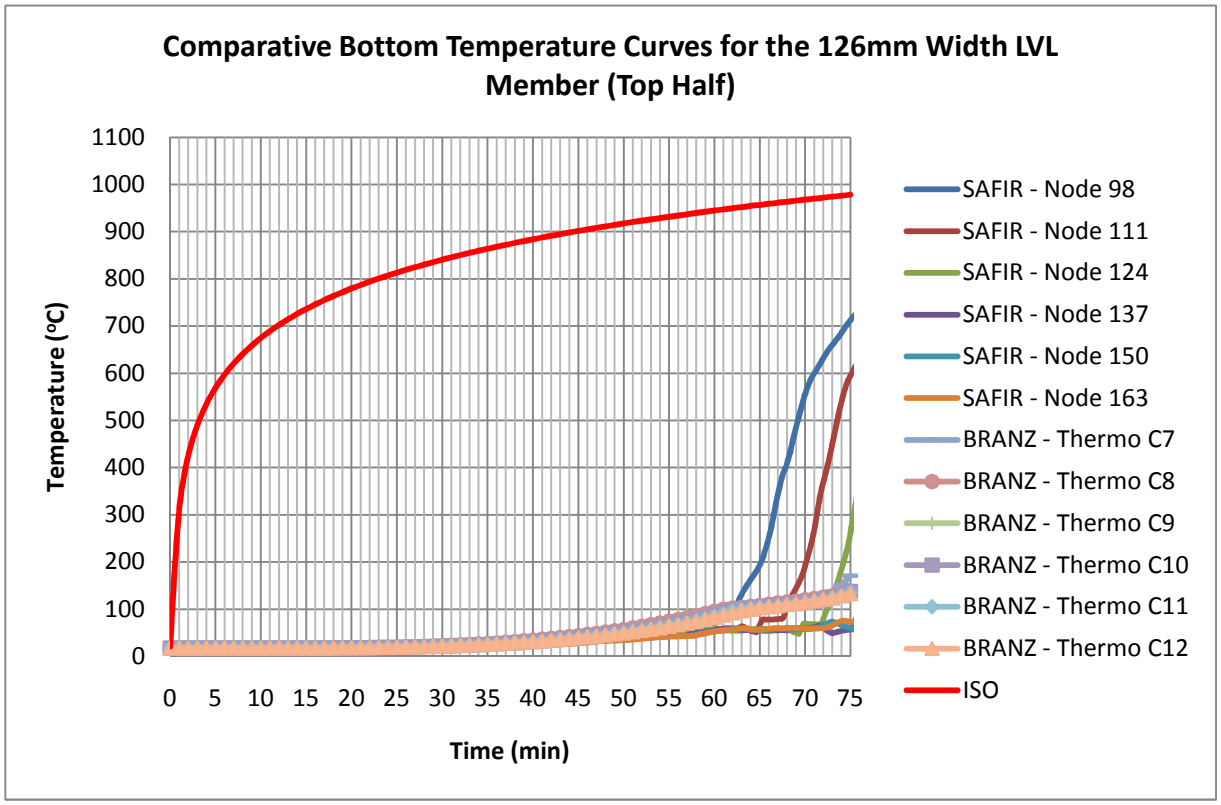

Figure 6-21: Comparative bottom temperature curves for the 126mm width LVL member (Top Half)

7. SPREADSHEET ANALYSIS

7.1. Background

Yeoh (2009), during his PhD research at the University of Canterbury, developed a spreadsheet design tool to analyse the behaviour of the semi-prefabricated composite floor system which can accommodate both short and long term loading. Yeoh's spreadsheet, however, was not able to evaluate the floors in fire conditions. O'Neill (2009) continued Yeoh's work by introducing a standalone tool for estimating expected fire resistance of the composite floor system in a spreadsheet model. This model is then able to provide a fast method of estimating the expected fire resistance time of a floor under user defined load conditions and floor geometries. Refer to O'Neill's thesis for the development and calibration of his spreadsheet.

The aim of this exercise, therefore, is to make modifications to O'Neill's spreadsheet design tool based on the experimental findings from this research.

7.2. Modifications to O'Neil's Spreadsheet

Three modifications were applied to the O'Neill's spreadsheet design tool. These modifications are described in more detail in following sections.

7.2.1. Rate of Charring

In O'Neill's spreadsheet, the default one-dimensional charring rate is set at 0.55mm/min, which was recorded during the large scale tests performed by O'Neill (2009). However in this research, test results from BRANZ showed that the average side charring rates for the 90mm and 126mm width LVL members were 0.72mm/min and 0.76mm/min respectively. Therefore in the current spreadsheet, the default charring rate is changed from 0.55mm/min to 0.74mm/min.

7.2.2. Bottom Charring Factor

In his spreadsheet, O'Neill (2009) proposed a bottom charring factor of 15 to adjust the change in the bottom charring rate from one-dimensional charring to two-dimensional charring. This value was an estimated number which was derived based on trial and error in in order to match his full-scale test results.

Test results from the first and the fourth pilot furnace tests show that a change in the bottom charring rate from one-dimensional to two-dimensional was approximately 9 to 10 times.

This is based on the ratio between the one-dimensional bottom charring rate and the two-two-dimensional bottom charring rate as shown in Figure 7-1. In Figure 7-1 the gradient of the second part of the curve, i.e. two-dimensional charring, was approximately 9 to 10 times higher than the gradient of the first part of the curve, i.e. one-dimensional charring. Therefore in the current spreadsheet, the proposed bottom charring factor is changed from 15 to 10.

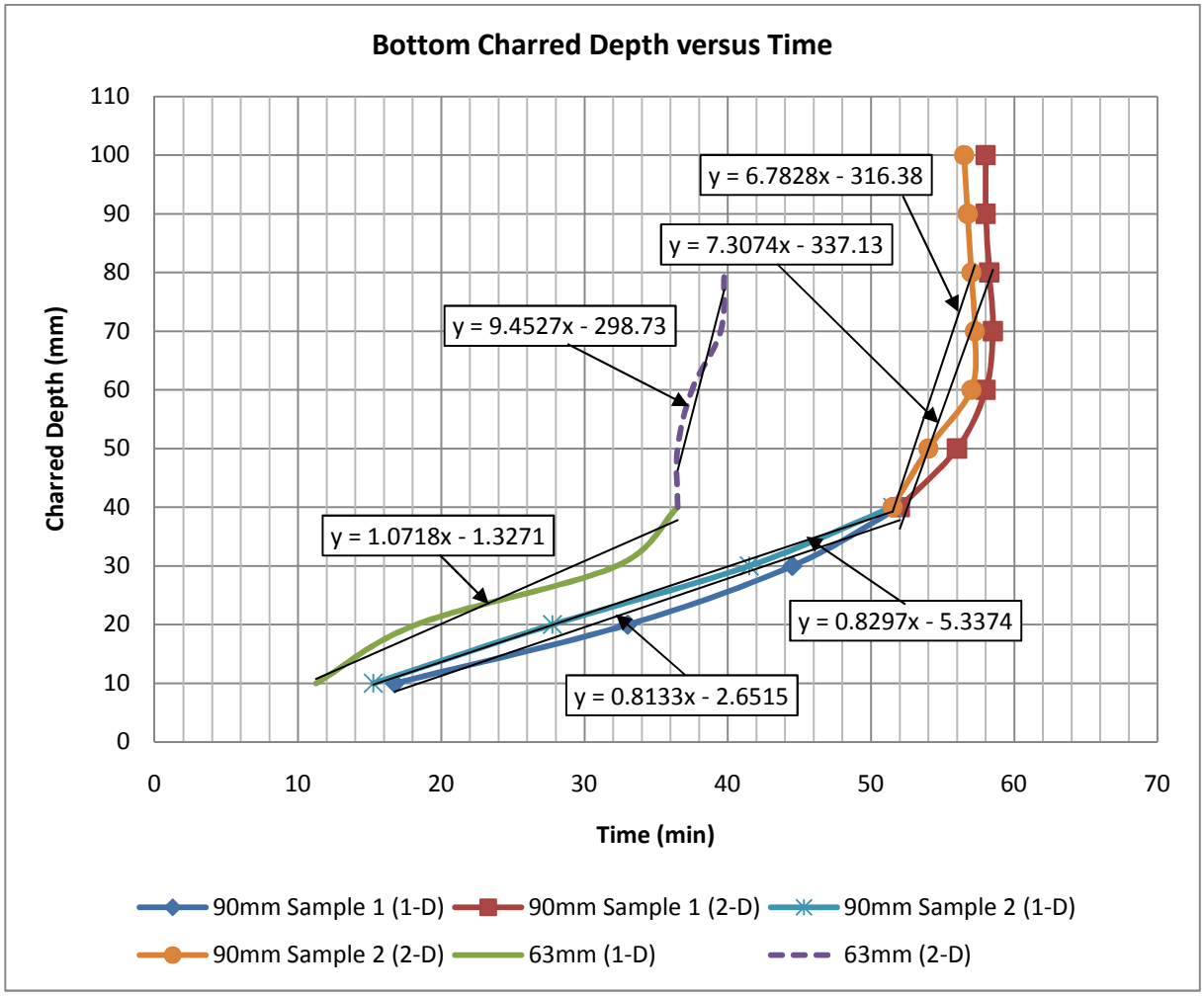

Figure 7-1: Comparison between the rate of one-dimensional charring and two-dimensional charring

7.2.3. Lower Limit of Beam Width

In his spreadsheet, O'Neill (2009) proposed that when the beam width reduces past a lower limit of 62mm beam thickness remaining, the bottom face will start to experience a two-two-dimensional charring. However, based on the experimental findings from the fourth pilot furnace test, it was observed that for the 90mm width LVL member, the bottom face started to experience a two-dimensional charring when the beam width reduced to approximately 20mm beam thickness remaining. Therefore in the current spreadsheet, the proposed lower limit of beam thickness width is changed from 62mm to 20mm.

7.3. Spreadsheet Calculations

Based on the modified spreadsheet design tool, the new expected fire resistance time outputs which encompass a variety of load combinations, member spans and section sizes, are summarised in Table 7-1 through Table 7-3. Users should be aware that all sections are based on the double LVL "M" panel configuration, and denote two beams of the specified size. These are all designed with four notched connections per beam, spaced a minimum of 650mm from the beam ends and nominally throughout the length of the beam.

Table 7-1: Fire resistance – Span table for SDL = 0.5kPa, Q = 1.5kPa

Fire Resistance Time (min) SDL = 0.5 kPa, Q = 1.5 kPa									
Beam Dimensions (mm)	**Span (m)**								
	4	**5**	**6**	**7**	**8**	**9**	**10**	**11**	**12**
200x45x2	47	40	-	-	-	-	-	-	-
240x45x2	48	43	-	-	-	-	-	-	-
300x45x2	49	46	41	-	-	-	-	-	-
360x45x2	-	48	45	41	-	-	-	-	-
400x45x2	-	-	46	43	39	35	-	-	-
450x45x2	-	-	-	45	42	39	35	-	-
600x45x2	-	-	-	-	47	45	43	40	38
200x63x2	69	63	53	-	-	-	-	-	-
240x63x2	72	66	59	-	-	-	-	-	-
300x63x2	73	69	64	58	-	-	-	-	-
360x63x2	-	72	68	64	59	-	-	-	-
400x63x2	-	-	70	66	62	58	-	-	-
450x63x2	-	-	-	69	65	62	58	-	-
600x63x2	-	-	-	-	71	69	67	64	61
200x90x2	102	97	85	-	-	-	-	-	-
240x90x2	107	100	91	-	-	-	-	-	-
300x90x2	109	104	98	92	84	-	-	-	-
360x90x2	-	107	103	98	93	86	-	-	-
400x90x2	-	-	105	101	97	91	86	-	-
450x90x2	-	-	-	104	100	96	92	87	-
600x90x2	-	-	-	-	107	105	102	99	96

Table 7-2: Fire resistance – Span table for SDL = 0.5kPa, Q = 2.0kPa

Fire Resistance Time (min) SDL = 0.5 kPa, Q = 2.0 kPa									
Beam Dimensions (mm)	**Span (m)**								
	4	**5**	**6**	**7**	**8**	**9**	**10**	**11**	**12**
200x45x2	45	39	-	-	-	-	-	-	-
240x45x2	47	42	-	-	-	-	-	-	-
300x45x2	49	45	40	-	-	-	-	-	-
360x45x2	-	47	44	40	-	-	-	-	-
400x45x2	-	-	45	42	38	-	-	-	-
450x45x2	-	-	-	44	41	38		-	-
600x45x2	-	-	-	-	47	44	42	39	37
200x63x2	68	61	51	-	-	-	-	-	-
240x63x2	71	65	57	-	-	-	-	-	-
300x63x2	73	68	63	57	-	-	-	-	-
360x63x2	-	71	67	63	57	-	-	-	-
400x63x2	-	-	69	65	61	56	-	-	-
450x63x2	-	-	-	68	64	61	56	-	-
600x63x2	-	-	-	-	70	68	66	63	60
200x90x2	101	95	82	-	-	-	-	-	-
240x90x2	106	99	89	-	-	-	-	-	-
300x90x2	108	103	97	90	-	-	-	-	-
360x90x2	-	106	102	97	91	-	-	-	-
400x90x2	-	-	104	100	95	90	-	-	-
450x90x2	-	-	-	103	99	95	90	-	-
600x90x2	-	-	-	-	106	104	101	98	95

Table 7-3: Fire resistance – Span table for SDL = 1.0kPa, Q = 3.0kPa

Fire Resistance Time (min) SDL = 1.0 kPa, Q = 3.0 kPa									
Beam Dimensions (mm)	**Span (m)**								
	4	**5**	**6**	**7**	**8**	**9**	**10**	**11**	**12**
200x45x2	41	-	-	-	-	-	-	-	-
240x45x2	44	37	-	-	-	-	-	-	-
300x45x2	47	42	35	-	-	-	-	-	-
360x45x2	49	45	40	-	-	-	-	-	-
400x45x2	-	46	43	38	-	-	-	-	-
450x45x2	-	-	45	41	-	-	-	-	-
600x45x2	-	-	-	47	44	41	-	-	-
200x63x2	63	54	-	-	-	-	-	-	-
240x63x2	67	59	-	-	-	-	-	-	-
300x63x2	70	65	58	-	-	-	-	-	-
360x63x2	72	68	63	-	-	-	-	-	-
400x63x2	-	70	66	61	-	-	-	-	-
450x63x2	-	-	68	64	60	-	-	-	-
600x63x2	-	-	-	70	68	65	-	-	-
200x90x2	95	86	-	-	-	-	-	-	-
240x90x2	101	92	-	-	-	-	-	-	-
300x90x2	106	99	91	-	-	-	-	-	-
360x90x2	108	103	98	-	-	-	-	-	-
400x90x2	-	105	101	95	-	-	-	-	-
450x90x2	-	-	104	99	94	-	-	-	-
600x90x2	-	-	-	106	103	100	-	-	-

Overall, the newly proposed fire resistance times summarized in Table 7-1 through Table 7-3 were comparatively lower than the fire resistance time proposed by O'Neill (2009). This was largely due to the modification of the charring rate from 0.55mm/min to 0.74mm/min. The proposed modification results in a much more conservative design.

8. CONCLUSIONS AND RECOMMENDATIONS

8.1. Small Furnace Tests

The first phase of this research centred around performing small scale tests in the small furnace at the University of Canterbury. From these small furnace tests, a number of key conclusions can be drawn:

- The overall average side charring rate for a 30 minute fire exposure was 0.76mm/min whereas the overall average side charring rate for a 60 minute fire exposure was 0.66mm/min. A higher charring rate for the 30 minute fire exposure was expected as the initial burning of wood is generally higher due to the fact that the wood is not initially insulated by a char layer.

- The overall corner charring rates for the 30 and 60 minute fire exposures were 1.38mm/min and 1.40mm/min, respectively. These rates were approximately twice higher than their average side charring rate due to the fact that corners of the LVL member were experiencing two dimensional charring.

- For a 30 minute fire exposure, the average bottom charring rates for nail, screw and glue connected double LVL members were 1.00mm/min, 0.83mm/min and 0.83mm/min, respectively. For a 60 minute fire exposure, the average bottom charring rates for screw and glue connected double LVL members were 0.97mm/min and 0.57mm/min, respectively. The nail connected double LVL members experienced a highest bottom charring rate as it suffered the largest bottom separation which allowed the heat to travel into the mid-span causing a higher bottom charring rate. Out of these three connection types, the glued connection was the best connection type.

- As for the screwed connection, it was observed that the screw performed well when the threaded length bridged across the double LVL members. This bridging effect holds the double LVL members much more securely when they were trying to separate in fire. If designed effectively, the screw connected double LVL member can achieve a similar bottom charring rate compatible with the glue connected double LVL member.

- In terms of the charring rate after the fire is out, it was observed that if the LVL timber was moved to the ambient temperature environment without being extinguished, the timber continued to char. This is due to the insulation effect of the charred layer which sustains the burning of the LVL timber within.

8.2. Pilot Furnace Tests

The second phase of this research centred around performing large scale tests in the pilot furnace at BRANZ in Wellington under the standard ISO 834 fire design curve. From these pilot furnace tests, a number of key conclusions can be drawn:

- Based on the first and the fourth pilot furnace tests, the average side charring rate for the 90mm and 126mm width LVL members were 0.72mm/min and 0.76mm/min, respectively.

- Based on the first pilot furnace test, the initial bottom charring rates for the 63mm width LVL members were fairly constant. Once the bottom charred depth reached approximately 50mm, the bottom charring rate started to increase exponentially. This showed a transition from one-dimensional charring into two-dimensional charring occurred around this depth. The factor of increase in the bottom charring rate from one-dimensional charring to two-dimensional charring was approximately 10 times.

- Based on the fourth pilot furnace test, the initial bottom charring rates were also approximately constant for the 90mm width LVL member. Once the bottom charred depth reached approximately 50mm, the bottom charring began to increase exponentially. This showed that a transition from one-dimensional charring into two-dimensional charring occurred around this depth. The factor of increase in the bottom charring rate from one-dimensional charring to two-dimensional charring was also approximately 10 times.

- Based on the first pilot furnace test, the average bottom charring rate for the 126mm width LVL member was 0.78mm/min. This was fairly close to its average side charring rate which indicate that the bottom face didn't go into a two-dimensional charring during the 75 minute fire exposure.

- Based on the test results from the second and the third pilot furnace tests, a staggered screw layout with a spacing of 150mm centre-to-centre is recommended if screws are used to join the double LVL members. The bottom row of screws is installed at 75mm from the base whereas the top row of screws is installed at 100mm from the base. One screw located 50mm from either ends of the LVL member is also recommended to prevent the separation of the double LVL member at the ends.

8.3. SAFIR Thermal Analysis

- From SAFIR thermal analysis, it was observed that the average side charring rate for the 63mm, 90mm and 126mm width LVL members generated by SAFIR were fairly similar. Meanwhile it was also observed that all bottom charring rates generated by SAFIR were higher than respective side charring rates. In theory the initial bottom charring rate should be similar to the side charring as they are both experiencing one-dimensional charring during the initial stage of burning. This may suggest that SAFIR is providing a much more conservative bottom charring rates.

- The comparative temperature curves between the BRANZ test results and the SAFIR simulation showed significant disagreement. Although both the BRANZ test results and the SAFIR simulation showed reasonable approximation close to the surface, the mismatch became more and more pronounced for interior fibres.

8.4. Spreadsheet Analysis

- Based on the experimental findings from this research, three modifications were made to the spreadsheet design tool for the timber-concrete composite floor developed by O'Neill (2009). These modifications were incorporated into this spreadsheet and new fire resistance tables were developed.

8.5. Recommendations for Further Research

- Carrying out further small scale tests using the new small furnace system soon operational at the University of Canterbury. The internal dimension of this new furnace system is 300mm wide by 300mm deep by 700mm long, which can accommodate a larger LVL specimen. By using this new furnace system, a larger double LVL specimen with different connection types can be burnt for a longer duration which can subsequently affect the overall side and bottom charring rate.

- Performing a large scale fire test on the timber-concrete composite floor using the proposed screwed connection layout for the double LVL members. This is to examine if the proposed screwed connection layout will work effectively as a whole.

- Conducting further analytical modelling by using the SAFIR program or other computer program such as Abaqus (2006) to compare with the experimental results. Discrepancies were found between BRANZ test results and SAFIR simulated results in this research. Therefore further assessment is recommended to minimise such inconsistency.

REFERENCES

ABAQUS version 6.6 (2006), Hibbbitt, D., Karlsson, B., Sorensen, P., Dassault Systemes S.A.

Bobacz, D. (2006), *Behavior of Wood in Case of Fire*, Proposal for a Stochastic Dimensioning of Structural Elements, Doctoral Thesis, Civil Engineering and Water Management, University of Natural Resources and Applied Life Sciences, Vienna.

Buchanan, A. (2002), *Structural Design for Fire Safety*, John Wiley & Sons, Chichester, UK.

Buchanan, A. (2007), *Timber Design Guide*, 3rd Edition, New Zealand Timber Industry Federation Inc.

Carter Holt Harvey Woodproducts New Zealand (2008), *Hyspan Structural LVL – Spain Tables for Residential Buildings*, 3rd Edition, Futurebuild, Carter Holt Harvey Limited, Auckland, New Zealand.

Collier, P. C. R. (1992), *Charring Rates of Timber*, BRANZ Study Report No. 42., Building Research Association of New Zealand.

CEN – European Committee for Standadizaion (2003), prEN 1995-1-2:2003, Final Draft, Stage 49, 2003-08-12, Brussels.

Dorn, H. and Egner, K. (1967), *Brandversuche an brettschichtverleimten Holzträgern unter Biegebeanspruchung*, Holz als Roh- und Werkstoff 25, pp. 308-320, Springer Verlag, Berlin.

Drysdale, D. (1999), *An Introduction to Fire Dynamics*, Chichester, UK: John Wiley & Sons.

European Guideline (2010), *Fire Safety in Timber Building*, Chapter 6.

Forest Products Laboratory (1989), *Handbook of Wood and Wood-based Materials for Engineers, Architects, and Builders*, Forest Service, U.S. Department of Agriculture, Hemisphere Publishing Corporation, New York, USA.

Forest Products Society (1999), *Wood-handbook – Wood as an Engineering Material*, U.S. Department of Agriculture, USA.

Forman Building Systems, (2010), www.forman.co.nz

Fornather, J. et al. (2000), *Versuchsbericht – Kleinbrandversuchsreihe 1 – Teil 1 (KBV1/1)*, Institute of Structural Engineering, Department of Structural Engineering and Natural Hazards, University of Natural Resources and Applied Life Sciences, Vienna.

Fornather, J. et al. (2001), *Versuchsbericht – Kleinbrandversuchsreihe 1 – Teil 2 (KBV1/2)*, Institute of Structural Engineering, Department of Structural Engineering and Natural

Hazards, University of Natural Resources and Applied Life Sciences, Vienna.

Fragiacomo, M. et al. (2009), *Numerical and experimental evaluation of the temperature distribution within laminated veneer lumber (LVL) exposed to fire*, Journal of structural Fire Engineering.

Franssen, J.M., (2007), *User's Manual for SAFIR2007a: A Computer Program for Analysis of Structures subjected to Fire*, University of Liège, Department of ArGEnCO, Service Structural Engineering, Belgium.

Incorpera et al, (2007), *Fundamentals of Heat and Mass Transfer*, 6th Edition, Hoboken, New Jersey, Wiley.

ISO (1975), *Fire Resistance Tests – Elements of Building Construction*, ISO 834-1975, International Organization for Standardization.

Klingsch, W. et al (1993), *Temperaturentwicklung in brandbeanspruchten Holzquerschnitten*, Schluβbericht, Forschungsvorhaben (F-90/1), Bergische Universität Wuppertal.

Knublauch, E. and Rudolphi, R. (1971): *Der Abbrand als Grundlage zur theoretischen Vorausbestimmung der Feuerwiderstandsdauer von Holzbauteilen*, Bauen mil Holz 12/71, pp 590 – 593, Bruderverlag, Köln.

König, J. and Walleij, L. (1999), *One-Dimensional Charring of Timber Exposed to standard and Parametric Fires in Initial Unprotected and Postprotection Situation*, Trätek, Rapport I 9908029, Stockholm.

Kordina, K. and Meyer-ottens, C. (1983), *Holz Brandschutz Handbuch*, Verlag Deutsche Gesellschaft für Holzforschung e. V., München.

Lache, M. (1992), *Untersuchungen zur Abbrandgeschwindigkeit von Vollholz und zur Feuerwiderstandsdauer biegebeanspruchter Brettschichtholzträger*, Dissertation an der Ludwig-Maximilians-Universität München, München.

Lane, W. P (2005), *Ignition, Charring and Structural Performance of Laminated Veneer Lumber*, Fire Engineering Research Report March 2005, School of Engineering, University of Canterbury.

Nelson Pine Industries Limited, www.nelsonpine.co.nz

New Zealand Wood, http://www.nzwood.co.nz/ Accessed January, 2010.

New Zealand Standard, NZS 3603 (1993), Timber Design Code, NZS 3603:1993, Standards New Zealand.

Mikkola, E. (1990), *Charring of Wood*, Research Report 689, Technical Research Centre of Finland (VTT), Espoo.

Moss, P. et al. (2009), *Predicting the behaviour of timber connections subjected to fire*, Futures in Mechanics of Structures and Materials, T. Aravinthan, W. Karunasena & H. Wang (eds), Taylor & Francis Group, London, being Proc. 20th Australasian Conference on the Mechanics of Structures and Materials, Toowoomba, Australia, 2-5 December 2008, pp857-863.

O'Neill, J. (2009), *The Fire Performance of Timber-Concrete Composite Floors*, Master's Thesis in Civil Engineering, University of Canterbury, Christchurch, New Zealand.

Purkiss, J. A. (1996), *Fire Safety Engineering Design of Structures*, Butterworth-Heinemann, Oxford, UK.

Schaffer, E. L. (1967), *Charring Rate of Selected Woods – transverse to grain*, U.S. Forest Service Research Paper FPL 69, U.S. Department of Agriculture, Forest Products Laboratory, Madison, Wisconsin.

Structural Timber Innovation Company (STIC), (2010), www.stic.co.nz

Thelandersson, S. and Larsen, H.J. (2002), *Timber Engeneering*, Wiley, New York, USA

Tope, P. (1971), *Thermal Decomposition of Wood at Temperature up to 180^{o}C – Part II: Experiments of Self ignition, Loss of Weight, Calorific Value and Elementary Analysis*, Holz als Roh- und Werkstoff (1971), pp. 295 – 300, Springer-Verlag, Berlin/Heidelberg.

White, R. H. (2008), *Analytical Methods for Determining Fire Resistance of Timber Members*, Section 4, Chapter 13, SFPE Handbook of Fire Protection Engineering (4th Edition), Society of Fire Protection Engineers.

White, R. H. (1988), *Charring Rates of Different Wood Species*, A thesis submitted in partial fulfilment of the requirements for the degree of Doctor of Philosophy (Forestry), University of Wisconsin, Madison, USA.

Yeoh, D. (2009), *Behaviour and Design of Timber-concrete Composite Floor under Short and Long-Term Loading*, Doctorate Thesis in Civil Engineering, University of Canterbury, Christchurch, New Zealand.

LIST OF APPENDICES

Appendix A: Comparative picture between the initial and the residual cross-section of the 63mm width single LVL specimen (small furnace test)

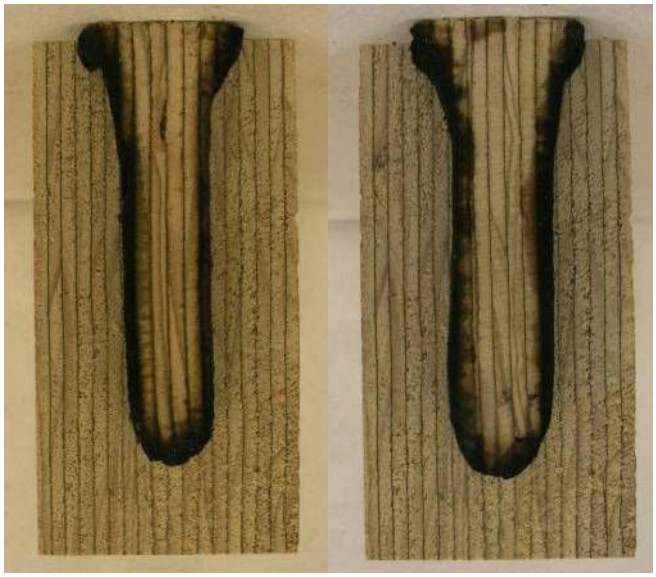

Figure A-1: 63mm width single LVL specimen (Left: Sample 1; Right: Sample 2)

Appendix B: Comparative picture between the initial and the residual cross-section of the 90mm width single LVL specimen (small furnace test)

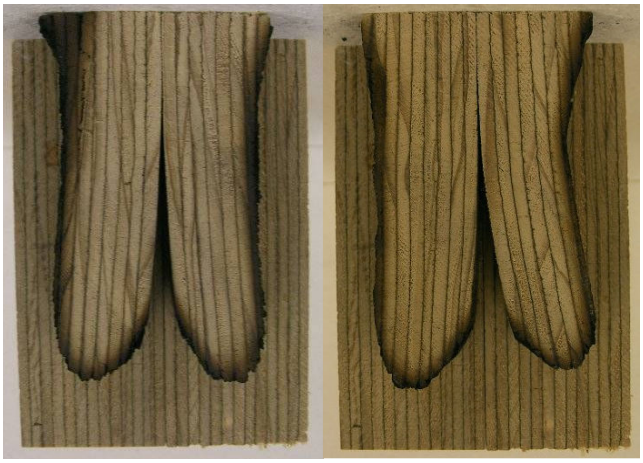

Figure B-1: No Connection (Left: Sample 1; Right: Sample 2)

Figure B-2: Nailed Connection (Left: Sample 1; Right: Sample 2)

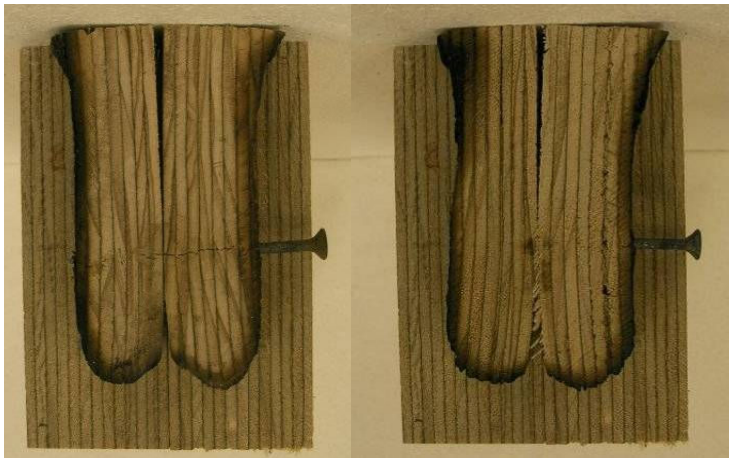

Figure B-3: Screwed Connection (Left: Sample 1; Right: Sample 2)

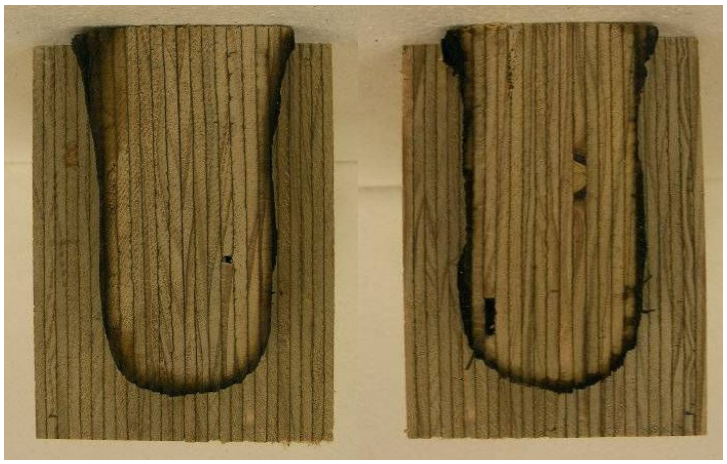

Figure B-4: Glued Connection (Left: Sample 1; Right: Sample 2)

Figure B-5: 2 Screws Connection

Appendix C: Comparative picture between the initial and the residual cross-section of the 126mm width single LVL specimen (small furnace test)

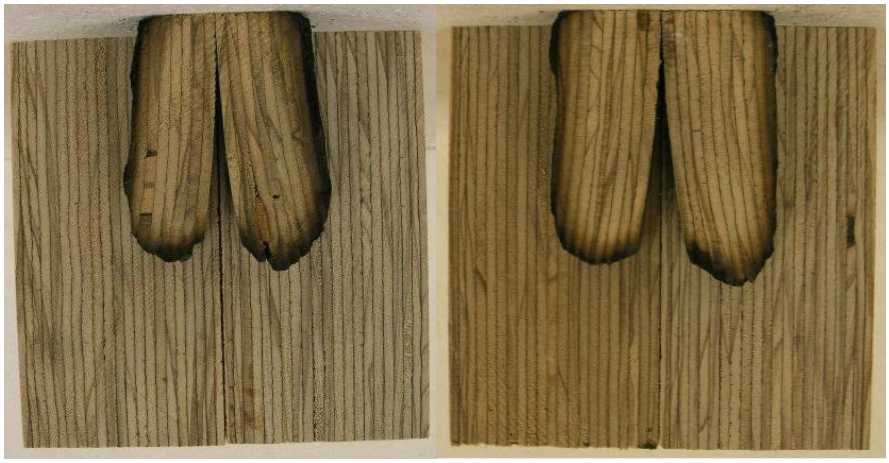

Figure C-1: No Connection (Left: Sample 1; Right: Sample 2)

Figure C-2: Screwed Connection (Left: Sample 1; Right: Sample 2)

Figure C-3: Glued Connection (Left: Sample 1; Right: Sample 2)

Appendix D: Thermocouple couple readings for 63mm width single LVL specimen (small furnace tests)

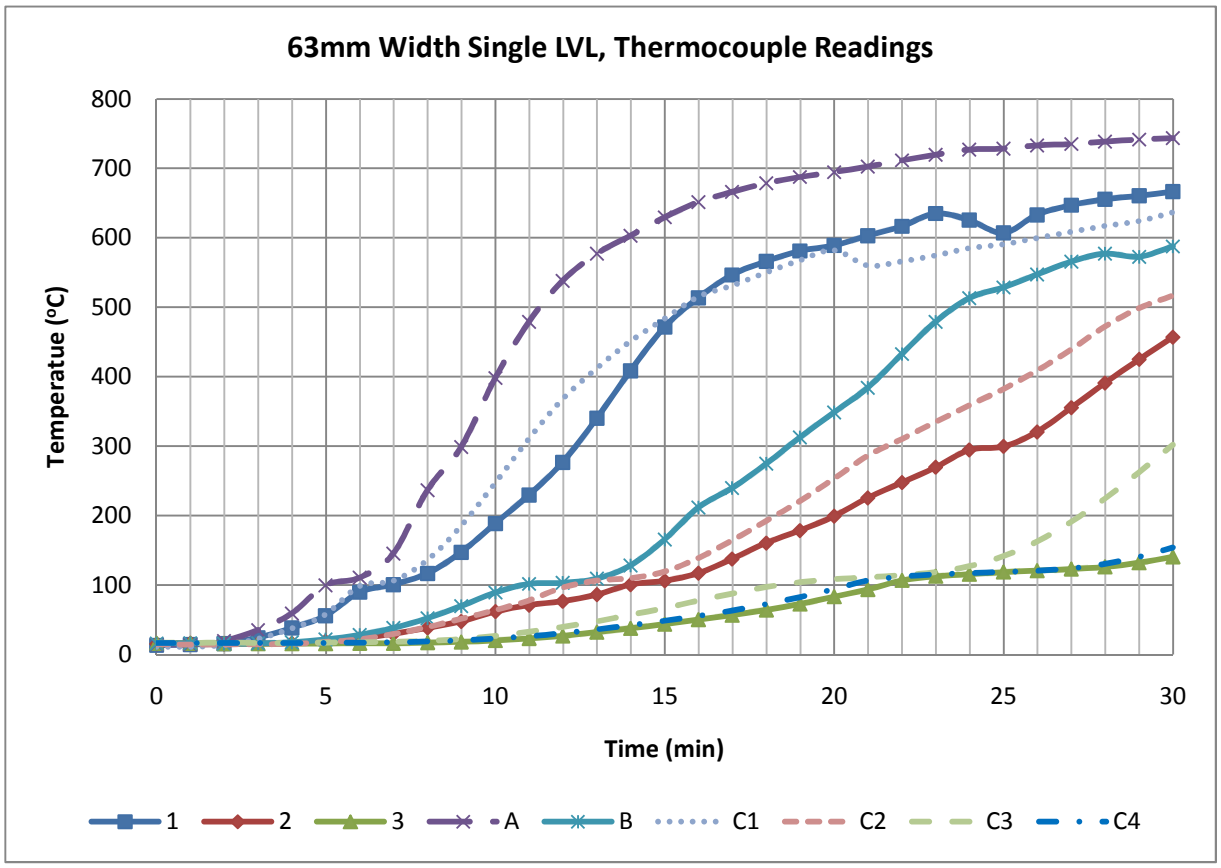

Figure D-1: Thermocouple readings for the 63mm width singled LVL specimen

Appendix E: Thermocouple couple readings for 90mm width double LVL specimens (small furnace tests)

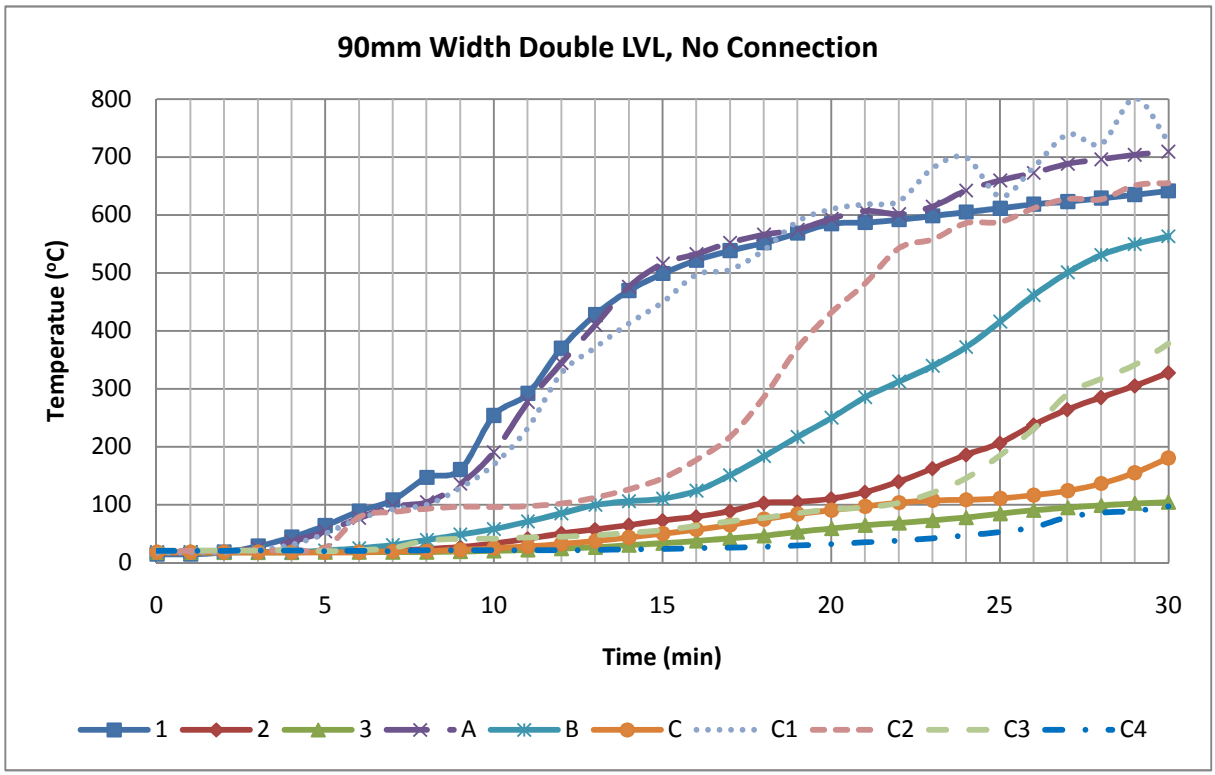

Figure E-1: 90mm, No connection

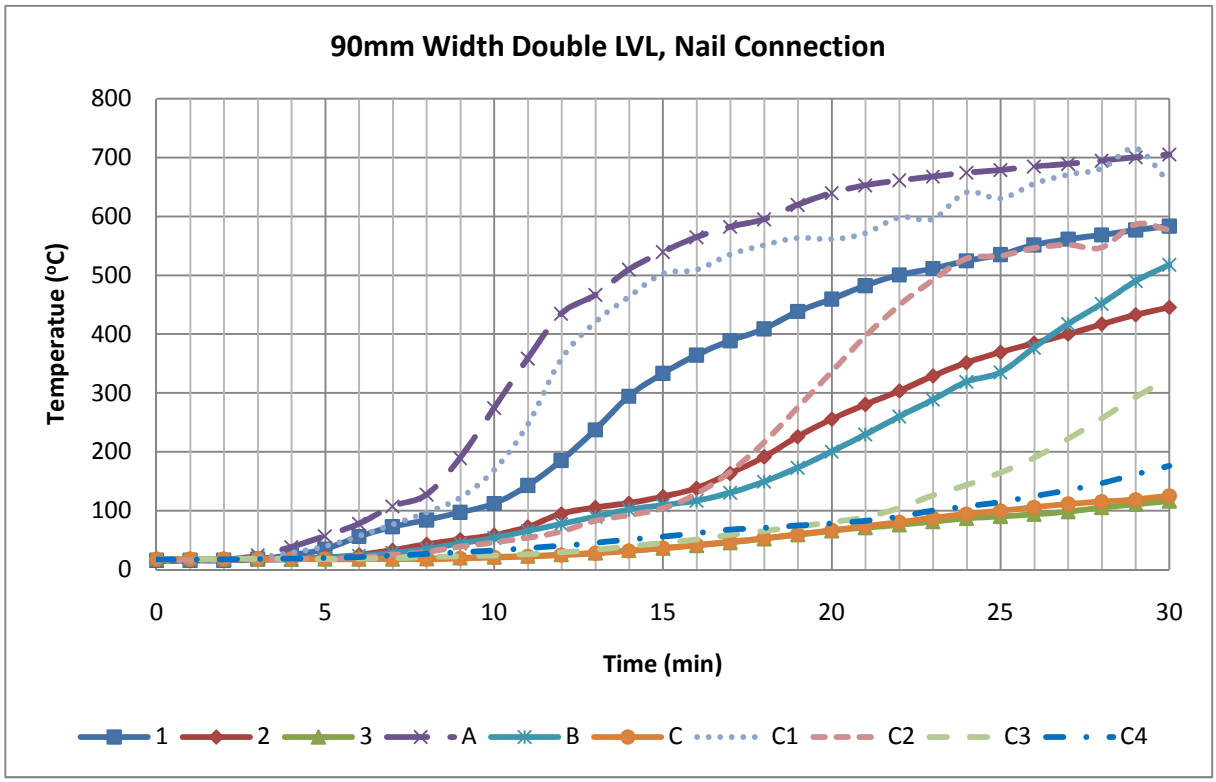

Figure E-2: 90mm, Nailed Connection

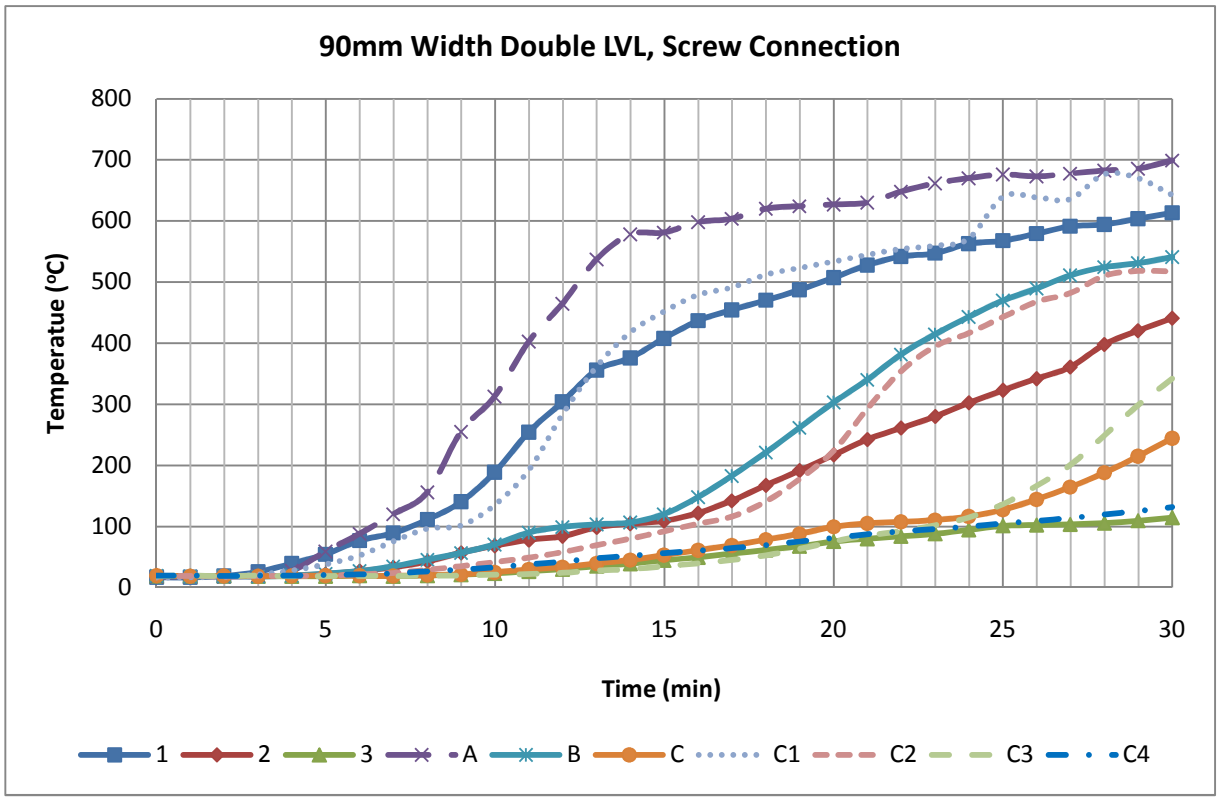

Figure E-3:90mm, Screwed Connection

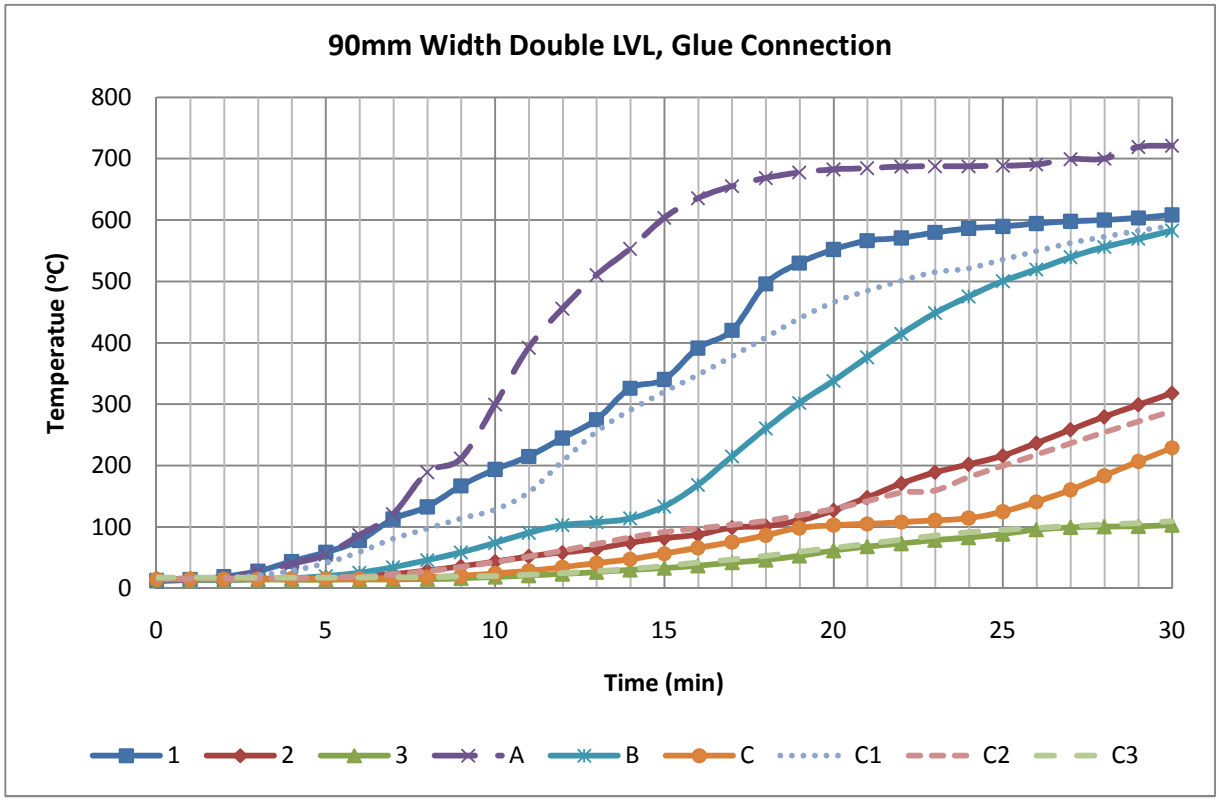

Figure E-4: 90mm, Glued Connection

Appendix F: Comparative thermocouple couple readings for 90mm width double LVL specimens (small furnace tests)

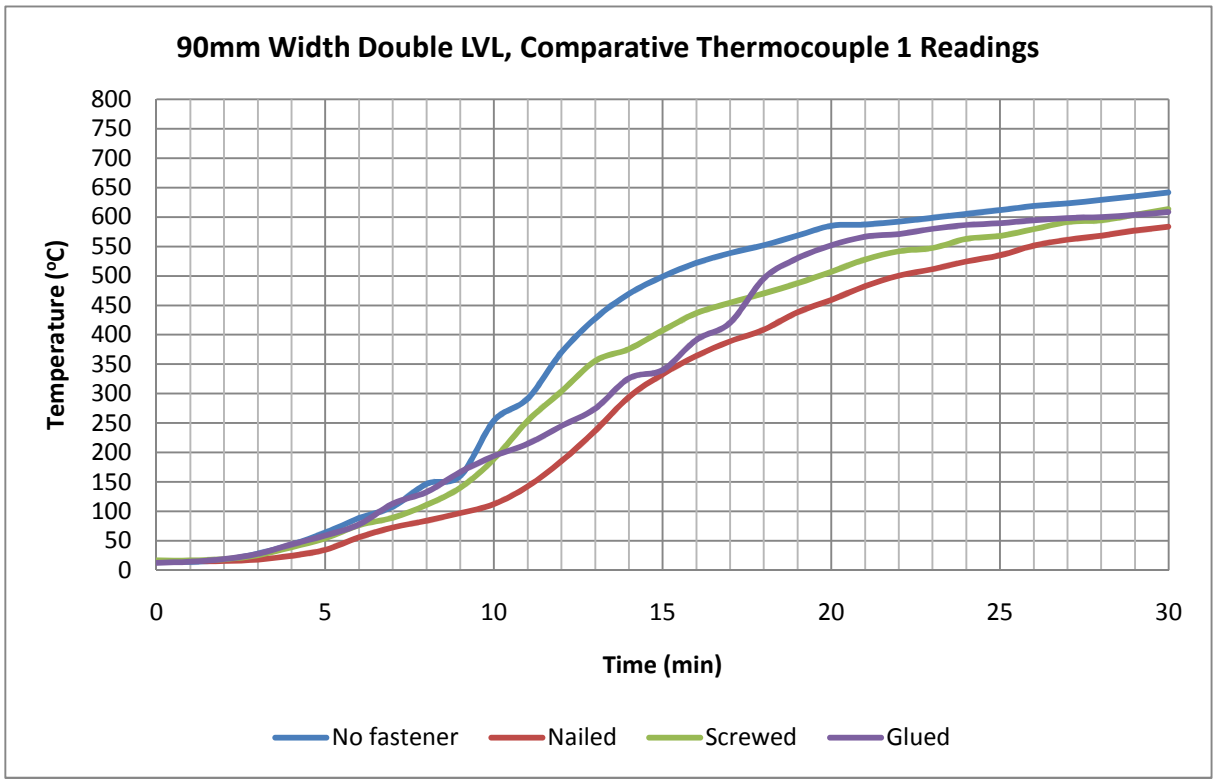

Figure F-1: Comparative thermocouple 1 readings

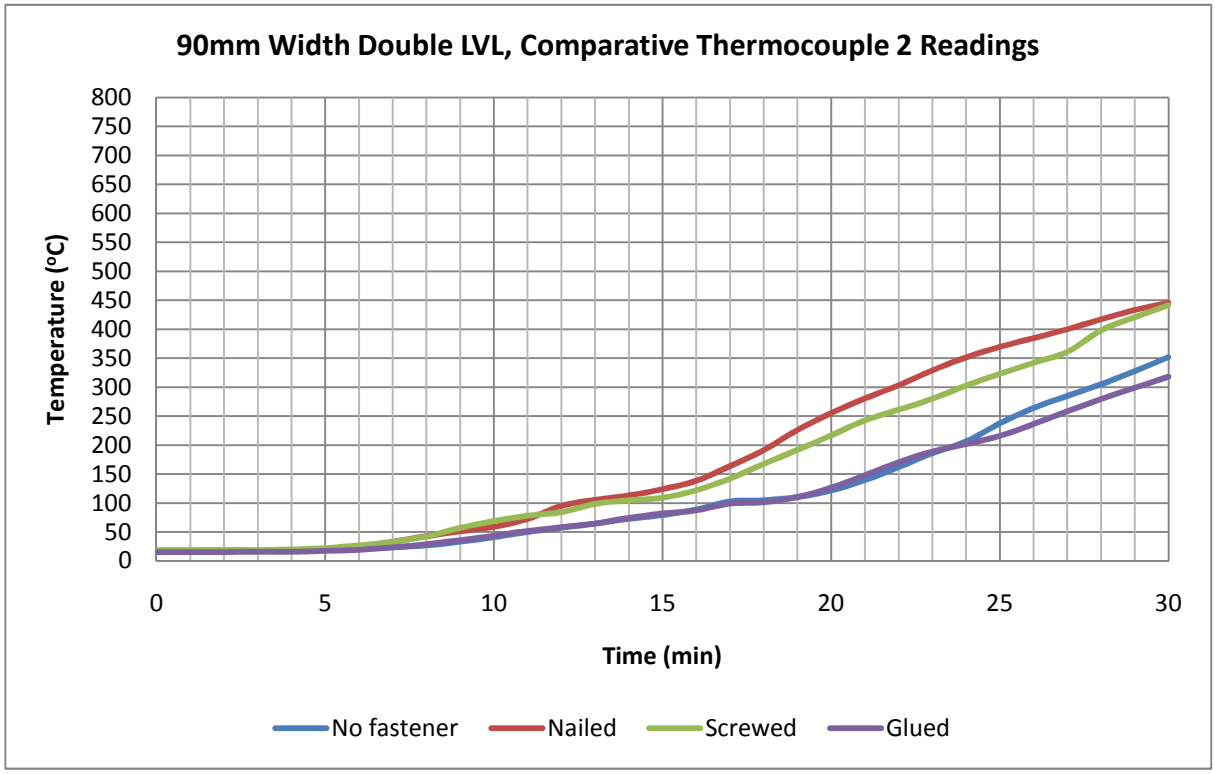

Figure F-2: Comparative thermocouple 2 readings

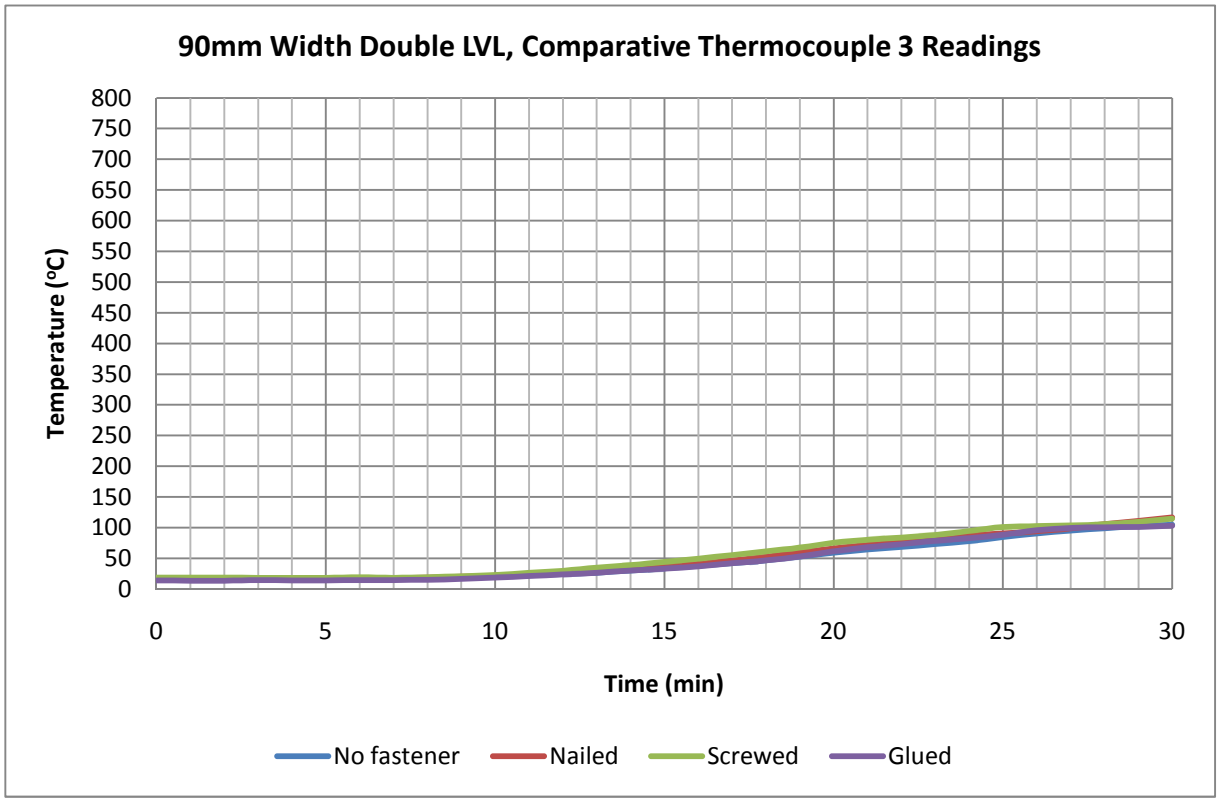

Figure F-3: Comparative thermocouple 3 readings

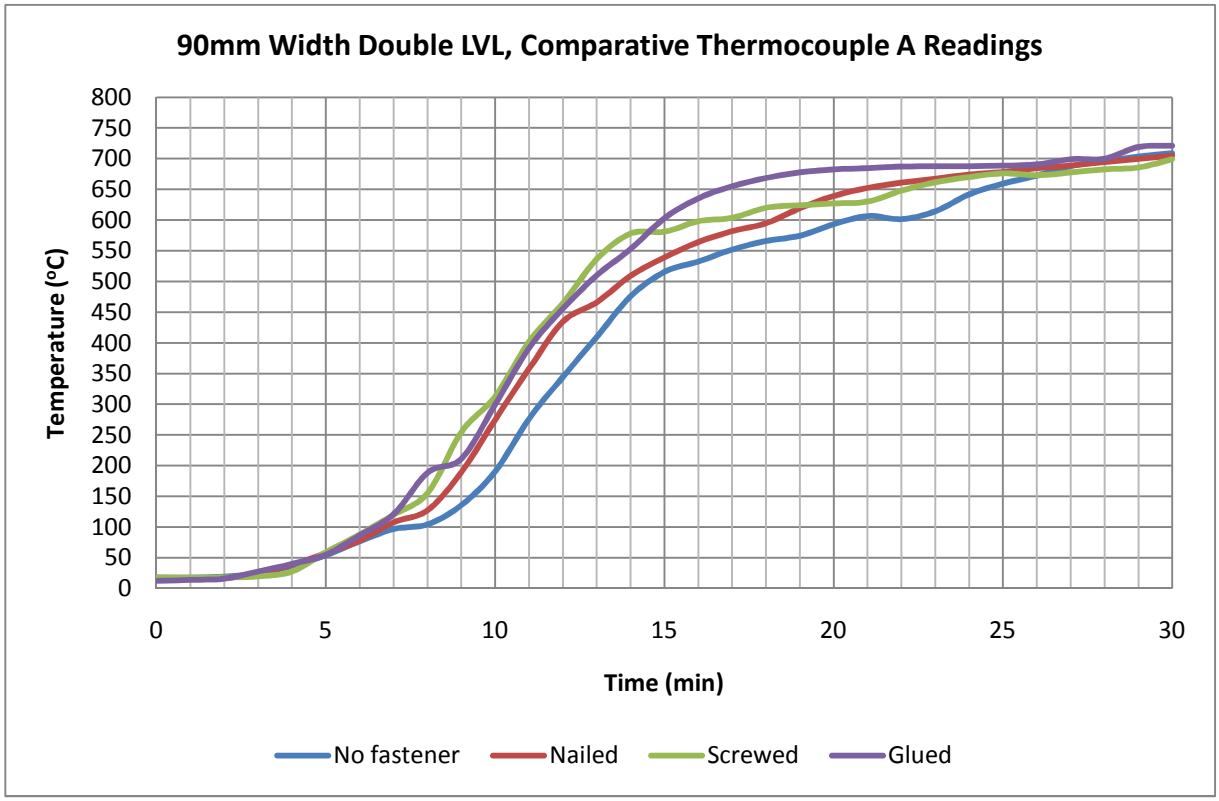

Figure F-4: Comparative thermocouple A readings

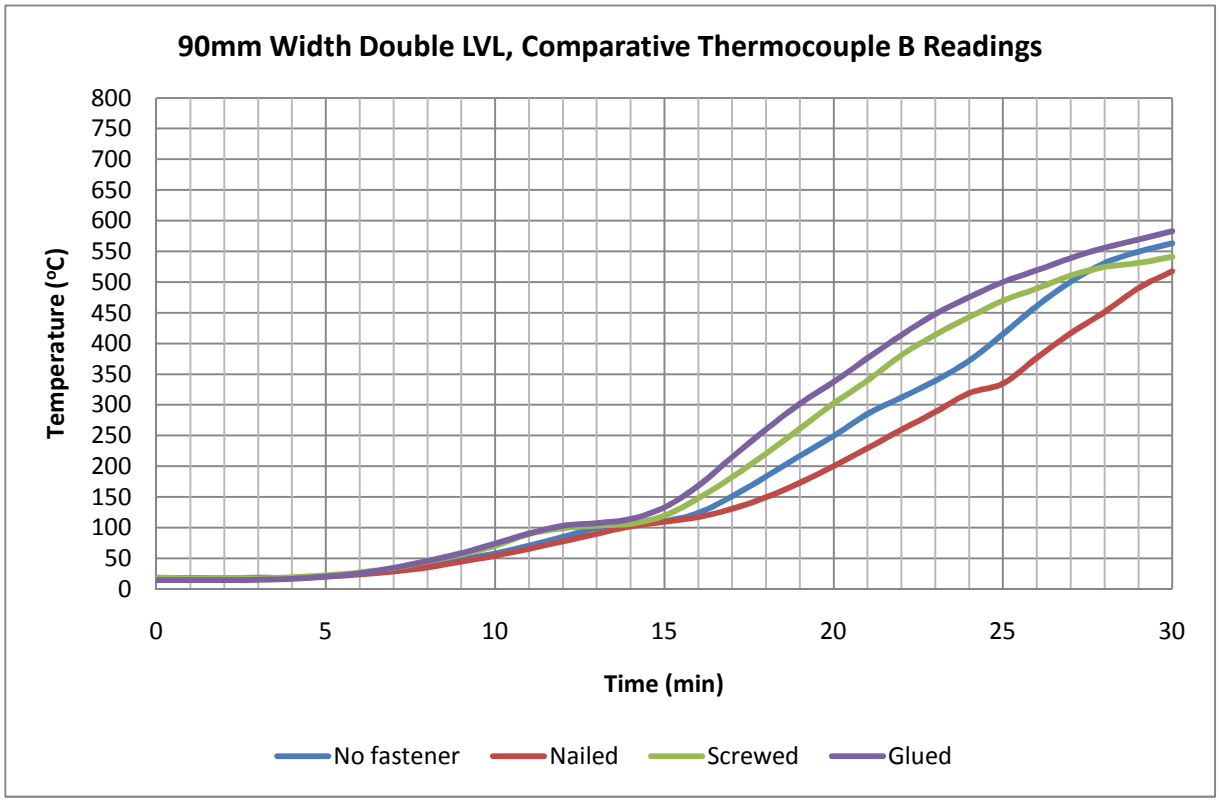

Figure F-5: Comparative thermocouple B readings

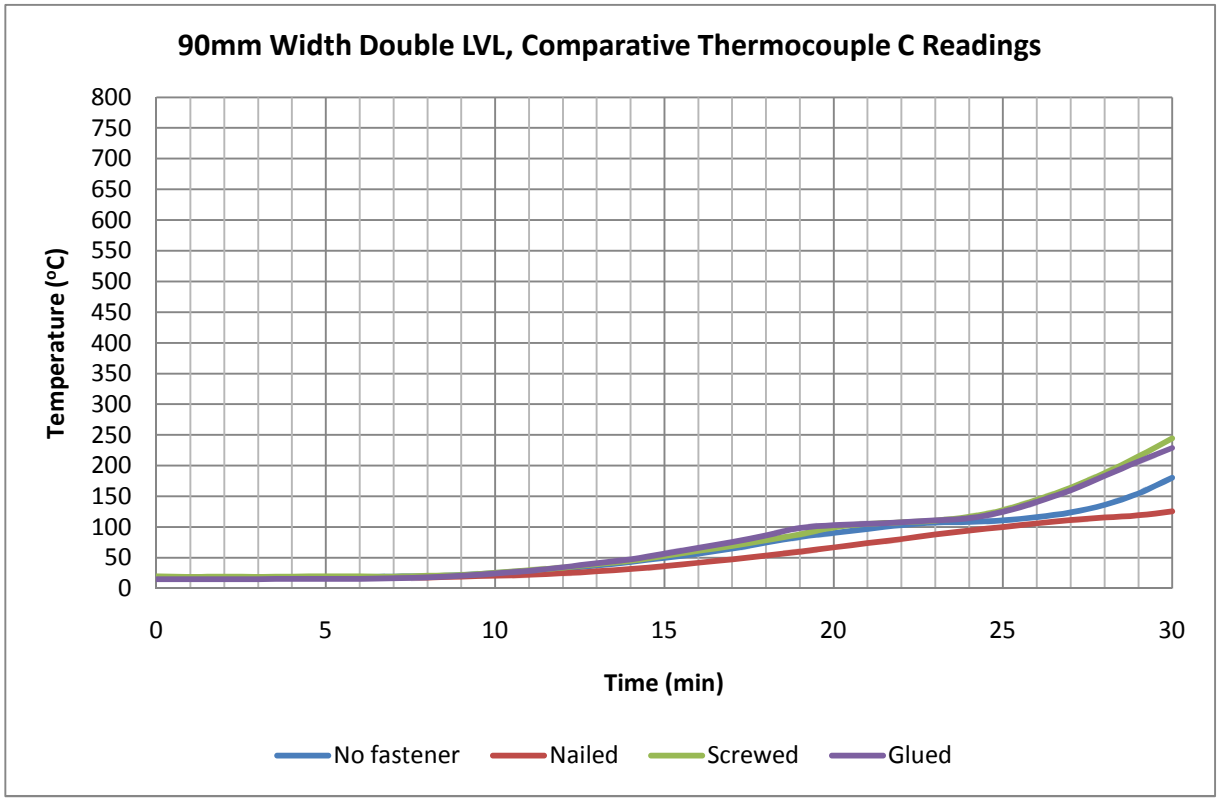

Figure F-6: Comparative thermocouple C readings

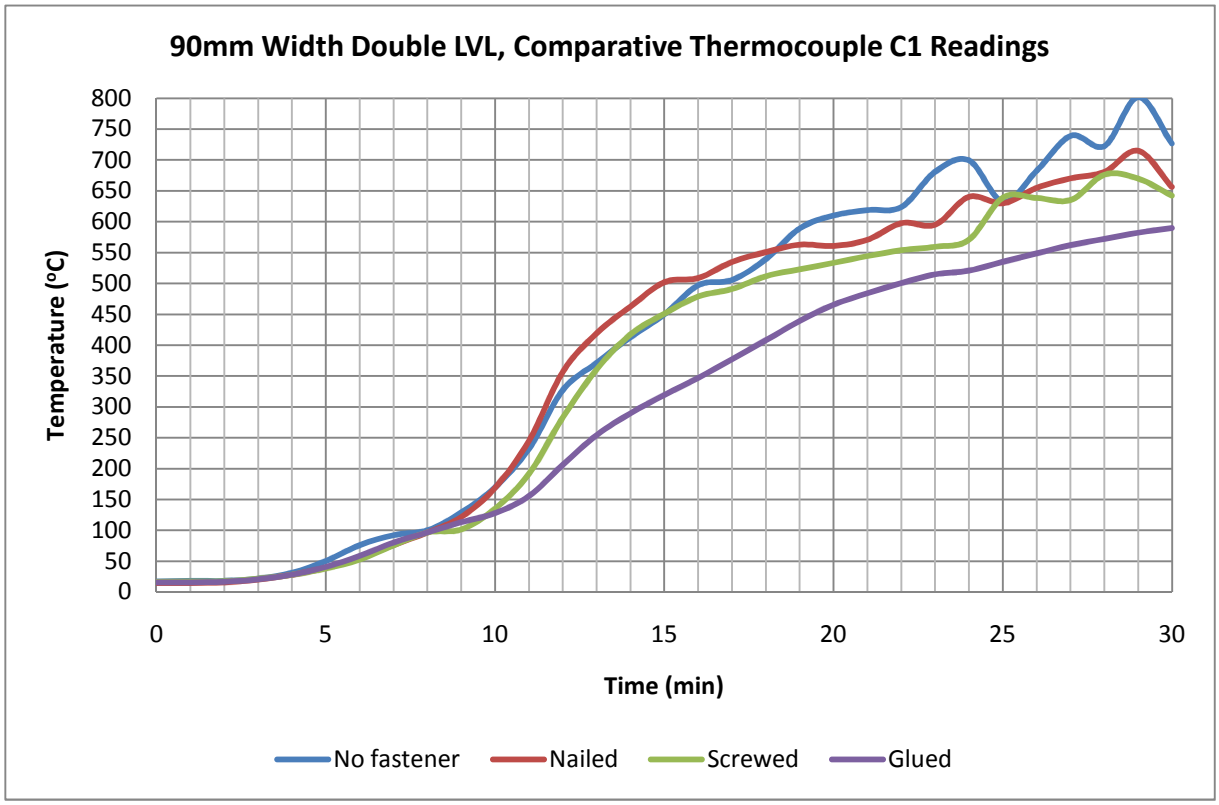

Figure F-7: Comparative thermocouple C1 readings

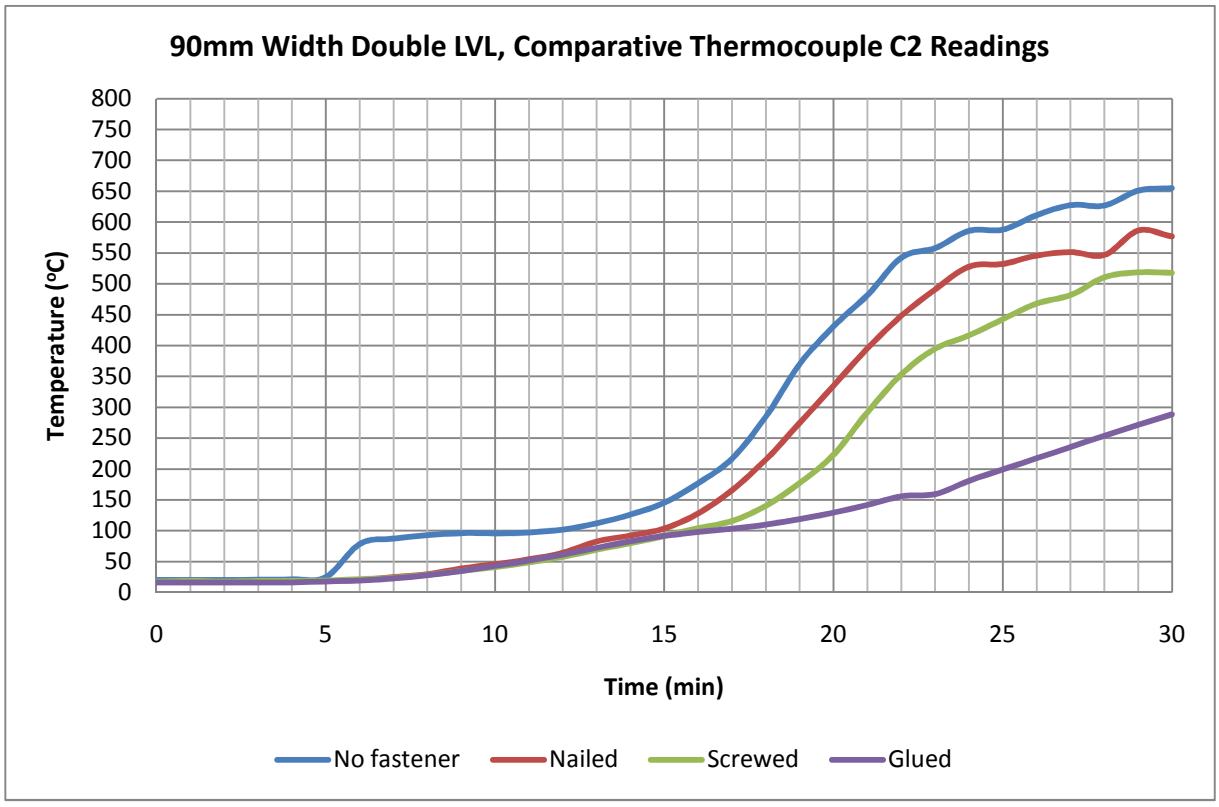

Figure F-8: Comparative thermocouple C2 readings

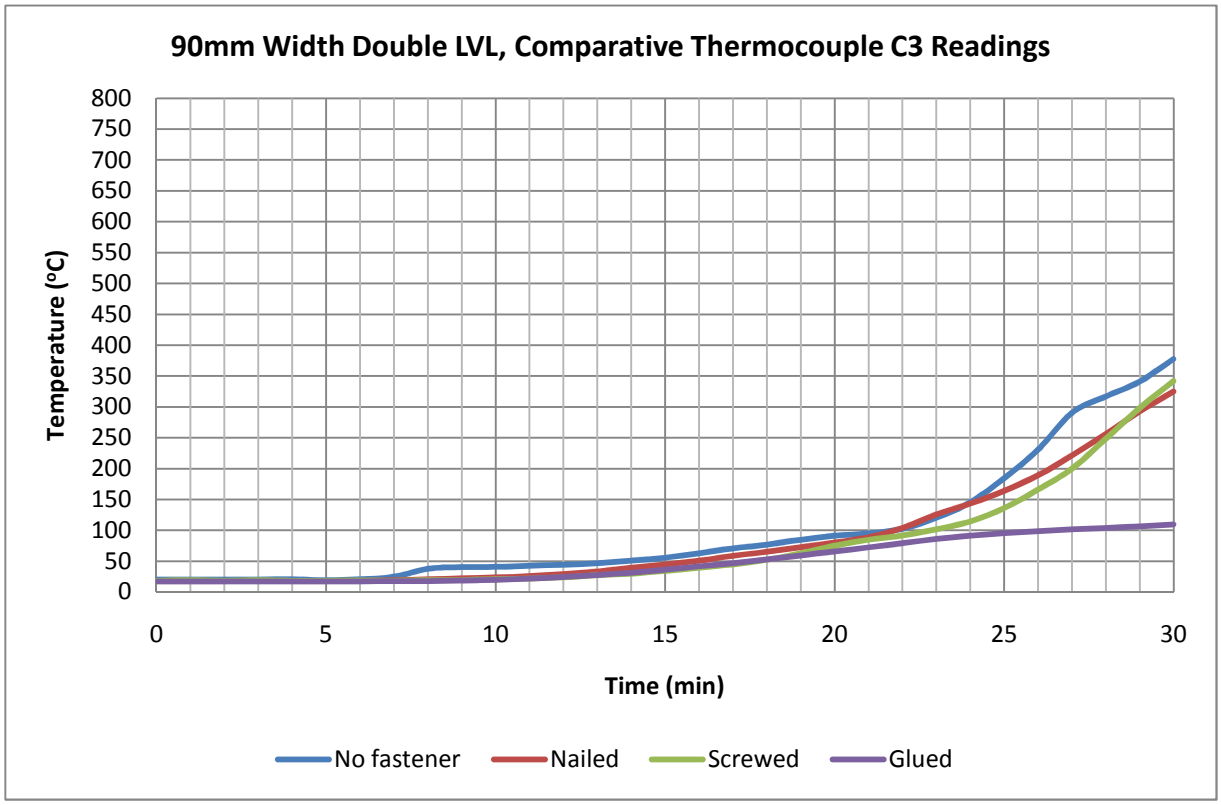

Figure F-9: Comparative thermocouple C3 readings

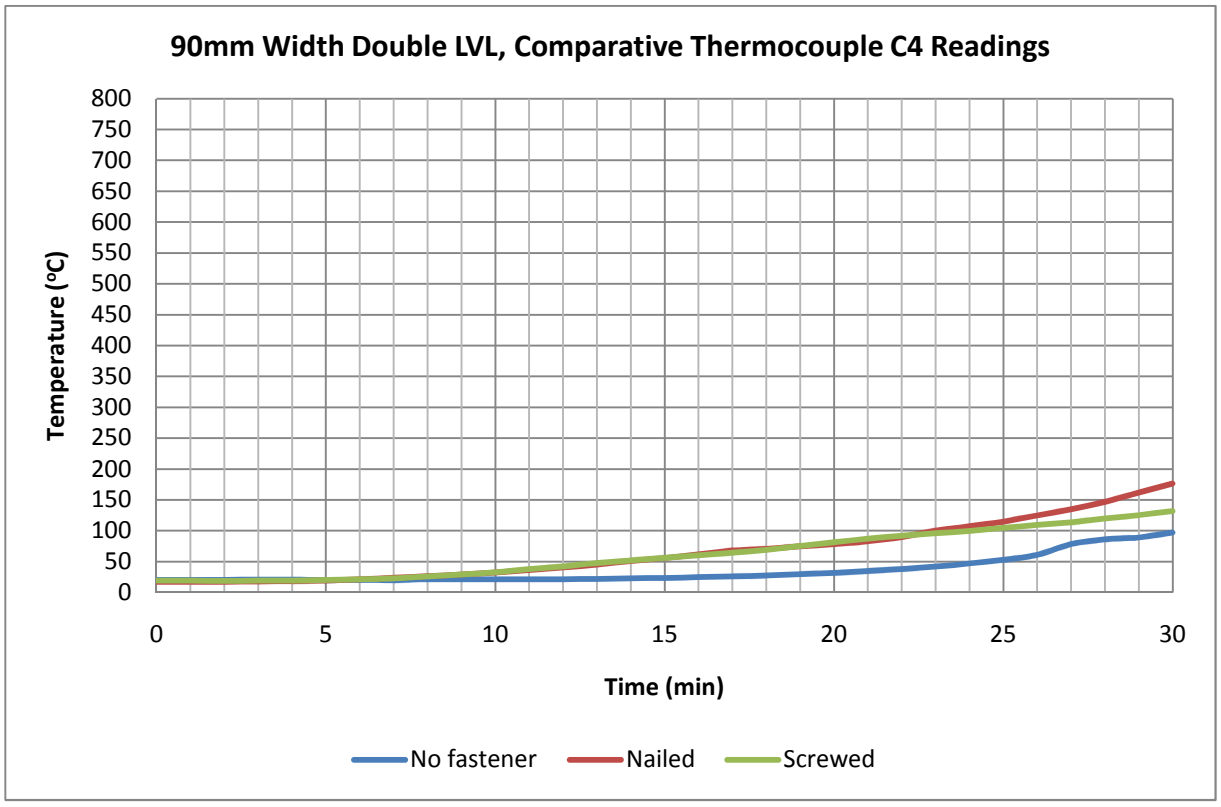

Figure F-10: Comparative thermocouple C4 readings

Appendix G: Thermocouple couple readings for 126mm width double LVL specimens (small furnace tests)

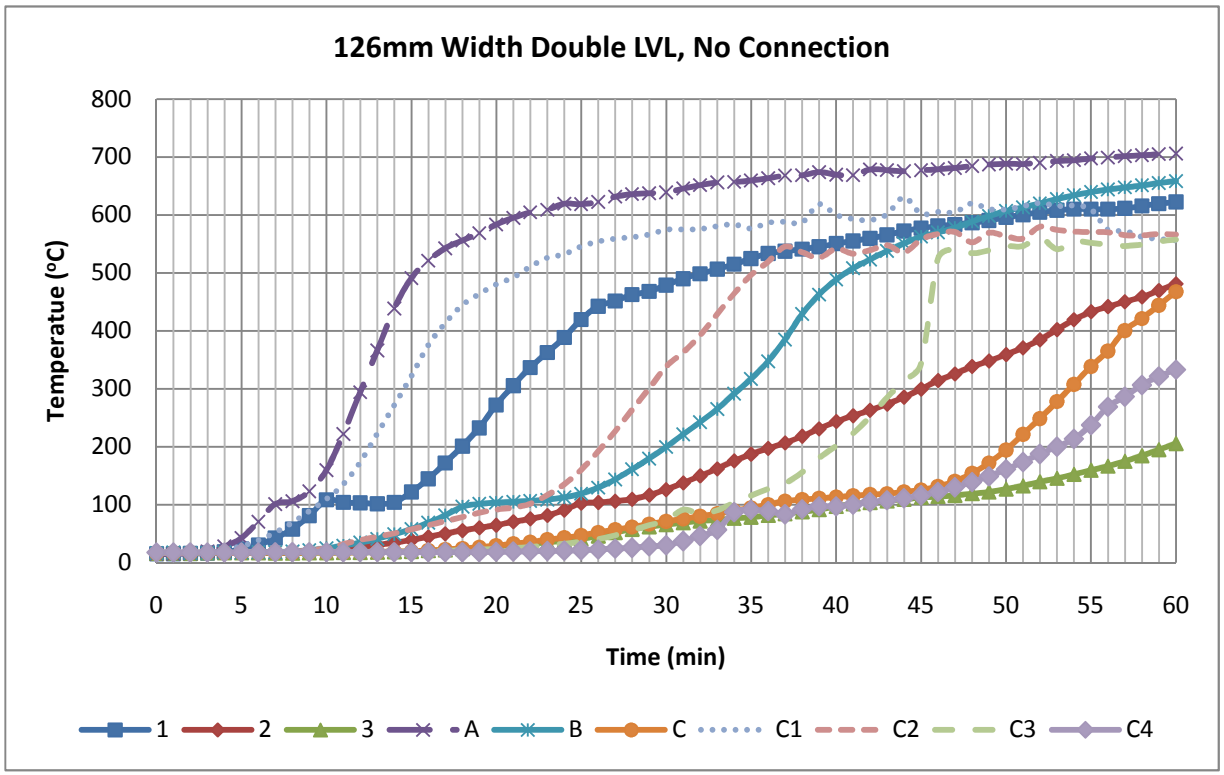

Figure G-1: 126mm, no connection

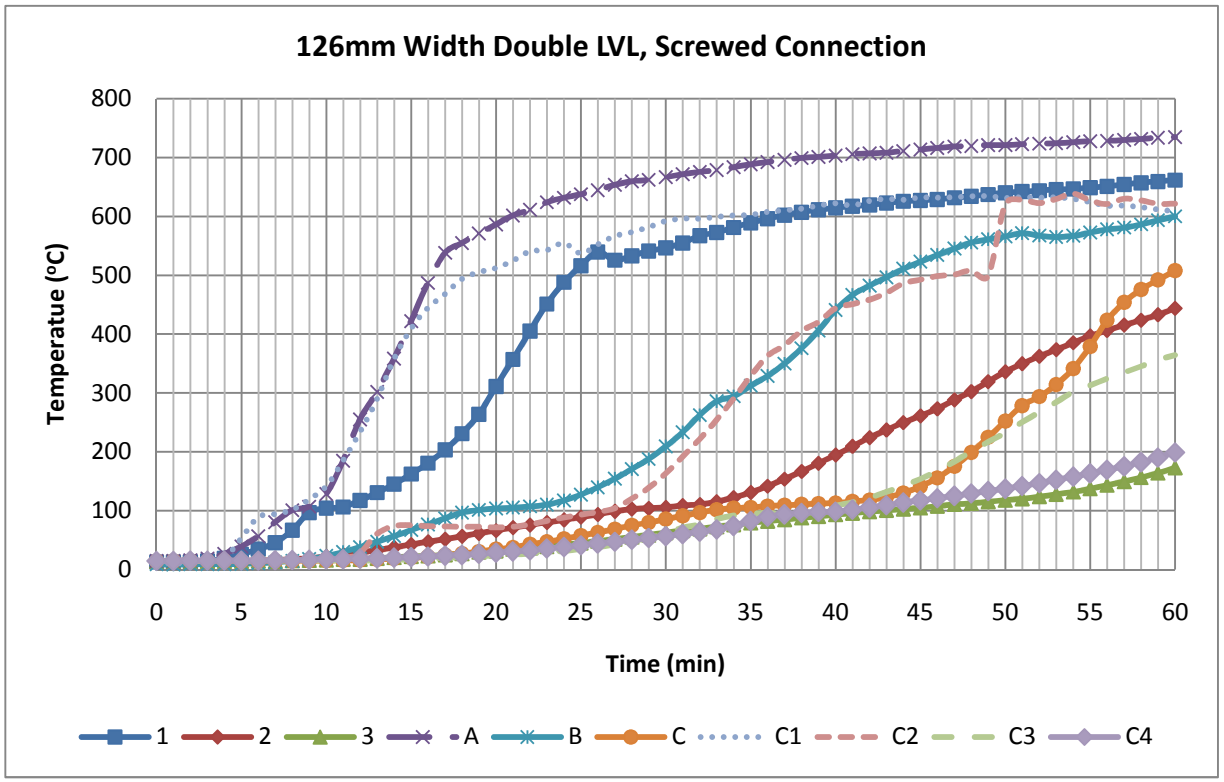

Figure G-2: 126mm, screwed connection

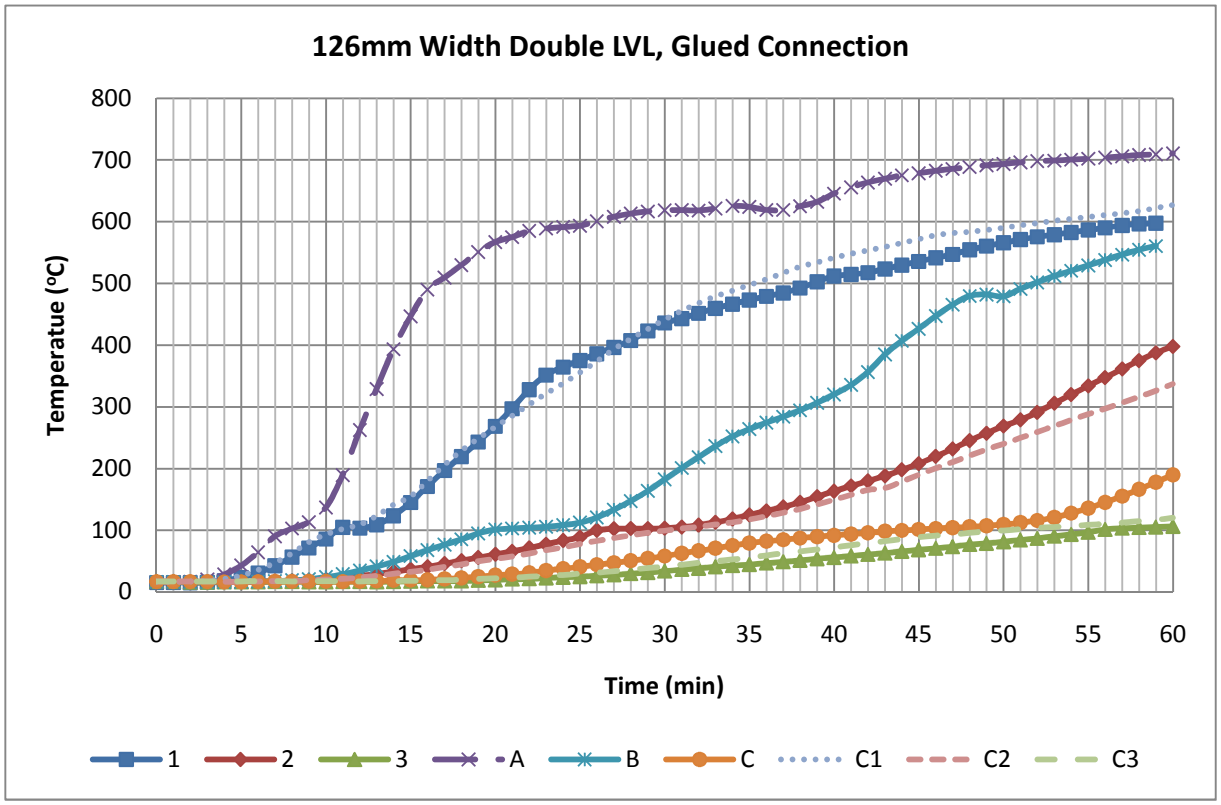

Figure G-3: 126mm, glued connection

Appendix H: Comparative thermocouple couple readings for 126mm width double LVL specimens (small furnace tests)

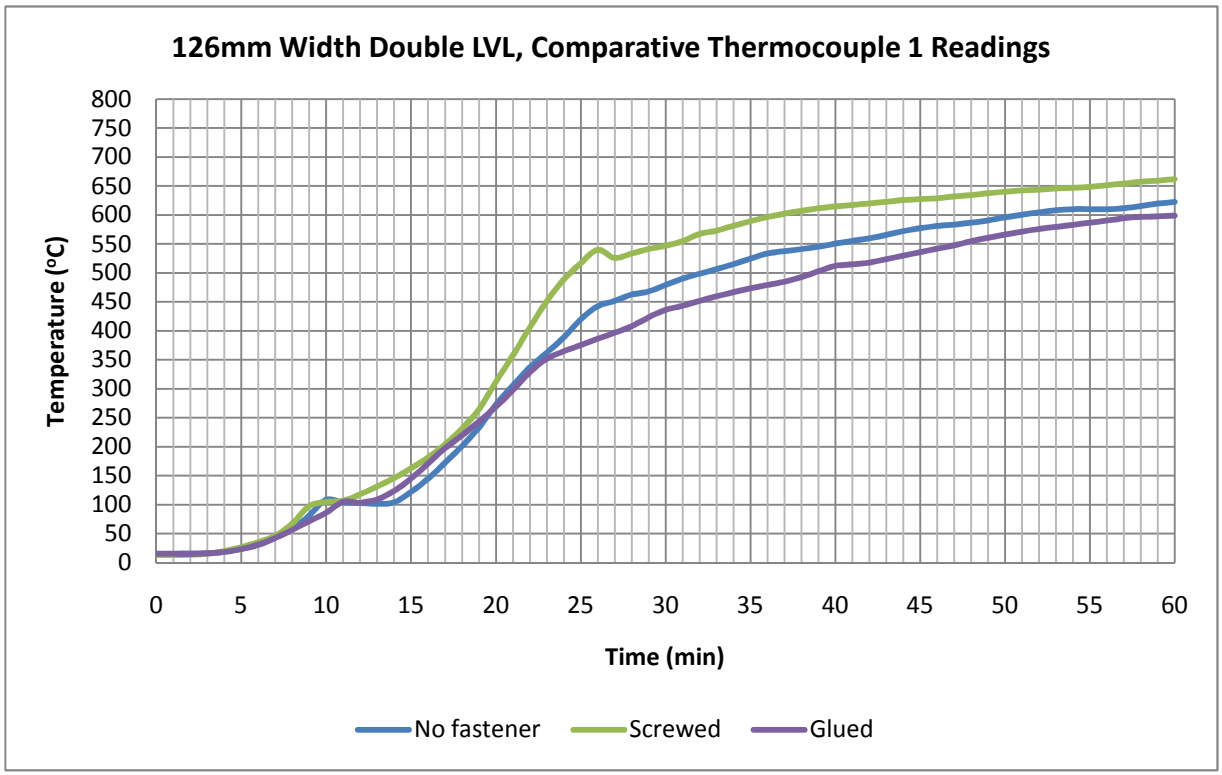

Figure H-1: 126mm, comparative thermocouple 1 readings

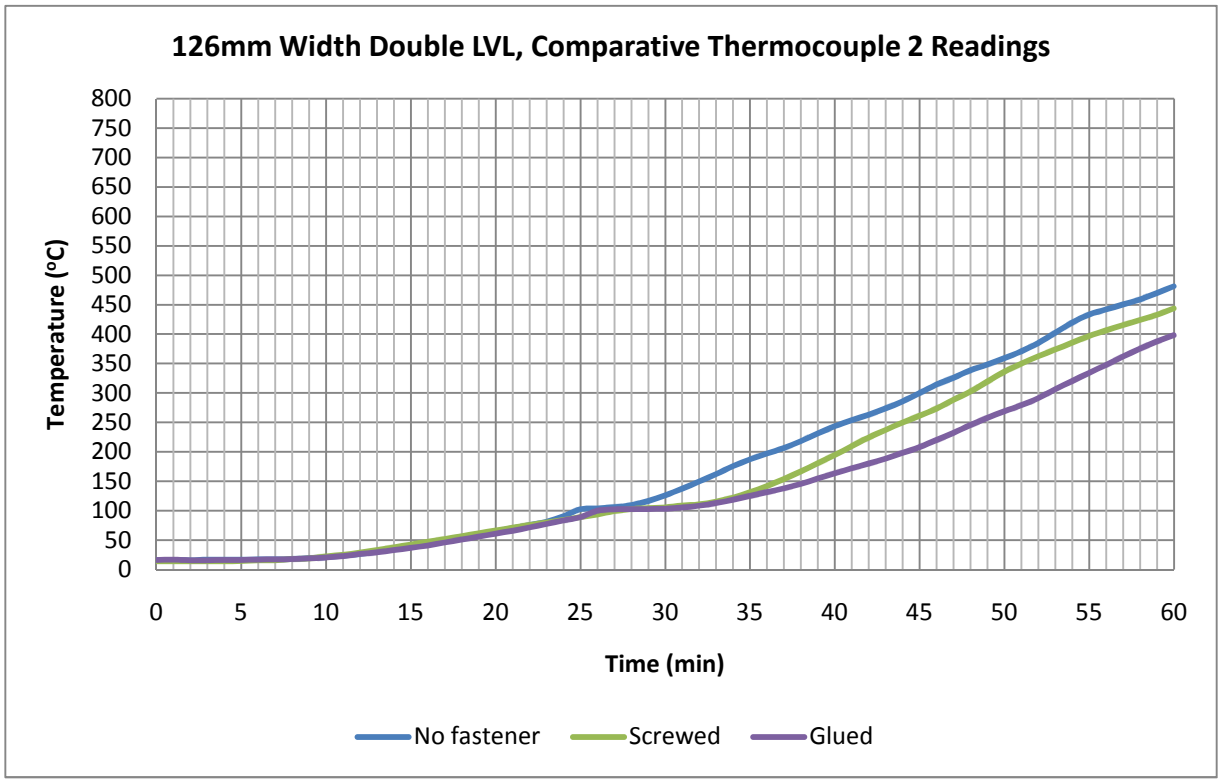

Figure H-2: 126mm, comparative thermocouple 2 readings

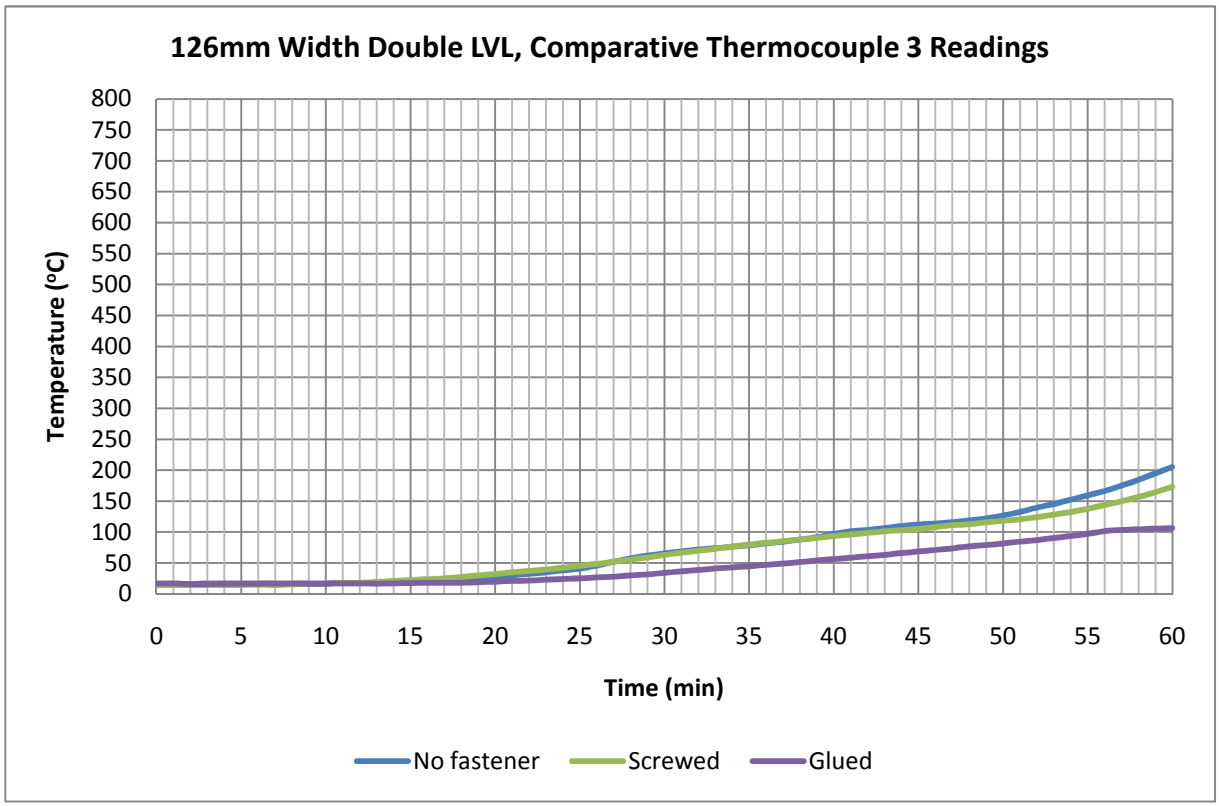

Figure H-3: 126mm, comparative thermocouple 3 readings

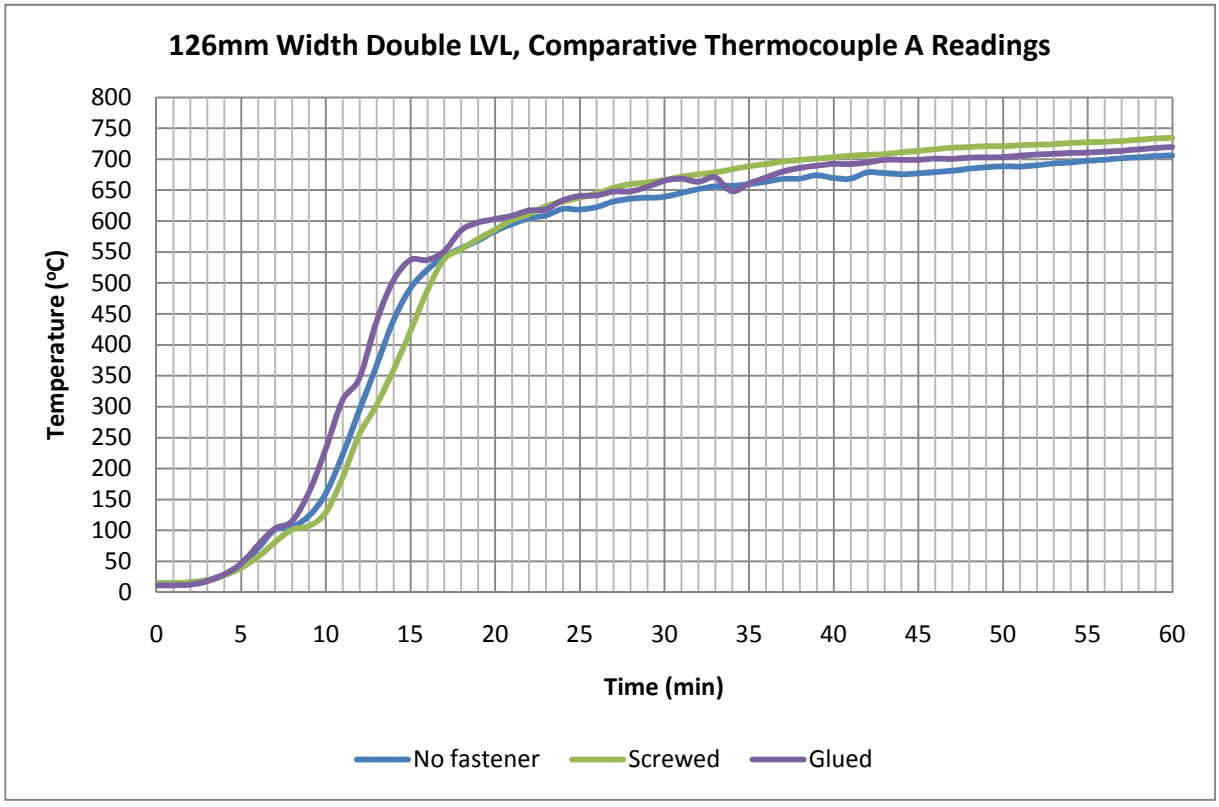

Figure H-4: 126mm, comparative thermocouple A readings

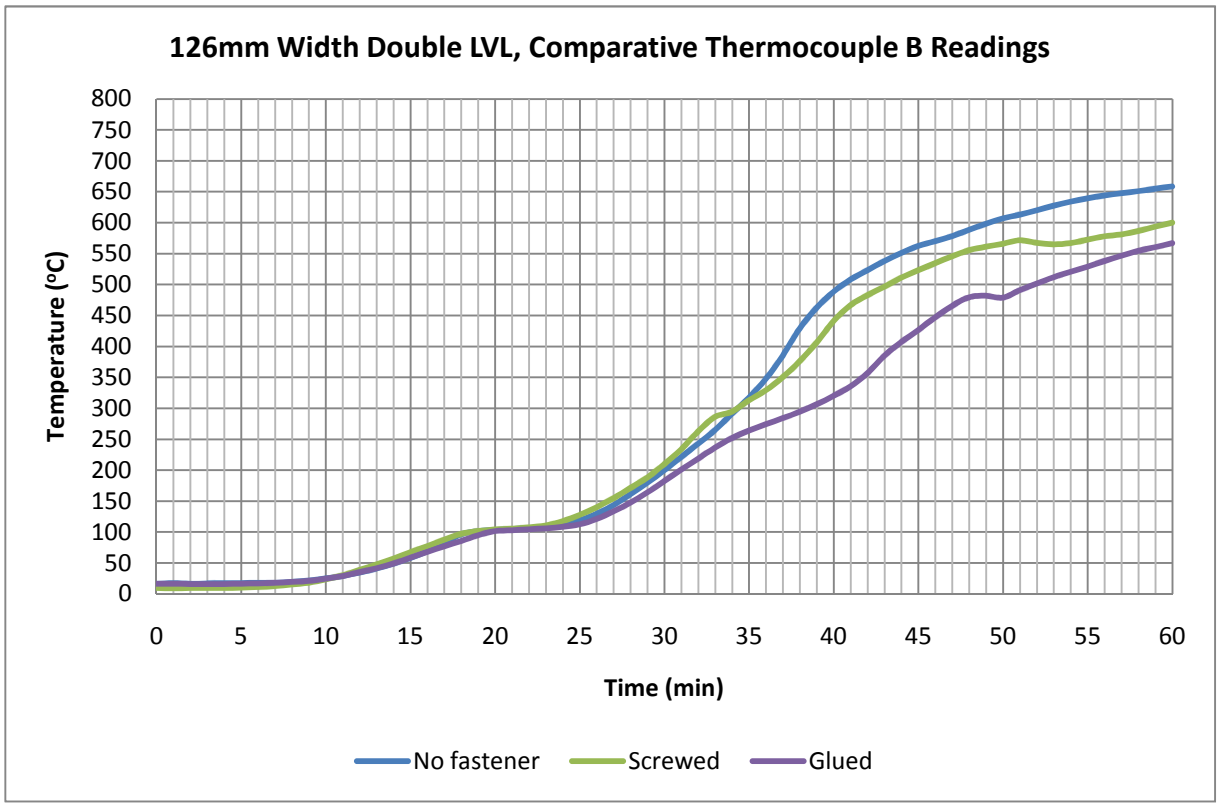

Figure H-5: 126mm, comparative thermocouple B readings

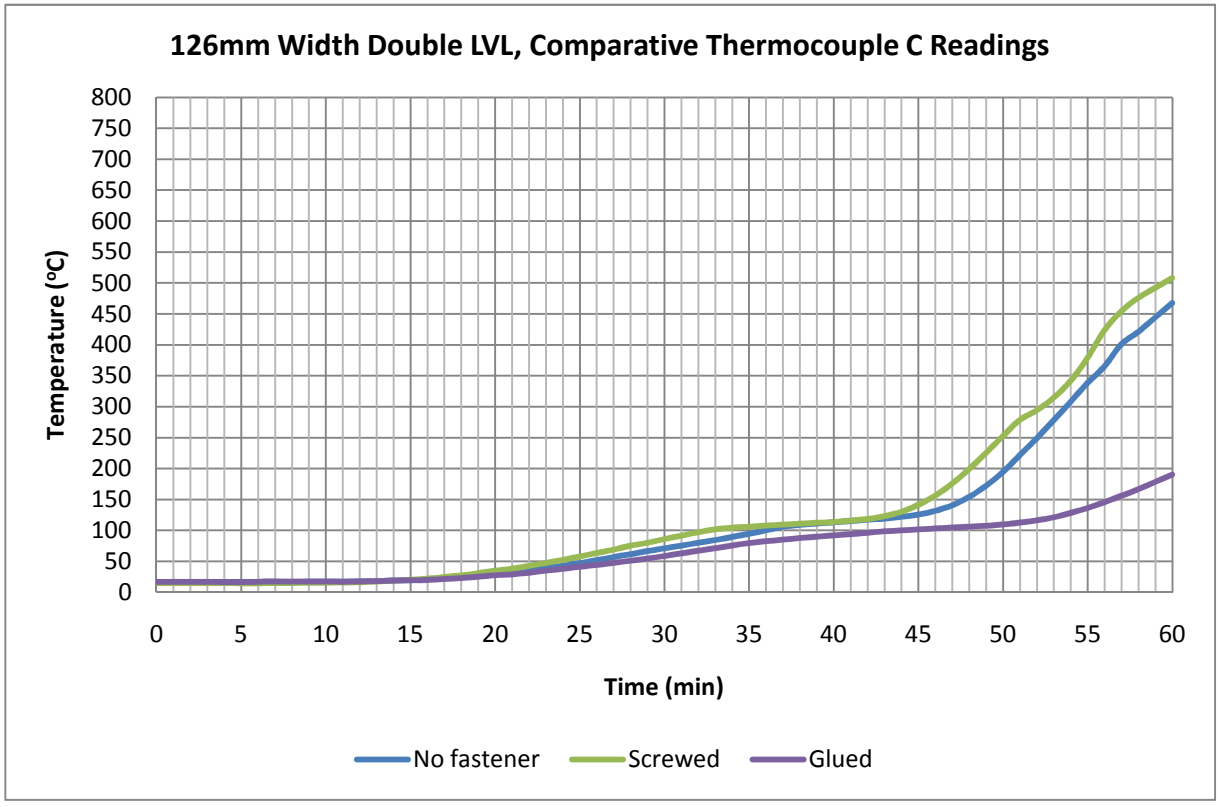

Figure H-6: 126mm, comparative thermocouple C readings

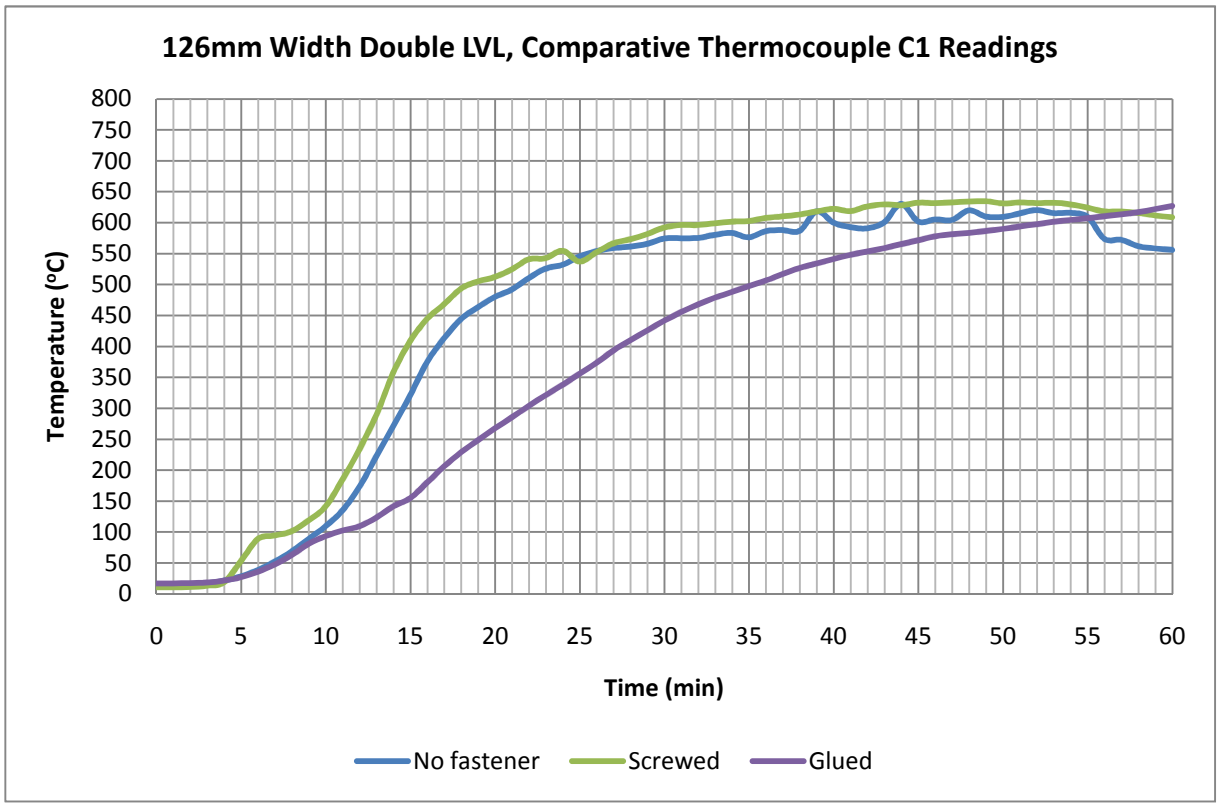

Figure H-7: 126mm, comparative thermocouple C1 readings

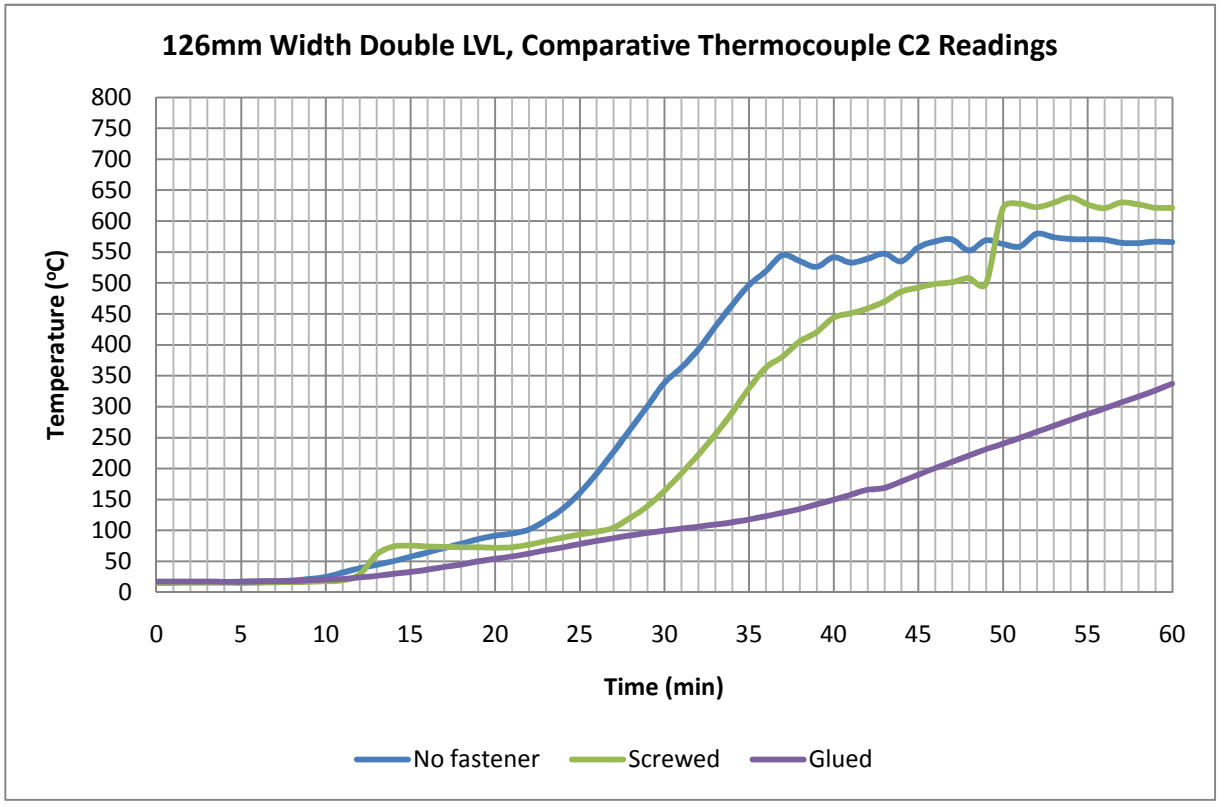

Figure H-8: 126mm, comparative thermocouple C2 readings

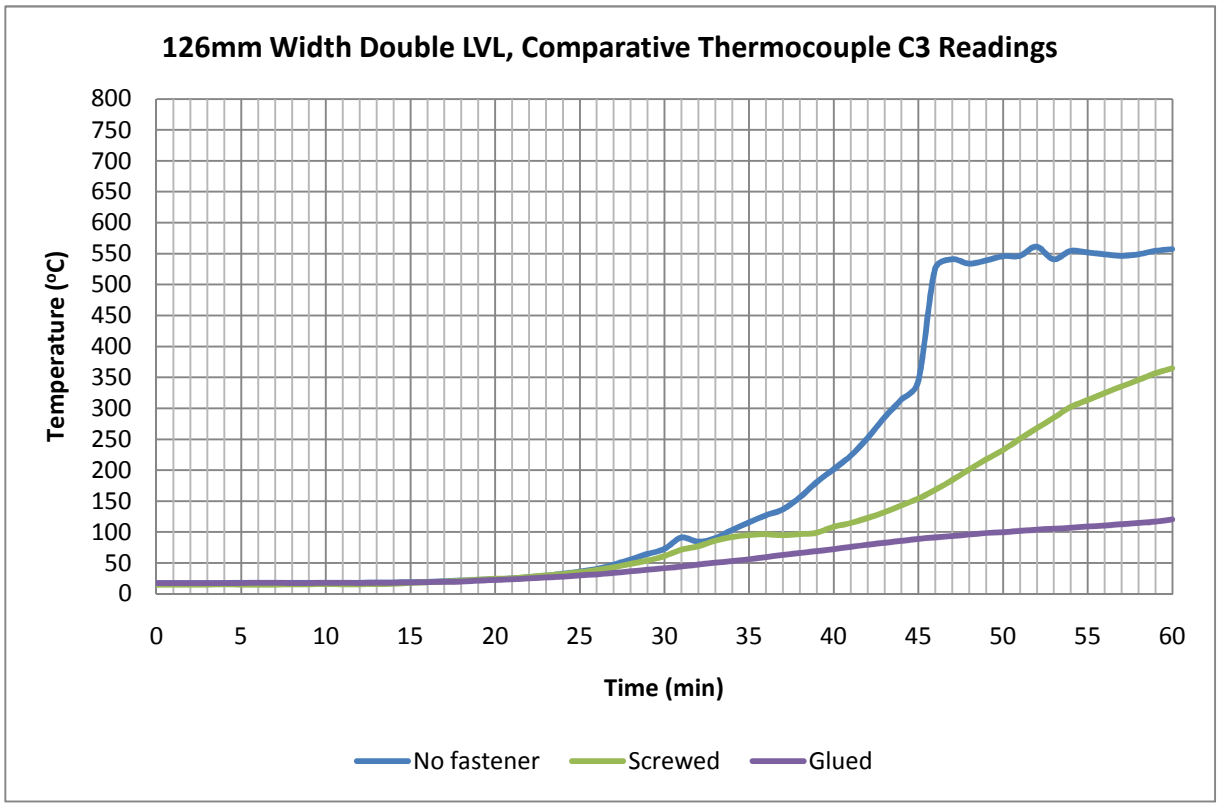

Figure H-9: 126mm, comparative thermocouple C3 readings

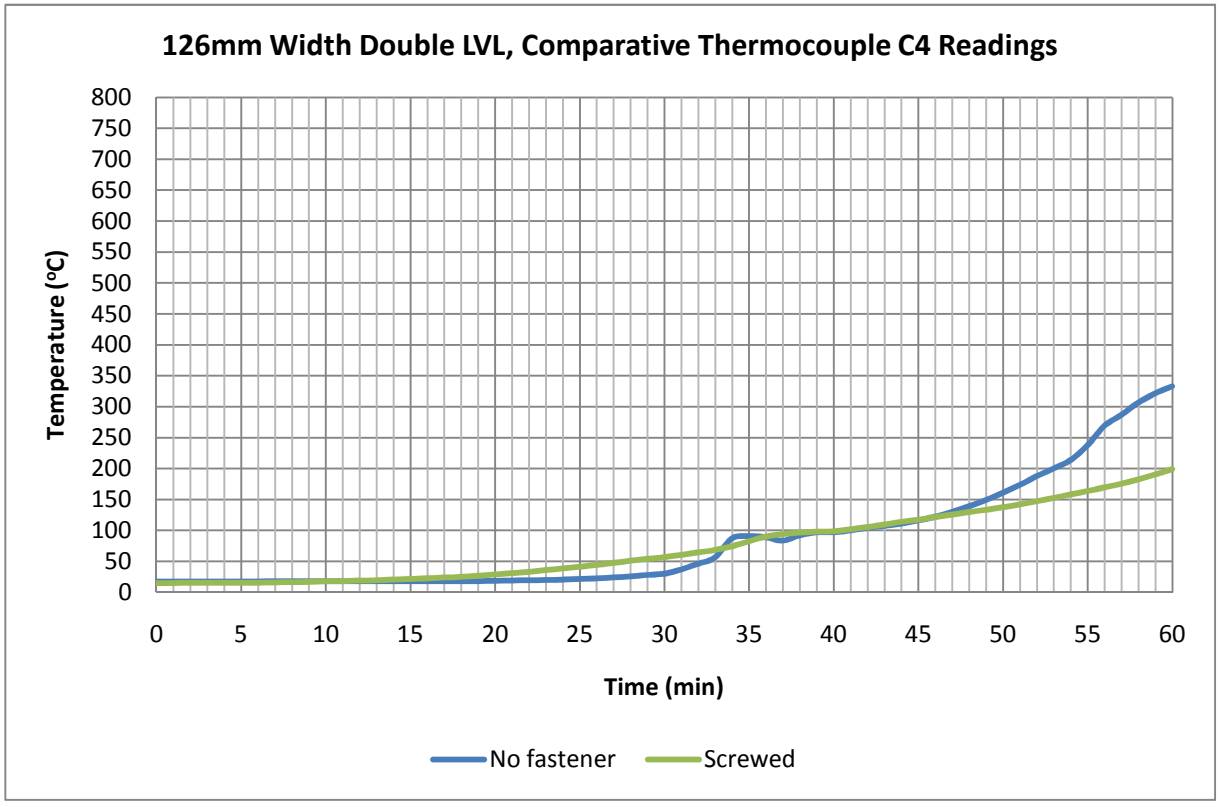

Figure H-10: 126mm, comparative thermocouple C4 readings

Appendix I: Thermocouple readings from first pilot furnace test

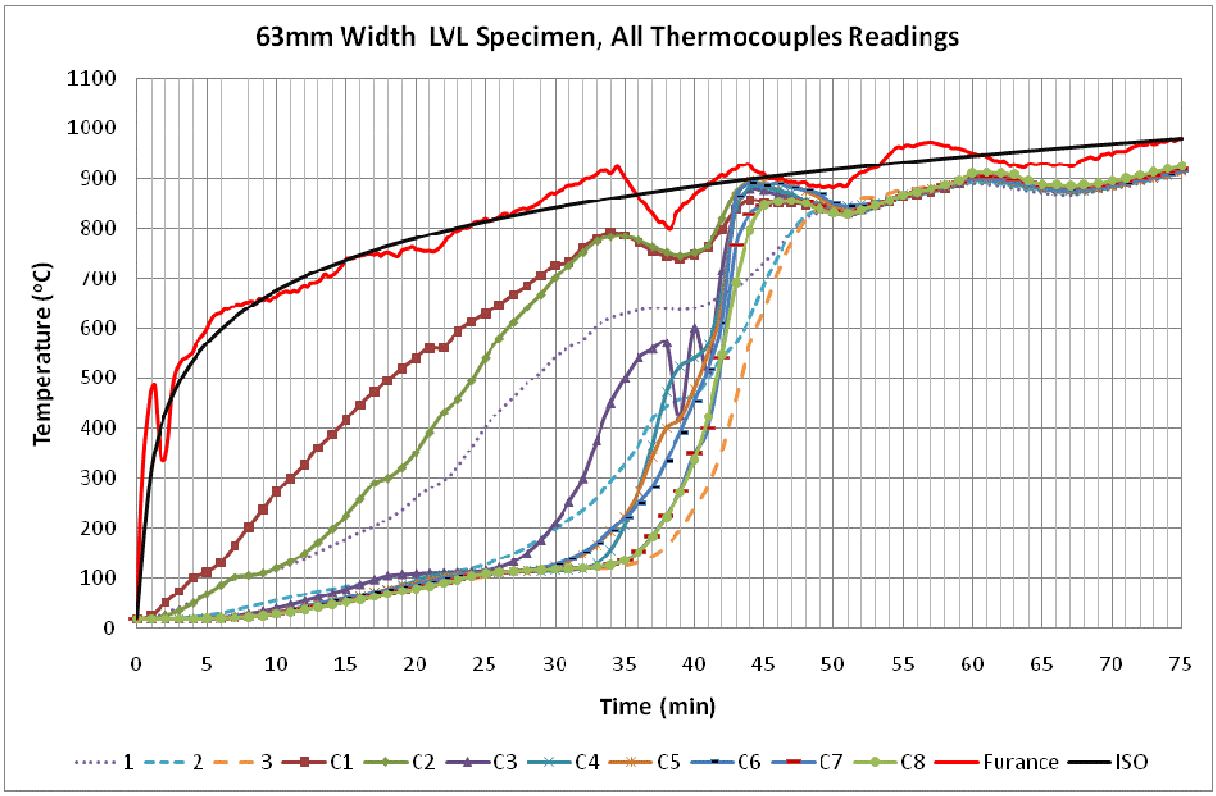

Figure I-1: 63mm, all thermocouples readings

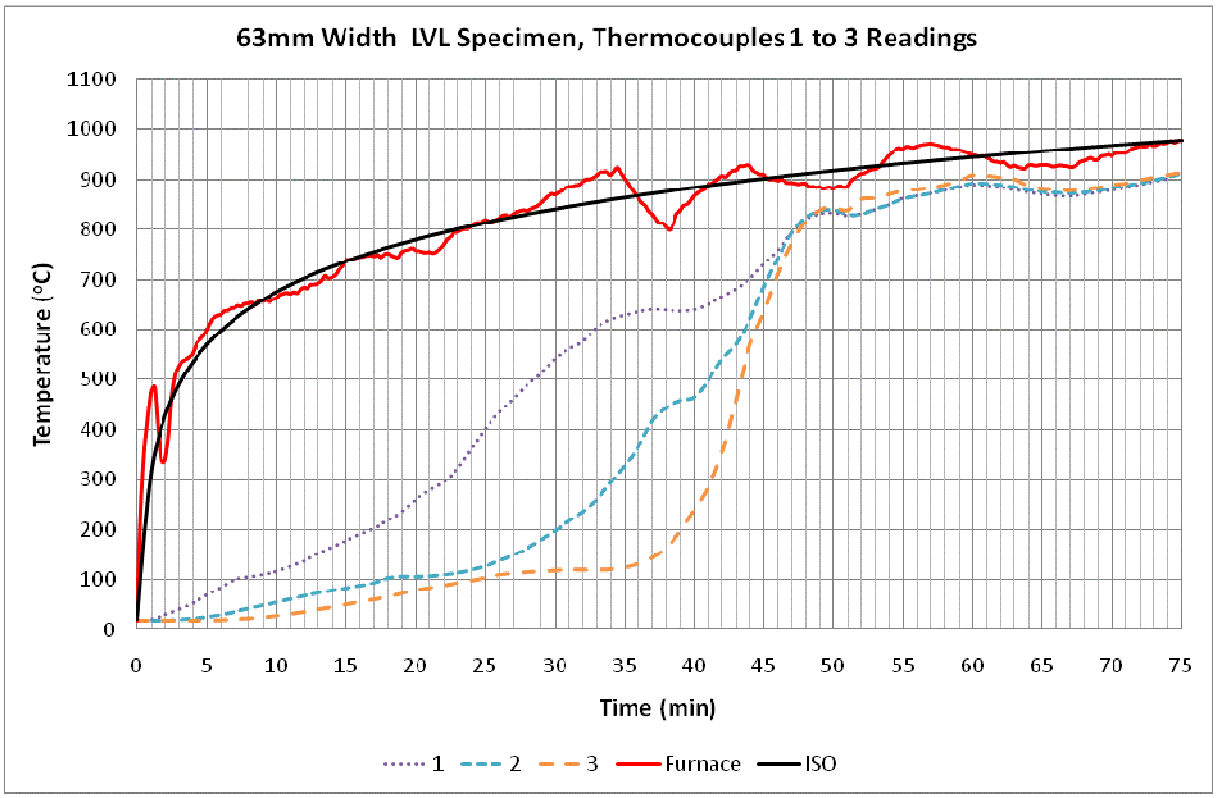

Figure I-2: 63mm, thermocouples 1 to 3 readings

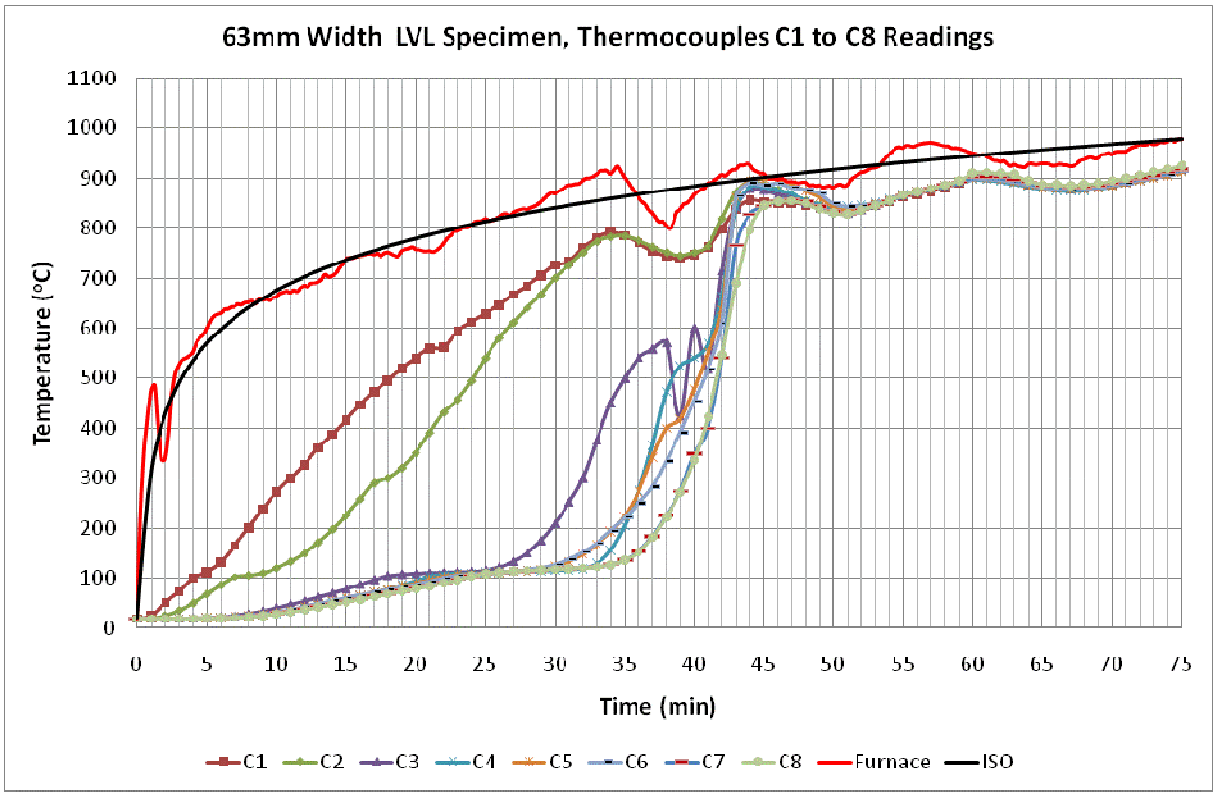

Figure I-3: 63mm, thermocouples C1 to C8 readings

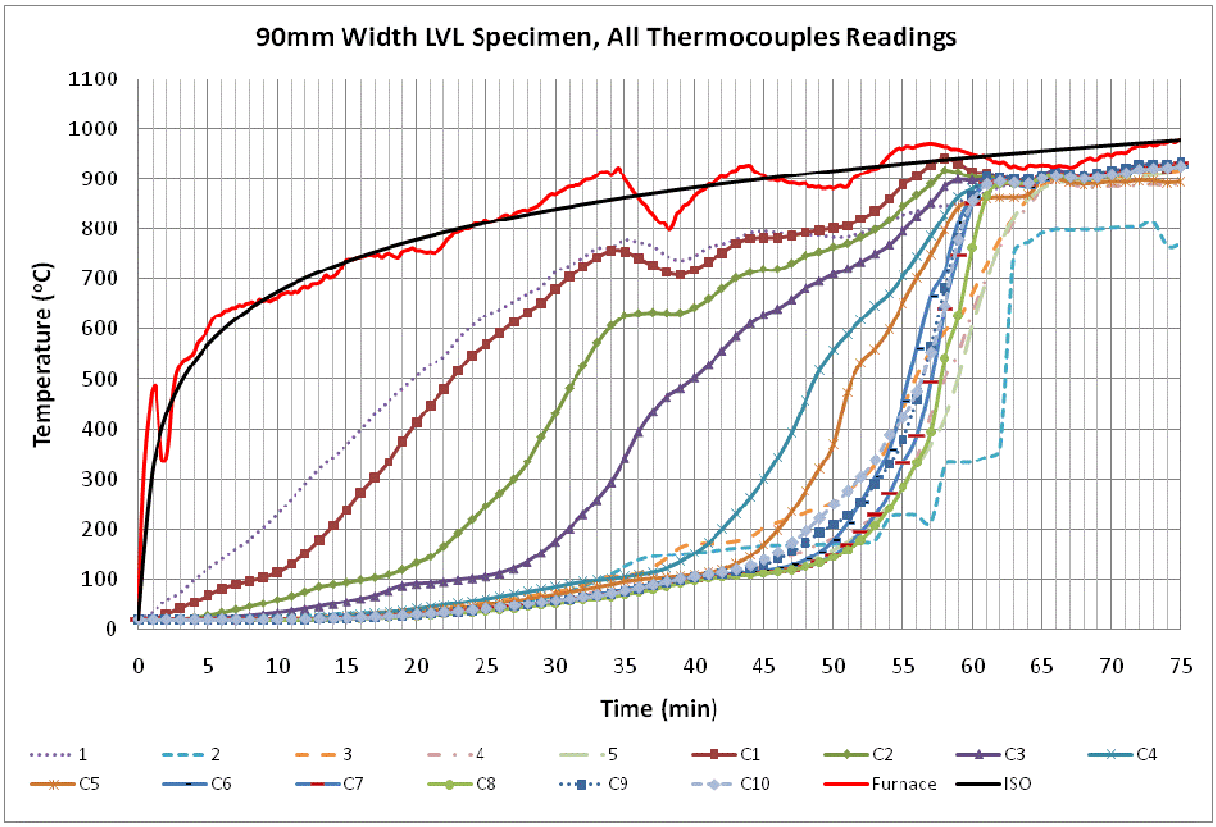

Figure I-4: 90mm, all thermocouples readings

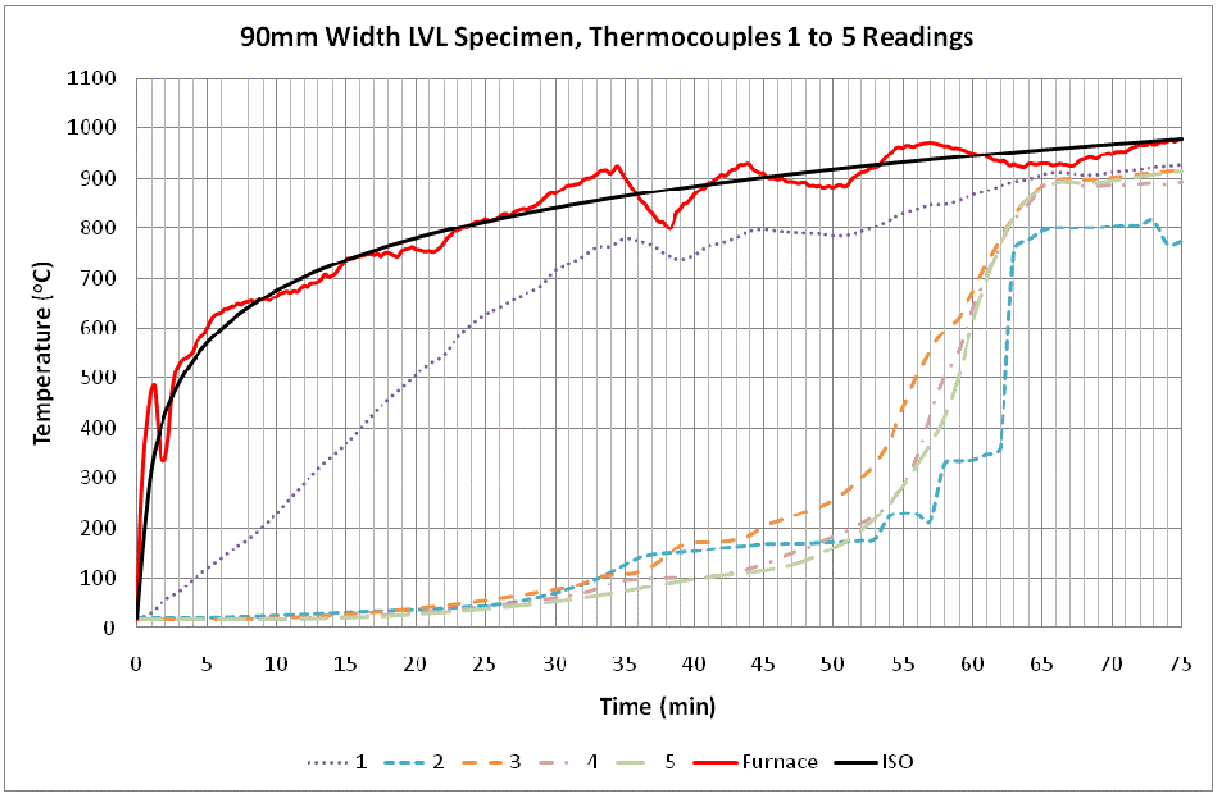

Figure I-5: 90mm, thermocouples 1 to 5 readings

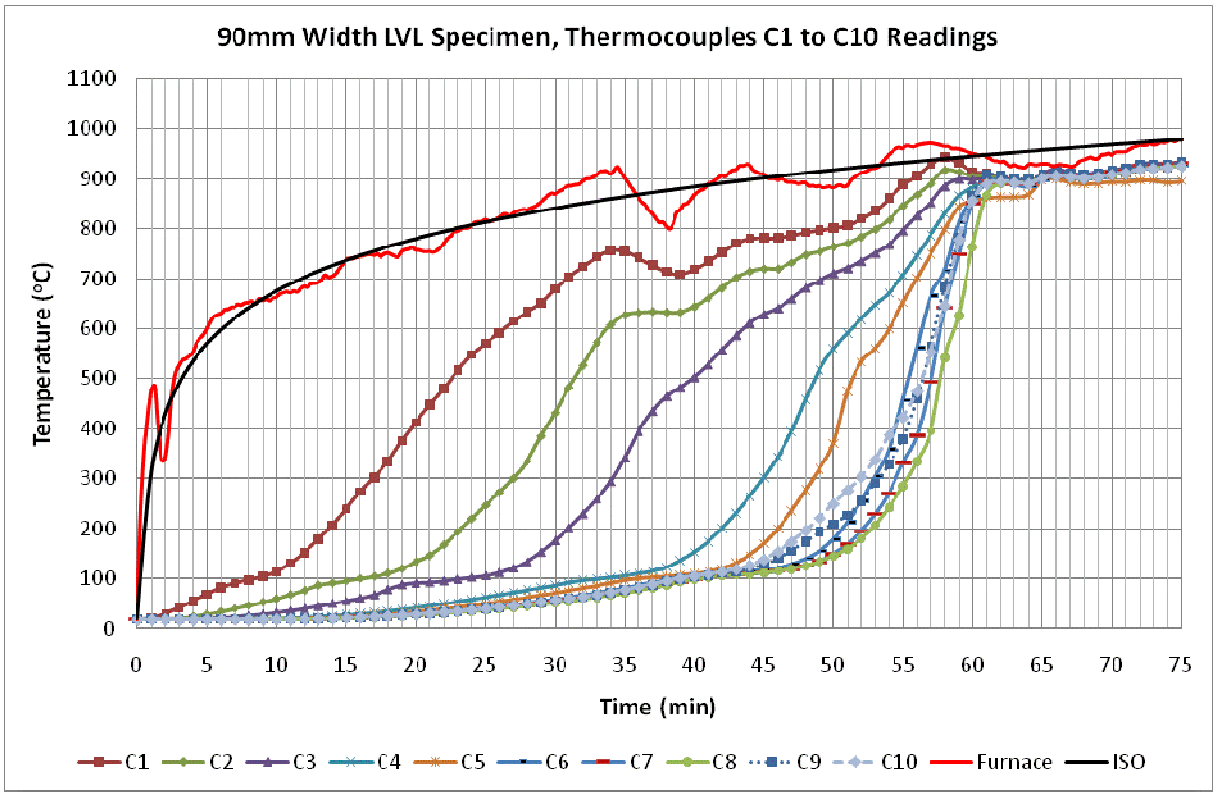

Figure I-6: 90mm, thermocouples C1 toC105 readings

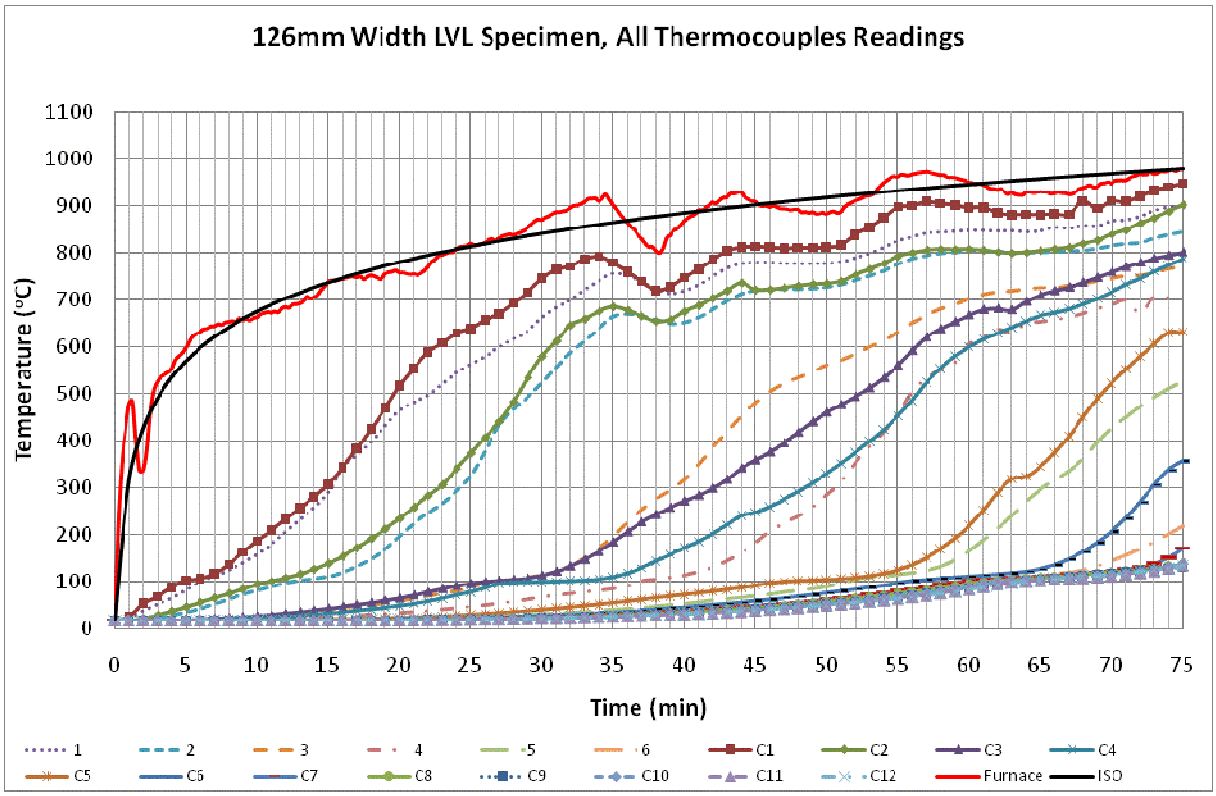

Figure I-7: 126mm, all thermocouples readings

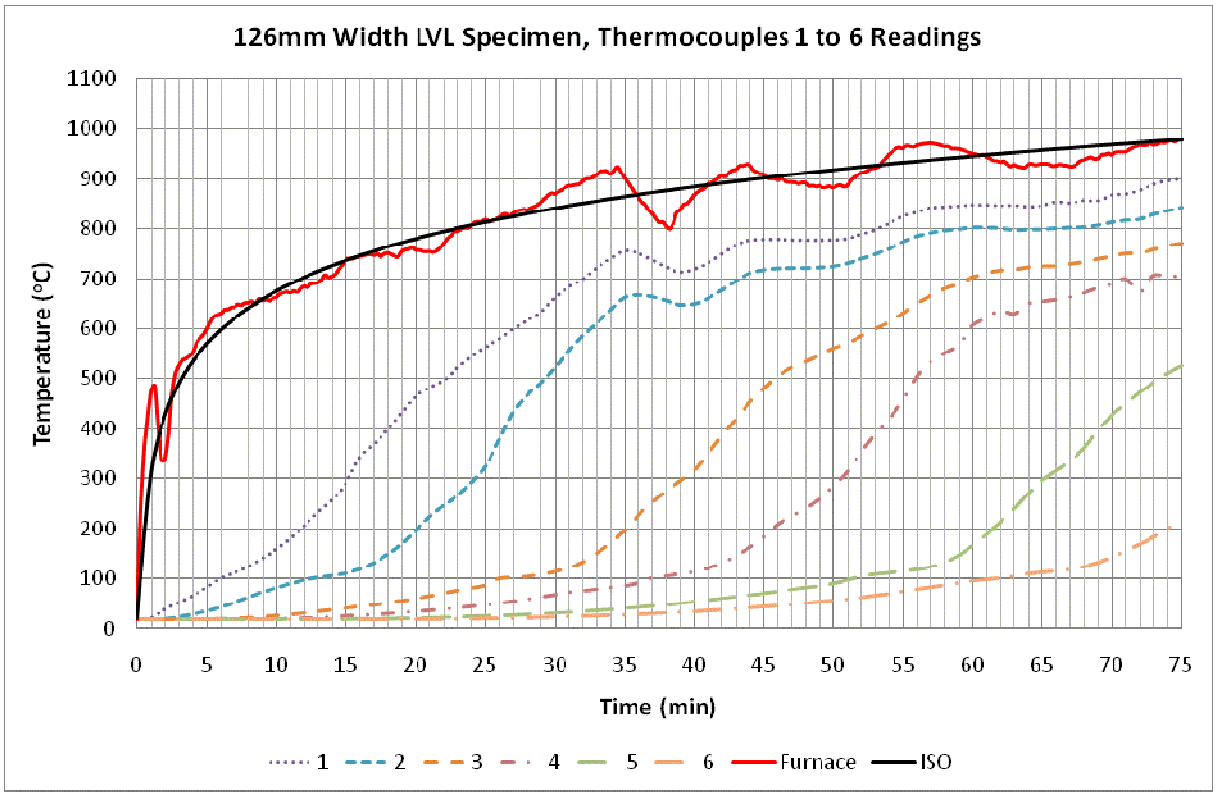

Figure I-8: 126mm, thermocouples 1 to 6 readings

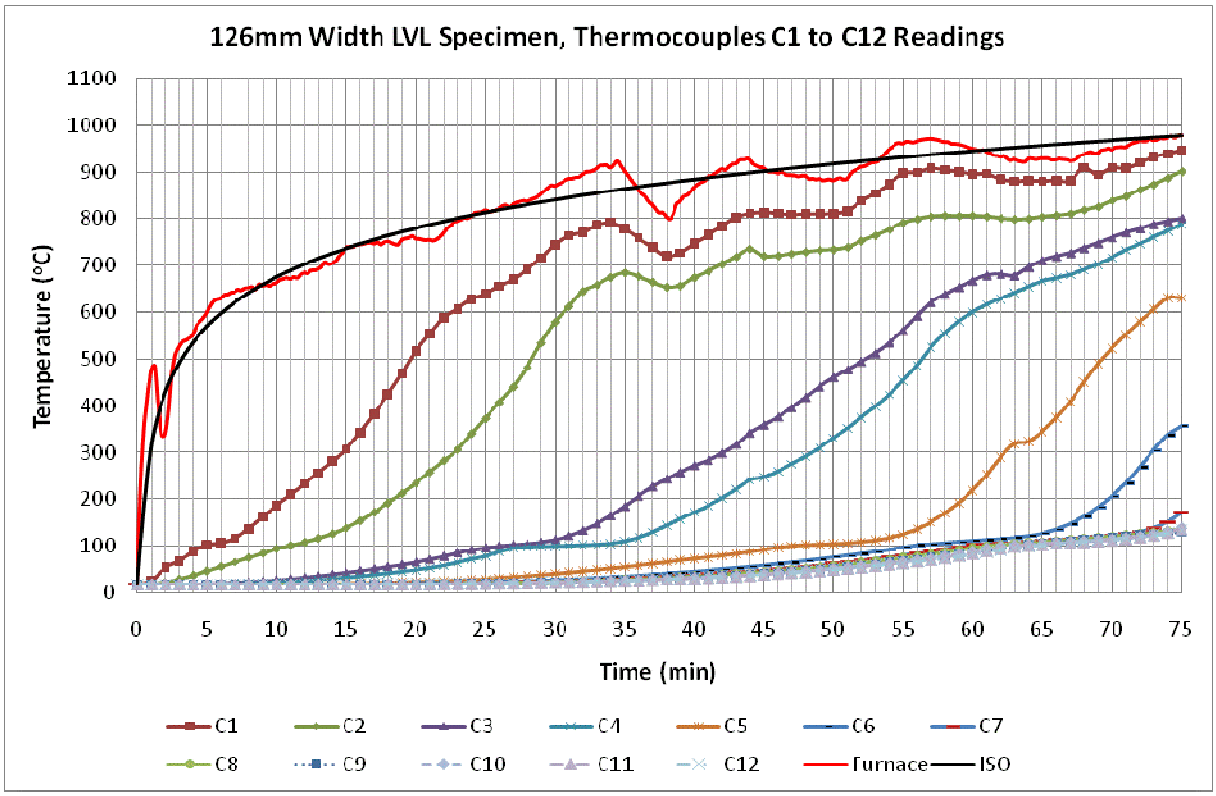

Figure I-9: 126mm, thermocouples C1 to C12 readings

Appendix J: Thermocouple readings from the fourth pilot furnace test

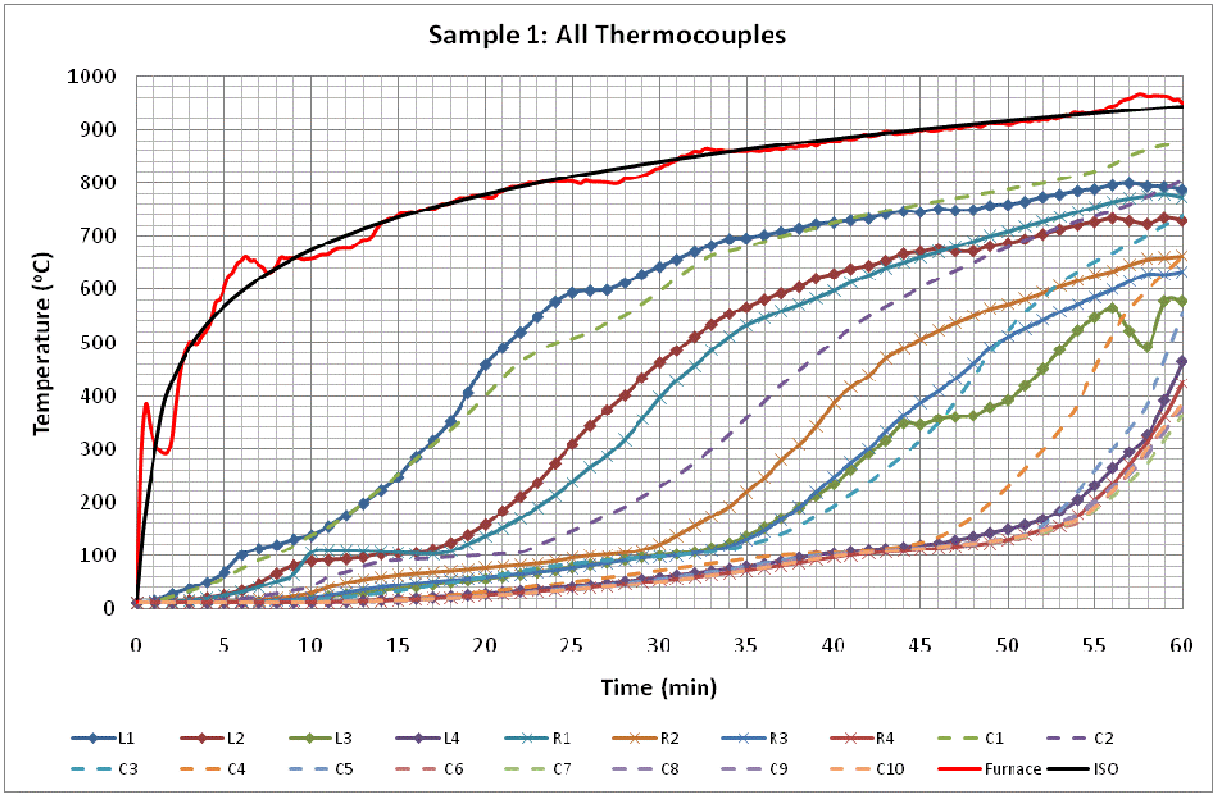

Figure J-1: Sample 1, all thermocouples readings

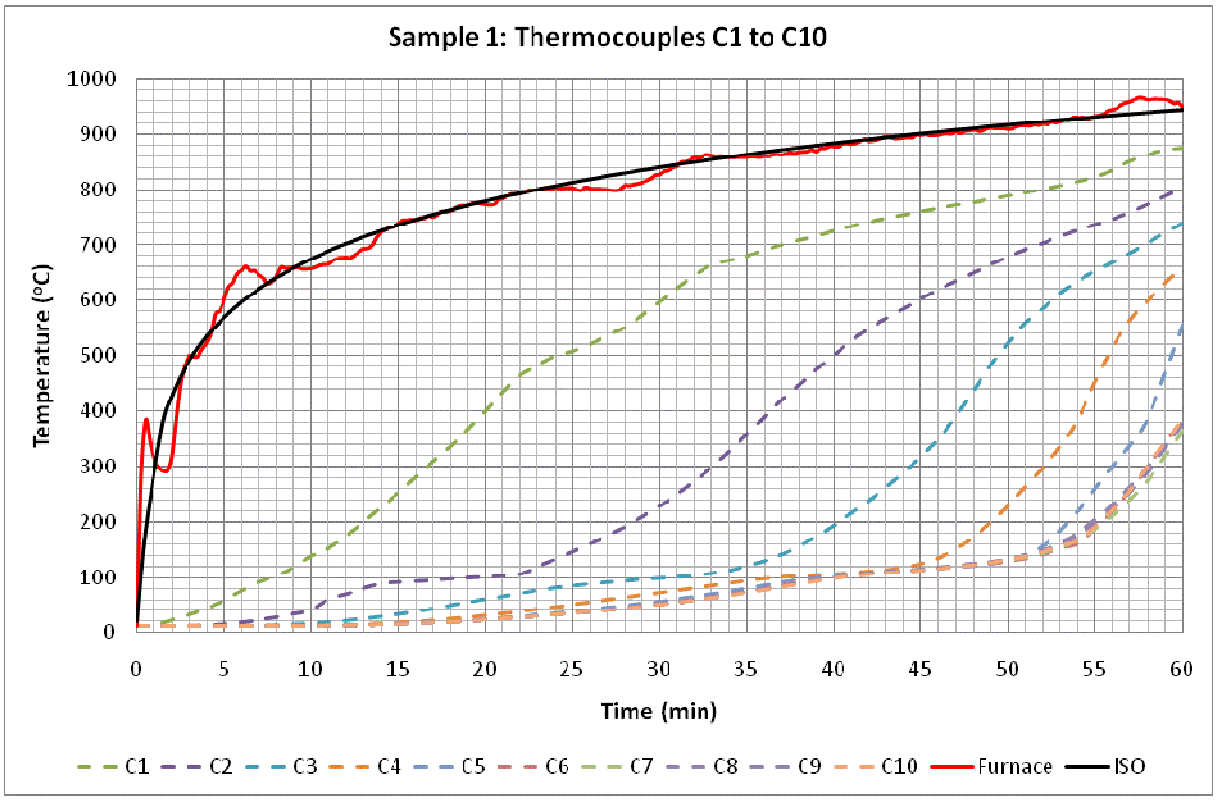

Figure J-2: Sample 1, thermocouples C1 to C10 readings

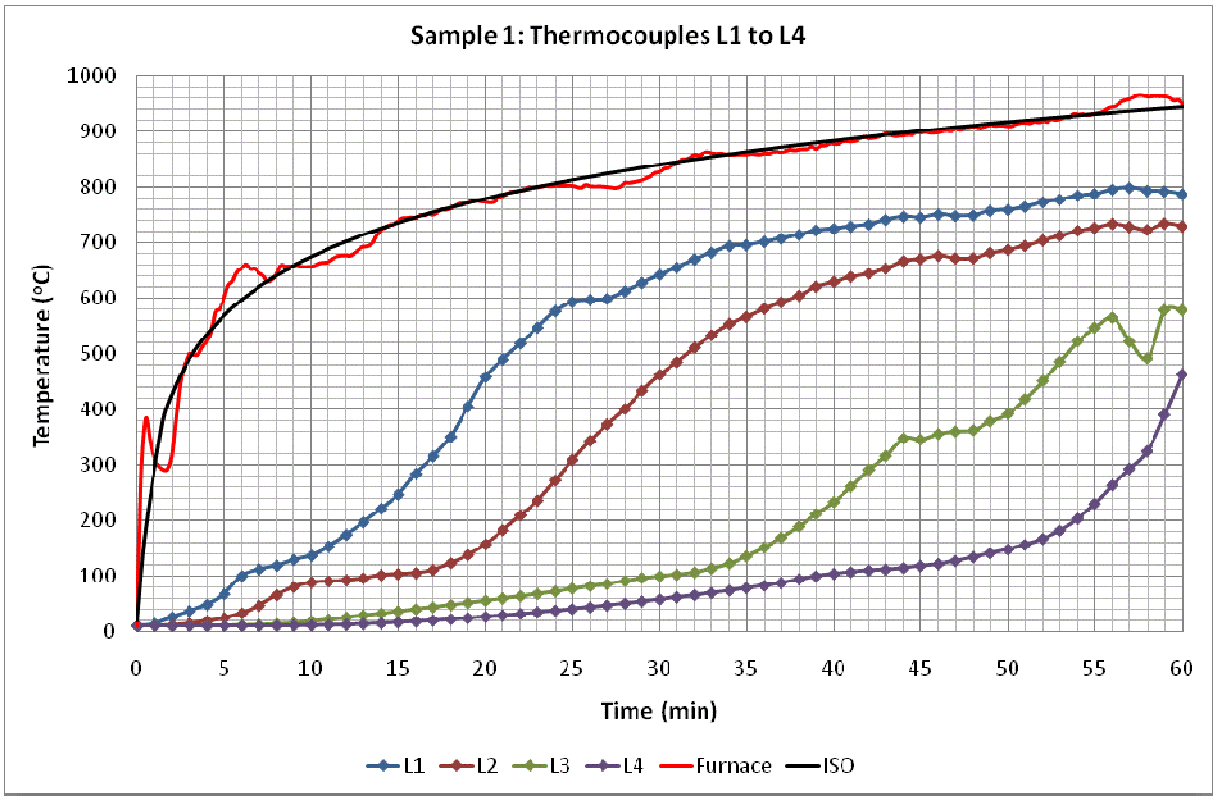

Figure J-3: Sample 1, thermocouples L1 to L4 readings

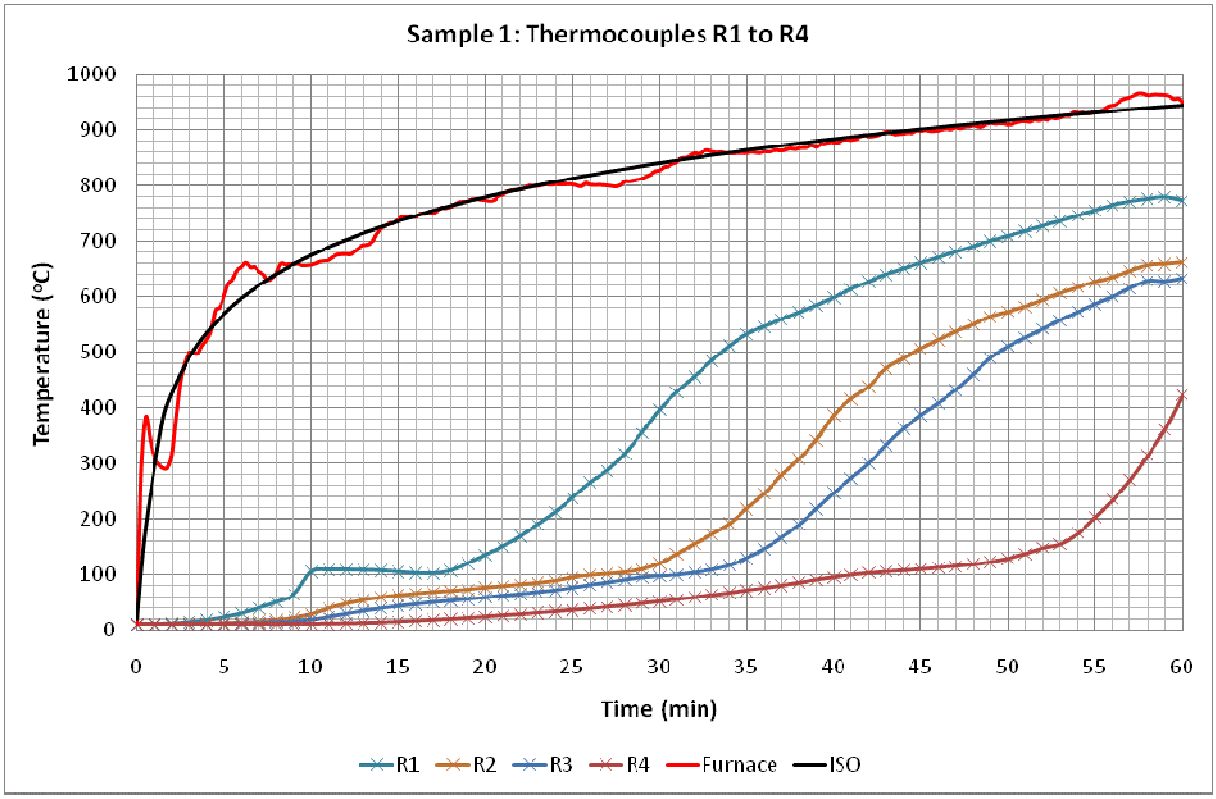

Figure J-4: Sample 1, thermocouples R1 to R4 readings

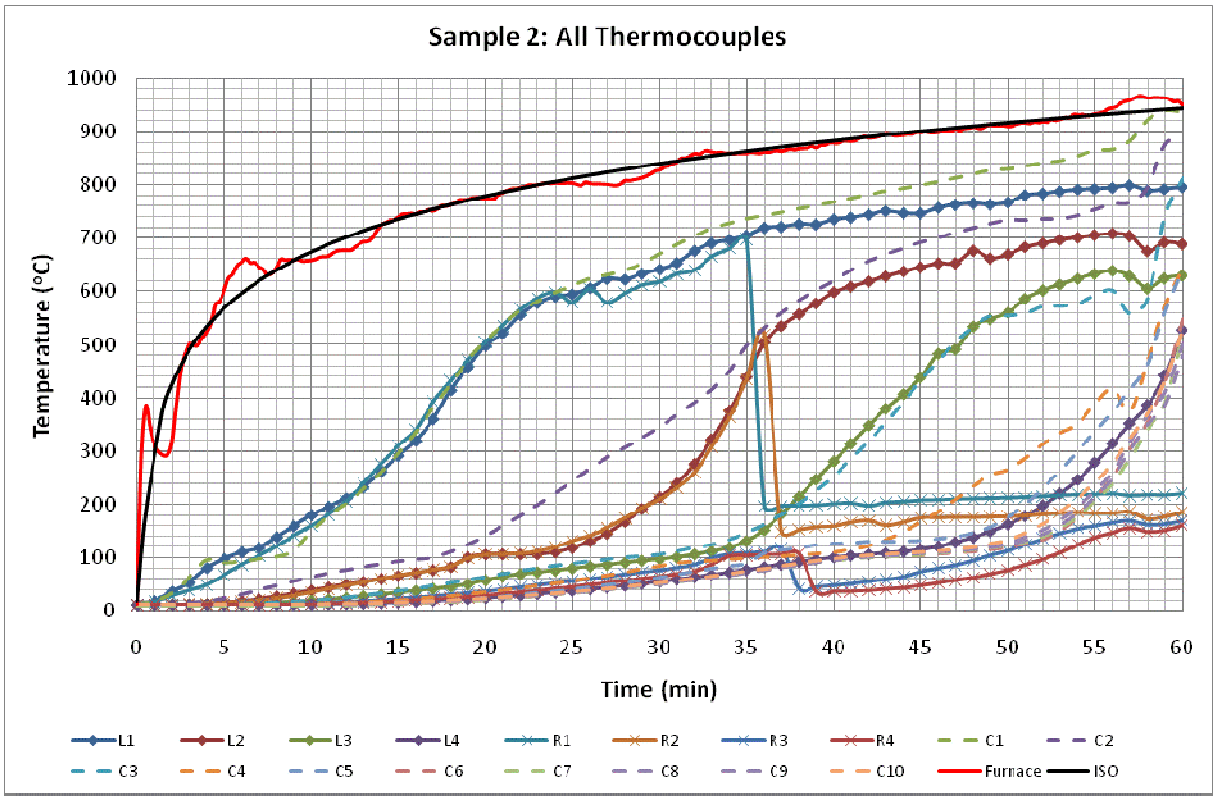

Figure J-5: Sample 2, all thermocouples readings

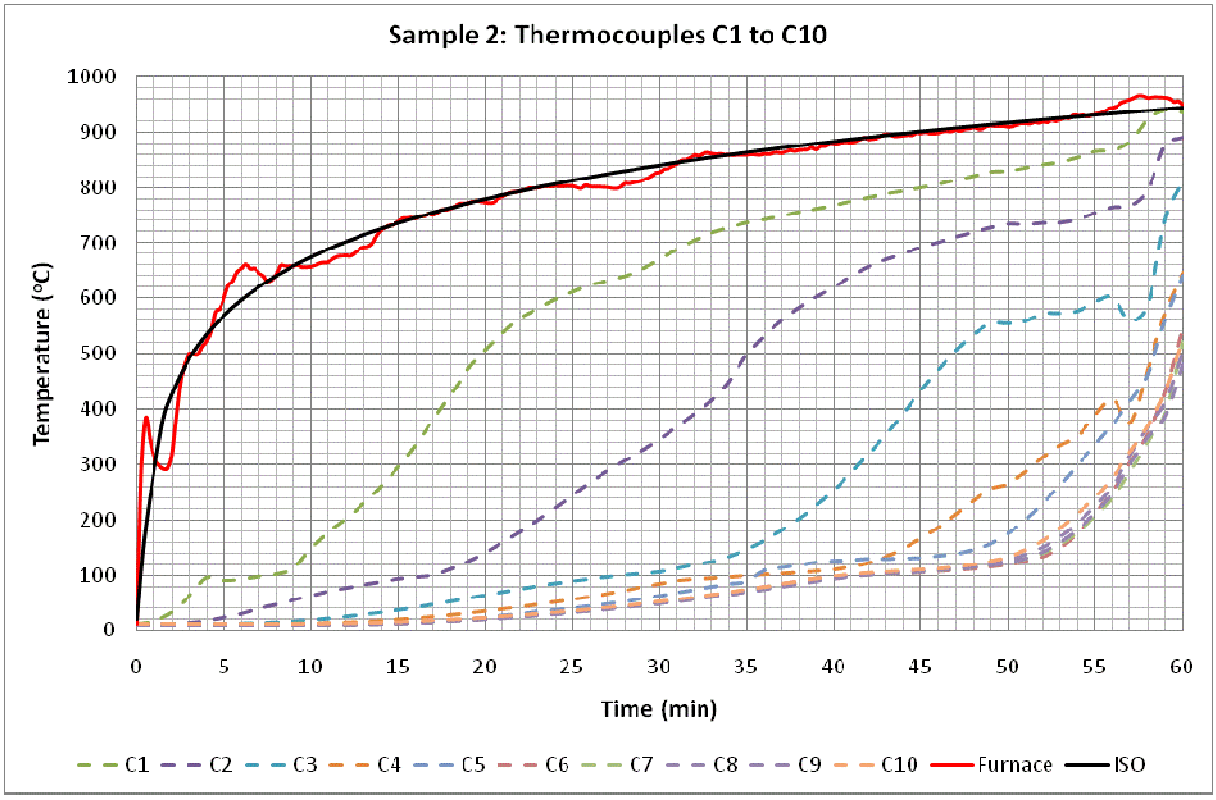

Figure J-6: Sample 2, thermocouples C1 to C10 readings

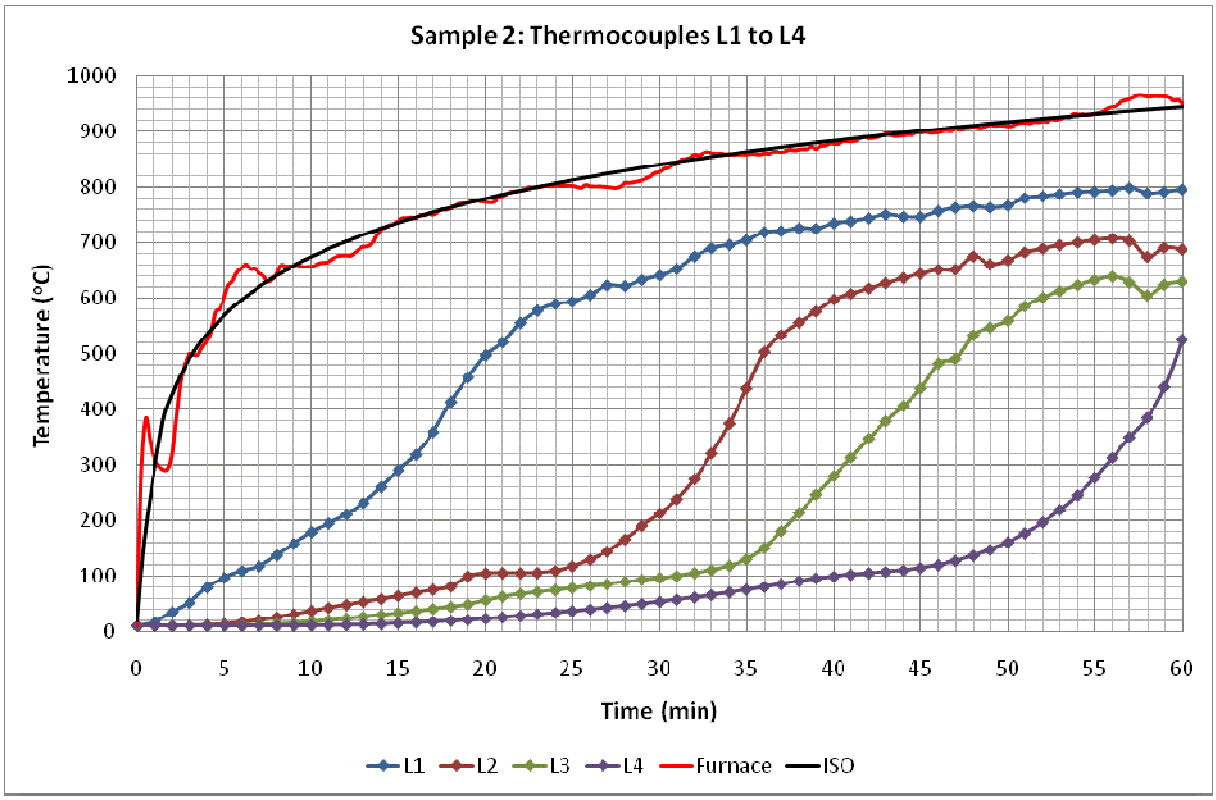

Figure J-7: Sample 2, thermocouples L1 to L4 readings

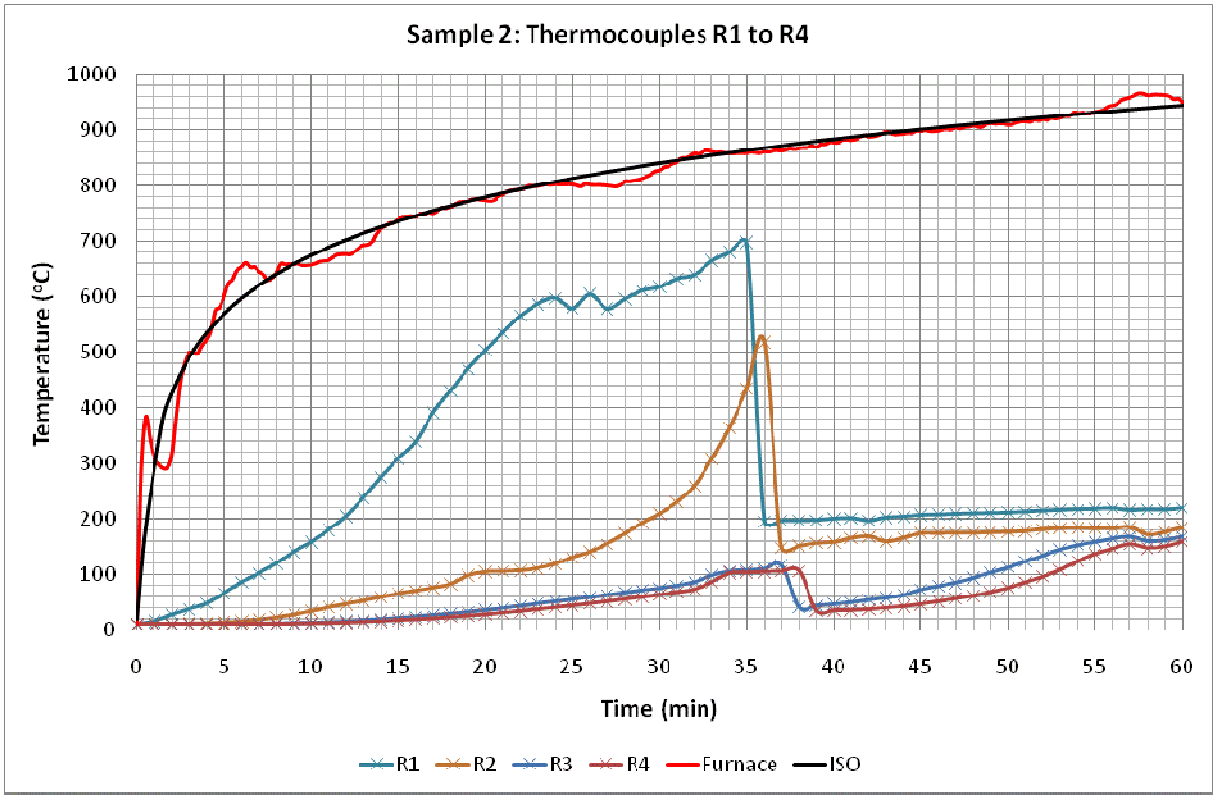

Figure J-8: Sample 2, thermocouples R1 to R4 readings

Appendix K: SAFIR Thermal Images for the 63mm width LVL Member

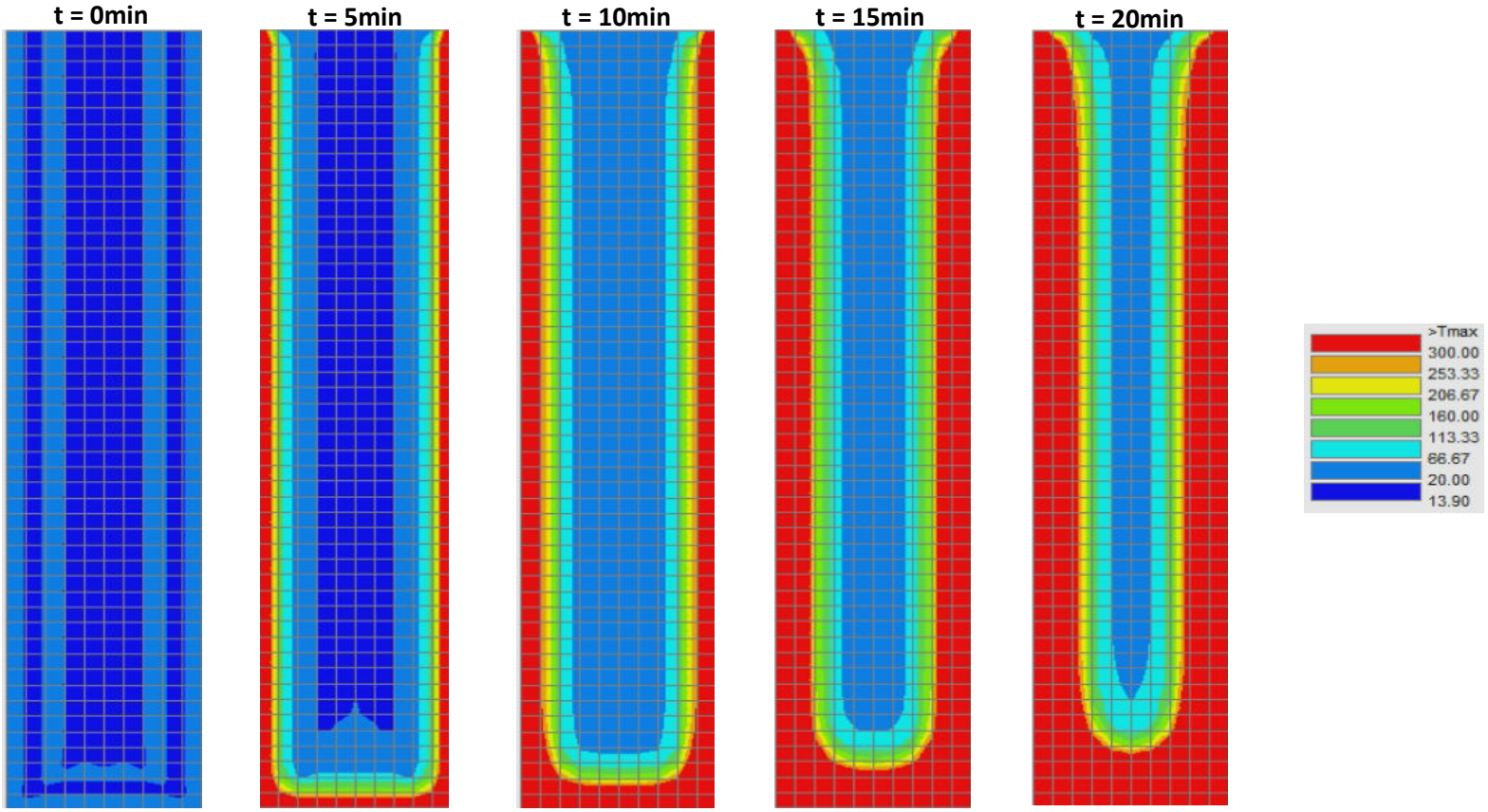

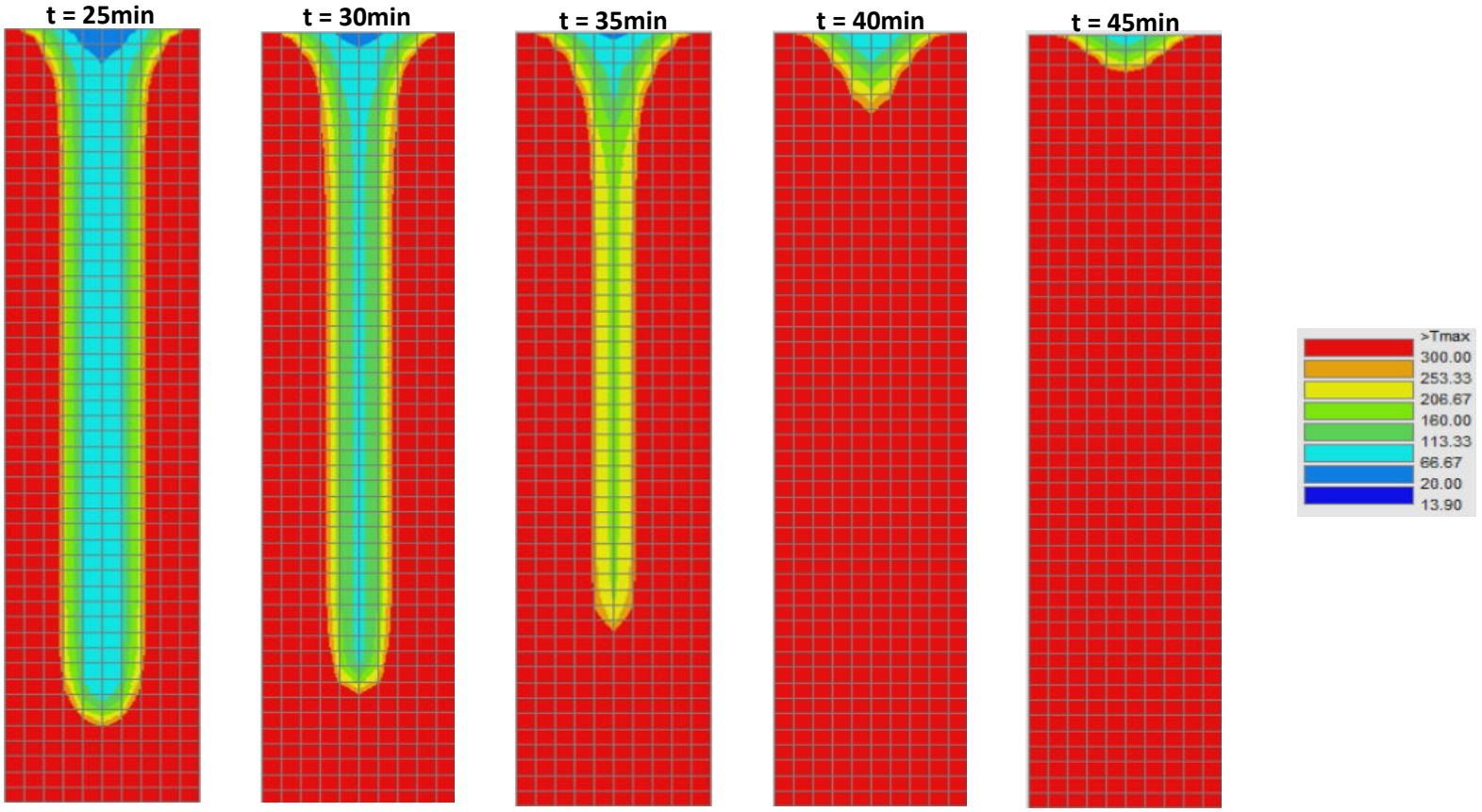
t = 25min
t = 30min
t = 35min
t = 40min
t = 45min
>Tmax
300.00
253.33
206.67
160.00
113.33
66.67
20.00
13.90

Appendix L: SAFIR Thermal Images for the 90mm width LVL Member

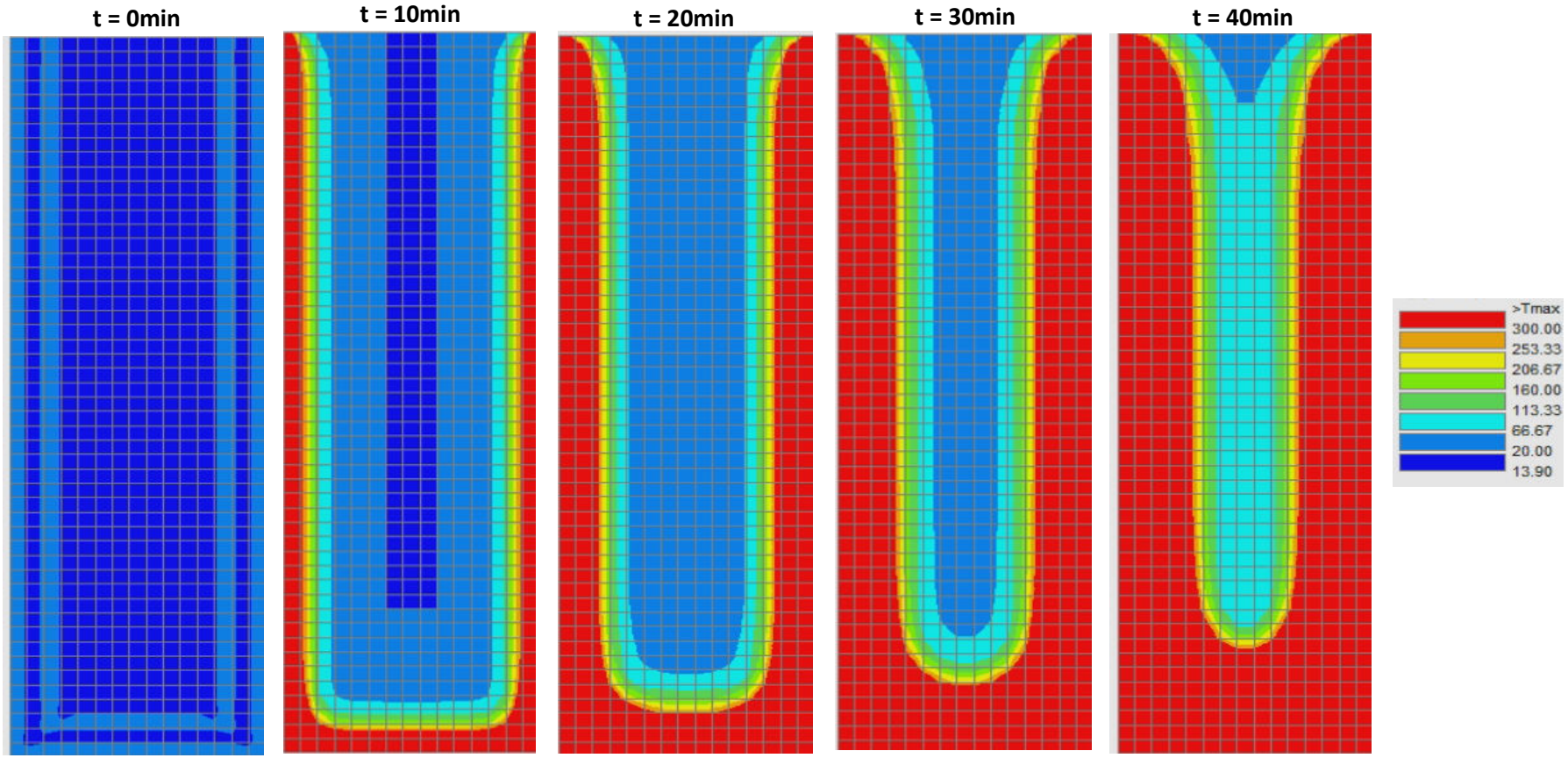

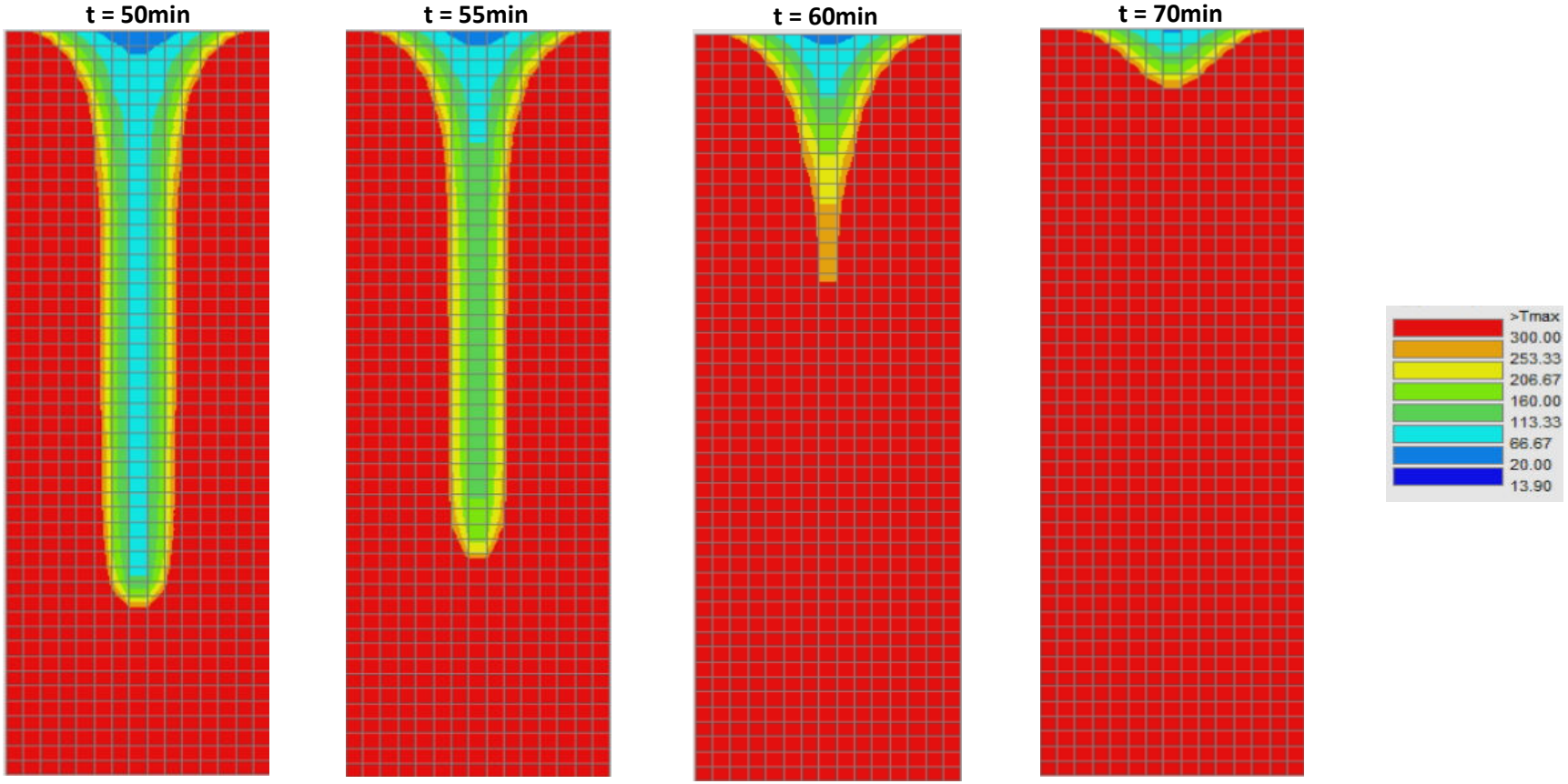
t = 50min
t = 55min
t = 60min
t = 70min
>Tmax
300.00
253.33
206.67
160.00
113.33
66.67
20.00
13.90

Appendix M: SAFIR Thermal Images for the 126mm width LVL Member

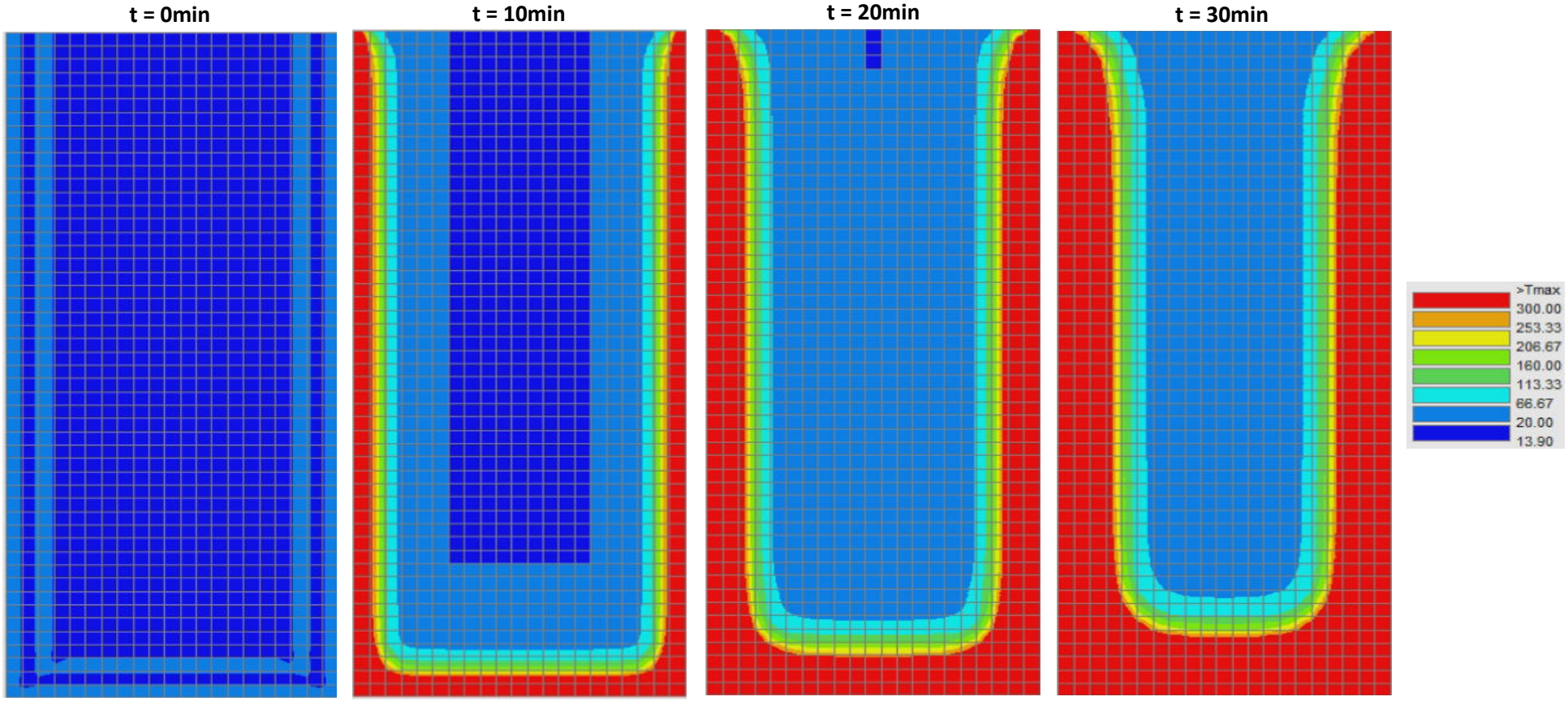

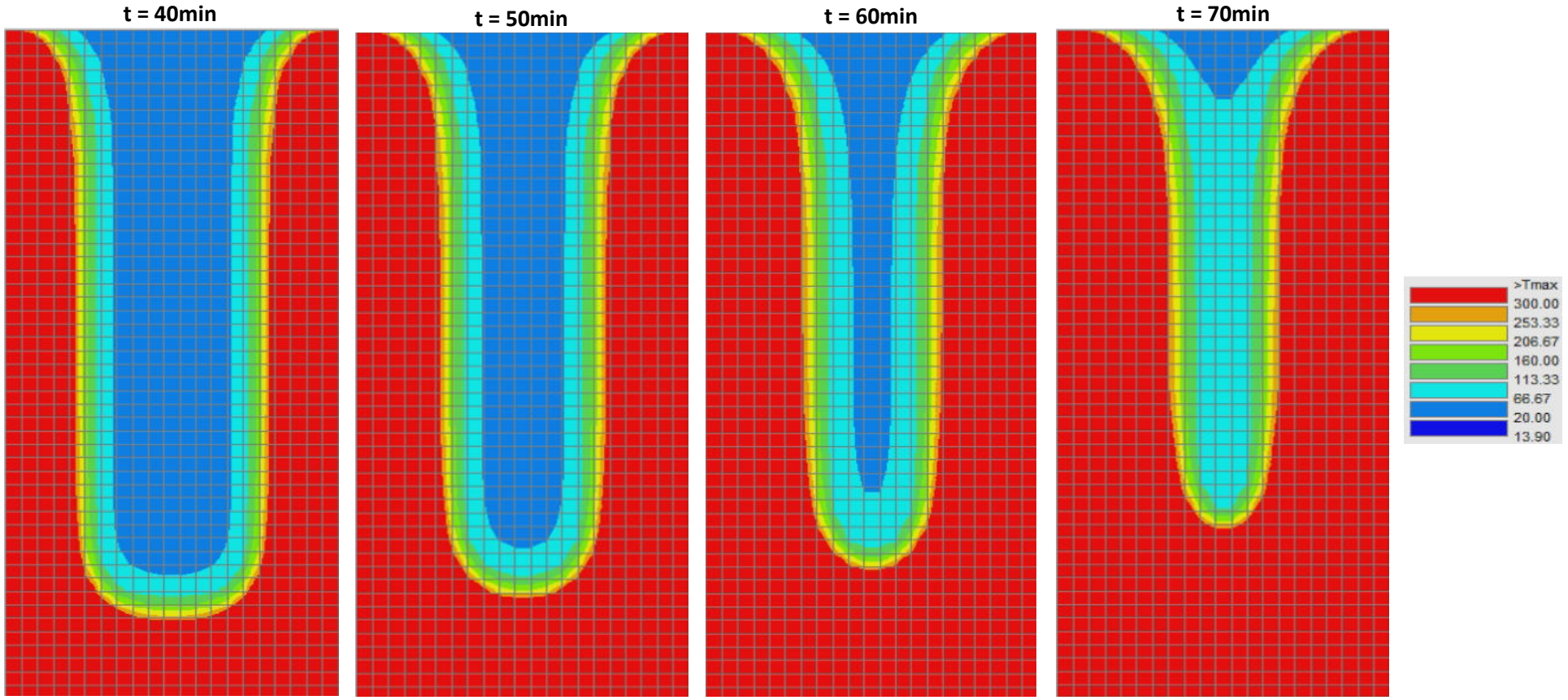
t = 40min
t = 50min
t = 60min
t = 70min
>Tmax
300.00
253.33
206.67
160.00
113.33
66.67
20.00
13.90

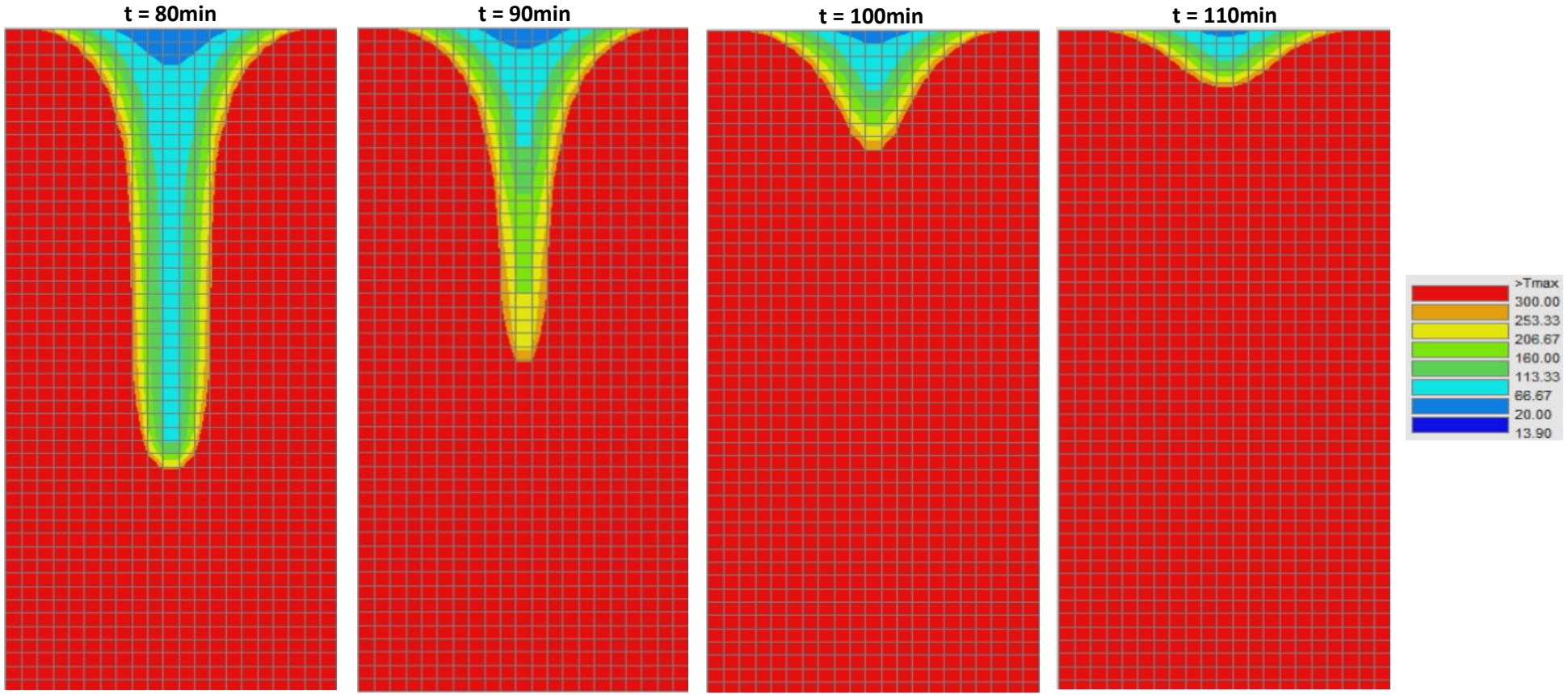
t = 80min
t = 90min
t = 100min
t = 110min
>Tmax
300.00
253.33
206.67
160.00
113.33
66.67
20.00
13.90